Suppression of Osteoblast Activity by Disuse is Prevented by Low Magnitude Mechanical Loading through a Bone Morphogenic Protein-Dependent Mechanism

A Dissertation
Presented to
The Academic Faculty

by

Mamta Jashvantlal Patel

In Partial Fulfillment
of the Requirements for the Degree
Doctor of Philosophy in the
School of Biomedical Engineering at the
Georgia Institute of Technology and Emory University

Georgia Institute of Technology
April 2008

Suppression of Osteoblast Activity by Disuse is Prevented by Low Magnitude Mechanical Loading through a Bone Morphogenic Protein-Dependent Mechanism

Approved by:

Dr. Hanjoong Jo, Chair
School of Biomedical Engineering
School of Medicine, Division of Cardiology
Georgia Institute of Technology
Emory University

Dr. Clint Rubin
School of Bioengineering
State University of New York at
Stony Brook

Dr. Barbara Boyan
School of Biomedical Engineering
School of Materials Science
Georgia Institute of Technology

Dr. Janet Rubin
School of Medicine
Division of Endocrinology/Metabolism
University of North Carolina

Dr. Robert Guldberg
School of Mechanical Engineering
Georgia Institute of Technology

Dr. Diana Risin
Space Medicine Division
NASA Johnson Space Center

Date Approved: December 17, 2007

The important thing is not to stop questioning. Curiosity has its own reason for existing. One cannot help but be in awe when he contemplates the mysteries of eternity, of life, of the marvelous structure of reality. It is enough if one tries merely to comprehend a little of this mystery every day. Never lose a holy curiosity.

-Albert Einstein (1879-1955)

To Ba and Dada for the heritage,
Mom and Dad for the opportunities,
Hemben for my childhood,
Daxaben for the indomitable support,
Pritty for the kindred friendship,
Bhikhu for the humor, and
Smita and Trisha for the future

Families are like fudge...mostly sweet with a few nuts.
-Author Unknown

PREFACE

I have been an inexorable dreamer my entire life, often aspiring for so many different ambitions that the immediate goals were frequently lost in thought. However, with every phase of my life, some things never changed. I always wanted to be just like my two older sisters, who could not be more disparate from one another. One sister wanted to be an astronaut, and thus, I, at the ripe age of seven, announced to the entire school during the morning announcements that *I* would one day become an astronaut. I always knew my forte embraced science and mathematics, quite contrary to the study of music, art, theatre, writing, and photography I commenced in vain. I recognized in myself a curiosity so reminiscent of scientists, and my perfectionist attitude and attention to detail often warranted teachers to suggest engineering as a profession. Thus, when sprinkled into the recipe of my life, these events led me to the Georgia Institute of Technology and Emory University in Atlanta, GA to write this dissertation in biomedical engineering.

In the epigraph, I quote the great Albert Einstein's thoughts on curiosity, a tenet that is arguably intrinsic in life. I wholly believe science requires a balance between the innate curiosity to question the reasons why certain entities exist and the acquired prudence to accept the things to which we have no answer. It is with this curiosity that science has delved into the puzzle of the human body, ascertaining the causes of pathologies that once evaded us and cultivating therapies to mitigate these medical maladies.

In the spirit of Einstein's words, I have completed my formal education by never losing my holy curiosity. From extensive "To Do" lists to three-week-in-advance experimental plans, this dissertation is brought to you after four years of diligence, vigilant thought, and an earnest aspiration to help others.

Mamta Patel, Ph.D.

ACKNOWLEDGEMENTS

I always knew that I enjoyed science and all things scientific in school but yearned to attempt my hand at various artistic ventures, which always seemingly failed. However, in graduate school, I found a wonderful balance among my many assorted interests and even managed to find a home for creativity in science. Along the way, I met a clan of the most eclectic personalities who inspired me scientifically and dazzled me personally. To them, I owe my heartfelt thank you, for this dissertation is the product of their indomitable support, charming friendship, constant encouragement, and invasive laughter.

I would like to acknowledge my advisor, Hanjoong Jo, who allowed me to work on a project related to microgravity and NASA. I am truly grateful to have been able to travel near and far to present our work at scientific sessions, which facilitated in my developing a knack for answering questions on-the-spot. My earnest admiration goes to my dissertation committee formed by Dr. Barbara Boyan and Dr. Robert Guldberg of Georgia Tech, Dr. Diana Risin of NASA, Dr. Clint Rubin of the SUNY Stony Brook, and Dr. Janet Rubin of the UNC. When we formed this committee, I was unaware that there were existing friendships among this group, making my committee meetings a joy...a sincere joy. After comments about my project had been laid on the table, the culmination of the meeting was more of a reunion of old friends. In turn, I benefited from a relaxed atmosphere of scientific discussion among mentors whose advice to me sincerely had my best interests at heart. To Dr. Boyan, thank you for taking me under your wing and leading by example in being an amazingly interesting and capturing lecturer. I am forever thankful to have had the opportunity to lecture to a room full of young undergraduates because when I first received an email saying "You make science

fun.", I knew teaching was in my future. To Dr. Guldberg, thank you for taking an interest in me as a person, inviting Srin and me to spend time with your beautiful (ideal) family, and for being a fantastic teacher. To Dr. Clint Rubin, your down-to-earth attitude and honest criticism have made our e-mentorship so rewarding, and to Dr. Janet Rubin, thank you for your appreciation of the details. Dr. Diana Risin, my genuine gratitude goes to you for always having my interests at the forefront of your actions. You were a wonderful mentor when I worked at NASA with the perfect balance of guidance and freedom.

To the Jo lab, transitioning from the start of this uphill climb to finally reaching the summit was indeed a hike that I could not have made without the resolute support I found in your presence. You, as a whole, are an amazingly talented group of fun, intelligent, and stylish people. Waking up and coming to work for what would surely have been a dreadful balance between classes and research ended up being one of my favorite things to do because of your shining personalities. Of course, all sorts of mad love and thank yous go to Tress, Ames, and Rando for being three of the coolest people I have ever met!

Tress, I can still remember meeting you at recruiting weekend and thinking you were such a sweet person. It was a most pleasant surprise to find that you had joined the same lab as I, and it was instantly apparent that we would share this frustrating, undulating, and exhilarating journey with persistent support and unwavering friendship. During these past four and a half years, we have laughed, shared, shopped, failed, succeeded, and persevered together. I am truly most fortunate to have had you along the way. Your sense of humor, innate quality for baking desserts, and enviable "nice" attribute make you a marvelous friend. We have often remarked that you and Pritty are identical, and as such, I often feel like you are my own sister.

Ames, my wonderful, beautiful, words-do-not-do-justice-to-you Ames. It often feels like speaking to you is like looking in a mirror. You read my mind with uncanny accuracy, and together we have celebrated our ups and commiserated our downs. I secretly hoped you would join our lab when you rotated that summer, but I never imagined we would form a friendship that is without a doubt centered about a sincere appreciation for each other. I have lived and learned vicariously through your beautiful marriage, and I am eternally thankful to have had a friend who just "got it". Thank you for the laughter, the tears, the successes, and the lessons. You truly are a remarkable person. I actually cannot wait to share our future with each other.

Rando, you quickly became one of my favorite friends for your ability to listen and sincere love of music. Thank you for keeping me hip enough to listen to music outside of my country-filled iTunes. My many thanks go to you for sharing in my joy of college football, and Thanksgiving day games with you were one of the highlights of my years here in ATL (sorry I missed this year). I do not know if I will ever hear the words South Dakota without thinking of my farm friend Randy! For you, I would actually go to Yankton.

Maria, thank you for your no-holds-barred attitude and for being an awesome lab manager! Michelle, thank you for always being an open ear for my venting, sharing your drama-filled personal life with me ☺, for changing my media from those annoying Opticells, for not making me feel bad when I asked you to change my media, and for taking the time to listen to me no matter how busy you were. Dr. Hannah Song, thank you for always bringing a smile to work and being a wealth of information on those darn BMPs. Chih-Wen, you are without a doubt one of the most selfless and intelligent people with whom I have had the honor of working. Dr. Kyung-Hwa Chang, your laughter rings through the lab daily, and your perky personality makes me smile. I am so proud of how far you have come from when you joined the lab. You have opened up

and allowed your sarcastic, funny personality to shine, and your English is so much better. My appreciation also goes to Dr. Seth Brodie (thanks for sharing in my love of fine dining), Dr. Doug Nam, Dr. Kwon, and Dr. Won Jong Rhee.

I owe a particular bout of thanks to my two wonderfully intelligent mentees, Sauja Vadoothker and Christine Hartzell. Sauja, you are indeed fantastic. You are a fantastically exuberant student and a fantastic younger sister☺! I love that you called me for advice about your graduate lab, and I look forward to the indubitable things you accomplish. Little bits of Sauja are sprinkled in this dissertation because she joined me as I was barely figuring out why there was no Eastern blot and what it meant to "vortex" something. In particular, I owe a big shout out to her for the fluid shear stress data in Chapter 7. Christine, you are wise beyond your years, and your honest interest in science is palpable. I have no doubt that with the way you assert yourself, you will compile an impressive repertoire of academic achievements.

To the many Jo lab members who have come and gone during my tenure at Emory, thank you. Steve Pardo, without the fantastic platform you created for me, this dissertation would have been quite painful and certainly not as successful. Thank you for your patience in dealing with my anal tendencies and inquisitive nature. I am so grateful that you have kept in touch, and I look forward to seeing Matthew Javier grow up! Deb Smith, what do I say about one of the funniest, most organized, and most caring people I have had the pleasure of knowing? My many thanks go to you for often holding my hand as I ventured into this unknown territory of research and for being a solid sounding board early on as I searched and found my own role in science. To Dr. Manu Platt, let me just say that anyone who has not had the pleasure of hearing the most joyous, infectious laughs from Manu is missing out on one of the definite wonders of the world. It is impossible to resist being caught up in Manu's energy. Thank you for teaching me to pipette (what's a pipette?), inaugurating me into the wonderful world of

ix

Western goodness, for being my partner in singing out loud in lab, for loving the soundtrack to *Rent*, and for sharing in my love for all things space-related.

To the other former Jo lab members, I thank Sarah Coleman for gracing us with the drama of her life, as I am certain no one's Wednesday night is as exciting as hers. To Dr. Cass Reyes, despite a brief stint in the lab, your sweet smile and notable organization were a pleasant addition to daily life in science. To Dr. Nolan Boyd, my gratitude goes to you for teaching me the despicable art of real time PCR, an assay that became the pillar of my dissertation. To Dr. George Sorescu, thank you for being willing to answer any pesky questions during my early years in graduate school.

There are many scientists and engineers spanning the globe to whom I owe my acknowledgement. From the European Space Agency, I thank Dr. Jack van Loon, Ron Huijser, J. Frans Hommes, and Luc van den Berg for their assistance with the RPM. Thank you for being available and for promptly responding to my many fear-filled emails of RPM parts frayed or missing. At NASA, I would like to thank Dr. Nancy Ward for teaching me about the world of the RWV and to Dr. Kamal Emami for cell suspension culture. From Juvent, I thank Roger Talish and Tommy Wilson for their assistance in preparing a platform for our lab, directly resulting in a large portion of my dissertation. From Emory University, I graciously offer my gratitude to Linda Gilbert, who answered my many random calls for cells and media. To Leita Young, thank you for your administrative support. Finally, to the Division of Cardiology and its many members, thank you for accepting me into the world of hearts, arteries, smooth muscle cells, and endothelial goodness despite that my research related to systems almost completely unrelated to yours. Initially, I often felt out of place and left out of the group, but as my tenure progressed, I found comfort in the Division and realized my insecurities were only in my head. In particular, I would like to thank the Taylor lab for a rather big whooping in softball and more seriously for the daily camaraderie.

xi

to my face! And on top of that, you can move faster than lightning on the dance floor!

Duvall, I will always remember your ravenous need for Krystal's and the "That just

happened" moment during the Days of Blaise. I still smile at the memory! To 'Gela Lin,

you are one of the most sincere girls with a fabulous sense of self who I have had the

pleasure of getting to know. You never seem too busy to help anyone, and the word fun

seems to follow you around! Dr. Catherine Reyes, although we never hung out when

you resided in ATL (except for the random time that you and Kevin happened to be in

the Lenox Mall when my car broke down), our e-conversations have absolutely taken me

by surprise! I have never had so many quirky qualities and interests in common with

someone. Your emails make me happy, and I am pretty certain I made it through the

drab library days by emailing you.

I am quite a privileged person who rarely is happy without a multitude of

simultaneous obligations. As such, my four short years in Atlanta were packed with

socials, community service, and education outreach, which inevitably balanced my

insatiable need to be the best graduate student ever. During my first year, I suffered

from a bite of the athletic bug, causing me to crazily sign up to run a marathon when

prior to that day I had only ever run (I use the word "run" loosely here) a couple of miles.

In true Mamta fashion, I could not just run the marathon. I signed up to not only

accomplish a seemingly impossible athletic goal but also to join Team in Training for the

Leukemia and Lymphoma Society in raising funds towards cancer research. The

fabulously wonderful thing about TNT is that they do not let anyone give up on herself.

Congratulations to them—what a wonderfully built organization with the right intentions.

With TNT, I managed to impress myself by finishing the San Diego marathon (barely)

and raising $4,000 along the way. To my donors and supporters, who are too numerous

to name, I am indebted to you for allowing me to embark on a journey I thought was

ludicrous in the least and commendable at the most.

I have participated in many community events that made my world complete and fulfilled, and although too copious to list, I am certainly thankful to have been surrounded by others who share my desire in ridding the world of the bad and burgeoning the world with the good. I must single out GTEC Education Outreach and Asha for Education in my quest to make a difference. I joined GTEC in my first year of graduate school as education outreach was special to me from my undergraduate activities at Texas A&M and NASA. I quickly learned that science, in the right hands, could draw a crowd of young students' interest when properly advertised. I thank Sally Gerrish, Shawna Young-Garcia, and Meg McDevitt for their staff support and my co-chairs Sean Coyer and Christiane Gumera in making GTEC Outreach bigger and better. Asha for Education is special to me because volunteering for this group allowed me the opportunity to give to back to the world that molded my parents. Asha aims to cultivate socio-economic change through education, and we strive to provide education to those in remote regions of India who would otherwise have no access to schools. We bring school to them. I was fortunate enough to have the entire world in my hands living in the Land of the Free, but these children knew not the world in which I have become so comfortable. For the efforts of the many volunteers who endeavor to make a difference, I offer my sincerest gratitude. Last, but certainly not the least, is Team Asha, a program I co-organized for Asha Atlanta during my tenure as president. Team Asha is a marathon training program for those who want to achieve the goal of a lifetime and help someone along the way. With sub-par ☺ coaching in 2006, Srin and I managed to support 27 runners to cross the finish line and raise almost $30,000, of which 100% was sent to India. Congratulations to Team Asha!

I honestly feel that friends make the world go round, and I am blessed to have been surrounded by a host of people who were brilliantly fun, silly, mature, and fabulous chefs. I call them my Pot Luck family, and thank goodness I already work out because

when we get together, it is like we are trying to feed the Indian Army! To Yash and Ayona, thank you for always planning our get togethers, for many great conversations, and for the delectable food I will dearly miss. To KB and Smitha, thank you for hosting random pot lucks and the sensational South Indian dosas! Murali, your sincere smile is always so welcoming and your mad Indian cooking skills never seize to amaze me! Sathe, thank you for your anal tendencies (mostly because they make me seem "normal") and for your vibrant, ebullient personality. The years you lived across the hall were some of the most fun-filled socials we had (although the Amicalola reunion was my favorite!). Popo, thank you so much for all of the work you did for Srin and me as our computer expert during Asha. You are one of the most dedicated people with a drive reminiscent of a true Patel. I am proud to know you! To Dr. Ramesh Singh, thank you for having the biggest, truest heart I have ever seen. You are one of the few people who embodies a truly selfless gene, and I am impressed by your desire to return to Bihar in hopes of giving to them what you were blessed to have yourself. When you return to the States, I hope you remember to look me up. I could use another Ramesh meal☺. Kartik! How do I say thank you to my big brother, K, who has always looked out for me since the day I entered ATL? Thank you for constantly being by my side and for searching my apartment when I was sure there was an intruder. Thank you for the many lunches, dinners, phone calls, and for never seeming like my annoying requests to pick something up for me inconvenienced you! On top of everything, I do not know if I will ever meet another South Indian boy who can make paneer like you! Finally, to all of the other friends who have made my years in ATL richer and full of memories, my many thanks. To Nate Bunderson, the Heffernan family, and Sarah West, thank you for the many conversations that left me feeling like I had gained something in life. Sarah, I am so thankful to have shared the Chicago marathon with you and Jenn. To Sujay, thank you for whipping me into the best shape of my life. Your unique sense of humor and

rugged good looks☺ make you an awesome friend! Andrea, aka Running Twin, I do not know if I can ever run without you! You may have to move to Houston☺! Swathi, spending time with you is always filled with laughter. Thanks for always making the time to hang out with Pritty and me! Jenny Porter, you make me feel like I am part of that family, and you always remind me that there are others out there who are thoughtful, sophisticated, and caring. Brini, you were the only reason I was not scared to come to ATL because I figured no one could love a city THAT much if it was not remotely attractive! Thank you for making me feel welcome and that I had a home away from home. Remember, you always have a sister in me. Lastly, to Srinidhi Nagaraja, thank you for the friendship we built and the relationship we nurtured for the last three years. Your enthusiasm for my little bits of news (when you listen, that is) and award-winning hugs make me wish we were together all of the time! I admire your intelligence, generosity, sense of humor, and wacky sense of self more than I ever express. Your dedication to your family and friends is evident, and I am grateful to be a part of your life.

Finally, I must acknowledge the unconditional support of my family, without whom I would never have achieved a life full of success and joy. You are the reason for my happiness, for my triumphs, and for saving me from my tribulations. Mom and Dad, I am not sure words can do justice to the opportunities you gave us by sacrificing your own luxuries. I strive to make you proud, to constantly thank you for putting the world in my hands, and to honor your name. Everything I have become is because of you. Hemben, thank you for sacrificing your own opportunities to help raise us, for teaching me that it did not matter who thought what of me, for leading by example, and for blessing my life with two beautiful nieces, Smita and Trisha. D, I am not sure how to thank you for your undying love and support for each of us. You constantly surprise me with your dedication, such as coming to my first marathon, surprising me for my defense (I still cannot get over that), going to Europe with me, and moving me to Florida and

ATL. I do not think I will ever understand how you balance being a doctor and a sister/daughter/fiancée so well, and for the all of the times I grunt about getting you a diet Pepsi (with ice and a paper towel), I am officially apologizing right now (do not expect it in person!). To Eddie and Patel, I am thankful that you joined the family and gave my sisters richer lives. P, I am not so sure that I can properly thank the one person who has shared the vast majority of my life with me. I often think you know me better than I know myself, and I am constantly impressed with your intelligence, integrity, and humor so much more than I ever admit. You can literally do anything you want to in life (you just do not think you can), and you should know that I always want better for you than I ever had. Your unwavering dedication to the big moments in my life reminds me that we really are best friends. Bhik, I doubt that these words can accurately articulate just how proud I am of you. In the last five years, you have grown, matured, and succeeded while maintaining your sense of humor and sense of family. You always had to learn by doing things yourself, and I admire the person you have become as a result. Ultimately, I wrote this dissertation in the memory of my maternal grandparents for providing my life with a sense of culture and diligence. For my entire family, I am indebted to you (even though you make fun of me ☺) because you constantly challenge me to be a better me.

This dissertation is brought to you in honor of those who use pipette tips from left to right, fear not the name Voldemort, appreciate the art of succulent living, and lastly, the letters and numbers of gtg668v.

TABLE OF CONTENTS

LIST OF TABLES

LIST OF FIGURES

LIST OF SYMBOLS AND ABBREVIATIONS

1-RM	One Repeat Maximum
3D	Three Dimensional
ALK	Activin Receptor-like Kinase
ALP	Alkaline Phosphatase
AP-1	Activator Protein 1
ATF2	Activating Transcription Factor 2
bFGF	Basic Fibroblastic Growth Factor
BFR	Bone Formation Rate
BMD	Bone Mineral Density
BMP	Bone Morphogenic Protein
BMP4	Bone Morphogenic Protein 4
BMPR	Bone Morphogenic Protein Receptor
BSP	Bone Sialoprotein
BUA	Broadband Ultrasound Attenuation
Ca2+	Calcium ion
cox-2	Cyclooxygenase 2
ctsk	Cathepsin K
dChip	DNA Chip Analyzer
DPD	Deoxypyridinoline
DSS	Dynamic Strain Similarity
DTGS	Deuterated Triglycine Sulfate
ECM	Extracellular Matrix
EP1	Prostaglandin E1
ERK	Extracellular Signaling-Regulated Kinase
FDR	False Discovery Rate
fgf-2	Fibroblast Growth Factor 2
FTIR	Fourier Transform Infrared Spectroscopy
g	Earth's gravitational field or acceleration due to gravity
GAPDH	Glyceraldehyde-3-Phosphate Dehydrogenase
GEO	Gene Expression Omnibus
GLA	γ-Carboxyglutamic Acid
GPCR	G-Protein Coupled Receptor
HLU	Hindlimb Unloading
hMSC	Human Mesenchymal Stem Cells
Hz	Hertz (frequency)
IGF	Insulin-like Growth Factor
IGF-1R	Insulin-like Growth Factor Receptor 1
iNOS	Inducible Nitric Oxide Synthase
ISS	International Space Station
JNK	c-jun N-terminal Kinase
kDa	kilodalton (unit of weight)
LBNP	Lower Body Negative Pressure

LMHF	Low Magnitude and High Frequency
MAPK	Mitogen-Activated Protein Kinase
MBEI	Model-Based Expression Index
MMP	Matrix Metalloproteinases
NO	Nitric Oxide
NTX	N-telopeptide
OCN	Osteocalcin
OGN	Osteoglycin
OMD	Osteomodulin
OPG	Osteoprotegerin
OPN	Osteopontin
PBS	Phosphate Buffered Saline
PCNA	Proliferating Cell Nuclear Antigen
PGE2	Prostaglandin E2
PICP	c-terminal Peptide of Pro-Collagen Type 1
PRX	Peroxiredoxin
PTH	Parathyroid Hormone
PTHR1	Parathyroid Hormone Receptor 1
PYD	Pyridinium
RANK	Receptor Activator of Nuclear Factor κB
RANKL	Receptor Activator of Nuclear Factor κB Ligand
RPM	Random Positioning Machine
RTK	Receptor Tyrosine Kinase
RTPCR	Reverse Transcriptase Polymerase Chain Reaction
runx2	Runt Homology Domain Transcription Factor 2
RWV	Rotating Wall Vessel
SLRP	Small Leucine-Rich Proteoglycan
smurf	Smad Ubiquitination Regulatory Factors
STS	Space Transportation System
TGFβ	Transforming Growth Factor β
vTBMD	Volumetric Trabecular Bone Mineral Density
μ-CT	Micro-Computed Tomography
με	Microstrain

Summary

Musculoskeletal pathologies associated with decreased bone mass, including osteopenia, osteoporosis, disuse-induced bone loss, and microgravity-induced bone loss, affect millions of Americans annually. According to the National Osteoporosis Foundation, 10 million Americans currently suffer from osteoporotic bone loss while 34 million more are estimated to have osteopenia, or low bone mass, a strong risk factor for osteoporosis. Bone loss is particularly dangerous since it is typically asymptomatic and can lead to fractures of any bone, most usually those in the hip, spine and wrist. These fractures can greatly decrease the quality of life and often cause hospitalization. While osteoporosis usually affects the elderly, it can afflict both men and women of any age. Additionally, bone loss occurs in spaceflight, rendering astronauts at-risk for fractures during long term space travel. Despite health implications, it is still a national and international interest to continue and to expand human-based space exploration. As such, it is imperative to develop countermeasures for bone loss in space. On average, astronauts lose 1-2% of bone mass per month during spaceflight, losing 6-12% in a typical six month International Space Station (ISS) mission.

While many pharmaceutical treatments have slowed osteoporosis, there is still no countermeasure that can effectively mitigate bone loss observed in astronauts. The inadequacy of current countermeasures is at least partially due to a lack of understanding of the cellular and molecular mechanisms underlying bone loss caused by osteoporosis and microgravity. In recent years, investigators have begun addressing these issues by studying changes in gene expression induced by disuse, spaceflight, and ground-based simulated microgravity. The assumption is that the knowledge of changes in key gene expression may provide means for new, target-specific therapies to adequately counteract bone loss due to osteoporosis, disuse, or microgravity.

Additionally, it has long been regarded that mechanical stimuli are anabolic to bone. High magnitude, low frequency impact has been recognized to increase bone and muscle mass under normal but not microgravity conditions. However, the opposite stimulus, a low magnitude and high frequency (LMHF) mechanical load experienced in activities as low impact as standing, has also been shown to be anabolic to bone and has never been used in spaceflight. LMHF mechanical loading has been shown to be effective in treating musculoskeletal pathologies in a number of subjects during research and clinical trials, including animals, children with musculoskeletal diseases such as cerebral palsy or muscular dystrophy, young women with low bone mass, and post-menopausal osteoporotic women. While several preclinical and clinical trials have demonstrated that LMHF mechanical loading affects bone formation *in vivo*, the target tissues of the mechanical load and underlying mechanisms mediating the responses are not known.

As such, this research project focuses on understanding how a LMHF mechanical load mediates prevention of bone loss *in vivo* and developing a countermeasure for microgravity-induced bone loss. **The *objectives* of the project are to analyze the cellular and molecular changes induced in osteoblasts by simulated microgravity or disuse and LMHF loading to identify potential targets for therapeutic interventions and to investigate the utility of a LMHF mechanical load in mitigating microgravity-induced bone loss. The *central hypothesis* of the project is that simulated microgravity or disuse conditions induce bone loss by inhibiting expression of genes critical in regulating bone formation, osteoblast differentiation, and subsequent mineralization while a LMHF mechanical load prevents these effects.**

In these studies, we developed an *in vitro* system that simulates microgravity or disuse conditions using the Random Positioning Machine (RPM) to study the effects of

disuse on 2T3 preosteoblast cells grown in gas-permeable culture disks. Exposure of 2T3 cells to the RPM for up to nine days significantly inhibited alkaline phosphatase activity (ALP), recapitulating a bone loss response as seen in spaceflight without altering cell morphology or proliferation. Next, we carried out gene expression analysis using DNA microarrays to determine gene expression profiles of 2T3 cells exposed to the RPM for three days. Among 10,000 genes examined with the microarray, 88 were downregulated while 52 were upregulated statistically significantly by disuse by more than two-fold in comparison to the static 1g control conditions. We then verified the microarray data for select genes relevant in bone biology by using real time PCR assays and immunoblotting. We confirmed that disuse downregulated levels of *ALP*, *runt-related transcription factor 2 (runx2)*, *osteomodulin (OMD)*, and *parathyroid hormone receptor 1 (PTHR1)* mRNA, upregulated *cathepsin K (ctsk)* mRNA, and did not significantly affect bone morphogenic protein 4 (BMP4) and cystatin C protein levels.

The Rotating Wall Vessel (RWV) and the RPM are the two most commonly used simulators of microgravity, but these simulators have not been systematically compared to each other or to mechanical stimulating models. These comparisons are vital to validate their use in modeling a disuse phenotype. In the ensuing studies, we hypothesized that exposure to RWV inhibits differentiation and alters gene expression profiles of 2T3 cells, and a subset of these mechanosensitive genes behaves in a manner consistent to the RPM and opposite to the trends incurred by mechanical stimulation of mouse tibiae. Exposure of 2T3 preosteoblast cells to the RWV for three days inhibited ALP activity, a marker of differentiation, and downregulated 61 and upregulated 45 genes by more than two-fold compared to static 1g controls, as shown by microarray analysis. The microarray results were confirmed by real time RTPCR and/or immunoblots for seven distinct genes and proteins including *OMD*, *runx2,* and *osteoglycin (OGN)*. Comparison of the RWV data to the RPM microarray study that we

previously published showed 17 mechanosensitive genes that changed in the same direction. Further comparison of the RWV and RPM results to independently published microarray data from mechanically loaded mouse tibiae revealed three genes including *osteoglycin* that were upregulated by mechanical loading and downregulated by disuse.

Finally, in subsequent studies, we hypothesized that direct application of LMHF mechanical loading to osteoblasts alters their cell responses, preventing decreased bone formation induced by disuse or microgravity conditions. To test our hypothesis, preosteoblast 2T3 cells were exposed to a disuse condition using the RPM and intervened with a LMHF mechanical load (0.1-0.4g at 30Hz for 10-60 min/day). Exposure of 2T3 cells to the RPM decreased bone formation responses as determined by ALP activity and mineralization even in the presence of a submaximal dose of BMP4 (20ng/ml). However, LMHF mechanical loading prevented the RPM-induced decrease in ALP activity and mineralization. Mineralization induced by LMHF mechanical loading was enhanced by treatment with BMP4 and blocked by the BMP antagonist noggin, suggesting a role for BMPs in this response. In addition, LMHF mechanical loading rescued the RPM-induced decrease in gene expression of *ALP*, *runx2*, *OMD*, *PTHR1*, and *OGN*. These findings show that osteoblasts directly respond to LMHF mechanical loading to induce bone formation responses, potentially leading to normalization or prevention of bone loss caused by disuse or microgravity conditions. The mechanosensitive genes identified in this project may provide potential targets for pharmaceutical treatments that could be used in combination with low level mechanical loading to better treat osteoporosis, disuse-induced bone loss, or microgravity-induced bone loss.

Chapter 1

Introduction

Bone Function

The average, mature adult skeleton is comprised of 206 bones, forming the framework of the human body. The skeleton serves four primary functions: 1) mechanical support and locomotion, 2) vital organ protection, 3) blood cell production, and 4) mineral storage (40). Mechanical support includes supplying a shape and frame while providing attachment points for muscles at joints, allowing locomotion. Vital organs are protected by the strength and rigidity of specific bones, including the cranium covering the brain, the ribs and sternum cosseting the heart and lungs, and the vertebral column sheltering the spinal cord. The marrow cavities of certain bones serve as housing for the body's immune cells, hematopoietic stem cells, and mesenchymal stem cells. These stem cells differentiate into a multitude of critical cells for the body, including red blood cells responsible for oxygen delivery and osteoblasts responsible for bone formation. Lastly, bone acts as a reservoir for minerals such as calcium, sodium, magnesium, and phosphate ions. Bone stores 99% of the body's calcium and regulates its release to tissues that need it. These minerals are needed for various processes, including blood clotting, cell signaling, and neural messaging (53).

Bone Structure and Composition

There are four types of bone including long, short, flat, and irregular. Long bones, such as the tibia and femur, are longer than they are wide. They are characterized by a central cylindrical shaft called a diaphysis flanked by two extremities composed of an epiphysis and metaphysis (Figure 1.1). Carpals and tarsals are types of short bones, which are characterized as having approximately the same dimensions in all directions.
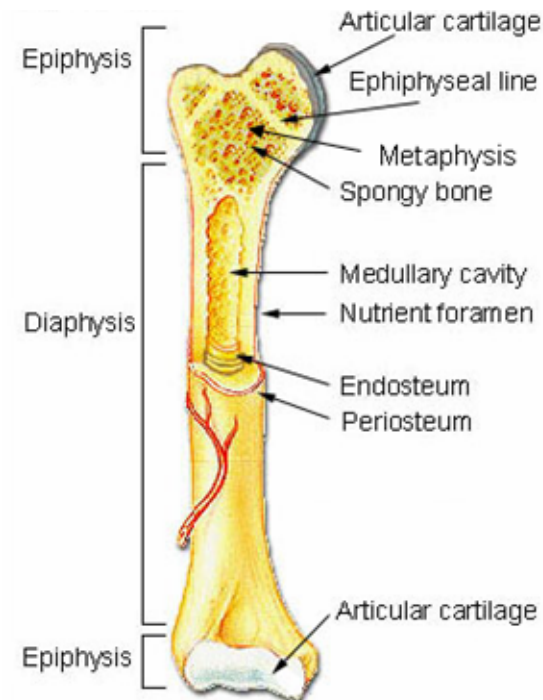
Figure 1.1 Anatomy of a long bone showing various characteristic components of bone, including the two epiphyses flanking the long cylindrical diaphysis
(Ref: Image adapted from www.web-books.com)

Flat bones, such as the cranium, have one dimension distinct from the other two and are thin, flattened, and usually curved. Irregular bones comprise any bones that do correspond to the aforementioned categories, such as the vertebrae (53).

Morphologically, there are two types of bone called cortical (compact) and trabecular (cancellous) bone as shown in Figure 1.2 (40, 53). Each type is distinguished macroscopically by its location in the whole bone tissue and microscopically by the orientation of mineral and collagen fibers. Cortical bone primarily comprises the diaphysis of long bones and forms a thin outer wall of other bones. It is a dense, compact material, and at the microstructural level, it is organized with parallel structural units called osteons. An osteon is a set of concentric lamellae formed from packed collagen fibrils, resembling the rings of a tree (Figure 1.3). Cortical bone is predominantly accountable for the supportive and protective functions of the skeleton.

2
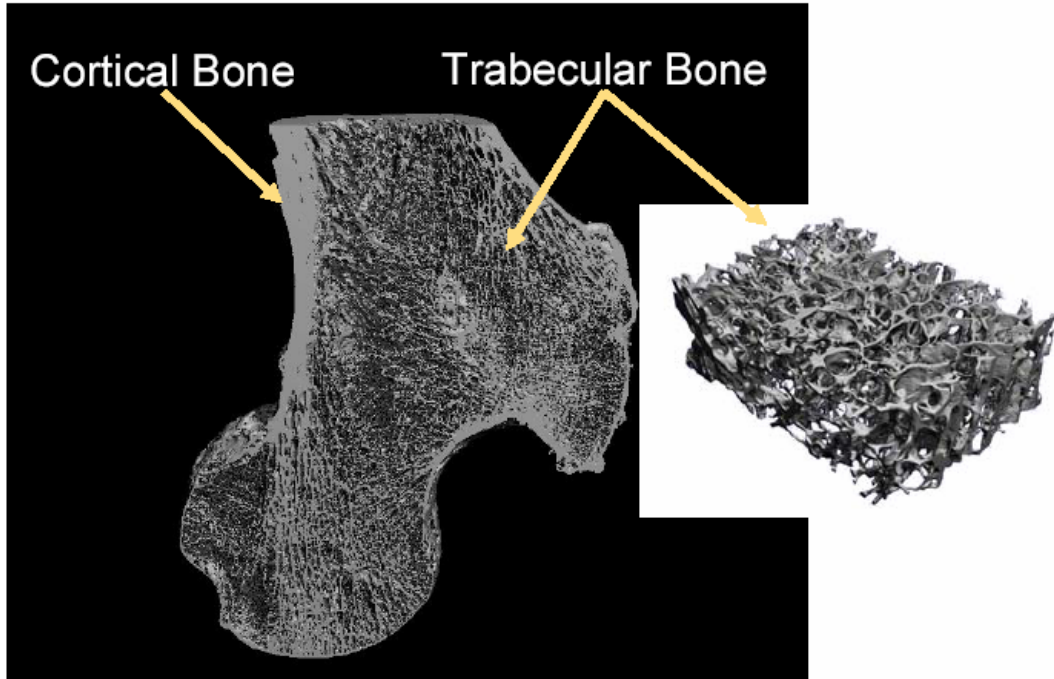
Figure 1.2 Architecture of bone showing near-solid cortical bone and porous trabecular bone (27)
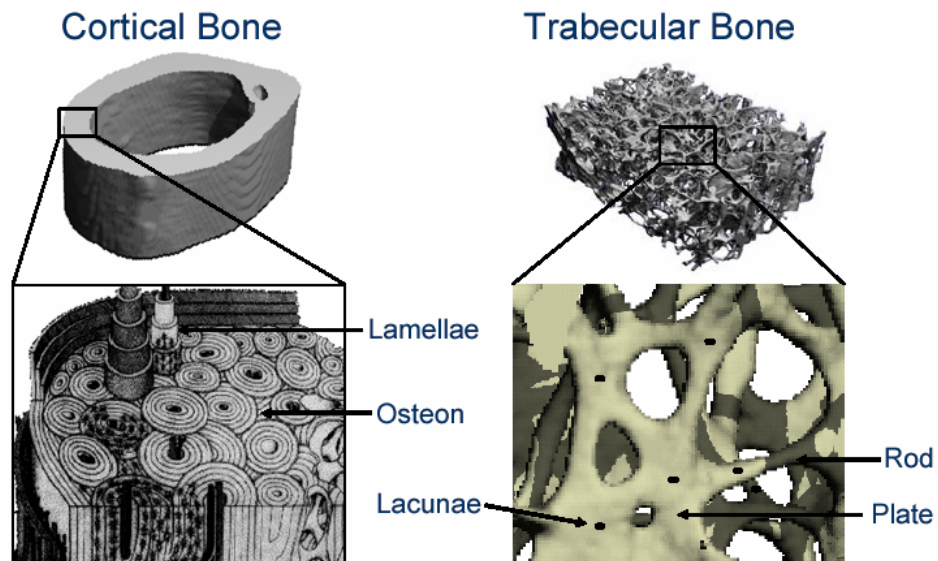
Figure 1.3 Microstructural features of cortical and trabecular bone showing the osteon, the building unit of cortical bone, and a rod and plate comprising the trabecula, the building unit of trabecular bone (27)
(Portion of figure also from T. Eienhorn, 1994)

Its structure is designed to provide a high moment of inertia to resist bending and remain relatively lightweight. In contrast, trabecular bone encompasses the metaphysis and epiphysis of long bones, interior of short bones, and the areas between the outer surfaces of flat bones. It is a loosely organized, porous solid characterized by interconnecting units called trabeculae, which are composed of rods and plates of bones. These trabeculae form a lattice-like structure with a large surface area, allowing absorption and dissipation of energy when joints are loaded and serving as the principal site of bone's metabolic functions (53). Bones are equipped with the appropriate structural integrity, strength, stiffness, and fracture resistance properties, enabling the human body to withstand diverse physiologic loads and changes to those loads.

Bone is a composite material containing three main constituents: mineral matrix (inorganic phase), organic matrix, and water. The mineral phase comprises 65% of the bone tissue and encompasses calcium phosphate and calcium carbonate in the form of hydroxyapatite mineral. The mineral in bone gives it strength and stiffness, primarily resisting compressive forces. The organic matrix makes up 30% of the bone tissue and contains 95% collagen fibers, primarily type I collagen, and 5% of proteoglycans and non-collagenous proteins such as osteocalcin (OCN), osteopontin (OPN), bone sialoprotein (BSP), and osteonectin (12, 40). Collagen fibers in the organic matrix act as reinforcement and provide ductility, fracture toughness, and tensile strength to bone tissue (48). Water constitutes the remainder of bone at approximately 5% weight and is located within the collagen fibers, in the pores, and bound to the mineral phase. Although seemingly inert, water plays a role in defining the mechanical properties of bone. Dehydrated bone samples have been shown to display increased strength and stiffness and decreased ductility (29, 41).

Bone Cell Types

There are four main cell types in bone: osteoblasts, bone lining cells, osteocytes, and osteoclasts (Figure 1.4) (2). Together, these cells form and maintain bone so that it can maintain its properties and perform its functions as previously discussed. Osteoblasts, osteocytes, and bone lining cells originate from local osteoprogenitor cells while osteoclasts differentiate from hematopoietic stem cell lineage. Osteoblasts are differentiated cells accountable for deposition and mineralization of the bone matrix, and bone lining cells are flat, elongated, and inactive while covering the bone surface. Osteocytes are mature osteoblasts that have become embedded into the mineralized matrix and are responsible for tissue maintenance. The cytoplasmic processes of osteoblasts propagate through the unmineralized matrix, called the osteoid, to the mineralized matrix and interact with osteocytes. A single osteocyte occupies a small
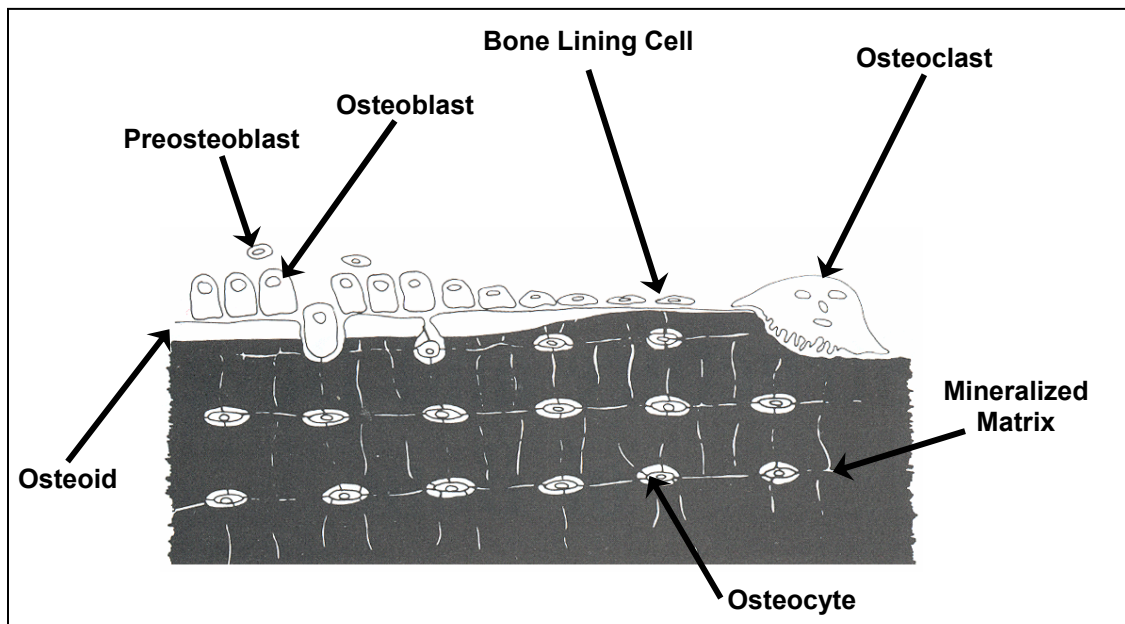
Figure 1.4 Bone is composed of multiple cell types to maintain skeletal homeostasis (2).

space called a lacuna and forms long, branching processes through the canaliculus, or a small channel, to contact another cell, such as an osteoblast. In this way, cell-to-cell communication occurs, potentially creating a diverse and intricate network that is hypothesized to sense deformation and instigate bone remodeling. Osteoclasts are large, multi-nucleated cells that resorb bone through dissolving the inorganic mineral matrix and enzymatically digesting the organic matrix. An activated osteoclast rests directly on the cell surface and has two distinct plasma membrane characteristics: a ruffled border and a clear zone. The ruffled border is where the bone resorption takes place while the clear zone is a microfilament-rich, organelle-free area that serves as a point of attachment to the bone matrix (2).

Bone Remodeling

Bone is a live, dynamic tissue undergoing constant remodeling, and perturbations to this process lead to bone loss. Bone remodeling occurs throughout life in a series of steps known as: 1) Quiescence, 2) Activation, 3) Bone Resorption, 4) Reversal, and 5) Bone Formation (Figure 1.5) (2, 40). During the quiescent phase, bone lining cells reside in the bone in an inactive state, and when bone remodeling begins, these cells secrete factors to recruit preosteoclasts to begin the activation phase. The activated preosteoclasts then differentiate into osteoclasts, signifying the beginning of the bone resorption phase. During this phase, osteoclasts close off portions of the old bone into areas called the Howship's lacunae. The large, multinucleated osteoclasts pump hydrogen ions into these areas to create an acidic environment for the lysozomal matrix metalloproteinases (MMPs) and cathepsins. These proteins first dissolve the hydroxyapatite mineral in the bone and then the organic matrix (2, 40). Once the bone is resorbed, the osteoclasts migrate out, and osteoblasts enter the region to begin laying down the extracellular matrix with type I collagen and numerous noncollagenous
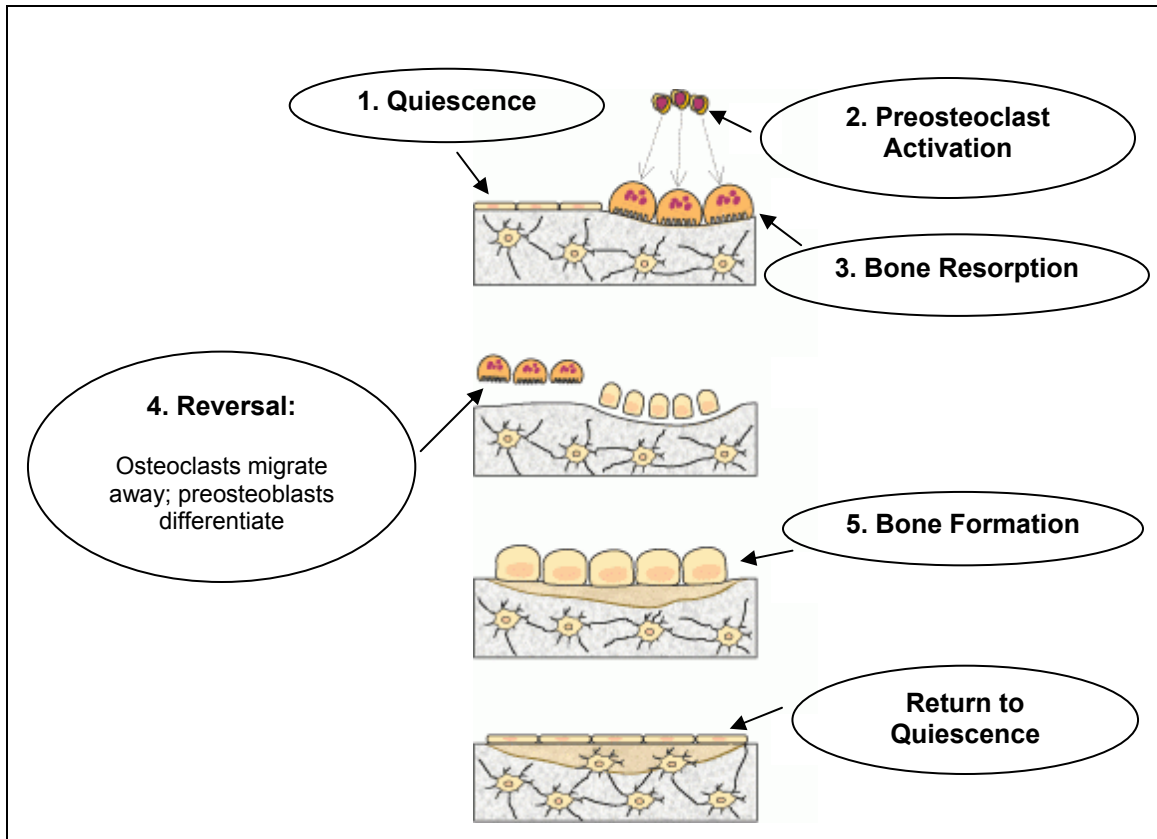
Figure 1.5 Bone remodeling occurs through a series of five steps to adapt to changes in environment.
(Ref: Image adapted from International Osteoporosis Foundation)

proteins such as OPN, osteomodulin (OMD), and osteonectin. The osteoid is eventually mineralized by deposition of calcium salts in the form of hydroxyapatite to provide bone with rigidity (2). The cycle returns to the quiescent phase and repeats throughout life as needed. As such, the new bone is called woven bone and is replaced by mature, lamellar bone by the process of remodeling (53). Woven bone is characterized by randomly deposited collagen fibers, which become organized in lamellar bone, giving it a directed mineral phase and anisotropic properties (53). The tightly coupled processes of bone formation and bone resorption in skeletal remodeling ultimately make bones structurally stronger (2, 40).

The process of bone formation can occur in a number of contexts, including new bone on existing bone (appositional bone formation), within cartilage (endochondral ossification), and within an organic matrix (intramembranous ossification) (53). Appositional bone formation ensues during enlargement of bones during remodeling and growth. In this type of formation, osteoblasts align on the existing bone surface, synthesizing osteoid in resultant layers forming bone lamellae. Endochondral ossification occurs during embryonic formation of long bones and weight-bearing bones through pre-existing cartilage. The cartilage cells called chondrocytes become hypertrophic and cause a cascade to resorb portions of the cartilage, creating marrow cavities. Preosteoblast cells invade these cavities, differentiate, and form bone matrix on the mineralized cartilage. Osteoclasts resorb the calcified cartilage, and bone remodeling replaces the immature bone with lamellar bone. Intramembranous ossification occurs in the development of flat bones without a cartilage template. This bone is formed directly from mesenchymal tissue, synthesizing an organic matrix that contains blood vessels, fibroblasts, and preosteoblasts. The osteoprogenitor cells differentiate and form an osteoid layer, and trabecular bone structures form within the

tissue. As the rods fuse, forming continuous plates, the woven bone is replaced with lamellar bone (53).

Bone Loss Pathologies

Bone loss occurs when there is an imbalance in the rate of bone formation and bone resorption, favoring the latter (Figure 1.6). Many different perturbations can cause bone loss, including alterations in hormonal balance, microgravity exposure, prolonged bed rest, malnutrition, or old age. Bone loss predominantly affects post-menopausal women because of sharp decreases in estrogen, which plays a role in inhibiting osteoclast function, and progesterone, which plays a role in stimulating osteoblast function. This pathology can, however, affect women and men of any age as well. The onset of bone loss is regarded as a condition called osteopenia, and when the bone loss reaches the point of fracture vulnerability, the condition is called osteoporosis. Osteoporosis is defined as a disease characterized by low bone mass and structural deterioration of bone tissue, eventually leading to bone fragility and an increased susceptibility to fractures. Osteoporotic fractures usually affect load-bearing bones such as those in the hip, spine, and wrist. According to the National Osteoporosis Foundation, an estimated 44 million Americans, or 55 percent of the people 50 years of age and older, have been diagnosed with osteopenia. Currently, there are approximately 10 million individuals in the United States already diagnosed with osteoporosis, and of these, eight million are women and two million are men. Bone loss leading to hip fractures or collapsed vertebrae severely lower the quality of life. Moreover, about 20% of those who have hip fractures die from complications incurred after the reconstructive surgery, such as blood clot impediments and pneumonia. Lastly, in many aspects, bone loss in spaceflight has been compared to age-related osteoporosis; however, the extent of bone mass loss due to spaceflight occurs in a shorter span of time than age-related

9
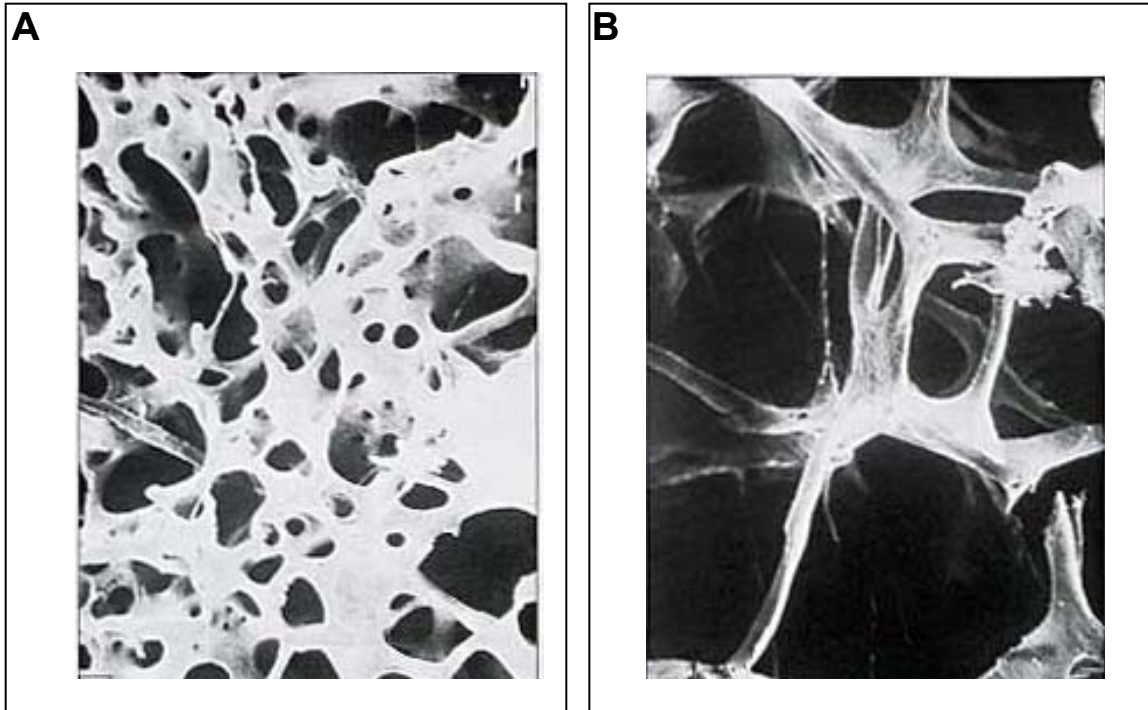
Figure 1.6 Normal bone (A) is composed of many connections between thick and healthy trabeculae while osteoporotic bone (B) is characterized by fewer connections of thinning trabeculae.
(Ref: Physicians Desktop Reference: PDR Health)

bone loss where astronauts lose as much bone mass in one month as post-menopausal women lose in one year (6).

Further progress in multidisciplinary studies on bone composition, structure, function, and diseases has significantly changed views on bone physiology (9). It is now understood that mechanical loading is not alone in altering the skeleton. In addition to mechanics, the skeleton is influenced by hormones, cytokines, nutrition, and genetic factors. The current observations continually trigger research to answer the questions of why and how bones adapt to their mechanical environment or how they change their structure to meet the demands of increased loading such as in exercise or decreased loading such as in spaceflight. Despite almost 50 years of human spaceflight and countermeasure efforts, researchers are still deliberating why bone loss occurs in

spaceflight and how to best counteract it. To date, there are no clear answers to these questions, and to continue and to expand development of countermeasures, scientists have ventured into studying these effects in ground-based systems. Research in this field could also benefit other bone pathologies such as osteoporosis.

Cellular Sense of Gravity

In order to develop countermeasures against bone loss in spaceflight, it is important to understand how a cell actually senses gravity, which is not certain and poses a challenge to understanding the role microgravity plays in pathology. Much of what is known regarding sensing gravity is in the plant cell. Weight causes differential mass displacement, due to differences in masses among disparate organelles. The cytoskeleton has traditionally been regarded as a mediator in the perception of gravity both in animals and plants (5, 18, 19, 31, 47). In plants, the mechanism used to sense gravity is most likely through the movement of statoliths, which are the suspected gravitropic organelle in Lepidium roots, in specialized cells when an organelle is displaced from its natural orientation (15). The concept of perception time is the minimum duration of the stimulation interval necessary to induce gravitropic bending of the plant root. Hejnowicz, et al. stated that the shortest stimulation time was one second, and therefore, they assumed that the perception time was less than second (15). The notion of perception time is important because it implies that the perception of gravity involves not only the magnitude of the gravity vector but also the constant alignment of the gravity vector for some minimal time.

Spaceflight is a constant state of freefall about the Earth, thereby eliminating the effects of gravity. Therefore, in spaceflight, cell signaling by gravitropic organelles is altered because there is no force displacing them to a specific gravity-dependent target for gravity-sensing signaling. Thus, a method of continually changing the direction of the

11

gravity vector faster than the cell's perception time may inhibit gravitropic responses. As such, simulating microgravity or disuse under normal ground conditions by using devices such as the Random Positioning Machine (RPM) that rotate and move the gravity vector continuously are based on the hypothesis that sensing no weight would have similar effects as being weightless. These devices, described in more detail below, are known as gravity vector-averaging systems.

Ground-based Simulators of Microgravity or Disuse

Many of the known space-inflicted pathologies have been the subject of research, and unfortunately, to date, they have not been adequately counteracted with dietary supplements (3, 14, 45) or rigorous exercise (22). Accordingly, scientists have tried to simulate microgravity using Earth-based models to study the mechanisms that might be responsible for causing pathologies such as bone loss in astronauts (1, 23, 28, 38).

Clinostats

A clinostat is a device that rotates around at least one axis with a platform that has a small enough radial distance to minimize centrifugal forces. Gravity still exists around the clinostat, but the gravity vector relative to the biological species on the clinostat continuously changes directions with the rotation. Over time, the gravity vector averages to a net zero force relative to the specimen because it does hot have enough time to sense it. The 2D clinostat, RPM, and the Rotating Wall Vessel (RWV) simulate microgravity or disuse by continuously moving the gravity vector, a method called gravity-vector averaging (Figure 1.7). The pertinent variable in the system is the speed of the rotation, for the gravity vector must move before the cell gravireceptors have time to sense it (17, 39). The dynamic stimulation of the gravity vector seems to displace the statoliths in the plant cells. Cytoskeletal elements, especially microfilaments, seem to be key players in the gravity-dependent change of statoliths. As the statoliths are displaced,

12

the cytoskeletal tension is disrupted, which alters the chain of cellular events leading to gravity-dependent responses (19, 47).

Hindlimb Unloading (HLU)

The animal hindlimb unloading (HLU) model has been used to partially mimic aspects of microgravity exposure such as removal of skeletal weight-bearing loads and the cephalic fluid shift (Figure 1.8). The hindlimbs are unloaded while the forelimbs remain loaded and used as internal controls. The head-down tilt from raising the hindlimbs provides the cephalic fluid shift seen in spaceflight. The HLU system applies minimal stress on the animal as noted by normal weight gain and eating habits of acclimated animals compared to controls (26). In comparison to spaceflight, the HLU model causes skeletal changes similar to spaceflight, with a few differences. Muscle atrophy occurs in both spaceflight and HLU in only load-bearing muscles, and the HLU model is most accurate and useful in studying the response of the skeleton to short duration spaceflight. Bone formation in rats seems to correct itself back to the level of control during long term HLU exposure, but in spaceflight, bone formation seems to remain suppressed until weeks to months upon return to Earth. It is also important to note that the entire body is unloaded in spaceflight whereas only the hindlimbs are unloaded in this model (25, 26).

Bed Rest

The bed rest studies are currently the only human-based ground analog to microgravity or disuse (Figure 1.9). Subjects are required to remain in bed at a 6-degree head-down tilt from weeks to months in time. Subjects perform all daily functions including eating and sleeping in bed, and cameras are placed in discreet places to ensure that subjects do not deviate from the protocol. In comparison to spaceflight, bone and mineral loss are site-specific phenomena in both studies. In addition, as
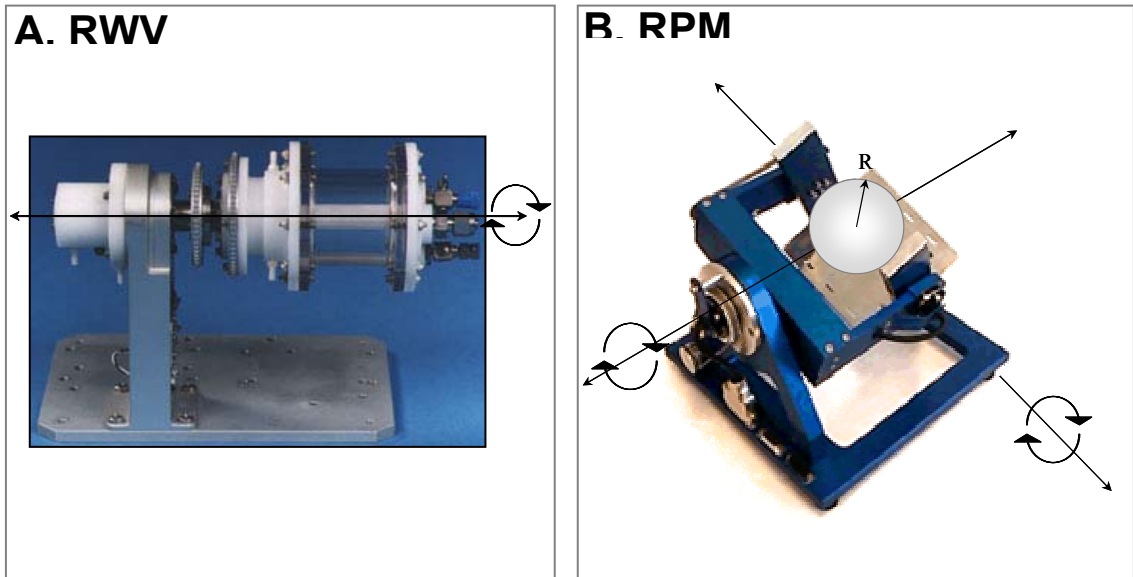
Figure 1.7 Clinostats that simulate microgravity or disuse conditions shown here are the Rotating Wall Vessel (A) and Random Positioning Machine (B) (30)

Figure 1.8 Animal hindlimb unloading (HLU) model showing a rat in a cage equipped with a rotary clip such that the hindlimbs are raised and forelimbs allow ambulation
(Ref: www.scielo.br)

bone is lost, there is a risk of kidney stones from increased urinary calcium excretion. Furthermore, muscles in the calf shrink up to 30% within a few months accompanied by a 50% decrease in strength. The headward shift of blood and other fluids mimics the cephalic fluid shift observed in spaceflight, and after approximately one day, the body adapts to the increased volume by increased urination, as also detected in spaceflight. Additionally, bed rest subjects develop a mild vertigo, causing nausea and dizziness. Microgravity is known to alter the neurovestibular system, where sensors in the ears and nerves in the soles of the feet are unbalanced, causing nausea and dizziness (20).
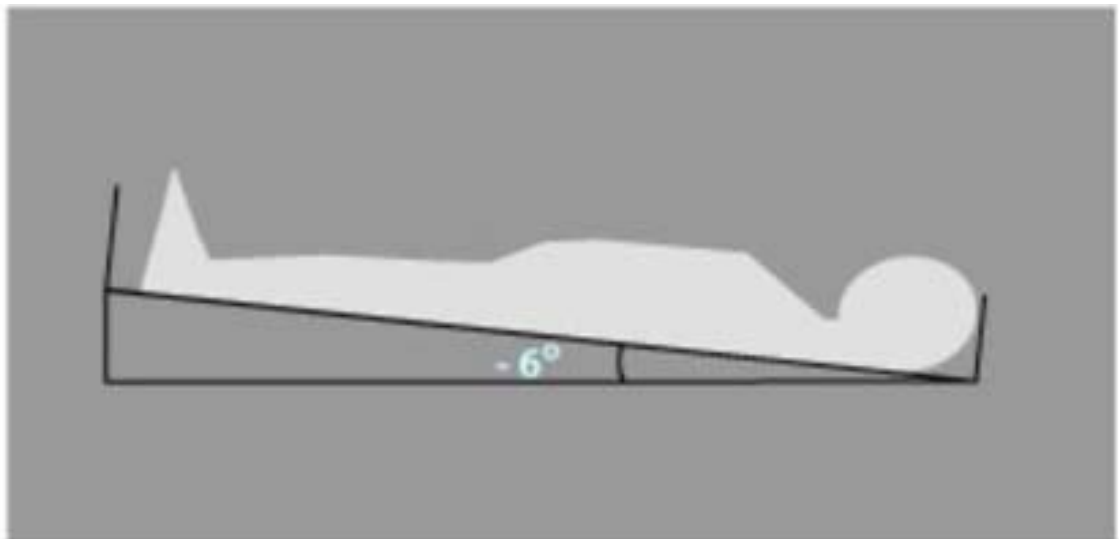
Figure 1.9 Human bed rest with head-down tilt showing 6 degree downward inclination
(Ref: Cleveland Clinic Lerner Research Institute, P. Cavanagh)

Countermeasures for Bone Loss: Current Status and Prospective

Exercise

Exercise has been the primary countermeasure to combat many of the pathologies induced by microgravity, including musculoskeletal alterations. It has long been recognized that exercise is beneficial to both muscles and bones, increasing their strength and size (11, 43, 46). When a clinical study of young, college-aged women was performed evaluating the effects of exercise, it was found that bone mineral density (BMD) of the spine increased in women who performed aerobic activity and in those who lifted weights. Additionally, improvements were seen in their back and leg muscles (43).

Exercise in spaceflight is not identical as on Earth since the loss of the force due to gravity yields no reaction force during movement. Therefore, exercise in spaceflight has been centered mainly on elastic-type machinery to load the muscles and bones of the body using devices such as bungee cords as early as the Gemini flights of the 1960s. Exercise machinery progressed to an adapted treadmill and bicycle as early as the Skylab missions of the 1970s, and updated machinery is still used today on the International Space Station (ISS). However, exercise has not been an adequate countermeasure for bone and muscle loss since astronauts continue to lose skeletal mass (6). Therefore, to defy the pathological changes induced by microgravity on the skeleton, distinct countermeasures must be developed targeting specific changes in bone cell adaptation.

Nutrition and Supplementation

Nutritional countermeasures have been integrated into crew meals, but the supplementations have not mitigated bone loss. Despite vitamin D and multivitamin intake, post-flight serum levels of 25-hydroxycholecalciferol (25(OH)-D3) were lower than pre-flight values for astronauts from the Skylab missions (24, 42). In another study, astronauts from the ISS consumed a vitamin D supplement for an average of five times

per week and a multivitamin for approximately three per week. These 11 astronauts had approximately 25% less serum vitamin D post-flight compared to pre-flight (42). The combination of calcium and vitamin D did not mitigate bone loss in astronauts because neither compound countered the increase in bone resorption or decrease in bone formation (4, 16, 54). Another vitamin that plays a role in bone health is vitamin K, which is involved in forming γ-carboxyglutamic acid (GLA) proteins such as osteocalcin (OCN) in the extracellular matrix of bone. An independent study showed that vitamin K supplementation during spaceflight increased urinary GLA excretion and lowered the secretion rate of undercarboxylated OCN. These data suggest that vitamin K is altered by spaceflight and that supplementation with vitamin K may be useful for astronauts since it counteracts the decrease in bone formation marked by decreased undercarboxylated OCN and bone specific alkaline phosphatase (ALP) (4, 45). However, vitamin K did not counteract the increased bone resorption as marked by the absence of an effect on type 1 collagen C-terminal telopeptide (44, 45). Although there seems to be promising benefits of vitamin K on bone health, there are limitations to supplementation of vitamin K because of its classical role in coagulation (50, 51).

In summary, the limited data available on nutrition show that the nutritional status of the astronauts changes in spaceflight. The dietary intake of specific vitamins or a multivitamin alone or in combination with an exercise regime is currently unable to mitigate bone loss.

Low magnitude and High Frequency (LMHF) Mechanical Loading

Julius Wolff (1892) was the first to suggest that stress imparted to bone impacted its architecture (52), and Harold Frost (1987) elucidated the role of a mechanical stimulus to bone (10). Frost defined a minimum effective strain that was required from a mechanical stimulus in order to stimulate bone adaptation, and he defined the

mechanostat as the biological machinery that determines bone strength (7-9). Therefore, it has long been regarded that mechanical stimuli are anabolic to bone. High magnitude, low frequency impact such as running has been recognized to increase bone and muscle mass (11, 43, 46). However, the opposite stimulus at a low magnitude (0.3g where 1g is Earth's gravitational field) and high frequency (30-90 Hz) (LMHF) is experienced in activities as low impact as standing (33). Figure 1.10 shows the platform (A) that applies these frequent oscillating acceleration and deceleration signals (B) to the subject upon it. The notion of stimulating bone formation or inhibiting bone resorption in
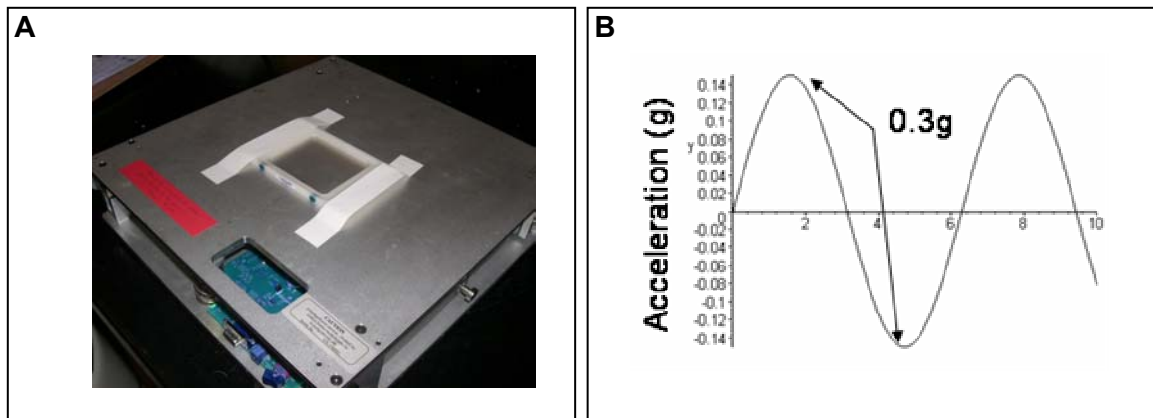
Figure 1.10 A low magnitude and high frequency (LMHF) platform (A) applies tiny vertical oscillations, where the magnitude of the load is characterized from the peak-to-peak value of each waveform (B).

patients with musculoskeletal diseases such as cerebral palsy and muscular dystrophy (13, 49), osteopenia (37), and post-menopausal osteoporosis (32) with a LMHF mechanical signal is a new, non-invasive treatment. It has been shown through animal and clinical trials that a LMHF mechanical stimulation is anabolic to bone (21, 32, 34-36, 49). Although not yet experimented in spaceflight, this potential osteoporosis countermeasure may provide benefit to the musculoskeletal system in a non-invasive manner for microgravity-induced bone loss.

References

1.   **Al Ajmi N, Braidman I, and Moore D.** Effect of clinostat rotation on differentiation of embryonic bone in vitro. *Adv Space Res* 17: 189-192, 1996.

2.   **Bilezikian JP, Raisz LG, and Rodan GA.** *Principles of bone biology*. San Diego: Academic Press, 1996.

3.   **Caillot-Augusseau A, Vico L, Heer M, Voroviev D, Souberbielle J-C, Zitterman A, Alexandre C, and Lafage-Proust M-H.** Space Flight Is Associated with Rapid Decreases of Undercarboxylated Osteocalcin and Increases of Markers of Bone Resorption without Changes in Their Circadian Variation: Observations in Two Cosmonauts. *Clin Chem* 46: 1136-1143, 2000.

4.   **Caillot-Augusseau A, Vico L, Heer M, Voroviev D, Souberbielle JC, Zitterman A, Alexandre C, and Lafage-Proust MH.** Space flight is associated with rapid decreases of undercarboxylated osteocalcin and increases of markers of bone resorption without changes in their circadian variation: observations in two cosmonauts. *Clin Chem* 46: 1136-1143, 2000.

5.   **Carmeliet G and Bouillon R.** The effect of microgravity on morphology and gene expression of osteoblasts in vitro. *FASEB J* 13: 129-134, 1999.

6.   **Cavanagh PR, Licata AA, and Rice AJ.** Exercise and pharmacological countermeasures for bone loss during long-duration space flight. *Gravit Space Biol Bull* 18: 39-58, 2005.

7.   **Frost HM.** A 2003 update of bone physiology and Wolff's Law for clinicians. *Angle Orthod* 74: 3-15, 2004.

8.   **Frost HM.** Bone "mass" and the "mechanostat": a proposal. *Anat Rec* 219: 1-9, 1987.

9.   **Frost HM.** From Wolff's law to the mechanostat: a new "face" of physiology. *J Orthop Sci* 3: 282-286, 1998.

10.   **Frost HM.** *The Laws of Bone Structure*. Springfield, IL: Thomas, 1964.

11.   **Galloway MT and Jokl P.** Aging successfully: the importance of physical activity in maintaining health and function. *J Am Acad Orthop Surg* 8: 37-44, 2000.

12.   **Gorski JP.** Is all bone the same? Distinctive distributions and properties of non-collagenous matrix proteins in lamellar vs. woven bone imply the existence of different underlying osteogenic mechanisms. *Crit Rev Oral Biol Med* 9: 201-223, 1998.

13.   **Gray B, Hsu JD, and Furumasu J.** Fractures caused by falling from a wheelchair in patients with neuromuscular disease. *Dev Med Child Neurol* 34: 589-592, 1992.

14.   **Heer M, Kamps N, Biener C, Korr C, Boerger A, Zittermann A, Stehle P, and Drummer C.** Calcium metabolism in microgravity. *Eur J Med Res* 4: 657-660, 1999.

15.   **Hejnowicz Z, Sondag C, Alt W, and Sievers A.** Temporal course of graviperception in intermittently stimulated cress roots. *Plant Cell Environ* 21: 1293-1300, 1998.

16.   **Holick MF.** Perspective on the impact of weightlessness on calcium and bone metabolism. *Bone* 22: 105S-111S, 1998.

17.   **Hoson T.** Evaluation of the three-dimensional clinostat as a simulator of weightlessness. *Planta* 203: S187-197, 1997.

18.   **Hou G, Mohamalawari DR, and Blancaflor EB.** Enhanced gravitropism of roots with a disrupted cap actin cytoskeleton. *Plant Physiol* 131: 1360-1373, 2003.

19.   **Ingber D.** How cells (might) sense microgravity. *Faseb J* 13 Suppl: S3-15, 1999.

20.   **Jones N.** Space physiology: lie back and think of science. *Nature* 435: 730-731, 2005.

21.   **Judex S, Zhong N, Squire ME, Ye K, Donahue LR, Hadjiargyrou M, and Rubin CT.** Mechanical modulation of molecular signals which regulate anabolic and catabolic activity in bone tissue. *J Cell Biochem* 94: 982-994, 2005.

22.   **Katkovsky BS PY.** Cardiac output during physical exercises following real and simulated space flight. *Life Sci Space Res* 14, 1976.

23.   **Kobayashi K, Kambe F, Kurokouchi K, Sakai T, Ishiguro N, Iwata H, Koga K, Gruener R, and Seo H.** TNF-[alpha]-Dependent Activation of NF-[kappa]B in Human Osteoblastic HOS-TE85 Cells Is Repressed in Vector-Averaged Gravity Using Clinostat Rotation. *Biochemical and Biophysical Research Communications* 279: 258-264, 2000.

24.   **Michel EL, Johnston RS, and Dietlein LF.** Biomedical results of the Skylab Program. *Life Sci Space Res* 14: 3-18, 1976.

25.   **Morey-Holton ER and Globus RK.** Hindlimb unloading of growing rats: a model for predicting skeletal changes during space flight. *Bone* 22: 83S-88S, 1998.

26.   **Morey-Holton ER and Globus RK.** Hindlimb unloading rodent model: technical aspects. *J Appl Physiol* 92: 1367-1377, 2002.

27.   **Nagaraja S.** Microstructural stresses and strains associated with trabecular bone microdamage, 2006.

28.   **Nakamura H, Kumei Y, Morita S, Shimokawa H, Ohya K, and Shinomiya K.** Suppression of osteoblastic phenotypes and modulation of pro- and anti-apoptotic features in normal human osteoblastic cells under a vector-averaged gravity condition. *J Med Dent Sci* 50, 2003.

29.   **Nyman JS, Roy A, Shen X, Acuna RL, Tyler JH, and Wang X.** The influence of water removal on the strength and toughness of cortical bone. *J Biomech* 39: 931-938, 2006.

30.   **Patel MJ.** Identification of Mechanosensitive Genes in Osteoblasts by Comparative Microarray Studies Using the Rotating Wall Vessel and the Random Positioning Machine. *Journal of Cellular Biochemistry* 101: 587-599, 2007.

31.   **Ross MD.** The influence of gravity on structure and function of animals. *Adv Space Res* 4: 305-314, 1984.

32.   **Rubin C, Recker R, Cullen D, Ryaby J, McCabe J, and McLeod K.** Prevention of postmenopausal bone loss by a low-magnitude, high-frequency mechanical stimuli: a clinical trial assessing compliance, efficacy, and safety. *J Bone Miner Res* 19: 343-351, 2004.

33.   **Rubin C, Turner AS, Bain S, Mallinckrodt C, and McLeod K.** Anabolism. Low mechanical signals strengthen long bones. *Nature* 412: 603-604, 2001.

34.   **Rubin C, Turner AS, Mallinckrodt C, Jerome C, McLeod K, and Bain S.** Mechanical strain, induced noninvasively in the high-frequency domain, is anabolic to cancellous bone, but not cortical bone. *Bone* 30: 445-452, 2002.

35.   **Rubin C, Turner AS, Muller R, Mittra E, McLeod K, Lin W, and Qin YX.** Quantity and quality of trabecular bone in the femur are enhanced by a strongly anabolic, noninvasive mechanical intervention. *J Bone Miner Res* 17: 349-357, 2002.

36.   **Rubin C, Xu G, and Judex S.** The anabolic activity of bone tissue, suppressed by disuse, is normalized by brief exposure to extremely low-magnitude mechanical stimuli. *Faseb J* 15: 2225-2229, 2001.

37.   **Rubin CT, Sommerfeldt DW, Judex S, and Qin Y.** Inhibition of osteopenia by low magnitude, high-frequency mechanical stimuli. *Drug Discov Today* 6: 848-858, 2001.

38.   **Sarkar D, Nagaya T, Koga K, Nomura Y, Gruener R, and Seo H.** Culture in vector-averaged gravity under clinostat rotation results in apoptosis of osteoblastic ROS 17/2.8 cells. *Journal of Bone and Mineral Research* 15: 489-498, 2000.

39.   **Sievers A and Hejnowicz Z.** How well does the clinostat mimic the effect of microgravity on plant cells and organs? *ASGSB Bull* 5: 69-75, 1992.

40.   **Sikavitsas VI, Temenoff JS, and Mikos AG.** Biomaterials and bone mechanotransduction. *Biomaterials* 22: 2581-2593, 2001.

41.   **Smith JW and Walmsley R.** Factors affecting the elasticity of bone. *J Anat* 93: 503-523, 1959.

42.   **Smith SM, Zwart SR, Block G, Rice BL, and Davis-Street JE.** The nutritional status of astronauts is altered after long-term space flight aboard the International Space Station. *J Nutr* 135: 437-443, 2005.

43.   **Snow-Harter C, Bouxsein ML, Lewis BT, Carter DR, and Marcus R.** Effects of resistance and endurance exercise on bone mineral status of young women: a randomized exercise intervention trial. *J Bone Miner Res* 7: 761-769, 1992.

44.   **Vergnaud P, Garnero P, Meunier PJ, Breart G, Kamihagi K, and Delmas PD.** Undercarboxylated osteocalcin measured with a specific immunoassay predicts hip fracture in elderly women: the EPIDOS Study. *J Clin Endocrinol Metab* 82: 719-724, 1997.

45.   **Vermeer C, Wolf J, Craciun A, and Knapen M.** Bone markers during a 6-month space flight: effects of vitamin K supplementation. *J Gravit Physiol* 5: 65-69, 1998.

46.   **Vuori I.** Exercise and physical health: musculoskeletal health and functional capabilities. *Res Q Exerc Sport* 66: 276-285, 1995.

47.   **Wang N, Naruse K, Stamenovic D, Fredberg JJ, Mijailovich SM, Tolic-Norrelykke IM, Polte T, Mannix R, and Ingber DE.** Mechanical behavior in living cells consistent with the tensegrity model. *Proc Natl Acad Sci U S A* 98: 7765-7770, 2001.

48.   **Wang X, Bank RA, TeKoppele JM, and Agrawal CM.** The role of collagen in determining bone mechanical properties. *J Orthop Res* 19: 1021-1026, 2001.

49.   **Ward K, Alsop C, Caulton J, Rubin C, Adams J, and Mughal Z.** Low magnitude mechanical loading is osteogenic in children with disabling conditions. *J Bone Miner Res* 19: 360-369, 2004.

50.   **Weber P.** Management of osteoporosis: is there a role for vitamin K? *Int J Vitam Nutr Res* 67: 350-356, 1997.

51.   **Weber P.** Vitamin K and bone health. *Nutrition* 17: 880-887, 2001.

52.   **Wolff J.** *Das Gesetz der Transformation der Knochen*. Berlin, Hirschwald: Stuttgart : Schattauer, 1892.

53.   **Yaszemski MJ, Payne RG, Hayes WC, Langer R, and Mikos AG.** Evolution of bone transplantation: molecular, cellular and tissue strategies to engineer human bone. *Biomaterials* 17: 175-185, 1996.

54.   **Zittermann A, Heer M, Caillot-Augusso A, Rettberg P, Scheld K, Drummer C, Alexandre C, Horneck G, Vorobiev D, and Stehle P.** Microgravity inhibits intestinal calcium absorption as shown by a stable strontium test. *Eur J Clin Invest* 30: 1036-1043, 2000.

Chapter 2

Specific Aims

Project Significance

Musculoskeletal pathologies associated with decreased bone mass, including osteopenia, osteoporosis, disuse-induced bone loss, and microgravity-induced bone loss, affect millions of Americans annually. According to the National Osteoporosis Foundation, 10 million Americans currently suffer from osteoporotic bone loss while 34 million more are estimated to have osteopenia, or low bone mass, a strong risk factor for osteoporosis. Bone loss is particularly dangerous since it is typically asymptomatic and can lead to fractures of any bone, most usually those in the hip, spine and wrist (2). In the US alone, there are approximately 1.5 million fractures annually due to osteoporosis (www.nof.org). Additionally, bone loss occurs in spaceflight, rendering astronauts at-risk for fractures during long term space travel. Despite health implications, it is still a national and international interest to continue and to expand human-based space exploration. As such, it is imperative to develop countermeasures for bone loss in space. On average, astronauts lose 1-2% of bone mass per month during space missions (6), losing 6-12% in a typical six month International Space Station (ISS) mission. While many pharmaceutical treatments have slowed osteoporosis, there is still no countermeasure that can effectively mitigate bone loss observed in astronauts.

It has long been regarded that mechanical stimuli are among the many factors that are anabolic to bone as shown in Figure 2.1. High magnitude, low frequency impact has been recognized to increase bone and muscle mass (1, 9, 10) under normal but not microgravity conditions. However, the opposite stimulus, a low magnitude and high frequency (LMHF) mechanical load experienced in activities as low impact as standing,

has also been shown to be anabolic to bone but has never been used in spaceflight. The LMHF mechanical load has been shown to be effective in treating musculoskeletal pathologies in a number of subjects during research and clinical trials, including animals (8), children with musculoskeletal diseases such as cerebral palsy or muscular dystrophy (4, 11), young women with low bone mass (3), and post-menopausal osteoporotic women (7). While several preclinical and clinical trials have demonstrated that the LMHF mechanical loading normalizes bone loss *in vivo*, the target tissues of the mechanical load and underlying mechanisms mediating the response are not known.
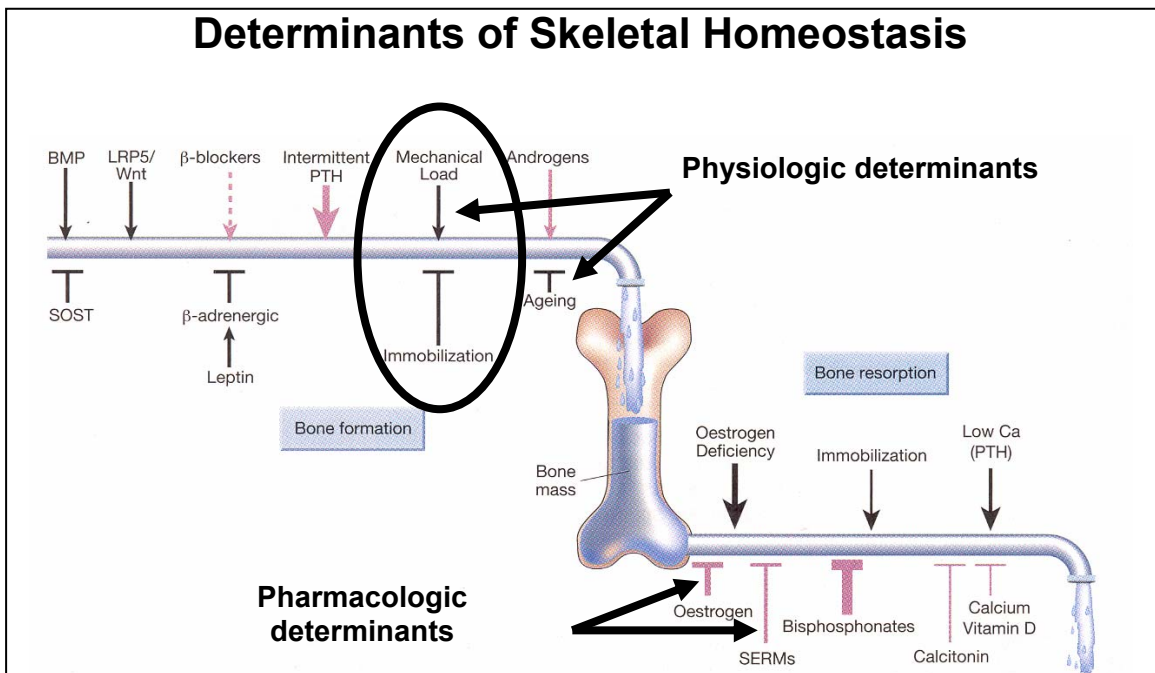
Figure 2.1 The determinants of skeletal homeostasis include many different factors, including physiologic aspects such as mechanical loads that instigate bone formation while ageing and disuse promote bone resorption (5).

Project Objectives and Hypothesis

This research project focuses on understanding how a LMHF mechanical load mediates prevention of bone loss *in vivo* and developing a countermeasure for microgravity-induced bone loss. **The *objectives* of the project are to analyze the cellular and molecular changes induced in osteoblasts by simulated microgravity or disuse and LMHF loading to identify potential targets for therapeutic interventions and to investigate the utility of a LMHF mechanical load in mitigating microgravity-induced bone loss. The *central hypothesis* of the project is that simulated microgravity or disuse conditions induce bone loss by inhibiting expression of genes critical in regulating bone formation, osteoblast differentiation, and subsequent mineralization while a LMHF mechanical load prevents these effects.** A LMHF mechanical loading platform has counteracted bone loss in both animal and human clinical trials. However, the mechanisms by which the low magnitude loading instigate an osteogenic response or whether it promotes an anabolic response in a microgravity setting has not been shown.
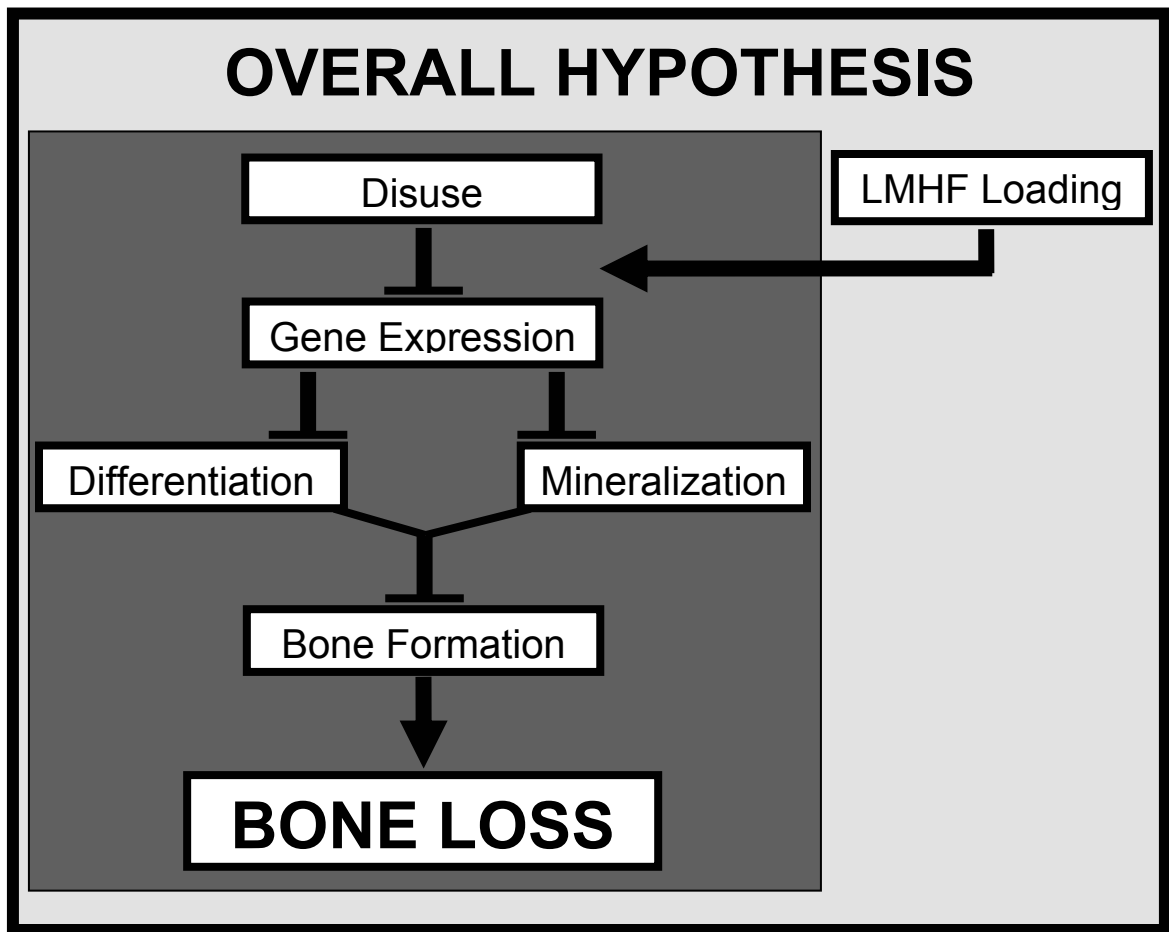
Figure 2.2 Project hypothesis conjecturing that microgravity or disuse causes bone loss through molecular alterations of osteoblasts while a low magnitude and high frequency (LMHF) mechanical loading intervention prevents bone loss through promoting osteoblast function

Specific Aims

      The central hypothesis of this project will be tested with three specific aims, as follows:

Specific Aim 1: **To determine the effect of simulated microgravity or disuse on cell differentiation and mineralization of mouse calvarial 2T3 preosteoblasts**

Working Hypothesis: Microgravity or disuse inhibits genes necessary for preosteoblast cell differentiation and subsequent mineralization.
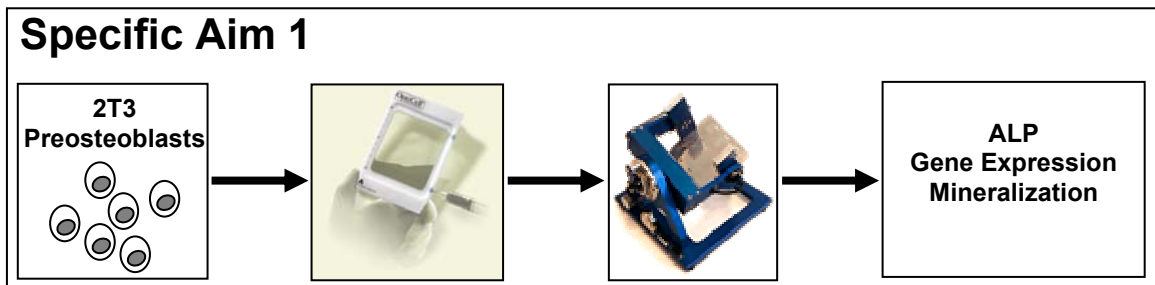
Figure 2.3 General experimental layout for specific aim 1
(Ref: Picture of Opticell from Opticell, Inc)

      As shown in Figure 2.3, preosteoblast cells plated in Opticells will be exposed to simulated microgravity or disuse conditions using the Japanese-designed and European-manufactured Random Positioning Machine (RPM) and assessed for markers of bone formation. Alkaline phosphatase (ALP) is an enzyme that is expressed early in osteoblast differentiation while mineralization is a late *in vitro* marker of bone formation. Several genes also are expressed during osteoblast differentiation, including *parathyroid hormone receptor 1 (PTHR1)*, *osteomodulin (OMD)*, and *runt homology domain transcription factor 2 (runx2)*. In this aim, various markers will be evaluated to determine if the decreased bone formation observed in spaceflight can be recapitulated using the RPM system. Most importantly, a high throughput DNA microarray will be performed to evaluate alterations in gene expression in 2T3 cells due to RPM exposure, providing the first systemic gene expression study performed under disuse conditions.

Specific Aim 2: **To compile a list of selected genes that change upon exposure to simulated microgravity or disuse conditions**

Working Hypothesis: Microgravity or disuse alters gene expression profiles of 2T3 preosteoblasts consisting of critical genes regulating osteoblast differentiation and mineralization.
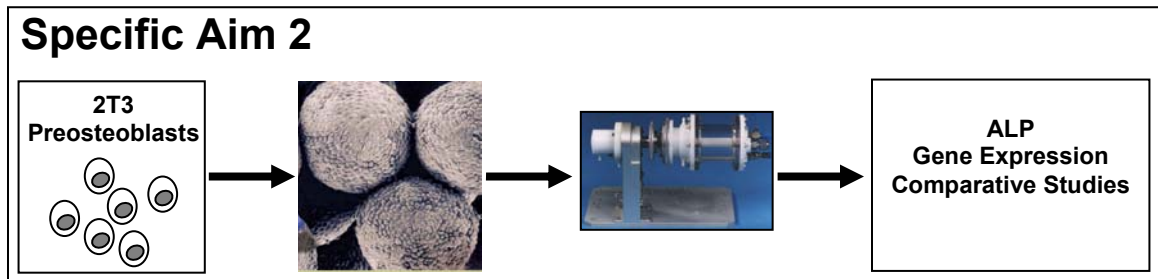
Figure 2.4 General experimental layout for specific aim 2
(Ref: Picture of cells on microcarriers from Solohill Engineering)

There are many simulators of microgravity used in the field, although the validity of data obtained from them is often rigorously questioned. The most substantial criticism is whether the simulators accurately replicate changes observed in spaceflight or disuse. While it is difficult to currently perform scientific experiments in actual spaceflight, it is possible to compare the various ground-based simulators to each other and to the small dataset of gene expression available from past spaceflight experiments. The NASA-designed simulator of microgravity called the Rotating Wall Vessel (RWV) is employed abundantly in the United States in studying various pathologies and tissue engineering. As depicted in Figure 2.4, 2T3 preosteoblast cells plated on microcarriers will be exposed to RWV simulated microgravity, and the results will be compared to those of the RPM. The critical information gained here will be a confined list of genes that change due to two models of simulated microgravity or disuse conditions. This confined list of genes will provide a group of target genes from which to continue molecular-based studies.

Specific Aim 3:   To determine whether LMHF mechanical loading prevents microgravity- or disuse-induced decrease in bone formation

Working Hypothesis: LMHF mechanical loading prevents decreased bone formation responses caused by the RPM.
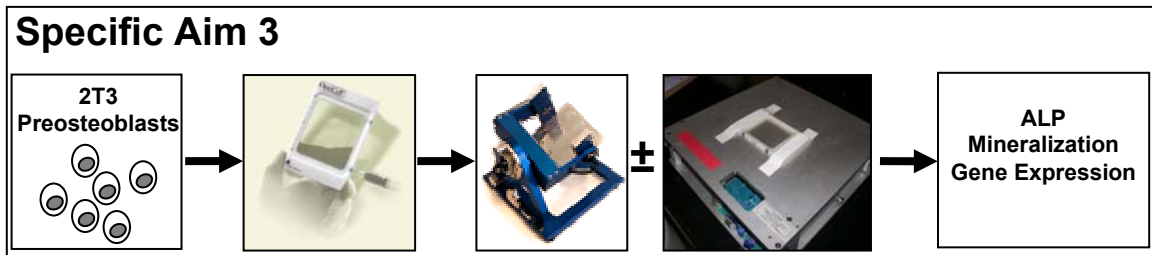
Figure 2.5 General experimental layout for specific aim 3
(Ref: Picture of Opticell from Opticell, Inc)

It is classically recognized that high magnitude and low frequency signals such as in exercise benefit the musculoskeletal system by maintaining bone density. However, a LMHF mechanical loading, which characterizes the load that muscles apply to the skeleton during activities such as standing, has also been shown to slow bone loss in post-menopausal women, young women with low bone mass, and various animal models.   However, the mechanism by which LMHF mechanical loading elicits an anabolic response is not known because cellular and molecular studies have not been performed. As illustrated in Figure 2.5, 2T3 cells plated in Opticells will be exposed to the RPM and intervened with a daily LMHF loading treatment.   Markers of bone formation such as ALP, mineralization, and gene expression will be evaluated to assess the utility of the LMHF platform in alleviating microgravity-induced bone loss.   More importantly, *in vitro* experiments will provide the means to begin studying molecular changes induced by a LMHF mechanical loading, and future therapies may be developed by combining the platform with pharmaceutical treatments based on molecular targets from this research to better treat bone loss due to osteoporosis, disuse, or microgravity.

References

1.   **Galloway MT and Jokl P.** Aging successfully: the importance of physical activity in maintaining health and function. *J Am Acad Orthop Surg* 8: 37-44, 2000.

2.   **Gass M and Dawson-Hughes B.** Preventing osteoporosis-related fractures: an overview. *Am J Med* 119: S3-S11, 2006.

3.   **Gilsanz V, Wren TA, Sanchez M, Dorey F, Judex S, and Rubin C.** Low-level, high-frequency mechanical signals enhance musculoskeletal development of young women with low BMD. *J Bone Miner Res* 21: 1464-1474, 2006.

4.   **Gray B, Hsu JD, and Furumasu J.** Fractures caused by falling from a wheelchair in patients with neuromuscular disease. *Dev Med Child Neurol* 34: 589-592, 1992.

5.   **Harada S and Rodan GA.** Control of osteoblast function and regulation of bone mass. *Nature* 423: 349-355, 2003.

6.   **Lang T, LeBlanc A, Evans H, Lu Y, Genant H, and Yu A.** Cortical and trabecular bone mineral loss from the spine and hip in long-duration spaceflight. *J Bone Miner Res* 19: 1006-1012, 2004.

7.   **Rubin C, Recker R, Cullen D, Ryaby J, McCabe J, and McLeod K.** Prevention of postmenopausal bone loss by a low-magnitude, high-frequency mechanical stimuli: a clinical trial assessing compliance, efficacy, and safety. *J Bone Miner Res* 19: 343-351, 2004.

8.   **Rubin C, Xu G, and Judex S.** The anabolic activity of bone tissue, suppressed by disuse, is normalized by brief exposure to extremely low-magnitude mechanical stimuli. *Faseb J* 15: 2225-2229, 2001.

9.   **Snow-Harter C, Bouxsein ML, Lewis BT, Carter DR, and Marcus R.** Effects of resistance and endurance exercise on bone mineral status of young women: a randomized exercise intervention trial. *J Bone Miner Res* 7: 761-769, 1992.

10.   **Vuori I.** Exercise and physical health: musculoskeletal health and functional capabilities. *Res Q Exerc Sport* 66: 276-285, 1995.

11.   **Ward K, Alsop C, Caulton J, Rubin C, Adams J, and Mughal Z.** Low magnitude mechanical loading is osteogenic in children with disabling conditions. *J Bone Miner Res* 19: 360-369, 2004.

Chapter 3

Evidence of Bone Loss and Alterations in Gene Expression in Spaceflight and Disuse

Summary

Significant evidence of bone loss in microgravity is available from early spaceflight experiments and from observations on current astronauts and cosmonauts. However, spaceflight is infrequent and expensive to study the biomedical effects of microgravity on the human body. Thus, it is critical to have adequate *in vitro* and *in vivo* ground-based models to simulate the effects of microgravity or disuse environments. Currently, the most commonly used *in vitro* simulators of microgravity or disuse are clinostats while *in vivo* simulators include the human-based bed rest studies and animal-based hindlimb unloading experiments. Despite the numerous studies that have marked a bone loss phenotype in wide ranges of multiple crew members, this pathology remains in astronauts without any effective countermeasures. Development and implementation of adequate countermeasures is hampered because little is known regarding the molecular changes regulating bone loss in microgravity. Recently, researchers have begun to investigate the molecular alterations in response to both spaceflight, simulated microgravity, and disuse, and it is believed that future prophylactic and therapeutic approaches may be directed towards specific molecular targets. In this chapter, we review data showing a bone loss phenotype in spaceflight, bed rest, hindlimb unloading, and clinostats. Additionally, we review the limited data on gene expression changes in each of these environments.

Bone Loss Response in Microgravity or Disuse

Spaceflight

It is well documented that spaceflight induces a decrease in bone mass in animals and humans after prolonged stay in space. In rodent animal studies, it has been shown that 17 days of spaceflight altered the biomechanics of femur bones, mostly concentrated on tissue properties rather than bone structure (47). Spaceflight did not affect maximum stress capability of the femur but did decrease the flexural rigidity compared to ground controls (47). There was no change in cortical bone mass, but endocortical bone resorption was decreased along with a trend towards decreased bone formation (47). To test whether changes in bone due to spaceflight exposure could impact ossification of new bone, growing rats were exposed to 11 days of spaceflight. There was no change in the width or longitudinal growth rate of the tibial growth plate (43). Other studies have shown that 16 days of spaceflight decreased mineral content in the distal section of the femur diaphysis, which correlated to reduced *type I collagen* (1). In some of the earliest observations of spaceflight, it was found that after nearly 20 days in space, rats suffered a drastic decrease in periosteal bone formation with no change in bone resorption (36). After 26 days of post-flight, the loss of bone mass was regained (36). This phenomenon was observed in another flight where rats exposed to nearly 19 days of spaceflight experienced an inhibition of periosteal bone formation in the tibial and humeral diaphyses and subsequent correction post-flight (53). These results suggest that spaceflight alters bone remodeling in animal models.

There is a vast amount of individual variation among the data available in human studies because of a relatively small sample size, leaving it difficult to draw definitive conclusions. However, a few patterns remain fairly consistent through the years of human-based spaceflight, namely an increase in bone resorption and decrease in bone formation. In the Mir missions, one cosmonaut experienced a 7.74% decrease in bone

mass of the calcaneus by one month as well as 2.27% in the tibial trabecular bone, as measured by broadband ultrasound attenuation (BUA) (14). After six months exposure to microgravity, another cosmonaut lost 4.5% of trabecular bone and 2.9% of cortical bone in the tibia compared to measurements before launch (14). After six months of return to Earth's gravitational field, there was no difference between pre-flight and post-flight bone mass in the cortical bone and still a 2.55% decrease in the trabecular bone mass, suggesting a site-specific partial recovery (14). Both cosmonauts showed a trend toward decreased bone formation markers, including osteocalcin (OCN), bone alkaline phosphatase (ALP), and the C-terminal peptide of pro-collagen type 1 (PICP) during spaceflight. There was an increase in PICP and a decrease in OCN post-flight (14). Additionally, there was a trend towards an increase in two bone resorption markers during flight (14). One of the Mir missions consisting of four European astronauts showed no change before, during, and after launch in stress-related hormones insulin growth factor 1 (IGF-1) and cortisol in three astronauts while one experienced an increase in cortisol before launch (11). Figure 3.1 shows a summary of bone mineral density (BMD) data for over 17 astronauts in various locations of the skeleton (27). In another study, parathyroid hormone (PTH) decreased during flight compared to pre-flight levels in one astronaut (Figure 3.2). Initially during post-flight, PTH remained within the normal range and then sharply increased for a short time, eventually returning to normal levels. In another astronaut, PTH did not change during flight but increased above normal range after flight and returned to normal levels after one week (11). Additionally, bone resorption can be marked by the breakdown of collagen, including the products N-telopeptide (NTX), pyridinium (PYD), and deoxypyridinoline (DPD). In these astronauts, bone resorption markers were increased, with the exception of pyridinium, during flight compared to pre-flight. These markers decreased post-flight, with the exception of one astronaut who experienced a sharp, unexplainable increase in pyridinium (11). In more

34

Variable	N	%/Month	SD
BMD Spine	18	-1.06*	0.63
BMD Neck	18	-1.15*	0.84
BMD Troch	18	-1.56*	0.99
BMD Total	17	-0.35*	0.25
BMD Pelvis	17	-1.35*	0.54
BMD Arm	17	-0.04	0.88
BMD Leg	16	-0.34*	0.33
Lean Total	17	-0.57*	0.62
Lean Leg	16	-1.00*	0.73
Lean Arm	17	0.00	0.77
Fat Total	17	+1.79	4.66

*p<0.01

Figure 3.1 Average BMD and lean muscle data for over 16 astronauts for various locations of the musculoskeletal system (27).
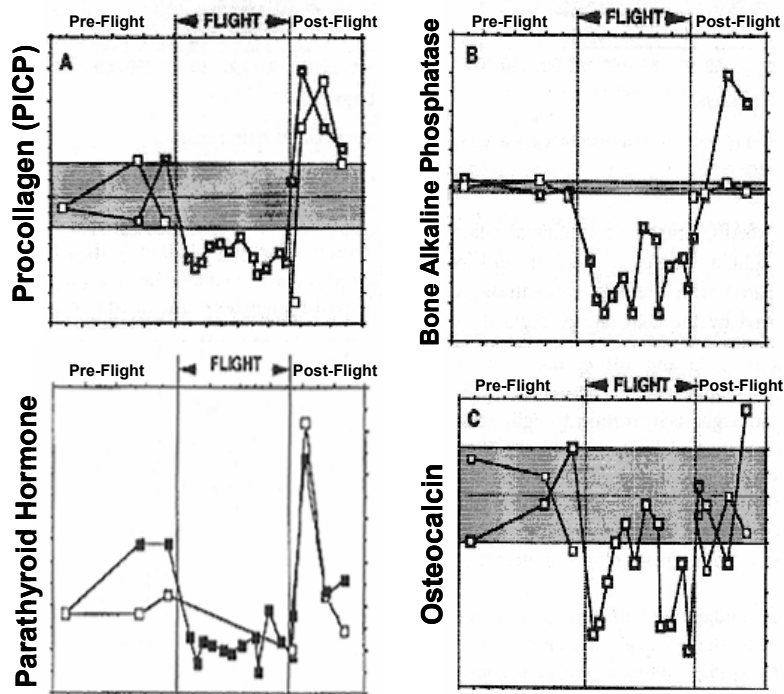
Figure 3.2 Spaceflight decreased various bone formation markers in two astronauts (45).

recent spaceflight missions aboard the International Space Station (ISS), seven of eight cosmonauts experienced decreased BMD in the range of 2.5-10.6% in the lumbar vertebrae. All eight cosmonauts experienced a loss of total BMD in the range of 3-10% in the femur and four of the eight had 1.7-10% loss in the femoral neck (26). In another study on astronauts from the Skylab missions, there was an increase in bone resorption markers due to exposure to spaceflight for 28-84 days. As shown in Figure 3.3, there was a steady increase in urinary excretion of collagen breakdown products during spaceflight and a recovery after landing (45).

N-telopeptide cross-links

Pyridinium (PYD) cross-links

Deoxypyridinoline (DPD) cross links
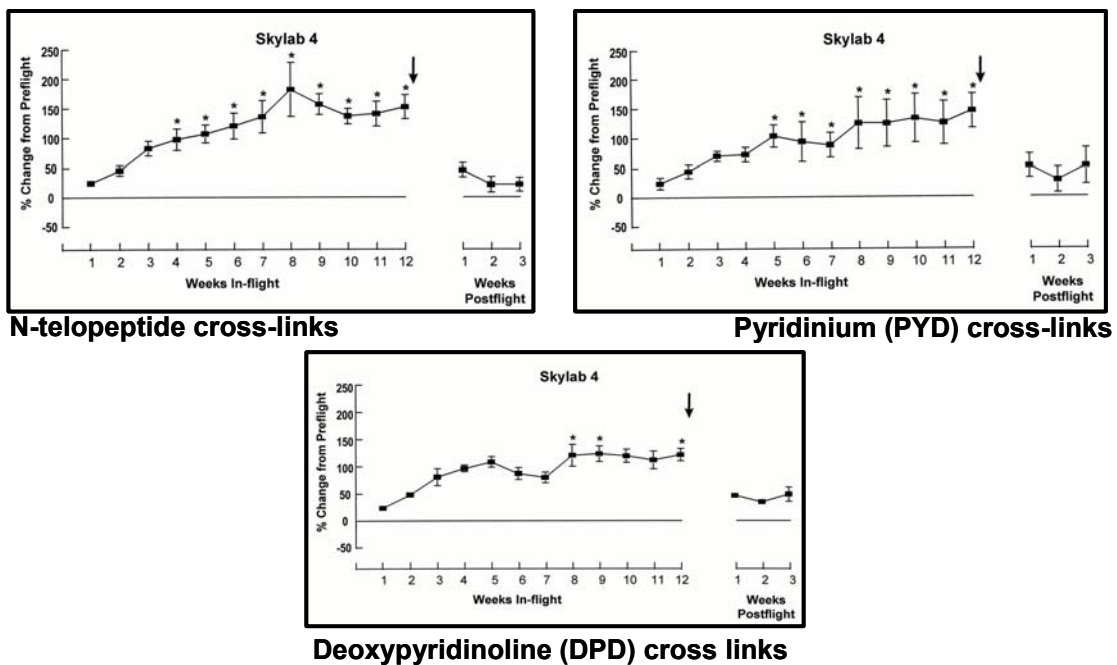
Figure 3.3 Spaceflight increased various bone resorption markers during long term spaceflight missions (45).

While long term spaceflight poses the most imminent danger to astronauts, some short term spaceflight missions have also induced changes in skeletal remodeling. A mission of 8-15 days induced a 3% decrease in the lumbar vertebrae BMD while the

BMD increased in the calvarius post-flight compared to pre-flight (32). Both astronauts experienced urinary calcium excretion after flight compared to pre-flight, which eventually corrected itself, but calcium regulators such as PTH, calcitriol, and calcitonin did not change (32). Elevated bone resorption markers were observed in the urine, and bone formation, as marked by total and bone-specific ALP, decreased in both astronauts one week after flight (32). There was no significant change in total BMD over the whole body by x-ray measurements in both astronauts, but a trend towards a decrease in lumbar spine and increase in the calvarius BMD were observed (32). Perhaps, these observations could be due to redistribution of bone formation due to microgravity and may be related to the cephalic fluid shift associated with spaceflight.

These reported results suggest that regardless of significant individual variability in the astronauts' physiological response to microgravity, there is a pattern of an increase in bone resorption and a decrease in bone formation, leading to site-specific loss of bone mineral density.

Bed Rest Studies

Bed rest studies are currently the only human-based ground analog to microgravity. Subjects are required to remain in bed at a 6-degree head-down tilt from weeks to months in time. Subjects perform all daily functions including eating and sleeping in bed, and cameras are placed in discreet places to ensure that subjects do not deviate from the protocol.

A potential countermeasure for microgravity-induced alterations in the cardiovascular system consists of treadmill exercise in a lower body negative pressure (LBNP) chamber. A LBNP environment creates a hypergravity load on the lower body, causing both mechanical and cardiovascular adaptation, and it is used to simulate orthostatic stress by unloading of the arterial and cardiopulmonary baroreceptors (9).

This countermeasure has recently been evaluated on bone response in identical twins. In one study using male identical twins, collagen cross-links and serum and urinary calcium concentrations, both measurements marking bone resorption, increased during 30 days of bed rest in non-exercise control subjects compared to the LBNP group as shown in Figure 3.4 (44). There was a smaller increase in pyridinium collagen cross-links above pre-bed rest levels in the LBNP group compared to the increase in the control group. In this study, there was no change in the markers of bone formation in both groups (44). They concluded that LBNP exercise partially mitigated bone loss as marked by decreased bone resorption (44). In a follow up study, female identical twins were subjected to similar conditions. Bone resorption markers were excreted in both control and LBNP groups throughout the 30 days of bed rest, and bone formation markers showed either no significant change or a tendency towards decreased expression (60). The exercise group showed less urinary calcium and helical peptide excretion than the control group, and the BMD in the femoral shaft and total hip was not different in the exercise group after bed rest compared to their pre-bed rest values while the control group had decreased BMD (60). Therefore, LBNP had a smaller protective effect on bone mass loss in women than men, signifying that the impact of disuse may be gender-specific. In another study, ten healthy males were exposed to 35 days of bed rest and five additional males were control subjects. In this study, subjects experienced decreased muscle strength in the knee and hip, and bed rest caused atrophy in the extensor muscles of the gluteus, thigh, calf, and knee. Bone density was decreased in the proximal tibia and was not recaptured after four weeks of recovery time that included exercise. However, muscle mass and strength was partially recovered by exercise after four weeks (4).
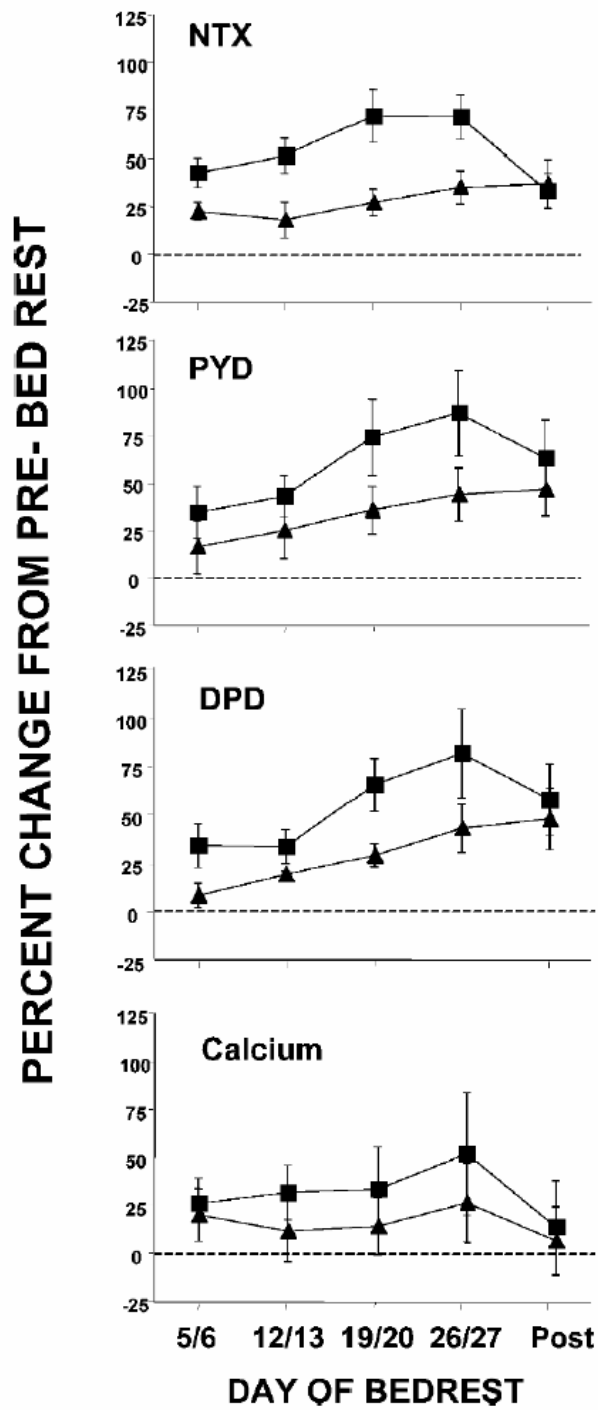
Figure 3.4 Effects of bed rest and LBNP on urinary excretion of bone resorption markers after 30 days exposure. Bed rest control (square) group showed higher levels of excretion than LBNP (triangle) group (44).

In comparison to spaceflight, mineral loss and regional bone loss is similar in both environments. As bone is lost, there is a risk of kidney stones from the increased urinary calcium excretion in both bed rest and spaceflight (23). The headward shift of blood and other fluids mimics the puffy faces seen in spaceflight, and after approximately one day, the body adapts to the increased volume by increased urination, as also observed in spaceflight. Additionally, bed rest subjects develop a mild vertigo, causing nausea and dizziness. Spaceflight microgravity is known to alter the neurovestibular system, where sensors in the ears and nerves in the soles of the feet are unbalanced, causing nausea and dizziness (23).

Hindlimb Unloading (HLU)

The rodent hindlimb unloading (HLU) animal model has been used to partially mimic aspects of microgravity exposure such as removal of skeletal weight-bearing loads and cephalic fluid shift. The hindlimbs are unloaded while the forelimbs remain physiologically loaded and used as internal controls. The head-down tilt from raising the hindlimbs provides the cephalic fluid shift, mimicking the situation observed in spaceflight. The HLU system applies minimal stress on the animal as noted by normal weight gain and eating habits of acclimated animals compared to controls (34).

One HLU study showed a small increase in serum calcium and a decrease in 1,25-dihydroxyvitamin D, and the levels returned to control after 5-15 days of unloading (19). There was no change in PTH in the serum in response to unloading (17, 19). The changes in fat-free bone mass depended on the type of bone, where unloading reduced the weights of both the tibia and vertebrae in the lumbar spine but not the humerus or vertebrae of the cervical spine (18). These findings suggest a decrease in calcium content of the bone (18, 49), and the mineralized matrix of the unloaded bones appeared to be more immature than control bones based on density-gradient fractionation studies

(5). The decrease in bone mass was most likely due to a combination of changes in both bone formation and bone resorption. An indicator of bone formation is the radius of the periosteum, and this marker decreased with HLU. However, in these HLU studies, the radius of the endosteum did not change, marking the absence of a change in bone resorption (17, 48). HLU decreased the number of osteoblasts in the metaphysis of the tibia after five days, but this change was normalized by 14 days (19, 29, 52). Subsequently, there was a decrease in trabecular bone volume by 14 days of HLU in multiple independent studies as represented in Figure 3.5 (8, 19, 30, 50, 52). These data suggest that HLU-related changes in rodents are partially due to changes in osteoblast function. However, after 14 days of unloading, there was no change in ALP activity (29), but the mRNA levels for *transforming growth factor β-2 (TGFβ2), insulin-like growth factor 2 (IGF2),* and *osteopontin (OPN),* all markers of bone formation, decreased in an independent study (58). There have been conflicting reports regarding HLU effects on osteoclast regulation and activity, depending on animal weight changes. If there was no difference between control and HLU animal weight, there was no change in bone resorption (19, 28, 30). However, if there was a change in weight, osteoclast activity increased (49, 50, 52).

Taken together, despite the variability among independent studies, these data show a pattern of bone loss induced by animal HLU. Comparison with spaceflight data shows that the HLU model causes skeletal changes similar to spaceflight, with few differences (6, 7, 50). The model is most accurate and useful in studying the response of bone in short duration spaceflight. Spaceflight and HLU both decrease bone strength (31, 46), and reloading triggers bone formation rates to return to control both after stimulus exposure. Additionally, the model induces a similar cephalic fluid shift as observed in spaceflight. Although there is a significant similarity in the functional and

41

structural changes in spaceflight and in HLU, it is important to note that spaceflight

unloads the entire body whereas this model only unloads the hindlimbs (34, 35).
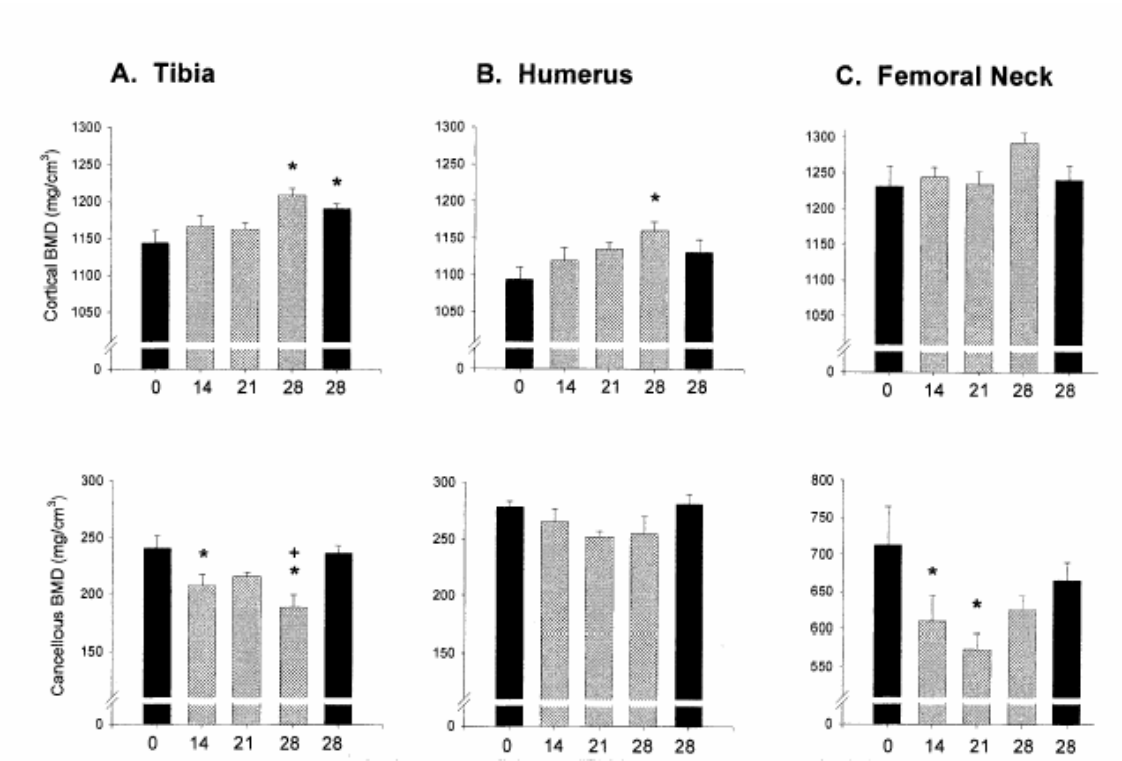
Figure 3.5 Effects of HLU on BMD in the cortical and trabecular (cancellous) bone in the tibia (A), humerus (B), and femoral neck (C). *HLU (gray bar) significant compared to 0 day control (black bar), +HLU (gray bar) significant compared to 28 day control (black bar) (8)

Clinostats

A clinostat is a device that rotates around at least one axis with a platform that

has a small enough radial distance to minimize centrifugal forces. Gravity still exists

around the clinostat, but the gravity vector relative to the biological specimen on the

clinostat is changing directions with the rotation. Over time, the gravity vector averages

to a net zero force (20, 22), a method called gravity-vector averaging.   The Random

Positioning Machine (RPM) and the Rotating Wall Vessel (RWV) are the two most commonly utilized clinostats for ground-based studies.

Both the RWV (38, 40, 51, 57) and the RPM (37, 39, 40) have been previously used by various groups to assess the effects of microgravity or disuse on bone cells as well as on other cells and tissue constructs. Various markers of bone formation have been assessed using the two simulators, including *ALP*, *osteocalcin* (*OCN*), matrix mineralization, and *runt homology domain transcription factor* (*runx2*). *ALP*, *OCN*, and matrix mineralization have been shown to decrease after exposure to the RWV in primary mouse calvariae (57), and *ALP*, *runx2*, and *OCN* decreased in human mesenchymal stem cells (hMSC), MC3T3 mouse pre-osteoblasts, and 2T3 mouse pre-osteoblasts compared to static controls (38, 40, 57). In contrast, in ROS.SMER #14 rat osteoblast cells, RWV induced an increase in *ALP* and *OCN* expression (41), signifying the dependence of clinostat results on species and cell type. Many of these results are comparable to findings obtained with the three dimensional (3D) clinostat. For example, *ALP*, *runx2*, and mineralization have been shown to decrease with exposure to the 3D clinostat compared to static controls as represented in Figure 3.6 (37, 39, 56). There are a limited number of studies on bone resorption and clinostats. One study exposed preosteoclasts to the RPM and found an increase in apoptosis and differentiation into osteoclast-like cells due to RPM exposure compared to static control (33). Using reverse transcriptase polymerase chain reaction (RTPCR), they found elevated expression of osteoclast markers, including receptor activator of the nuclear factor κB (RANK) and its ligand (RANKL) (33).

Despite conflicting results, these studies show that the ground-based simulators closely mimic changes observed in astronauts after spaceflight by showing an inhibition of osteoblast differentiation and matrix mineralization and increased differentiation into osteoclast-like cells. These investigations partially validate the use of the clinostat

43

experimental systems for studying changes associated with the exposure to microgravity. In general, accumulated knowledge from spaceflights and experiments on Earth demonstrate certain patterns of skeletal tissue response to real and modeled microgravity that constitute a specific bone loss phenotype, implying possible changes at the genomic level.

(Bar: 100 μm)
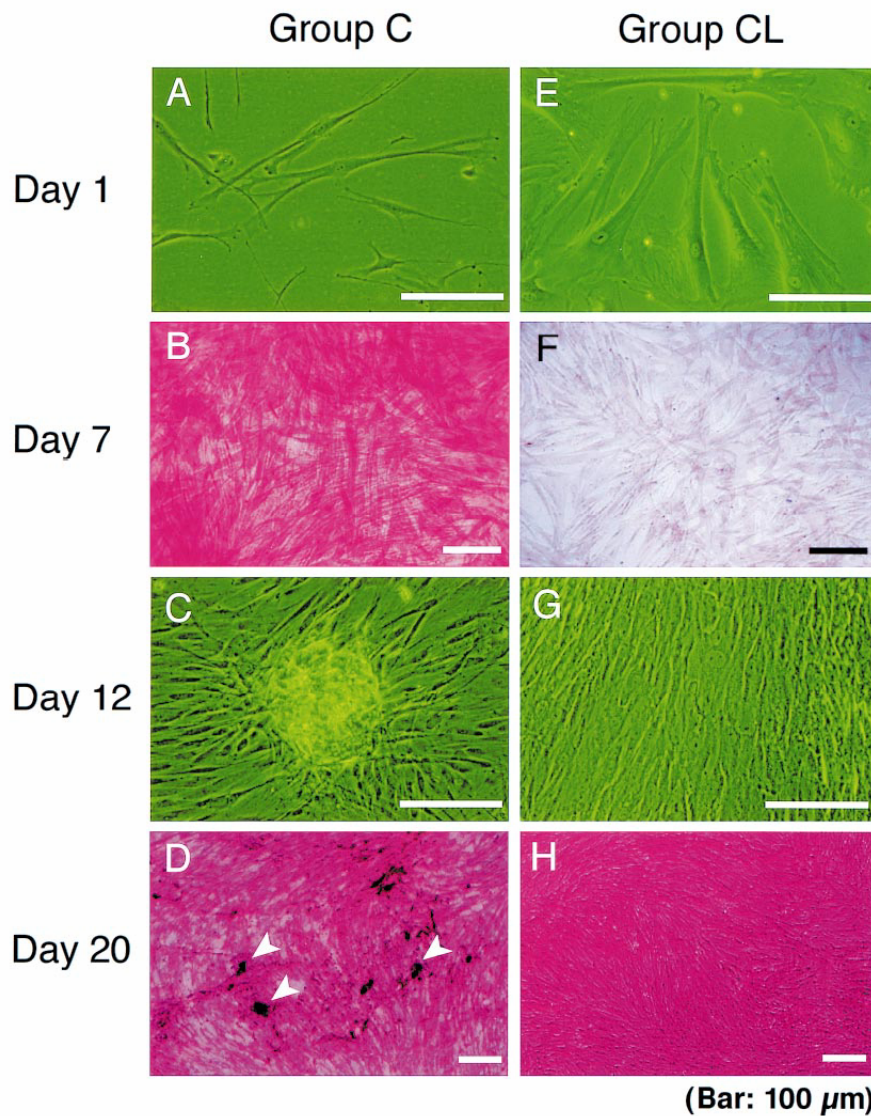
Figure 3.6 The 3D clinostat (Group CL) decreased ALP and mineralized nodules compared to control (Group C) in human osteoblasts. Cells were enlarged and bulged in the clinostat group (E vs A) on day 1, and bone nodules formed by day 12 in the control (C and D) but not clinostat group (G and H). ALP activity was detected by day 7 in control (B) but not in the clinostat group (F) until day 20 (H) (56).

Alterations in Gene Expression in Microgravity or Disuse

Spaceflight

Although it is extremely difficult to design and conduct gene expression studies on humans and animals in space, there is some evidence of gene alterations in animal and cell culture after spaceflight. However, there has been no large-scale gene expression study performed on samples from spaceflight exposure.

In animal studies, after 11 days of spaceflight, there was a significant reduction in the mRNA levels for *aggrecan* and a trend towards reduced *type II collagen*, both members of the skeletal extracellular matrix, in rat tibia (43). Additionally, spaceflight transiently increased mRNA expression of *IGF-1, insulin-like growth factor receptor 1 (IGF-1R), ALP,* and decreased *OCN* (7). The rise in *ALP* countered with the decrease in *OCN* may suggest decreased bone maturation over time. The changes in *IGF-1* and its receptor may indicate compensation by the animal to decreased bone formation. Here, the authors concluded that spaceflight altered the pattern of gene expression in rat, resulting in a less mature genomic profile (7). In an independent spaceflight study, after ten days of exposure, there was no change in ribosomal RNA or *glyceraldehyde-3-phosphate dehydrogenase* (*GAPDH*), and after four days, there was decreased *actin* in the muscles of growing rats (2). In the long bone and calvarial periosteum, both four day and ten day spaceflight decreased *OCN* and *type I pro-collagen* (2). In another spaceflight study for 14 days, there was a decrease in mRNA levels for *GAPDH* and *OCN* in the proximal metaphysis and in *osteonectin* and *type I collagen* in the distal and proximal metaphysis compared to ground controls (16). There was no change in any of these proteins in the diaphysis or distal epiphyses (16). This study shows that spaceflight induces a decrease in bone formation markers in a site-specific manner.

In cellular studies, MC3T3 preosteoblast cells were exposed to spaceflight for nine days and examined for the effects of microgravity with or without a centrifugal 1g

field on the expression of 24 genes (21). In this study, there was a significant reduction in expression of genes such as *cyclooxygenase 2 (cox-2), TGFβ1, fibroblast growth factor 2 (fgf-2),* apoptosis regulators *bcl2* and *bax*, *proliferating cell nuclear antigen (PCNA), OCN, cpla2,* and *c-myc* compared to ground controls (21). An in-flight control was used to investigate the ability of a 1g field to normalize the changes in gene expression, and *c-myc, cox-2, TGFβ1, bcl2, bax,* and *fgf-2* were normalized after 1g exposure (21). Spaceflight did not alter *cyclin A, cyclin E, actin, 18s,* or *fibronectin* (21). In another study, MG-63 osteosarcoma cells flown for nine days showed no change in total protein or DNA content in ground unit-gravity, in-flight 1g gravity, or microgravity groups. With vitamin D and TGFβ2 treatment, cells showed a reduced response to in ALP activity increase in microgravity compared to ground controls, and microgravity did not affect the response of type I collagen protein production to vitamin D and TGFβ2 treatments. However, there was decreased gene expression of *type 1 collagen*, *ALP*, and *OCN* genes with the largest change in the *OCN* gene (13). Perhaps most interesting, this study showed the time-dependent sequence of protein expression, where type I collagen production occurred before ALP activity and then was trailed by moderate OCN expression. Additionally, the study found that gene expression for *ALP* and *OCN* preceded protein changes; however, conflicting results were found for *type I collagen* message and protein levels (12, 13). These data suggest that differentiation is thwarted by microgravity as matrix maturation leads into matrix mineralization.

These investigations highlight the vast number of changes induced by spaceflight in the genetic profiles of the skeleton and bone cells. Perhaps, it would be useful to further explore these changes to advance our knowledge of the mechanisms underlying bone loss in spaceflight microgravity.

Hindlimb Unloading (HLU) and Mechanical Loading

The HLU system is a widely accepted model of animal-based simulated microgravity. To date, there has not been a large scale gene expression study performed from bones of animals exposed to HLU. However, there have been a limited number of small scale studies investigating specific gene expression. After four days of HLU of BALB mice, two independent studies found decreased expression of *type I collagen, osteonectin, osterix,* and *matrix metalloproteinase 2 (MMP-2)* (24, 59). In the Judex, et al. study, each of these genes was corrected to the level of control by day 21 of HLU, and there was no change observed in *cathepsin K (ctsk)* and *runx2* expression (24). Moreover, Zhong, et al. showed that *ALP* expression decreased in BALB mice after four days of HLU exposure (59).

Mechanical loading to the skeleton is beneficial to maintain musculoskeletal health. Various types of loading have been applied to animal models, and gene expression was evaluated. In the Judex, et al. study, HLU-exposed mice were treated with a low magnitude and high frequency (LMHF) mechanical load. LMHF mechanical loading increased gene expression of *inducible nitric oxide synthase (iNOS), MMP-2*, and *RANKL* after 21 days of treatment (24). These evaluated genes are involved in bone remodeling. For example, *RANKL* is expressed by osteoblasts and is essential for osteoclastogenesis. *RANKL* attaches to the *RANK* receptor expressed on osteoclasts to stimulate cell proliferation and differentiation to begin bone resorption (3). In another study, mechanical loading by four-point bending was applied in the tibia of mice at 9 Newtons and 2 Hz, simulating loading incurred during exercise. After four days of exposure to mechanical loading, RNA was extracted from the loaded region, and DNA microarrays were used to evaluate gene expression (55). Many osteogenic genes were increased in expression due to mechanical loading, such as *pleiotrophin*, *osteoglycin (OGN),* and *legumain*.

Although no systemic gene evaluation data is available, smaller scale studies provide evidence that there are molecular alterations *in vivo* caused by simulated microgravity or disuse. Additionally, mechanical loading ranging from low impact to high impact has also been shown to alter gene expression. These studies suggest that molecular changes may be pertinent in the development of adequate countermeasures for bone loss due to disuse, microgravity, or osteoporosis.

Clinostats

The RPM and RWV have been used for small scale studies evaluating alterations in gene expression of bone cells. There are conflicting data regarding RWV effects on *ALP* mRNA and activity. Rucci, et al. found that *ALP* mRNA and activity expression increased when exposed to the RWV for two days using a rat osteoblast-like cell line that was grown in aggregate suspension (41). In contrast, Klement, et al. showed that exposure to the RWV for up to 14 days blunted ALP activity and bone matrix mineralization of mouse embryonic pre-metatarsal tissue explants (25). Similarly, Patel, et al. showed a decrease in *ALP* mRNA and activity after three days of exposure to the RWV (40). Additionally, an independent study using MC3T3-E1 preosteoblasts found that expression of *runx2* and downstream target genes *OCN* and *type I collagen* did not change while *ALP* was decreased in cells exposed to simulated microgravity for five days (10). In another study, the RWV had no effect on *ALP, runx2, OCN*, *OPN,* or *type 1collagen* mRNA expression (42). In human osteoblasts, exposure to the 3D clinostat blunted expression of both *cbfa1/runx2* (Figure 3.7) and *OCN* (56).

Additionally, it is known that the mitogen activated protein kinase (MAPK) pathway regulates *runx2* and the expression of its target genes *type I collagen* and *OCN* (54). A limited number of studies that have examined the effects of the simulators on MAPK, but the data are conflicting. The 3D clinostat and the RWV both did not alter c-

jun N-terminal kinase (JNK) phosphorylation (42, 56, 57), and the 3D clinostat inhibited

p38 phosphorylation (Figure 3.8) (56) while the RWV enhanced it (57) or did not alter it

(42). The RWV has been shown to enhance extracellular signaling-regulated kinase

(ERK) activity (42) and to repress it (57) while the 3D clinostat did not alter it (56). As

well, *TGFβ1* expression was downregulated by the RWV, comparable to spaceflight data,

but it was upregulated by the RPM. *Prostaglandin E1 (EP1)* was not altered in

spaceflight, corroborating with the RPM data, but the RWV upregulated its expression

(21, 39, 40). In another study, *AKT* and *ERK 1/2* were decreased after three days of

clinostat exposure (15). Additionally, growth factors, including *IGF1* and *basic*

fibroblastic growth factor (bFGF), stimulated bone marrow stem cell proliferation in

control conditions but only had a moderate effect under simulated microgravity (15).

These data suggest that there is likely an inhibitory effect induced by the clinostat

simulators of microgravity or disuse on osteoblast function depending on culture

conditions, recapitulating a bone loss phenotype similar to spaceflight. Despite apparent

differences among experiments due to distinct simulators, cell type, or culture conditions

used, these ground-based systems allow for molecular studies utilizing gene

manipulation.

Conclusion and Future Directions: Possible Impact of Gene Expression Studies on Countermeasure Development

In general, the reviewed studies from spaceflight, HLU studies, and clinostat

investigations confirmed that there is a certain pattern of genomic response to

microgravity or disuse that could create a foundation for development of molecular-

based countermeasures. Studies in animal and cellular models indicate the significance
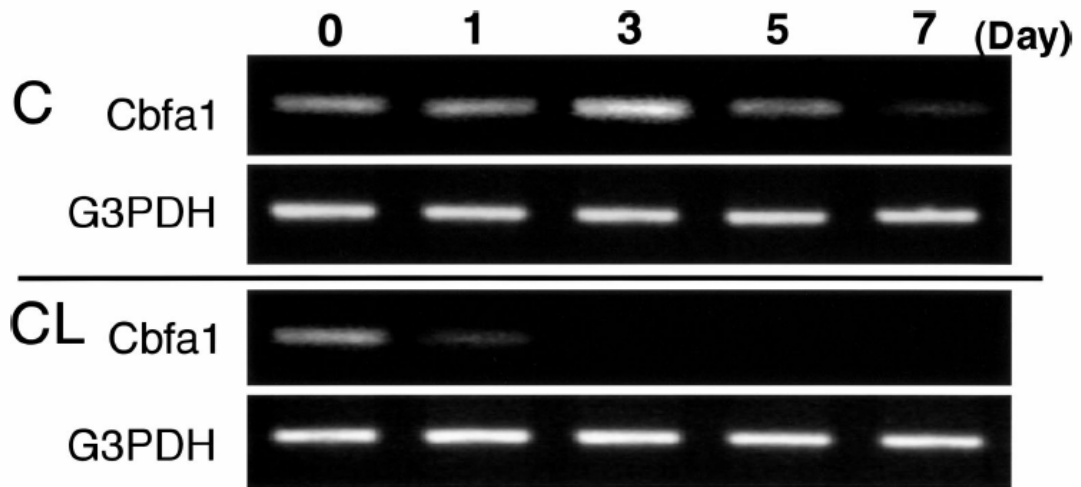
Figure 3.7 The 3D clinostat (Group CL) decreased cbfa1/runx2 compared to control (Group C) in human osteoblasts (56).
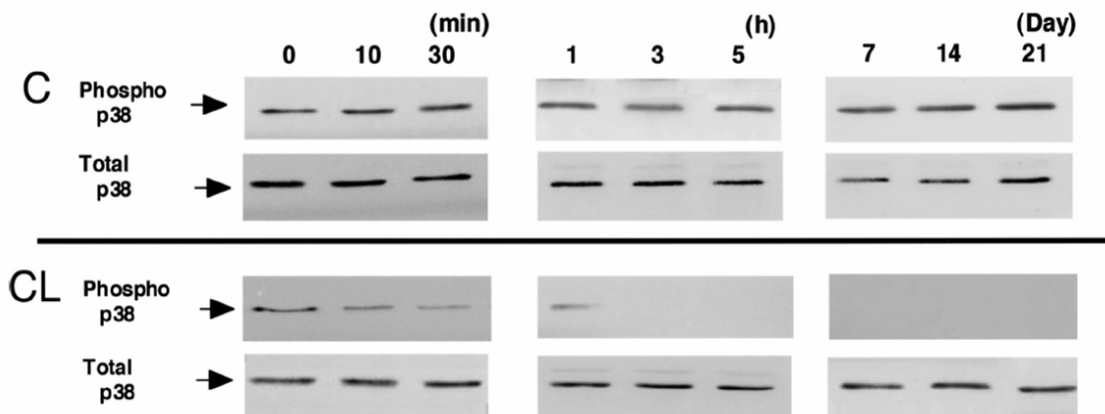
Figure 3.8 The 3D clinostat (Group CL) decreased p38 compared to control (Group C) in human osteoblasts (56).

of the gravitational vector and gravity sensing for cellular regulatory processes involving the genomic level. This is likely due to specific conditions of the evolution of life on Earth. It is perhaps these gravity-sensitive regulatory processes and genes that should be used as potential molecular targets for future therapeutic interventions to mitigate bone loss in astronauts. Although data from the different astronauts are not completely consistent, patterns have emerged depicting an obvious bone loss phenotype. Despite almost 50 years of human-based spaceflight, there is still no effective countermeasure available, hindering the possibility of pursuing longer term spaceflight mission such as those to Mars. It seems convincing that current studies investigating the molecular changes induced by spaceflight and ground-based simulators will provide targets for therapeutic interventions to mitigate bone loss in spaceflight, disuse, and osteoporosis. In the next decade, targeting molecular changes induced by microgravity or disuse could provide new, exciting, and feasible molecular countermeasures for bone loss.

References

1. **Arnaud SB, Buckendahl P, Durnova G, Bromage T, and Yamauchi M.** Bone biochemistry in rat femoral diaphysis after space flight. *J Gravit Physiol* 7: 7-15, 2000.

2. **Backup P, Westerlind K, Harris S, Spelsberg T, Kline B, and Turner R.** Spaceflight results in reduced mRNA levels for tissue-specific proteins in the musculoskeletal system. *Am J Physiol* 266: E567-573, 1994.

3. **Bell NH.** RANK ligand and the regulation of skeletal remodeling. *J Clin Invest* 111: 1120-1122, 2003.

4. **Berg HE, Eiken O, Miklavcic L, and Mekjavic IB.** Hip, thigh and calf muscle atrophy and bone loss after 5-week bedrest inactivity. *Eur J Appl Physiol* 99: 283-289, 2007.

5. **Bikle DD, Halloran BP, Cone CM, Globus RK, and Morey-Holton E.** The effects of simulated weightlessness on bone maturation. *Endocrinology* 120: 678-684, 1987.

6. **Bikle DD, Halloran BP, and Morey-Holton E.** Spaceflight and the skeleton: lessons for the earthbound. *Gravit Space Biol Bull* 10: 119-135, 1997.

7. **Bikle DD, Harris J, Halloran BP, and Morey-Holton E.** Altered skeletal pattern of gene expression in response to spaceflight and hindlimb elevation. *Am J Physiol* 267: E822-827, 1994.

8. **Bloomfield SA, Allen MR, Hogan HA, and Delp MD.** Site- and compartment-specific changes in bone with hindlimb unloading in mature adult rats. *Bone* 31: 149-157, 2002.

9. **Brown CM, Hecht MJ, Neundorfer B, and Hilz MJ.** Effects of lower body negative pressure on cardiac and vascular responses to carotid baroreflex stimulation. *Physiol Res* 52: 637-645, 2003.

10. **Bucaro MA, Zahm AM, Risbud MV, Ayyaswamy PS, Mukundakrishnan K, Steinbeck MJ, Shapiro IM, and Adams CS.** The effect of simulated microgravity on osteoblasts is independent of the induction of apoptosis. *J Cell Biochem* 102: 483-495, 2007.

11.   **Caillot-Augusseau A, Lafage-Proust M-H, Soler C, Pernod J, Dubois F, and Alexandre C.** Bone formation and resorption biological markers in cosmonauts during and after a 180-day space flight (Euromir 95). *Clin Chem* 44: 578-585, 1998.

12.   **Carmeliet G and Bouillon R.** The effect of microgravity on morphology and gene expression of osteoblasts in vitro. *FASEB J* 13: 129-134, 1999.

13.   **Carmeliet G, Nys G, and Bouillon R.** Microgravity reduces the differentiation of human osteoblastic MG-63 cells. *J Bone Miner Res* 12: 786-794, 1997.

14.   **Collet P, Uebelhart D, Vico L, Moro L, Hartmann D, Roth M, and C A.** Effects of 1- and 6-month spaceflight on bone mass and biochemistry in two humans. *Bone* 20: 547-551, 1997.

15.   **Dai ZQ, Wang R, Ling SK, Wan YM, and Li YH.** Simulated microgravity inhibits the proliferation and osteogenesis of rat bone marrow mesenchymal stem cells. *Cell Prolif* 40: 671-684, 2007.

16.   **Evans GL, Morey-Holton E, and Turner RT.** Spaceflight has compartment- and gene-specific effects on mRNA levels for bone matrix proteins in rat femur. *J Appl Physiol* 84: 2132-2137, 1998.

17.   **Globus RK, Bikle DD, Halloran B, and Morey-Holton E.** Skeletal response to dietary calcium in a rat model simulating weightlessness. *J Bone Miner Res* 1: 191-197, 1986.

18.   **Globus RK, Bikle DD, and Morey-Holton E.** The temporal response of bone to unloading. *Endocrinology* 118: 733-742, 1986.

19.   **Halloran BP, Bikle DD, Wronski TJ, Globus RK, Levens MJ, and Morey-Holton E.** The role of 1,25-dihydroxyvitamin D in the inhibition of bone formation induced by skeletal unloading. *Endocrinology* 118: 948-954, 1986.

20.   **Hoson T.** Evaluation of the three-dimensional clinostat as a simulator of weightlessness. *Planta* 203: S187-197, 1997.

21.   **Hughes-Fulford M, Rodenacker K, and Jutting U.** Reduction of anabolic signals and alteration of osteoblast nuclear morphology in microgravity. *J Cell Biochem*, 2006.

22.   **Huijser RH.** Desktop RPM: New Small Size Microgravity Simulator for the Bioscience Laboratory. Fokker Space, 1-5, 2000.

23.   **Jones N.** Space physiology: lie back and think of science. *Nature* 435: 730-731, 2005.

24.   **Judex S, Zhong N, Squire ME, Ye K, Donahue LR, Hadjiargyrou M, and Rubin CT.** Mechanical modulation of molecular signals which regulate anabolic and catabolic activity in bone tissue. *J Cell Biochem* 94: 982-994, 2005.

25.   **Klement B, Young Q, George B, and Nokkaew M.** Skeletal tissue growth, differentiation and mineralization in the NASA rotating wall vessel. *Bone* 34: 487-498, 2004.

26.   **Kozlovskaya IB and Grigoriev AI.** Russian system of countermeasures on board of the International Space Station (ISS): the first results. *Acta Astronaut* 55: 233-237, 2004.

27.   **LeBlanc A, Schneider V, Shackelford L, West S, Oganov V, Bakulin A, and Voronin L.** Bone mineral and lean tissue loss after long duration space flight. *J Musculoskelet Neuronal Interact* 1: 157-160, 2000.

28.   **Machwate M, Zerath E, Holy X, Hott M, Godet D, Lomri A, and Marie PJ.** Systemic administration of transforming growth factor-beta 2 prevents the impaired bone formation and osteopenia induced by unloading in rats. *J Clin Invest* 96: 1245-1253, 1995.

29.   **Machwate M, Zerath E, Holy X, Hott M, Modrowski D, Malouvier A, and Marie PJ.** Skeletal unloading in rat decreases proliferation of rat bone and marrow-derived osteoblastic cells. *Am J Physiol* 264: E790-799, 1993.

30.   **Machwate M, Zerath E, Holy X, Pastoureau P, and Marie PJ.** Insulin-like growth factor-I increases trabecular bone formation and osteoblastic cell proliferation in unloaded rats. *Endocrinology* 134: 1031-1038, 1994.

31.   **Martin RB.** Effects of simulated weightlessness on bone properties in rats. *J Biomech* 23: 1021-1029, 1990.

32.   **Miyamoto A, Shigematsu T, Fukunaga T, Kawakami K, Mukai C, and Sekiguchi C.** Medical baseline data collection on bone and muscle change with space flight. *Bone* 22: 79S-82S, 1998.

33.   **Monici M, Fusi F, Paglierani M, Marziliano N, Cogoli A, Pratesi R, and Bernabei PA.** Modeled gravitational unloading triggers differentiation and apoptosis in preosteoclastic cells. *J Cell Biochem* 98: 65-80, 2006.

34.   **Morey-Holton ER and Globus RK.** Hindlimb unloading of growing rats: a model for predicting skeletal changes during space flight. *Bone* 22: 83S-88S, 1998.

35.   **Morey-Holton ER and Globus RK.** Hindlimb unloading rodent model: technical aspects. *J Appl Physiol* 92: 1367-1377, 2002.

36.   **Morey ER and Baylink DJ.** Inhibition of bone formation during space flight. *Science* 201: 1138-1141, 1978.

37.   **Nakamura H, Kumei Y, Morita S, Shimokawa H, Ohya K, and Shinomiya K.** Suppression of osteoblastic phenotypes and modulation of pro- and anti-apoptotic features in normal human osteoblastic cells under a vector-averaged gravity condition. *J Med Dent Sci* 50, 2003.

38.   **Ontiveros C, McCabe, Laura R.** Simulated microgravity suppresses osteoblast phenotype, Runx2 levels and AP-1 transactivation. *Journal of Cellular Biochemistry* 88: 427-437, 2003.

39.   **Pardo SJ, Patel MJ, Sykes MC, Platt MO, Boyd NL, Sorescu GP, Xu M, van Loon JJWA, Wang MD, and Jo H.** Simulated microgravity using the Random Positioning Machine inhibits differentiation and alters gene expression profiles of 2T3 preosteoblasts. *Am J Physiol Cell Physiol* 288: C1211-1221, 2005.

40.   **Patel MJ.** Identification of Mechanosensitive Genes in Osteoblasts by Comparative Microarray Studies Using the Rotating Wall Vessel and the Random Positioning Machine. *Journal of Cellular Biochemistry* 101: 587-599, 2007.

41.   **Rucci N, Migliaccio S, Zani BM, Taranta A, and Teti A.** Characterization of the osteoblast-like cell phenotype under microgravity conditions in the NASA-approved Rotating Wall Vessel bioreactor (RWV). *J Cell Biochem* 85: 167-179, 2002.

42.   **Rucci N, Rufo A, Alamanou M, and Teti A.** Modeled microgravity stimulates osteoclastogenesis and bone resorption by increasing osteoblast RANKL/OPG ratio. *J Cell Biochem* 100: 464-473, 2007.

43.   **Sibonga JD, Zhang M, Evans GL, Westerlind KC, Cavolina JM, Morey-Holton E, and Turner RT.** Effects of spaceflight and simulated weightlessness on longitudinal bone growth. *Bone* 27: 535-540, 2000.

44.   **Smith SM, Davis-Street JE, Fesperman JV, Calkins DS, Bawa M, Macias BR, Meyer RS, and Hargens AR.** Evaluation of treadmill exercise in a lower body negative pressure chamber as a countermeasure for weightlessness-induced bone loss: a bed rest study with identical twins. *J Bone Miner Res* 18: 2223-2230, 2003.

45.   **Smith SM, Nillen JL, Leblanc A, Lipton A, Demers LM, Lane HW, and Leach CS.** Collagen cross-link excretion during space flight and bed rest. *J Clin Endocrinol Metab* 83: 3584-3591, 1998.

46.   **Vailas AC, Zernicke RF, Grindeland RE, Kaplansky A, Durnova GN, Li KC, and Martinez DA.** Effects of spaceflight on rat humerus geometry, biomechanics, and biochemistry. *Faseb J* 4: 47-54, 1990.

47.   **Vajda EG, Wronski TJ, Halloran BP, Bachus KN, and Miller SC.** Spaceflight alters bone mechanics and modeling drifts in growing rats. *Aviat Space Environ Med* 72: 720-726, 2001.

48.   **van der Meulen MC, Morey-Holton ER, and Carter DR.** Hindlimb suspension diminishes femoral cross-sectional growth in the rat. *J Orthop Res* 13: 700-707, 1995.

49.   **Vico L, Bourrin S, Very JM, Radziszowska M, Collet P, and Alexandre C.** Bone changes in 6-mo-old rats after head-down suspension and a reambulation period. *J Appl Physiol* 79: 1426-1433, 1995.

50.   **Vico L, Novikov VE, Very JM, and Alexandre C.** Bone histomorphometric comparison of rat tibial metaphysis after 7-day tail suspension vs. 7-day spaceflight. *Aviat Space Environ Med* 62: 26-31, 1991.

51.   **Ward NE, Pellis NR, Risin SA, and Risin D.** Gene expression alterations in activated human T-cells induced by modeled microgravity. *J Cell Biochem*, 2006.

52.   **Wronski TJ and Morey-Holton ER.** Skeletal response to simulated weightlessness: a comparison of suspension techniques. *Aviat Space Environ Med* 58: 63-68, 1987.

53.   **Wronski TJ and Morey ER.** Effect of spaceflight on periosteal bone formation in rats. *Am J Physiol* 244: R305-309, 1983.

54.   **Xiao G, Jiang D, Thomas P, Benson MD, Guan K, Karsenty G, and Franceschi RT.** MAPK pathways activate and phosphorylate the osteoblast-specific transcription factor, Cbfa1. *J Biol Chem* 275: 4453-4459, 2000.

55.   **Xing W, Baylink D, Kesavan C, Hu Y, Kapoor S, Chadwick RB, and Mohan S.** Global gene expression analysis in the bones reveals involvement of several novel genes and pathways in mediating an anabolic response of mechanical loading in mice. *Journal of Cellular Biochemistry* 9999: n/a, 2005.

56.   **Yuge L, Hide I, Kumagai T, Kumei Y, Takeda S, Kanno M, Sugiyama M, and Kataoka K.** Cell differentiation and p38(MAPK) cascade are inhibited in human osteoblasts cultured in a three-dimensional clinostat. *In Vitro Cell Dev Biol Anim* 39: 89-97, 2003.

57.   **Zayzafoon M, Gathings WE, and McDonald JM.** Modeled microgravity inhibits osteogenic differentiation of human mesenchymal stem cells and increases adipogenesis. *Endocrinology* 145: 2421-2432, 2004.

58.   **Zhang R, Supowit SC, Klein GL, Lu Z, Christensen MD, Lozano R, and Simmons DJ.** Rat tail suspension reduces messenger RNA level for growth factors and osteopontin and decreases the osteoblastic differentiation of bone marrow stromal cells. *J Bone Miner Res* 10: 415-423, 1995.

59.   **Zhong N, Garman RA, Squire ME, Donahue LR, Rubin CT, Hadjiargyrou M, and Judex S.** Gene expression patterns in bone after 4 days of hind-limb unloading in two inbred strains of mice. *Aviat Space Environ Med* 76: 530-535, 2005.

60.   **Zwart SR, Hargens AR, Lee SM, Macias BR, Watenpaugh DE, Tse K, and Smith SM.** Lower body negative pressure treadmill exercise as a countermeasure for bed rest-induced bone loss in female identical twins. *Bone* 40: 529-537, 2007.

Chapter 4

The Effects of Disuse on Osteoblast Gene Expression*

Summary

The goals of specific aim 1 are to determine the effects of simulated microgravity or disuse using the Random Positioning Machine (RPM) on 2T3 pre-osteoblast function, creating an *in vitro* system that can recapitulate the effects of spaceflight microgravity on bone formation. An *in vitro* system would provide the means to study the cellular and molecular alterations caused by disuse, potentially yielding molecular targets for pharmaceutical treatments for bone loss. To achieve this aim, we investigated the effects of disuse on preosteoblast cells by evaluating various bone formation markers and, for the first time, systemic gene expression through microarrays.

Exposure to microgravity causes bone loss in humans, and the underlying mechanism is believed to be at least partially due to a decrease in bone formation by osteoblasts. Here, we examined the hypothesis that microgravity alters osteoblast gene expression profiles, resulting in decreased bone formation. For this study, we developed an *in vitro* system that simulates microgravity or disuse conditions using the RPM to study the effects of disuse on 2T3 preosteoblast cells grown in gas-permeable culture disks. Exposure of 2T3 cells to the RPM for up to nine days significantly inhibited alkaline phosphatase activity (ALP) and up to 15 days blunted mineralization, recapitulating a bone loss response as seen in spaceflight. Next, we carried out gene expression analysis using DNA microarrays to determine gene expression profiles of

2T3 cells exposed to the RPM for three days. Among 10,000 genes examined with the microarray, 88 were downregulated while 52 were upregulated significantly by disuse by more than two-fold in comparison to the static 1g control conditions. We then verified the microarray data for select genes relevant in bone biology by using real time RTPCR assays and immunoblotting. We confirmed that microgravity downregulated levels of *ALP*, *runt-related transcription factor 2 (runx2)*, *osteomodulin (OMD)*, and *parathyroid hormone receptor 1 (PTHR1)* mRNA, upregulated *cathepsin K (ctsk)* mRNA, and did not significantly affect *bone morphogenic protein 4 (BMP4)* and *cystatin C* protein levels. The identification of these mechanosensitive genes provides useful insight in generating further hypotheses regarding their roles not only in microgravity-induced bone loss but also in the general population of patients with similar pathologic conditions such as osteoporosis.

Introduction

Musculoskeletal pathologies such as osteoporosis and muscular dystrophy affect millions of Americans. Bone loss incurred by osteoporosis, disuse, or microgravity renders the skeleton at risk for bone fractures. The underlying mechanisms regulating bone formation are still largely unknown. Additionally, there is an increasing interest for manned space exploration, including extensive trips to deep space planets such as Mars. Microgravity conditions in space have been shown to cause decreased bone mass (6, 7, 10, 16), bone demineralization (8, 35, 38), skeletal muscle atrophy (20, 25), cardiovascular deconditioning (2, 39), and immune dysfunction (32). Many of these pathological changes cannot yet be counteracted adequately by physical exercise (20) or nutritional supplementation alone (7, 13, 36). Therefore, it is imperative to understand the mechanisms of microgravity-induced pathologies so that manned space exploration can continue with minimal negative effects on astronauts. Furthermore, the knowledge

of the mechanisms inducing spaceflight-dependent bone loss may also provide insight into the understanding of pathologies occurring in the general population, including osteoporosis and muscle atrophy.

Unfortunately, it is difficult and impractical to conduct well controlled and large numbers of *in vitro* studies in a microgravity environment due to the limited and expensive nature of spaceflight missions. Thus, to investigate pathologies that occur during spaceflight, several ground-based systems, including the 2D and 3D clinostats and the Rotating Wall Vessel (RWV), have been developed to simulate microgravity or disuse using cultured cells and tissues (1, 21, 26, 31). The RPM is a 3D clinostat that simulates disuse by continuously moving the gravity vector relative to the cells in three dimensions before the cells have enough time to sense it, which is a method called gravity-vector averaging (14, 15).

Previous studies have indicated that spaceflight-induced bone loss may be due in part to decreased osteoblastic function with or without enhancing osteoclastic bone resorption (9). Simulated microgravity has been shown to inhibit markers of bone formation such as ALP activity and *runx2* expression (26, 43). While these studies examined only a few candidate genes that are likely to be involved in bone mass regulation, systematic and unbiased characterization of gene expression profiles scanning the majority of genes has not been carried out. Here, we hypothesized that bone loss due to simulated microgravity or disuse is due to an inhibition of preosteoblast differentiation and alterations of gene expression critical in maintaining bone formation.

To test this hypothesis, we have 1) developed and characterized an *in vitro* cell culture system using 2T3 preosteoblast cells exposed to simulated microgravity or disuse conditions produced by the RPM, 2) examined cell proliferation, ALP activity, and mineralization of 2T3 cells, 3) performed gene expression analysis using DNA

microarrays, and 4) validated the microarray data using quantitative real time RTPCR and immunoblotting.

Methods

Cell culture–2T3 murine osteoblast precursor cells were kindly provided to us by Dr. Xu Cao at the University of Birmingham in Alabama (41). The cells were cultured in growth medium (α-minimal essential medium) containing 10% fetal bovine serum (Atlanta Biologicals) with 100 units/ml of penicillin and 100µg/ml of streptomycin in a standard humidified incubator (37°C, 5% CO2). For mineralization experiments, the growth medium was supplemented with ascorbic acid (50 µg/ml) and β-glycerolphosphate (5 mM) with or without BMP2 or BMP4 (0-50 ng/ml)

Seeding cells in OptiCells–Confluent 2T3 cells grown in T-75 flasks were trypsinized using 0.05% Trypsin/EDTA (Sigma), and two million cells were seeded into a gas-permeable cell culture disk (OptiCell) according to the manufacturer's instructions. As shown in Figure 1A, an OptiCell disk is a sealed cell culture disk encapsulated by two optically clear and gas-permeable polystyrene membranes containing two ports, which allow access to the contents of the disk. The internal disk dimensions are 74.8 x 65 x 2.06 mm, and it can be filled with 10 to 14 ml of medium. To seed cells on each membrane of the Opticell, the disks were turned over every five minutes for one hour after seeding. Cells were allowed to grow for three days to confluency in 14 ml of growth medium before exposure to the stimulus, and the day on which the OptiCells were mounted on the RPM was referred to as Day 0. On Day 0, the medium was changed with 14 ml of fresh growth medium, and air bubbles were removed to prevent potentially uncharacterized mechanical perturbation during RPM exposure.

Random Positioning Machine–A desktop RPM described by Huijser (17) and manufactured by Fokker Space was used to simulate microgravity or disuse conditions. As shown in Figure 1B, the dimensions of the entire RPM are 30x30x30 cm with an inner and outer frame creating a cargo volume of 150 mm^3. The OptiCell disks were mounted on the center of the platform located on the inner frame, and a maximum of eight disks were used in each experiment. The RPM was operated in random modes of speed and direction (0.1-2 radians/second) via a computer user interface with dedicated control software inside a humidified incubator (5% CO2 at 37°C). Under this experimental condition, the cells were exposed to the RPM with a range of 0 to 0.01g centrifugal forces (17). For static 1g controls, OptiCell disks seeded concurrently with the RPM group were placed in the same incubator as the RPM. Samples were harvested at Days 0, 1, 3, 5, 7 and 9. For a three day experiment, the Opticells were exposed to the RPM without interruption as there was no media change necessary over this period. However, for experiments longer than three days, the medium was changed every three days (Days 3 and 6) by stopping the RPM for approximately 20 minutes before restarting it.

Cell proliferation assay–To determine cell proliferation, attached cells were collected by trypsinization after experimental treatments. Cell number was determined using an aliquot of cell suspension and a Coulter counter.

Whole cell lysate and alkaline phosphatase (ALP) enzyme activity–After collecting the culture medium following the experiment, cells were scraped in 500 µl of lysis buffer containing 0.2% NP-40 in 1 mM MgCl2 and stored at -80°C until needed. ALP activity was determined using a Diagnostics ALP assay kit (Sigma) according to the manufacturer's instructions (28). Aliquots of lysate (20 µl) and p-nitrophenol standard

(Sigma) were used for the assay. ALP enzyme activity was normalized to total protein content as determined by a Biorad-DC protein assay and expressed in international enzyme activity units (µmol/min/mg protein).
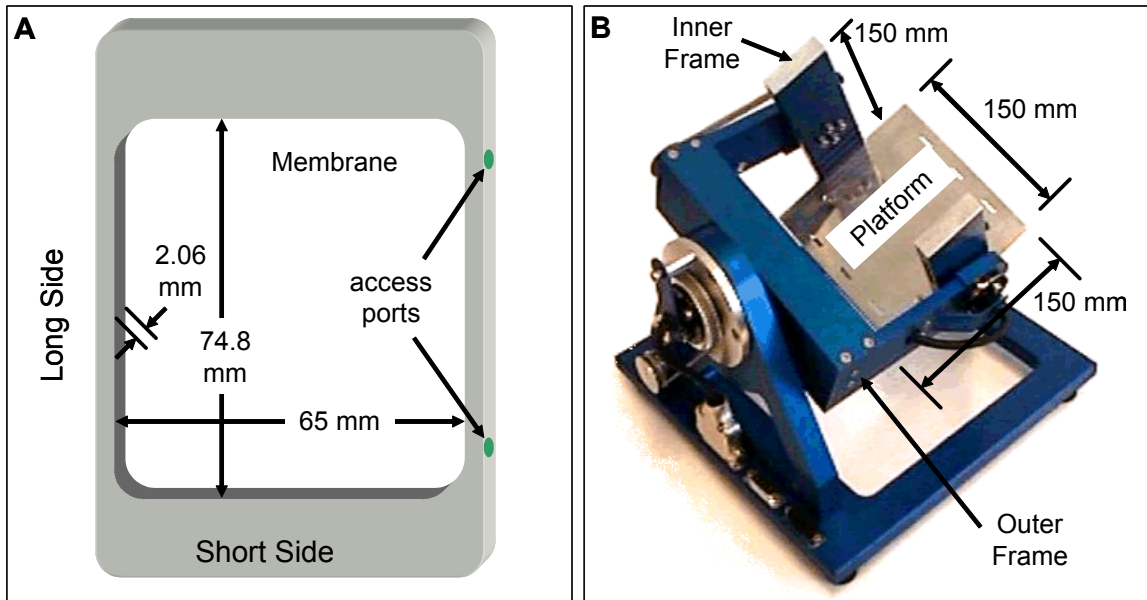
Figure 4.1 *In vitro* **simulated microgravity or disuse conditions using 2T3 cells cultured in OptiCell disks and the RPM**

Alizarin Red Stain—Following the experiment, cells were washed with ice-cold PBS two times and fixed in 70% ethanol for 15 minutes. Cultures were stained for two minutes with a 1% Alizarin red solution for calcium detection. Following the stain, cultures were rinsed with a 0.01%HCl-ethanol solution and dH_20. The plates were dried overnight before being scored for percent mineralization using ImageJ analysis software. Quantification graphs express mineralization as a percent of the experimental control.

Codelink Gene Microarrays–Total RNA was isolated from 2T3 cells exposed to RPM or static 1g control conditions for three days using the RNeasy kit (Qiagen), and

experiments were performed in triplicate. The total RNA was reverse transcribed, and the second strand was synthesized using T7 RNA polymerase and biotinylated dNTPs according to Amersham Biosciences instructions (29). Each cRNA preparation was then hybridized to individual Uniset Mouse 1 microarrays (CodeLink) containing synthetic oligonucleotide probes corresponding to 10,000 unique mouse genes in the Amersham Biosciences facility (Piscataway, NJ) (29). The gene expression intensity was determined by using streptavidin-Cy5 conjugated to the biotin. The processed slides were scanned using an Axon GenePix Scanner with CodeLink Expression Scanning Software (29). The fluorescence intensities of individual probes that were above the threshold levels determined by internal controls were considered to be genes expressed by the cells and were further analyzed by the CodeLink Software (Amersham). Using this software, the median intensity of all discovery probes in each microarray was used to normalize the fluorescence intensity of individual gene probes (normalized fluorescence intensity) in order to minimize inter-array variations. The filtered and normalized data were statistically analyzed by the Student's t-test, and the genes that changed in response to the RPM by more than two-fold above or below the static 1g controls with p-values of less than 0.05 were deemed considerable and significant. GoMiner software (http://www.miblab.gatech.edu/gominer) was used to sort the genes by biological processes and to assign some of the functions of each known gene (44). The entire RPM microarray can be accessed from Gene Expression Omnibus (GEO) with accession numbers GDS928 or GSE1367.

Reverse Transcriptase and Real-Time Polymerase Chain Reaction (RTPCR)—Total RNA was prepared by using the RNeasy Mini Kit (Qiagen) and reverse transcribed by using random primers and a Superscript-II kit (Life Technology) (33). The synthesized and purified cDNA was amplified using a LightCycler (Roche Applied Science), and the

size of each PCR product was verified by agarose gel electrophoresis as described by us (33). The mRNA copy numbers were determined based on standard curves generated with the genes of interest and *18S* templates. The *18S* primers (50 nM at 61ºC annealing temperature; Ambion) were used as an internal control for real time RTPCR using capillaries (Roche Applied Science), recombinant Taq polymerase (Invitrogen), and Taq start antibody (Clontech). The primer pairs for the quantitative real time RTPCR are listed in Table 1 along with their annealing temperatures, extension times, and base pair yields. Real-time RTPCR for the listed genes were carried out in PCR buffer (20mM Tris-Cl, pH 8.4, at 25°C, 4mM MgCl2, 250µg/ml bovine serum albumin, and 200µM deoxynucleotides) containing SYBR green (1:84,000 dilution), 0.05unit/µl Taq DNA polymerase, and Taq Start antibody (1:100 dilution) as described previously by us (33).

Table 4.1 List of mouse primers used for quantitative real time RTPCR

Accession #	Gene	Primers (5'-3')		bp	Conditions for LightCycler
NM_007431	*ALP*	Fw	CAGTATGAATTGAATCGGAACAACC	107	7 sec at 62ºC
		Rv	CAGCAAGAAGAAGCCTTTGAGG		6 sec at 72ºC
NM_009820	*runx2*	Fw	GACAGAAGCTTGATGACTCTAAACC	171	7 sec at 62ºC
		Rv	TCTGTAATCTGACTCTGTCCTTGT		9 sec at 72ºC
NM_011199	*PTHR1*	Fw	GCACACAGCAGCCAACATAA	531	7 sec at 63ºC
		Rv	CGCAGCCTAAACGACAGGAA		22 sec at 72ºC
NM_012050	*OMD*	Fw	GACGGGCTGGTGAATGTGACTATGCTTGA	147	7 sec at 63ºC
		Rv	CCAAGGGGCATTGATTCTAATCTGTTATT		10 sec at 72ºC
NM_007802	*ctsk*	Fw	AAGTGGTTCAGAAGATGACGGGAC	342	5 sec at 55ºC
		Rv	TCTTCAGAGTCAATGCCTCCGTTC		13 sec at 72ºC

Immunoblot (Western blot)—Aliquots of cell lysate were resolved on a SDS-PAGE gel and transferred to a polyvinylidene difluoride membrane (Millipore) (4). The membrane was incubated with a primary antibody overnight at 4°C and then incubated with a secondary antibody conjugated with alkaline phosphatase for one hour at room temperature. Expression was detected by a chemiluminescence method and the

intensities of the immunoreactive bands were determined by densitometry (4). Antibodies specific for BMP4 and cystatin C (Santa Cruz Biotechnologies) were used.

Statistical Analysis–Statistical analysis was performed by using the Student's t-test for all experiments. A significance of $p < 0.05$ from three or more independent experiments was considered statistically significant.

Results

Exposure of 2T3 cells to the RPM did not alter cell morphology or proliferation.

To examine the effects of simulated microgravity or disuse on osteoblasts, we developed an *in vitro* system to expose 2T3 cells grown in gas-permeable culture disks (OptiCell) to the RPM. The morphology of 2T3 cells grown in standard tissue culture dishes and OptiCells were indistinguishable (data not shown). When cells grown in OptiCells were exposed to RPM or static 1g conditions, the pH of the medium remained neutral at or near pH 7.4 (data not shown). As shown in Figure 2A, the morphology of 2T3 cells exposed to static 1g control and RPM conditions were not significantly different from each other.

Next, we examined whether RPM exposure induced any changes in 2T3 cell proliferation by using cell count as a marker. For this study, OptiCells were seeded with 2T3 cells, and three days later (Day 0 of the experiment), the cell number reached approximately three million cells per disk (Figure 2B). The cells were fed with fresh medium every three days during the experiment, and they continued to proliferate to a maximum of 13 ± 1.1 million cells (static 1g on Day 7) and 10.8 ± 0.3 million cells (RPM on Day 7), showing no statistical difference between the two groups ($p=0.10$, $n=6$ to 7). The cell number in both groups reached maximum by Day 5 and remained unchanged until Day 7. The static 1g control group showed a decrease in cell number at Day 9, and

66

to determine whether this decrease was due to increased cell detachment, we counted the number of dead cells in the media on Day 9 by trypan blue assay. Although the total number of detached cells tended to be higher in the RPM group (194,250 ± 6,475) than the static group (103,600 ± 33,645), there was no statistically significant difference (p>0.05, n=6). These results suggest that simulated microgravity or disuse does not have a significant effect on cell proliferation.
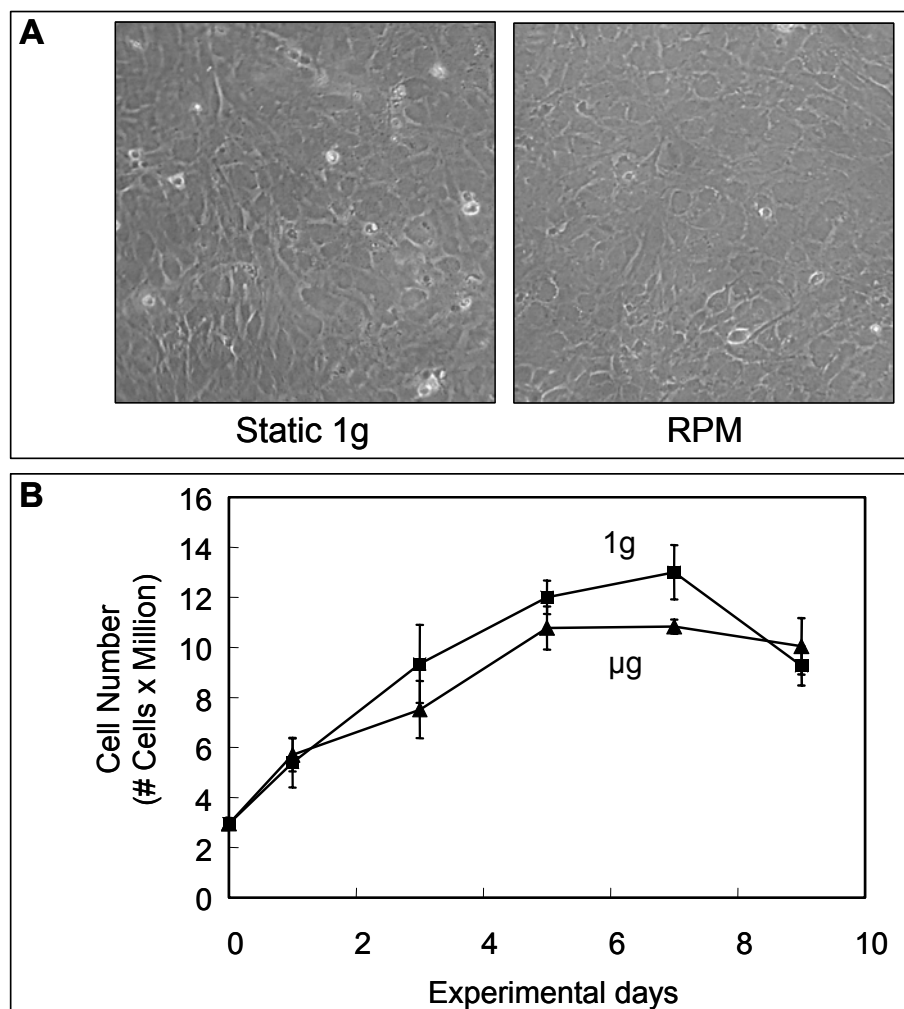
Figure 4.2 Simulated microgravity (μg) or disuse had no significant effect on 2T3 cell morphology and cell number. At Day 0, 2T3 cells grown in OptiCells were placed on the RPM or exposed to the static 1g condition for 1, 3, 5, 7 or 9 days. A phase contrast microscope was used to image cells after the experiment (A), and cell proliferation was assessed by cell number using a Coulter counter. Data are represented as mean ± SEM (n=6, *p<0.05).

2T3 cells experienced low shear stress and strain due to fluid movement caused by the RPM rotation.

The attached cells grown on the OptiCell membranes could be exposed to mechanical forces such as fluid shear stress and strain in addition to disuse during RPM rotation. In order to visualize the dynamics of the fluid within the OptiCell, we marked a disk with a calibrated grid and filled it with water and colored bead markers (density=1.018g/ml, Amersham Biosciences). The beads had a density close to that of water, allowing visualization of potential fluid movement. Short movies were recorded using a digital camera mounted on the RPM to track bead movement over the calibrated grid, and flow velocities, v, were estimated from the recordings. The shear stress, τ, was calculated using Newton's law of viscosity as shown in Equation 4.1:

$$\tau = \mu \left(\frac{v}{h} \right)$$

(4.1)

where, μ is the viscosity of water or growth medium at 37°C (6.92 x 10^{-4} and 7.8 x 10^{-4} kg· m-1 · s^{-1}, respectively) and h is half the height of the fluid within the OptiCell (1.028mm). These calculations suggested that the magnitude of shear stress caused by movement of the growth medium experienced at the membrane was close to 0 dyn/cm^2 for 43 seconds, 0.09-0.22 dyn/cm^2 for 13 seconds, and 0.22-0.44 dyn/cm^2 for 4 seconds during a one minute period of random rotation by the RPM. The maximum shear stress intensity was present at the larger radius of the OptiCell close to the rigid frame while the center portions of the membranes experienced minimum shear stresses.

Due to forces generated during the RPM rotation, cells in this experimental setup may experience mechanical strain. As such, mechanical strain, ε, was calculated using

the 1D wave equation with fixed boundary conditions at both ends of the OptiCell frame. We assumed that the maximum height of the stretched membrane, h, was located at half the membrane length, L. The static solution to this wave equation for the first harmonic with the aforementioned constraints can be described by Equation 4.2:

$$f(x) = h \times \sin\left(\frac{\pi}{2}\frac{x}{L}\right)$$
(4.2)

where f(x) is the assumed shape the membrane takes when filled with 14 ml of medium, h is the differential gap height between the stretched membrane at the center (when filled with medium) and the unstretched membrane (when unfilled), and L is equal to L_{short}, half the length of the membrane's short side, and L_{long}, half the length of the membrane's long side. To determine the length of these arcs, we used the integral formula in Equation 4.3:

$$arc = \int_0^L \sqrt{1 + [f'(x)]^2}\, dx$$
(4.3)

We calculated the arc for the filled OptiCell when the RPM is not rotating, where the height is equal to h (arc_h), and then we calculated the arc at h+Δh ($arc_{h+\Delta h}$), where Δh is the change in gap height due to *additional* membrane stretch occurring during sudden directional changes by the RPM rotation. The strain, ε, of the membrane along the short and long sides was calculated using Equation 4.4:

$$\varepsilon = \frac{arc_{h+\Delta h} - arc_h}{arc_h}$$
(4.4)

This calculation suggests that the maximum microstrain occurs at the center of the longer side of the membrane with a magnitude less than 200 microstrains. Although we

have not determined the time-dependent changes in the strain history, we assume that the maximum strain occurs only briefly during sudden directional changes of the RPM.

Exposure of 2T3 cells to the RPM inhibited ALP activity and mineralization.

Since ALP activity and mineralization are established indicators of osteoblast differentiation and bone mass formation (40), we determined whether exposing 2T3 cells to disuse using the RPM inhibited these markers. As shown in Figure 4.3A, ALP activity increased during culture as expected. ALP activity of static 1g control cells dramatically increased by more than eight-fold within two days of culture (Day 1 to 3). By Day 5, ALP activity in control cells reached maximum (24 ± 1 µmol/min/mg protein), which remained maximum at Day 7. In contrast, exposure of 2T3 cells to the RPM significantly blunted the culture time-dependent increase in ALP activity (Figure 4.3). Unlike the static 1g control group, ALP enzyme activity of the RPM group at Day 3 did not increase significantly above the Day 1 level. By Day 9, ALP activity increased by four-fold above the Day 1 level. As shown in Figure 4.3, ALP enzyme activity of the static 1g group was 2.7 times higher than that of the RPM group at Day 9. An additional group of cells was exposed to the RPM for three days and restored to static 1g conditions for the remainder of the experiment. As expected, the ALP activity of the restored group continued to increase to levels between the static 1g and RPM groups. Additionally, as depicted in Figure 4.3B and D, the RPM inhibited mineralization after 15-16 days of exposure even in the presence of BMP4 or BMP2. This finding that simulated microgravity or disuse significantly decreases ALP activity and mineralization is consistent with the inhibitory effects of spaceflight and disuse on osteoblast differentiation and bone formation.
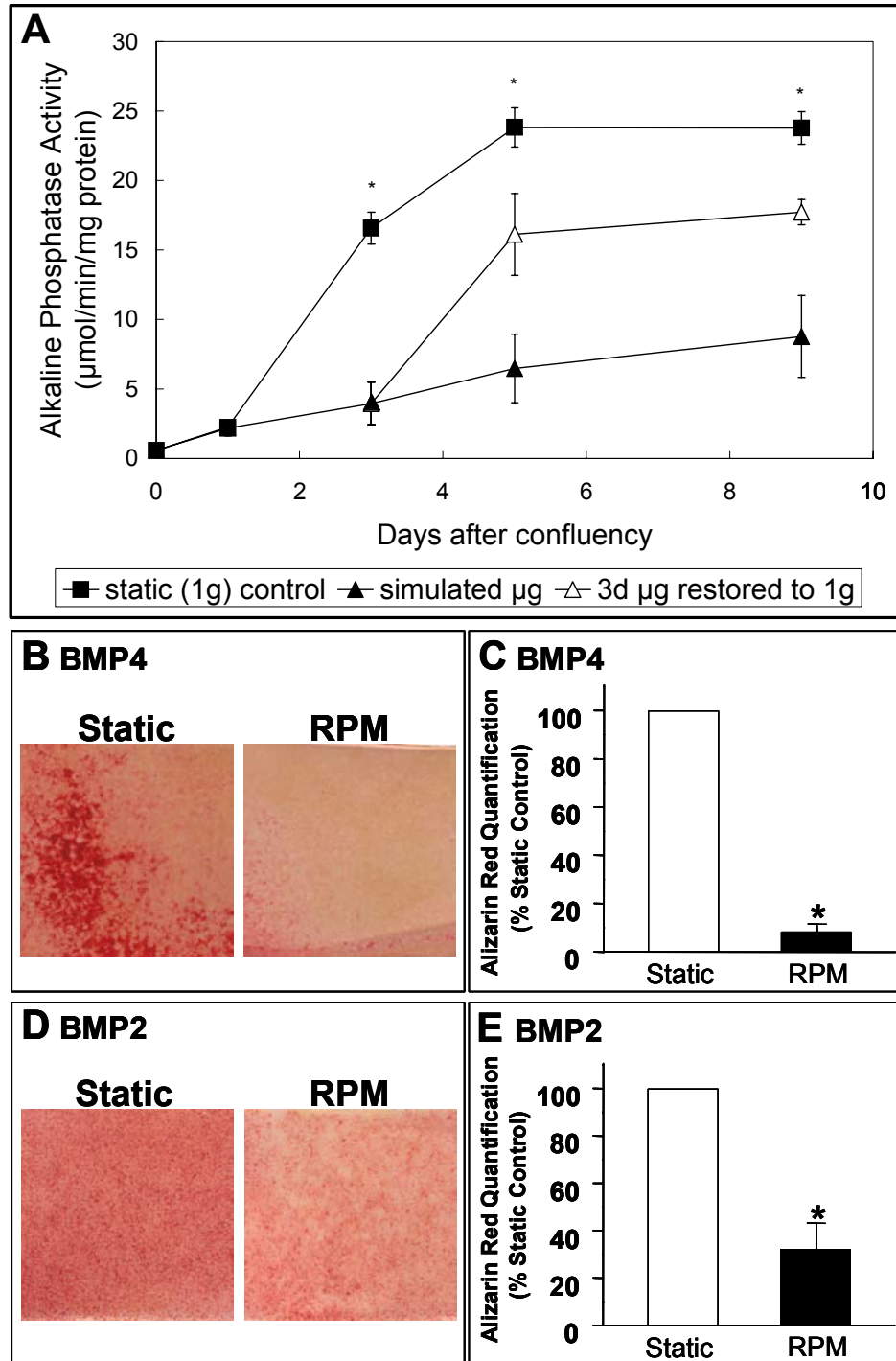
Figure 4.3 The RPM inhibited ALP activity and mineralization of 2T3 cells. Three days after seeding (on Day 0), 2T3 cells were exposed to the RPM or static 1g conditions for 1, 3 , 5 and 9 days. ALP activity in the cell lysate was determined by a colorimetric Sigma assay and graphed as averaged ALP activity normalized to total protein. For mineralization studies, cells were exposed to the RPM for 15-16 days and treated with BMP4 or BMP2 to support mineralization. Cultures were stained with Alizarin Red for calcium detection. Data are shown as mean ± SEM (n=6-10, * $p < 0.05$ between Static and RPM groups).

The RPM altered gene expression profiles of 2T3 cells as determined by microarray studies.

By performing microarray studies, we analyzed the global changes in gene expression profiles of 2T3 cells when exposed to simulated microgravity or disuse conditions. Among 10,000 genes examined with the microarray, only 88 were downregulated and 52 upregulated to statistically significant levels (p<0.05) by more than two-fold in comparison to the static 1g control level. Figure 4.4 shows a scatter plot of the averaged microarrays for both the RPM (μg) and static 1g control groups where each dot represents one gene. The diagonal line represents no change in expression due to RPM exposure (fold change=1), and genes upregulated by the RPM are above the diagonal while genes downregulated by the RPM are below the diagonal line. A heat map was generated (Figure 4.5) representing the data as low gene intensity (green) to high gene intensity (red). The genes are identified by their accession number (accn #) and sorted based on fold changes induced by the RPM (μg 1-3) when compared to static 1g conditions (st 1-3). Table 2 categorizes genes with known functions from the microarray study that were upregulated or downregulated by the RPM significantly (p<0.05) by more than two-fold above the static 1g control. Since these genes are sorted based on typical cell function using the GoMiner program, genes with unknown functions were not included in this analysis. Table 3 shows genes that have potential involvement in osteoblast differentiation and matrix mineralization regardless of the two-fold change threshold.

Many osteoblast genes that have been shown to be relevant in bone formation were influenced by simulated microgravity or disuse. *ALP*, a known marker for bone formation, was downregulated by the RPM by five-fold below the static 1g control. *Runx2*, a master transcription factor regulating osteocalcin levels, was downregulated by 1.88-fold by the RPM when compared to static 1g. *PTHR1*, which acts directly on the

72
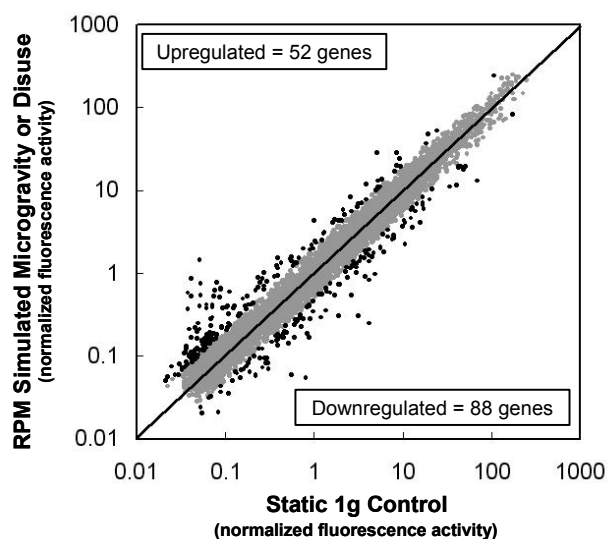
Figure 4.4 Scatter plot of gene expression profiles of 2T3 cells after exposure to RPM or static 1g control conditions. Total RNA was isolated from 2T3 cells exposed to the RPM or static 1g conditions for three days. For each group (n=3 RPM and static 1g), the RNA was reverse transcribed and hybridized to probes on Codelink microarrays corresponding to 10,000 mouse genes. Gene expression was determined by fluorescence intensity, and the scatter plot shows mean values of each gene as a single dot. Genes changed by the RPM are shown in black relative to the diagonal line and unchanged genes in gray.

skeleton to promote Ca2+ release from bone and on the kidney to enhance calcium reabsorption, was downregulated by five-fold by the RPM. In contrast, inducers of osteolytic activity were also upregulated by the RPM. For example, *ctsk* was upregulated by 1.66-fold above the static 1g control.

Although the fold changes for *runx2* and *ctsk* fall slightly below the two-fold change threshold for significance, these genes were included in the analysis because of their established relevance in bone formation and resorption. These results are consistent with the notion that disuse decreases the expression of genes necessary for differentiation, matrix formation, and subsequent mineralization while increasing the expression of genes that trigger osteoclast activity.

accn #	st1 st2 st3 µg1 µg2 µg3	fold Δ	accn #	st1 st2 st3 µg1 µg2 µg3	fold Δ
NM_009115		0.09	NM_010551		0.46
NM_012050		0.18	NM_026131		0.46
NM_011606		0.19	AK013035		0.47
NM_011199		0.20	AK003918		0.47
AK014166		0.20	W53823		0.47
NM_007431		0.21	NM_026486		0.47
AF064749		0.21	NM_013888		0.48
NM_030127		0.22	NM_010358		0.48
NM_053078		0.24	NM_011817		0.48
NM_008604		0.24	NM_010222		0.49
NM_008524		0.26	NM_020010		0.49
NM_010753		0.26	NM_010846		0.49
NM_007884		0.27	AK017193		0.49
NM_011253		0.27	AK013793		0.49
NM_008196		0.28	NM_021515		0.49
NM_025711		0.28	NM_010368		0.49
NM_011338		0.29	NM_011985		0.49
NM_007729		0.29	NM_019517		0.50
NM_020568		0.31	AF321817		2.00
NM_013456		0.31	NM_008654		2.00
AK017110		0.31	NM_019553		2.01
M58755		0.32	NM_008723		2.01
AF309508		0.33	NM_025640		2.01
NM_008185		0.34	AK011383		2.01
NM_013641		0.34	AK010437		2.02
NM_009128		0.35	NM_009138		2.04
NM_007934		0.35	NM_019425		2.04
NM_009964		0.35	NM_026631		2.04
AK005141		0.35	AK018113		2.08
NM_010941		0.37	NM_011710		2.08
NM_010357		0.37	NM_008361		2.10
AK010249		0.37	AJ002730		2.11
NM_013584		0.37	AK009010		2.14
NM_015744		0.38	NM_012006		2.17
AB040819		0.38	NM_011361		2.17
NM_009155		0.38	AK013772		2.18
NM_011058		0.38	NM_033320		2.18
NM_016911		0.38	NM_008987		2.20
NM_010354		0.38	NM_008462		2.21
NM_008760		0.38	NM_013525		2.20
NM_016867		0.38	NM_020562		2.20
AK017798		0.38	NM_009052		2.25
NM_009921		0.39	NM_008519		2.28
NM_019521		0.39	NM_010415		2.28
NM_009073		0.39	AK011873		2.30
AK002518		0.39	NM_015774		2.30
NM_010315		0.40	NM_010235		2.33
AK018128		0.40	AK008546		2.33
NM_010255		0.41	NM_011670		2.35
AK004002		0.41	NM_030556		2.35
NM_009144		0.41	NM_011433		2.36
NM_010497		0.41	AK010138		2.37
AF422245		0.41	NM_007703		2.38
AK008108		0.41	NM_007836		2.40
NM_016894		0.42	NM_029292		2.44
NM_007763		0.42	NM_026633		2.44
NM_012043		0.42	AK002480		2.49
AK018504		0.43	NM_009635		2.59
NM_008599		0.43	NM_013490		2.60
AK004556		0.43	NM_009943		2.67
NM_018887		0.43	NM_026626		2.77
NM_009923		0.44	AB059565		2.80
NM_016757		0.44	AK007530		2.86
NM_008492		0.44	AK006554		2.89
NM_021472		0.45	NM_016660		3.06
NM_008976		0.45	AK011900		3.18
AK004179		0.45	NM_020013		3.22
NM_054077		0.45	NM_007823		3.93
BC005529		0.45	NM_009731		4.41
NM_026428		0.46	NM_009802		5.57

Figure 4.5 The effects of the RPM on gene expression profiles of 2T3 cells. The heat map was generated by converting the fluorescent intensities of the 140 significantly changed genes to corresponding pseudo-colors. The pseudo-color bar represents data as low gene intensity (green), no change (yellow), and high gene intensity (red). The genes are identified by their accession number (accn #) and sorted based on fold changes induced by the RPM (µg 1-3) when compared to static 1g conditions (st 1-3).

Table 4.2 A list of selected mechanosensitive genes in 2T3 cells. Genes are sorted based on typical cell functions.

Accession #	Gene Name	Fold Δ	SEM	p-value	Molecular Function
Cell Adhesion					
NM_012050	osteomodulin	0.184	± 0.031	<0.01	aka osteoadherin, may mediate cell attachment
AF064749	collagen, type VI, alpha 3	0.213	± 0.012	<0.05	extracellular matrix structural constituent
NM_007729	procollagen, type XI, alpha 1	0.292	± 0.013	<0.025	extracellular matrix structural constituent
NM_008462	killer cell lectin-like receptor, subfamily A, member 2	2.202	± 0.311	<0.05	binding and signal transducer activity
Cell Cycle					
NM_011817	growth arrest and DNA damage inducible, gamma (GADD45G)	0.485	± 0.081	<0.025	structural constituent of ribosome
NM_021515	adenylate kinase 1	0.490	± 0.042	<0.025	nucleobase, nucleoside, nucleotide kinase activity
NM_008654	myeloid differentiation primary respose gene 116 (MYD116)	2.004	± 0.187	<0.025	myeloid differentiation primary response gene induced by IL6
NM_007836	growth arrest and DNA damage inducible 45 alpha (GADD45A)	2.405	± 0.193	<0.025	structural constituent of ribosome
Development					
NM_009964	crystalline, alpha B	0.351	± 0.061	<0.05	chaperone and heat shock protein activity
NM_009144	secreted frizzled-related sequence protein 2	0.409	± 0.009	<0.005	transmembrane receptor and signal transduction activity
Metabolism					
NM_007431	alkaline phosphatase 2, liver	0.210	± 0.017	<0.01	essential for hydroxyapatite formation and matrix mineralization
NM_008196	granzyme K	0.279	± 0.014	<0.025	hydrolase and peptidase activity
M58755	glucokinase	0.318	± 0.017	<0.01	hexokinase activity
NM_009128	stearoyl-coenzyme A desaturase 2	0.347	± 0.050	<0.01	metal_ion_binding and oxidoreductase activity
NM_007934	glutamyl aminopeptidase	0.350	± 0.042	<0.005	metalloexopeptidase activity
NM_010941	NAD(P) dependent steroid dehydrogenase-like	0.367	± 0.021	<0.025	oxidoreductase activity, acting on CH-OH group of donors
NM_015744	ectonucleotide pyrophosphatase/phosphodiesterase 2	0.376	± 0.087	<0.025	hydrolase activity
NM_010255	guanidinoacetate methyl transferase	0.406	± 0.069	<0.05	methyltransferase activity
NM_018887	cytochrome p450, 39A1	0.435	± 0.051	<0.05	oxidoreductase activity
NM_008976	protein tyrosine phosphatase, non-receptor type 14	0.451	± 0.034	<0.01	phosphoric monoester hydrolase activity
NM_020010	cytochrome p450, 51	0.486	± 0.011	<0.025	oxidoreductase activity
NM_019425	glucosamine-phosphate N-acetyltransferase 1	2.041	± 0.077	<0.01	transferase activity
NM_012006	cytosolic acyl-coA thioesterase 1	2.165	± 0.175	<0.025	CoA hydrolase activity
NM_033320	glucuronyl c5 epimerase	2.184	± 0.105	<0.025	racemase and epimerase activity, acting on carbohydrates
NM_007703	cig30 or (FEN1/ELO2, SUR4/ELO3, yeast)-like 3 (ELOVL3)	2.377	± 0.157	<0.025	involved in a pathway connected with brown fat hyperplasia
NM_009943	cytochrome C oxidase, subunit VI A, polypeptide 2	2.669	± 0.199	<0.01	oxidoreductase activity, acting on heme group of donors
NM_007823	cytochrome P450, subfamily IV B, polypeptide 1	3.925	± 0.241	<0.005	oxidoreductase activity
NM_009802	carbonic anhydrase 6	5.571	± 1.077	<0.05	carbon-oxygen lyase and hydro-lyase activity

Table 4.2-*Continued*

Accession #	Gene Name	Fold Δ	SEM	p-value	Molecular Function
Protein Metabolism					
NM_010222	*FK506 binding protein 7*	0.485	0.073	<0.05	peptidyl-prolyl cis-trans isomerase activity
NM_011985	*matrix metalloproteinase 23*	0.493	0.009	<0.025	metalloendopeptidase activity
NM_011710	*tryptophanyl-TRNA synthetase*	2.080	0.085	<0.025	ligase activity, forming phosphoric ester & carbon-oxygen bonds
NM_011361	*serum/glucocorticoid regulated kinase*	2.169	0.014	<0.005	serine/threonine kinase activity
NM_015774	*ERO1-LIKE*	2.305	0.108	<0.01	unknown
NM_011670	*ubiquitin carboxy-terminal hydrolase L1*	2.354	0.423	<0.05	thiolester hydrolase activity
Stress or Immune Response					
NM_010357	*glutathione S-transferase, α4*	0.368	0.046	<0.05	transferase activity, transferring alkyl or aryl groups
NM_008599	*small inducible cytokine B subfamily, member 9*	0.430	0.069	<0.025	G-protein-coupled receptor binding activity
NM_010358	*glutathione S-transferase, µ1*	0.482	0.085	<0.05	transferase activity, transferring alkyl or aryl groups
AF321817	*LPTS1*	2.001	0.293	<0.05	nucleic acid binding activity
NM_009635	*advillin*	2.588	0.308	<0.025	structural constituent of cytoskeleton
Sensory Perception					
NM_009073	*rod outer segment membrane protein 1 (ROM1)*	0.390	0.172	<0.05	G-protein-coupled photoreceptor activity
Signal Transduction					
NM_011338	*small inducible cytokine A9*	0.287	0.046	<0.005	G-protein-coupled receptor binding activity
NM_013641	*prostaglandin E receptor 1*	0.338	0.026	<0.005	transmembrane and G-protein-coupled receptor activity
AB040819	*RAC3*	0.377	0.012	<0.05	GTPase activity
NM_011058	*platelet derived growth factor receptor, alpha polypeptide*	0.378	0.025	<0.025	transmembrane receptor protein tyrosine kinase activity
NM_010315	*guanine-nucleotide binding protein, gamma 2 subunite*	0.404	0.041	<0.05	heterotrimeric G-protein GTPase activity
NM_016894	*RAMP1*	0.418	0.047	<0.025	coreceptor, soluble ligand activity
NM_009138	*small inducible cytokine A25*	2.038	0.117	<0.01	G-protein-coupled receptor binding activity
NM_008519	*leukotriene B4 receptor*	2.276	0.092	<0.025	rhodopsin-like transmembrane receptor activity
Skeletal Development					
NM_011199	*parathyroid hormone receptor*	0.198	0.010	<0.005	transmembrane receptor activity
NM_011606	*tetranectin*	0.187	0.027	<0.025	binds to plasminogen, may regulate matrix mineralization
NM_054077	*proline arginine-rich end leucine-rich repeat*	0.453	0.037	<0.005	extracellular matrix structural constituent
Transcription					
NM_010753	*max dimerization protein 4 (MAD4)*	0.261	0.058	<0.025	transcription regulator activity
NM_010497	*isocitrate dehydrogenase 1 (NAP+), soluble*	0.409	0.094	<0.025	oxidoreductase activity, acting on CH-OH group of donors
NM_010235	*FOS-like antigen 1*	2.328	0.199	<0.025	DNA binding activity
NM_016660	*high mobility group protein I*	3.060	0.442	<0.025	DNA binding activity

Table 4.3 The effect of the RPM on selected genes that may be involved in osteoblast differentiation and matrix mineralization. Genes are sorted based on fold changes.

Accession #	Gene Name	Fold Δ	SEM	p-value.	Molecular Function
NM_012050	Osteomodulin	0.184	± 0.031	<0.01	aka osteoadherin, may mediate cell attachment
NM_011606	Tetranectin	0.187	± 0.027	<0.025	binds to plasminogen, may regulate matrix mineralization
NM_011199	parathyroid hormone receptor	0.198	± 0.010	<0.005	transmembrane receptor activity
NM_007431	alkaline phosphatase 2, liver	0.210	± 0.017	<0.01	essential for hydroxyapatite formation and matrix mineralization
NM_008524	Lumican	0.259	± 0.030	<0.005	regulates collagen fibril formation in different extracellular matrices
NM_007729	procollagen, type XI, alpha 1	0.292	± 0.013	<0.025	present in cartilage
NM_007559	bone morphogenetic protein 8B	0.337	± 0.071	<0.1	growth factor and cytokine activity
NM_008760	Osteoglycin	0.380	± 0.003	<0.025	binds to TGF-beta, no GAG in bone, keratan sulfate in other tissues
NM_016894	RAMP1	0.418	± 0.047	<0.025	calcitonin signal transducer activity
NM_007743	procollagen, type I, alpha 2	0.431	± 0.091	<0.1	the major constituent of bone matrix
NM_021355	Fibromodulin	0.450	± 0.103	<0.1	binds to collagen, may regulate fibril formation, binds to TGF-beta
NM_019444	RAMP2	0.500	± 0.027	<0.005	calcitonin signal transducer activity
AF053954	cbfa1/runx2 (osf2)	0.533	± 0.058	<0.1	essential transcription factor for osteoblast differentiation and bone formation
NM_007833	Decorin	0.562	± 0.003	<0.005	binds to collagen and may regulate fibril diameter
NM_013691	thrombospondin 3	0.581	± 0.034	<0.01	involved in cell attachment
NM_011607	tenascin C	0.589	± 0.024	<0.025	noncollagenous macromolecule of cartilage matrix
NM_011693	vascular cell adhesion molecule 1	0.633	± 0.075	<0.05	cell adhesion molecule activity
NM_008970	parathyroid hormone-like peptide	0.655	± 0.233	>0.1	signal transduction and hormone activity
NM_007553	bone morphogenetic protein 2	0.704	± 0.065	<0.05	growth factor and cytokine activity
NM_016919	procollagen, type V, alpha 3	0.716	± 0.024	<0.1	present where there is collagen type I
NM_011581	thrombospondin 2	0.724	± 0.298	>0.1	involved in cell attachment
NM_013605	mucin 1	0.733	± 0.047	<0.05	cell adhesion receptor
NM_011146	peroxisome proliferator activated receptor γ	0.734	± 0.016	<0.1	RNA polymerase II transcription factor
NM_007433	alkaline phosphatase 5	0.736	± 0.108	>0.1	hydrolase activity, acting on ester bonds
NM_010514	insulin-like growth factor 2	0.752	± 0.077	<0.1	signal transduction and hormone activity
NM_007737	procollagen, type V, alpha 2	0.767	± 0.026	<0.1	present where there is collagen type I
NM_022415	prostaglandin E synthase	0.778	± 0.041	<0.05	intramolecular isomerase activity, other intramolecular oxidoreductases
NM_010512	insulin-like growth factor 1	0.785	± 0.190	>0.1	signal transduction and hormone activity
NM_007644	CD36 antigen-like 2	0.833	± 0.013	<0.025	signal transducer activity
NM_010181	fibrillin 2	0.842	± 0.172	>0.1	may regulate elastic fiber formation (calcium ion binding activity)
NM_013731	serum/glucocorticoid regulated kinase 2	0.848	± 0.348	>0.1	phosphotransferase activity, alcohol group as acceptor
NM_009262	osteonectin (SPOCK1)	0.853	± 0.210	>0.1	may mediate deposition of hydroxyapatite, binds to growth factors
NM_011707	Vitronectin	0.861	± 0.297	>0.1	binds to collagen, plasminogen and heparin
NM_008712	nitric oxide synthase 1	0.861	± 0.025	<0.1	nitric oxide synthase activity
L27439	protein S	0.864	± 0.170	>0.1	calcium ion binding activity
NM_008689	NFκB 1	0.875	± 0.027	<0.05	transcription factor activity
NM_011808	ETS 1	0.883	± 0.199	>0.1	transcription factor expressed in proliferating preosteoblastic cells
NM_007388	acid phosphatase 5, tartrate resistant	0.885	± 0.180	>0.1	enzyme identified in both the ruffled border of the osteoclast membrane
NM_011519	syndecan 1	0.890	± 0.047	>0.1	binds to type 1 collagen, fibronectin, tenascin-C
NM_007557	bone morphogenetic protein 7	0.905	± 0.063	>0.1	growth factor and cytokine activity
NM_009926	procollagen, type XI, alpha 2	0.913	± 0.121	>0.1	present in cartilage
NM_011347	platelet selectin	0.920	± 0.075	>0.1	cell adhesion molecule activity
NM_007542	Biglycan	0.920	± 0.024	>0.1	may bind to collagen, a genetic determinant of peak bone mass
M28621	interferon-γ	0.945	± 0.161	>0.1	inhibit bone resorption
NM_031163	procollagen, type II, alpha 1	0.947	± 0.171	>0.1	the major constituent of cartilage
NM_008318	integrin binding sialoprotein	0.953	± 0.151	>0.1	noncollagenous protein in bone

Table 4.3-*Continued*

Accession #	*Gene Name*	Fold Δ	SEM	p-value.	**Molecular Function**
NM_013712	*integrin β1 binding protein 2*	0.956	± 0.062	>0.1	muscle-specific integrin beta1-interacting protein
NM_031168	*interleukin 6*	0.964	± 0.065	>0.1	act as stimulators of an early stage of osteoclast formation
NM_008355	*interleukin 13*	0.966	± 0.345	>0.1	inhibit bone resorption
NM_020273	*glucocorticoid modulatory element binding protein 1*	0.979	± 0.077	>0.1	transcription factor activity
NM_007412	*adrenomedullin receptor*	0.981	± 0.125	>0.1	rhodopsin-like, G-protein coupled receptor activity
NM_011346	*lymphocyte selectin*	0.982	± 0.075	>0.1	cell adhesion molecule activity
NM_009367	*transforming growth factor, beta 2*	1.000	± 0.127	>0.1	growth factor and cytokine activity
NM_009758	*bone morphogenetic protein receptor 1A*	1.011	± 0.176	>0.1	TGF-β and BMP receptor
NM_007560	*bone morphogenetic protein receptor 1B*	1.024	± 0.144	>0.1	TGF-β and BMP receptor
NM_008713	*nitric oxide synthase 3*	1.026	± 0.151	>0.1	nitric oxide synthase activity
NM_007424	*aggrecan 1*	1.026	± 0.077	>0.1	glycosaminoglycan binding activity
NM_007554	*bone morphogenetic protein 4*	1.027	± 0.017	>0.1	growth factor and cytokine activity
NM_007558	*bone morphogenetic protein 8A*	1.049	± 0.186	>0.1	growth factor and cytokine activity
NM_007993	*fibrillin 1*	1.049	± 0.045	>0.1	may regulate elastic fiber formation
NM_011809	*ETS 2*	1.078	± 0.176	>0.1	transcription factor expressed in differentiating and mature osteoblasts
NM_010927	*nitric oxide synthase 2*	1.086	± 0.195	>0.1	nitric oxide synthase activity
NM_011196	*prostaglandin E receptor 3*	1.102	± 0.397	>0.1	rhodopsin-like, G-protein coupled receptor activity
NM_007643	*CD36 antigen*	1.102	± 0.461	>0.1	cell adhesion molecule activity
NM_008216	*hyaluronan synthase 2*	1.116	± 0.240	>0.1	with versican-like protein works to captures space destined to become bone
NM_008764	*osteoprotegerin*	1.127	± 0.260	>0.1	signal transducer activity
NM_008319	*intracellular adhesion molecule 5*	1.136	± 0.082	>0.1	cell adhesion molecule activity
X97991	*calcitonin*	1.149	± 0.096	>0.1	signal transducer activity
NM_010735	*lymphotoxin A*	1.149	± 0.129	>0.1	tumor necrosis factor receptor ligand activity
NM_052994	*osteonectin (SPOCK2)*	1.164	± 0.105	>0.1	may mediate deposition of hydroxyapatite, binds to growth factors
NM_019511	*RAMP3*	1.172	± 0.042	>0.1	calcitonin signal transducer activity
NM_008215	*hyaluronan synthase 1*	1.177	± 0.258	>0.1	with versican-like protein works to captures space destined to become bone
NM_013693	*tumor necrosis factor*	1.256	± 0.334	>0.1	growth factor and cytokine activity
NM_010577	*integrin α5*	1.304	± 0.251	>0.1	cell adhesion molecule
NM_008350	*interleukin 11*	1.312	± 0.379	>0.1	act as stimulators of an early stage of osteoclast formation
NM_008518	*lymphotoxin B*	1.330	± 0.031	<0.025	tumor necrosis factor receptor ligand activity
NM_007761	*calcitonin gene-related peptide-receptor*	1.345	± 0.102	<0.1	calcitonin receptor activity
NM_007588	*calcitonin receptor*	1.345	± 0.225	>0.1	calcitonin G-protein coupled receptor activity
NM_008217	*hyaluronan synthase 3*	1.357	± 0.198	>0.1	with versican-like protein works to captures space destined to become bone
NM_010494	*intracellular adhesion molecule 2*	1.362	± 0.550	>0.1	cell adhesion molecule activity
NM_010576	*integrin α4*	1.413	± 0.448	>0.1	cell adhesion molecule
NM_018782	*calcitonin receptor-like*	1.413	± 0.242	>0.1	calcitonin G-protein coupled receptor activity
NM_011580	*thrombospondin 1*	1.418	± 0.278	>0.1	cell attachment
NM_009627	*adrenomedullin*	1.426	± 0.176	<0.1	neuropeptide hormone activity
NM_008965	*prostaglandin E receptor 4*	1.445	± 0.581	>0.1	G-protein coupled receptor_activity
NM_008396	*integrin α2*	1.654	± 0.467	>0.1	cell adhesion molecule
NM_007802	*cathepsin K (Ctsk)*	1.661	± 0.076	<0.01	in the papain family of cysteine proteases
NM_010554	*Interleukin 1α*	1.875	± 0.224	<0.1	potent stimulators of bone resorption
NM_007556	*bone morphogenetic protein 6*	1.877	± 0.161	<0.1	growth factor and cytokine activity
NM_008361	*Interleukin 1β*	2.099	± 0.176	<0.025	potent stimulators of bone resorption
NM_011361	*serum/glucocorticoid regulated kinase*	2.169	± 0.014	<0.001	transferase activity, transferring phosphorus-containing groups
NM_054084	*calcitonin-related polypeptide β*	9.548	± 8.524	>0.1	signal transducer activity

The gene microarray was verified by quantitative real time RTPCR for select osteogenic genes.

To verify the microarray studies by real time RTPCR, we selected genes that have been shown to be involved in osteoblast differentiation and bone mass regulation. The same samples used for the CodeLink bioarray assays were used for the real time RTPCR. All real time RTPCR data shown in Figure 4.6 (A–E) was normalized to the internal control, *18S* rRNA, and fold changes were determined by dividing the amount of a gene exposed to the RPM by the static 1g control (Figure 4.6F). As evaluated by the Codelink microarray, 2T3 cells exposed to the RPM had decreased expression of *ALP, runx2, PTHR1*, and *OMD* gene expression by a fold change of 0.21, 0.53, 0.20 and 0.18, respectively. In addition, 2T3 cells showed an increase in *ctsk* by a fold change of 1.66. To verify these results, real time RTPCR was performed. The gene expression fold changes by real time RTPCR for *ALP, runx2, PTHR1,* and *OMD* were 0.21, 0.68, 0.25 and 0.17, respectively. The fold change for *ctsk* from RTPCR was 1.67. Additionally, we confirmed the expression of non-mechanosensitive genes such as *BMP4* and *cystatin C* protein levels by immunoblotting. We show that the fold changes for *BMP4* and *cystatin C* by Western were 1.12 and 1.13 and by Codelink were 1.03 and 0.71, respectively (Figure 4.6G). The different methodologies used, the microarray assay, real time RTPCR, and immunoblotting, produced highly consistent results, providing a level of assurance regarding the validity of the microarray data.

Discussion

The novel and most significant finding of the current study is that exposure of preosteoblasts to simulated microgravity or disuse using the RPM partially recapitulates the expected changes associated with the bone loss response observed in spaceflight.
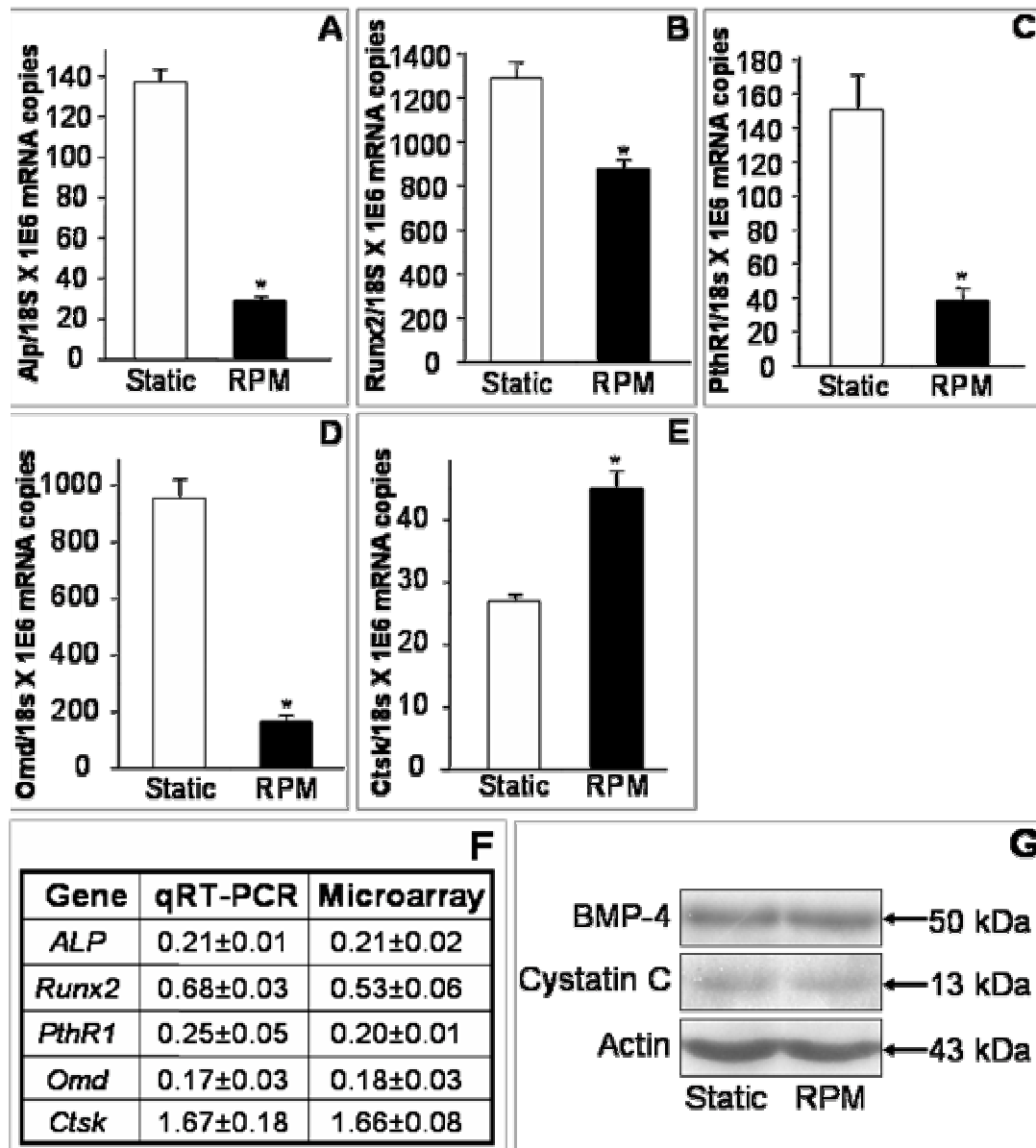
Figure 4.6 Verification of microarray results by real time RTPCR and immunoblot. Aliquots of total RNA were purified, reverse transcribed, and probed by real time RTPCR for ALP (A), runx2 (B), pthr1 (C), omd (D), and ctsk (E) using 18s rRNA as an internal control, and fold changes were compared to the microarray data (F). Cell lysate from additional experiments was obtained for immunoblotting and probed for BMP4 and cystatin C (G) using actin as an internal control. Data are shown as mean ± SEM (n=4-6, *p< 0.05).

The RPM induced a loss of *ALP* mRNA and activity, a marker of differentiation, and we found that this change occurred without altering cell proliferation or gross morphology of 2T3 cells. More importantly, the RPM inhibited mineralization, a long term marker of bone formation *in vitro* despite treatment with an osteogenic factor such as BMP2 or BMP4. Furthermore, using this *in vitro* system, the current study generated a list of genes that were upregulated, downregulated, or unchanged by the RPM. Several genes that are suspected to be involved in bone formation and bone resorption were found to change in the expected manner. We selected 7 genes (*ALP, runx2, PTHR1, OMD, ctsk, BMP4, and cystatin C*) from the list and verified the microarray results by real time RTPCR or immunoblot.

Disuse- and microgravity-induced bone loss in humans and animals has been shown to be mediated at least in part by osteoblast differentiation, and ALP and mineralization are well-known markers for it (3, 7, 22). Our current data showing a decrease in ALP activity and mRNA levels as well as mineralization is consistent with this notion (11). In addition, the decrease in *runx2* is also indicative of a disuse-response as *runx2* mRNA levels have been previously shown to decrease in both spaceflight and ground-based studies (3, 27). The current finding that 2T3 cell exposure to the RPM decreases *ALP* and *runx2* expression is consistent with the spaceflight data obtained with osteoblasts as well as other bioreactor data using MC3T3-E1 preosteoblast cells exposed to the Rotating Wall Vessel (RWV) (6, 8, 27). *Runx2*, a member of the runt homology domain transcription factor family and regulator of matrix protein osteocalcin, is an essential transcription factor for osteoblast differentiation and bone formation. We found that *runx2* was downregulated by almost two-fold below the static 1g control. Osteocalcin protein levels in the conditioned medium were too low to be detected in our studies due to a relatively short experimental duration of 9 days, and

81

this is consistent with previous findings (12). In other studies, osteocalcin level was shown to be decreased in MC3T3-E1 cells by exposure to the RWV (27).

Additionally, *OMD* belongs to the small leucine-rich proteoglycan (SLRP) family and is thought to be involved in bone matrix formation (5). Our current study showing the downregulation of *OMD* by the RPM supports the current hypothesis. A decrease in parathyroid hormone related protein, which plays a role in calcium mobilization, has been linked to the decrease in bone density and bone loss in space-flown rats (34). In this light, our result demonstrating that *PTHR1* mRNA level was decreased by the RPM is also consistent with the space-flown data. In addition to the downregulated genes, there were several genes that were upregulated. *Ctsk*, which is a member of the papain family of cysteine proteases, is mostly expressed in osteoclasts and plays a critical role in bone resorption (24, 42). More recently, however, *ctsk* has been found in non-osteoclastic cells such as thyroid epithelial cells (42). As far as we are aware, this is the first time that *ctsk* expression has been found in osteoblasts. At present, the biological and pathological implications of *ctsk* expression in osteoblasts are not clear. *Ctsk* induced by the RPM could be responsible for bone loss by either directly increasing osteoclastic activity or through an indirect osteoblast-dependent mechanism.

We also examined genes that were not unchanged in response to the RPM according to the microarray data. For example, *BMP4* and *cystatin C* mRNA levels in the RPM-exposed group showed 1.0- and 0.7-fold changes over the controls, respectively. We performed immunoblot analyses to examine their protein expression levels with specific antibodies to BMP4, cystatin C, and actin (as a control) using lysate obtained from 2T3 cells exposed to three days of RPM or static 1g control conditions. As expected, we did not find any significant difference in their protein expression levels as shown in Figure 4.6F.

In addition to simulated microgravity or disuse conditions, cells in this *in vitro* system experienced a low level of shear stress and subsequent strain based on computational modeling studies. The model predicted that a minor portion of the cells close to the edge of the long frame of the Opticell disk experienced significantly less than 1.0 dyn/cm^2 of shear stress for a brief moment (less than 4.0 sec/min) and less than 200 microstrains of mechanical strain for a fraction of the RPM exposure time. However, the levels of these forces are significantly lower than the reported stress or strain magnitudes (as low as 2 dyn/cm^2 shear stress and 500 microstrains) needed to stimulate signaling in osteoblasts (18, 19, 23, 30). It should be noted that it has been shown that 0.14 dyn/cm^2 of *continuous* shear exposure for four hours increased *cyclooxygenase 2 (cox-2)* expression (37). Therefore, these results should be taken with caution that the observed RPM effects may be partially attributed to mechanical forces other than simulated microgravity or disuse conditions.

In summary, we have developed a novel *in vitro* system using the RPM, Opticell disks, and 2T3 preosteoblast cells, which seems to recapitulate the bone loss-like response due to microgravity or disuse conditions. The data reported here show that exposure to the RPM alters gene expression profiles and inhibits differentiation of preosteoblasts to osteoblasts, eventually leading to reduced bone formation. At this point, it is not clear whether these two events, differentiation or gene expression changes, occur in sequence or concurrently. However, it is likely that these two events are closely interrelated. In addition to having tabulated a list of known and expected genes altered by disuse (e.g. *ALP, runx2, OMD, PTHR1, and ctsk*), we have a list of unknown and uncharacterized genes that have dramatically changed in 2T3 cells exposed to the RPM. The functional characterization of these expected and unexpected genes could provide critical insight into understanding the mechanisms driving disuse-induced bone loss. Moreover, these studies may also lead to the identification of novel

targets of therapeutic interventions to prevent bone loss not only in astronauts but also in the general population afflicted with metabolic bone diseases.

Acknowledgements

References

1.   **Al Ajmi N, Braidman I, and Moore D.** Effect of clinostat rotation on differentiation of embryonic bone in vitro. *Adv Space Res* 17: 189-192, 1996.

2.   **Arbeille P, Fomina G, Achaibou F, Pottier J, and Kotovskaya A.** Cardiac and vascular adaptation to 0g with and without thigh cuffs. *Acta Astronaut* 36: 753-762, 1995.

3.   **Bikle DD and Halloran BP.** The response of bone to unloading. *J Bone Miner Metab* 17: 233-244, 1999.

4.   **Boo YC, Sorescu G, Boyd N, Shiojima I, Walsh K, Du J, and Jo H.** Shear stress stimulates phosphorylation of endothelial nitric-oxide synthase at Ser1179 by Akt-independent mechanisms: role of protein kinase A. *J Biol Chem* 277: 3388-3396, 2002.

5.   **Buchaille R, Couble ML, Magloire H, and Bleicher F.** Expression of the small leucine-rich proteoglycan osteoadherin/osteomodulin in human dental pulp and developing rat teeth. *Bone* 27: 265-270, 2000.

6.   **Caillot-Augusseau A, Lafage-Proust M-H, Soler C, Pernod J, Dubois F, and Alexandre C.** Bone formation and resorption biological markers in cosmonauts during and after a 180-day space flight (Euromir 95). *Clin Chem* 44: 578-585, 1998.

7.   **Caillot-Augusseau A, Vico L, Heer M, Voroviev D, Souberbielle J-C, Zitterman A, Alexandre C, and Lafage-Proust M-H.** Space Flight Is Associated with Rapid Decreases of Undercarboxylated Osteocalcin and Increases of Markers of Bone Resorption without Changes in Their Circadian Variation: Observations in Two Cosmonauts. *Clin Chem* 46: 1136-1143, 2000.

8.   **Carmeliet G and Bouillon R.** The effect of microgravity on morphology and gene expression of osteoblasts in vitro. *FASEB J* 13: 129-134, 1999.

9.   **Carmeliet G, Vico L, and Bouillon R.** Space flight: a challenge for normal bone homeostasis. *Crit Rev Eukaryot Gene Expr* 11: 131-144, 2001.

10.   **Collet P, Uebelhart D, Vico L, Moro L, Hartmann D, Roth M, and C A.** Effects of 1- and 6-month spaceflight on bone mass and biochemistry in two humans. *Bone* 20: 547-551, 1997.

11.   **Garetto LP, Gonsalves MR, Morey ER, Durnova G, and Roberts WE.** Preosteoblast production 55 hours after a 12.5-day spaceflight on Cosmos 1887. *Faseb J* 4: 24-28, 1990.

12.   **Ghosh-Choudhury N, Windle JJ, Koop BA, Harris MA, Guerrero DL, Wozney JM, Mundy GR, and Harris SE.** Immortalized murine osteoblasts derived from BMP 2-T-antigen expressing transgenic mice. *Endocrinology* 137: 331-339, 1996.

13.   **Heer M, Kamps N, Biener C, Korr C, Boerger A, Zittermann A, Stehle P, and Drummer C.** Calcium metabolism in microgravity. *Eur J Med Res* 4: 657-660, 1999.

14.   **Hejnowicz Z, Sondag C, Alt W, and Sievers A.** Temporal course of graviperception in intermittently stimulated cress roots. *Plant Cell Environ* 21: 1293-1300, 1998.

15.   **Hoson T.** Evaluation of the three-dimensional clinostat as a simulator of weightlessness. *Planta* 203: S187-197, 1997.

16.   **Hughes-Fulford M.** Signal transduction and mechanical stress. *Science STKE* 12, 2004.

17.   **Huijser RH.** Desktop RPM: New Small Size Microgravity Simulator for the Bioscience Laboratory. Fokker Space, 1-5, 2000.

18.   **Kapur S, Baylink DJ, and Lau KH.** Fluid flow shear stress stimulates human osteoblast proliferation and differentiation through multiple interacting and competing signal transduction pathways. *Bone* 32: 241-251, 2003.

19.   **Kaspar D, Seidl W, Neidlinger-Wilke C, Ignatius A, and Claes L.** Dynamic cell stretching increases human osteoblast proliferation and CICP synthesis but decreases osteocalcin synthesis and alkaline phosphatase activity. *J Biomech* 33: 45-51, 2000.

20.   **Katkovsky BS PY.** Cardiac output during physical exercises following real and simulated space flight. *Life Sci Space Res* 14, 1976.

21.   **Kobayashi K, Kambe F, Kurokouchi K, Sakai T, Ishiguro N, Iwata H, Koga K, Gruener R, and Seo H.** TNF-[alpha]-Dependent Activation of NF-[kappa]B in Human Osteoblastic HOS-TE85 Cells Is Repressed in Vector-Averaged Gravity Using Clinostat Rotation. *Biochemical and Biophysical Research Communications* 279: 258-264, 2000.

22.   **LeBlanc A, Schneider V, Spector E, Evans H, Rowe R, Lane H, Demers L, and Lipton A.** Calcium absorption, endogenous excretion, and endocrine changes during and after long-term bed rest. *Bone* 16: 301S-304S, 1995.

23.   **McAllister TN, Du T, and Frangos JA.** Fluid shear stress stimulates prostaglandin and nitric oxide release in bone marrow-derived preosteoclast-like cells. *Biochem Biophys Res Commun* 270: 643-648, 2000.

24.   **McGrath ME.** The lysosomal cysteine proteases. *Annu Rev Biophys Biomol Struct* 28: 181-204, 1999.

25.   **Miyamoto A, Shigematsu T, Fukunaga T, Kawakami K, Mukai C, and Sekiguchi C.** Medical baseline data collection on bone and muscle change with space flight. *Bone* 22: 79S-82S, 1998.

26.   **Nakamura H, Kumei Y, Morita S, Shimokawa H, Ohya K, and Shinomiya K.** Suppression of osteoblastic phenotypes and modulation of pro- and anti-apoptotic features in normal human osteoblastic cells under a vector-averaged gravity condition. *J Med Dent Sci* 50, 2003.

27.   **Ontiveros C, McCabe, Laura R.** Simulated microgravity suppresses osteoblast phenotype, Runx2 levels and AP-1 transactivation. *Journal of Cellular Biochemistry* 88: 427-437, 2003.

28.   **Parhami F, Morrow AD, Balucan J, Leitinger N, Watson AD, Tintut Y, Berliner JA, and Demer LL.** Lipid oxidation products have opposite effects on calcifying vascular cell and bone cell differentiation. A possible explanation for the paradox of arterial calcification in osteoporotic patients. *Arterioscler Thromb Vasc Biol* 17: 680-687, 1997.

29.   **Ramakrishnan R, Dorris D, Lublinsky A, Nguyen A, Domanus M, Prokhorova A, Gieser L, Touma E, Lockner R, Tata M, Zhu X, Patterson M, Shippy R, Sendera TJ, and Mazumder A.** An assessment of Motorola CodeLink microarray performance for gene expression profiling applications. *Nucleic Acids Res* 30: e30, 2002.

30.   **Reich KM, Gay CV, and Frangos JA.** Fluid shear stress as a mediator of osteoblast cyclic adenosine monophosphate production. *J Cell Physiol* 143: 100-104, 1990.

31.   **Sarkar D, Nagaya T, Koga K, Nomura Y, Gruener R, and Seo H.** Culture in vector-averaged gravity under clinostat rotation results in apoptosis of osteoblastic ROS 17/2.8 cells. *Journal of Bone and Mineral Research* 15: 489-498, 2000.

32.   **Sonnenfeld G, Butel J, and Shearer W.** Effects of the space flight environment on the immune system. *Rev Environ Health* 18: 1-17, 2003.

33.   **Sorescu GP, Sykes M, Weiss D, Platt MO, Saha A, Hwang J, Boyd N, Boo YC, Vega JD, Taylor WR, and Jo H.** Bone Morphogenic Protein 4 Produced in Endothelial Cells by Oscillatory Shear Stress Stimulates an Inflammatory Response. *J Biol Chem* 278: 31128-31135, 2003.

34.   **Torday JS.** Parathyroid hormone-related protein is a gravisensor in lung and bone cell biology. *Adv Space Res* 32: 1569-1576, 2003.

35.   **Van Loon JJ, Bervoets DJ, Burger EH, Dieudonne SC, Hagen JW, Semeins CM, Doulabi BZ, and Veldhuijzen JP.** Decreased mineralization and increased calcium release in isolated fetal mouse long bones under near weightlessness. *J Bone Miner Res* 10: 550-557, 1995.

36.   **Vermeer C, Wolf J, Craciun A, and Knapen M.** Bone markers during a 6-month space flight: effects of vitamin K supplementation. *J Gravit Physiol* 5: 65-69, 1998.

37.   **Wadhwa S, Embree MC, Kilts T, Young MF, and Ameye LG.** Accelerated osteoarthritis in the temporomandibular joint of biglycan/fibromodulin double-deficient mice. *Osteoarthritis Cartilage* 13: 817-827, 2005.

38.   **Wang E.** Age-dependent atrophy and microgravity travel: what do they have in common? *FASEB J* 13 Suppl: S167-S174, 1999.

39.   **White R and Blomqvist C.** Central venous pressure and cardiac function during spaceflight. *J Appl Physiol* 85: 738-746, 1998.

40.   **Whyte MP.** Hypophosphatasia and the role of alkaline phosphatase in skeletal mineralization. *Endocr Rev* 15: 439-461, 1994.

41.   **Yang X, Ji X, Shi X, and Cao X.** Smad1 domains interacting with Hoxc-8 induce osteoblast differentiation. *J Biol Chem* 275: 1065-1072, 2000.

42.   **Zaidi M, Blair HC, Moonga BS, Abe E, and Huang CL.** Osteoclastogenesis, bone resorption, and osteoclast-based therapeutics. *J Bone Miner Res* 18: 599-609, 2003.

43.   **Zayzafoon M, Gathings WE, and McDonald JM.** Modeled microgravity inhibits osteogenic differentiation of human mesenchymal stem cells and increases adipogenesis. *Endocrinology* 145: 2421-2432, 2004.

44.   **Zeeberg B, Feng W, Wang G, Wang M, Fojo A, Sunshine M, Narasimhan S, Kane D, Reinhold W, Lababidi S, Bussey K, Riss J, Barrett J, and Weinstein J.** GoMiner: a resource for biological interpretation of genomic and proteomic data. *Genome Biology* 4: R28, 2003.

Chapter 5

A Confined List of Mechanosensitive Genes in Osteoblasts by Comparative Microarray Studies*

Summary

With a list of gene expression changes due to simulated microgravity or disuse from specific aim 1, it is the goal of specific aim 2 to confine this list to those genes that may be most important in regulating bone formation in disuse conditions. Specific aim 1 resulted in a relatively large list of 140 genes with potential roles in bone loss due to disuse. As such, to achieve this aim, we exposed 2T3 cells to a distinct simulator of microgravity or disuse called the Rotating Wall Vessel (RWV) and performed comparative microarray analyses.

Bone loss due to disuse, microgravity, or osteoporosis is caused in part by decreased bone formation by osteoblasts. There are simulators of microgravity or disuse used to study the mechanisms regulating bone loss in these environments at the *in vitro* level. Thus, this research has the potential to elucidate the role of certain mechanosensitive genes in bone loss. The RWV and RPM are the two most commonly used simulators of microgravity, but these simulators have not been systematically compared to each other or to mechanical stimulating models. These comparisons are vital to validate their use in modeling the disuse phenotype. Here, we hypothesized that exposure to the RWV inhibits differentiation and alters gene expression profiles of 2T3 cells, and a subset of these mechanosensitive genes behaves in a manner consistent to the RPM and opposite to the trends incurred by mechanical stimulation of mouse tibiae.

Exposure of 2T3 preosteoblast cells to the RWV for three days inhibited alkaline phosphatase (ALP) activity, a marker of differentiation, and downregulated 61 and upregulated 45 genes by more than two-fold compared to static 1g controls as shown by microarray analysis. The microarray results were confirmed by real time RTPCR and/or immunoblots for seven distinct genes and proteins including *osteomodulin (OMD)*, *runt homology domain transcription factor 2* (*runx2),* and *osteoglycin (OGN)*. Comparison of the RWV data to the RPM microarray study that we previously published showed 17 mechanosensitive genes that changed in the same direction. Further comparison of the RWV and RPM results to independently published microarray data from mechanically loaded mouse tibiae revealed three genes including *OGN* that were upregulated by mechanical loading and downregulated by disuse. These mechanosensitive genes may provide novel insight into understanding the mechanisms regulating bone formation and potential targets for countermeasures against decreased bone formation during spaceflight, disuse, and osteoporosis.

Introduction

Bone loss occurs due to a number of stimuli, including disuse due to illness or paralysis, microgravity in spaceflight, or ageing. Bone loss can lead to fractures, causing hospitalization and potentially invasive replacement surgery. Exposure to microgravity conditions induces several adaptive and pathological changes to the human body, posing health risks to astronauts during spaceflight. These pathological changes include decreased bone mass (12, 23) at 1%-2% per month during spaceflight, and this bone loss may be due to either decreased bone formation by osteoblasts or increased osteolytic functions of osteoclasts (3, 23). Bone loss in space may be regulated by similar mechanisms as bone loss due to disuse, and research in this area has the potential to benefit the general public. However, the underlying molecular mechanisms

91

driving bone loss in various environments remain unknown, making it difficult to develop adequate countermeasures to mitigate it.

Bioreactors such as the RPM and RWV provide unique environments to model disuse or microgravity for *in vitro* experiments. However, it has become increasingly important to have validated *in vitro* ground-based models. Whenever possible, comparisons of data from these systems should be made to spaceflight, *in vivo* models of disuse, and *in vivo* mechanical loading models to evaluate consistency of results. The RWV and the RPM are the two most commonly used *in vitro* simulators of microgravity or disuse. While the RWV models microgravity conditions by maintaining continuous free-fall, the RPM exposes cells and tissues to random speeds and orientation such that the gravity vector is randomly moved relative to the specimen (4, 22). The RWV (Figure 1A) is designed such that the particles within it are subjected to solid body rotation, which is achieved as the vessel rotates and the liquid accelerates such that the entire body of fluid is rotating at the same angular velocity as the vessel wall. The RWV generates minimum shear forces since there is no internal mixer, and thus, the cells in the RWV are subjected to solid body rotation and are constantly suspended (22). In contrast, the RPM (Figure 5.1B) is a three dimensional (3D) clinostat that rotates about two orthogonal axes. There are two frames, an inner and an outer frame, which rotate about distinct axes, and the platform where the cells rest is the inner frame. The RPM operates in a random mode, where rotation speeds and directions are randomized using software developed by the Dutch Space Agency (Leiden, the Netherlands). The continuous movement of the gravity vector averages the vector to zero over time, a method called gravity-vector averaging (6).

Both the RWV (18, 30) and the RPM (16, 19) have been previously used by various groups to assess the effects of microgravity or disuse on bone cells. However, it has not been reported whether these simulators induce similar changes with regard to

bone loss or bone formation. Since the RPM and RWV operate in distinct modes, it is imperative to compare the data produced by each simulator. Recently, we have characterized gene transcript expression profiles of 10,000 genes using Codelink gene chips in 2T3 murine preosteoblasts exposed to the RPM (19). We compiled a list of 140 genes (mechanosensitive genes) that changed in response the RPM, and a subset of these genes may be involved in regulation of bone formation. In contrast, a study by Xing et al., has characterized gene transcript profile changes induced by exposing mouse tibiae to mechanical stimulation, an apparent opposite of microgravity or disuse conditions, using a four-point bending method (29). Therefore, we hypothesized that exposure to the RWV inhibits differentiation and alters gene expression profiles of 2T3 cells, and a subset of these mechanosensitive genes behaves in a manner consistent to the RPM and opposite to the trends incurred by mechanical stimulation of mouse tibiae.

To test this hypothesis, we carried out an additional gene transcript profiling study with 2T3 cells exposed to the NASA-developed RWV bioreactor and compared the results to our previous transcript database obtained with the Japanese-designed and European-manufactured RPM. In addition, we compared both the RWV and RPM transcript databases to a database obtained from mechanically loaded mouse tibiae (29). From these comparisons, we produced a confined subset of genes that was affected in all three studies, suggesting that these genes may be implicated in disuse-induced decrease in bone formation.

Materials and Methods
Cell culture—2T3 murine osteoblast precursor cells were cultured in growth medium (α-minimal essential medium) containing 10% fetal bovine serum (Atlanta Biologicals) with 100 U/ml penicillin and 100 µg/ml streptomycin in a standard humidified incubator (37°C, 5% CO_2) as previously described by us (19). For RWV experiments, trypsinized cells

93

were seeded on microcarriers (#P102-1521, Solohill, Ann Arbor, MI), which have polystyrene cores and no extracellular matrix coating. The cells were allowed to grow in low adhesion 100 mm plates (Corning, Inc. #3262) for three days to confluency and then were exposed to simulated microgravity using the RWV or static 1g control conditions.

Rotating Wall Vessel (RWV)–Rotation of the RWV (Figure 5.1A) maintains microbeads coated with attached 2T3 preosteoblasts in a continuous free-fall state, simulating a microgravity environment (22). This RWV system has been shown to be an effective simulator of real microgravity conditions as demonstrated in comparative studies using blood mononuclear cells in space flight missions STS-54 and STS-56 (20). In the current study, 2T3 cells were exposed to the RWV for three days so that the data could be directly compared to data obtained with the RPM for the same time period (19).

Whole cell lysate and alkaline phosphatase (ALP) enzyme activity—Following the RWV or static 1g exposure, cells and beads were washed with ice-cold phosphate buffered saline (PBS) two times and lysed in 500 µl of a lysis buffer containing 0.1% Triton X-100 in 1mM $MgCl_2$, 20mM Tris-HCl, and 0.1 mM $ZnCl_2$. The lysate and bead mixture was centrifuged for three minutes at 1,500 rpm to separate the beads from the lysate. The lysate was pipetted out of the mixture and stored at –20°C until needed. A Bio-Rad DC protein assay and ALP activity assay (Sigma) were carried out as described previously (19).

Immunoblotting—Aliquots of cell lysate were resolved on a SDS-PAGE gel and transferred to a polyvinylidene difluoride membrane (Millipore) (1). The membrane was incubated with a primary antibody overnight at 4°C and then incubated with a secondary antibody conjugated with alkaline phosphatase for one hour at room temperature.

94
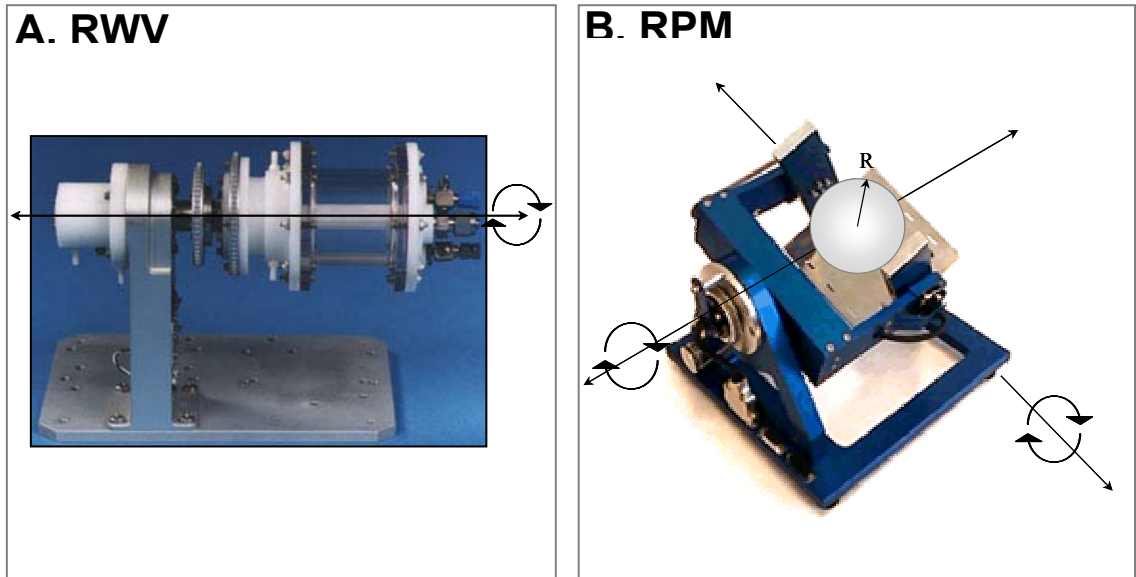
Figure 5.1 Simulated microgravity or disuse using the RWV and the RPM. The arrows indicate movement about the respective axis of rotation.

Expression was detected by a chemiluminescence method, and the intensities of immunoreactive bands were determined by densitometry (1). Antibodies specific for BMP4 (Santa Cruz Biotechnologies), OGN (R&D Biosciences), and peroxiredoxin I and peroxiredoxin IV (Lab Frontier, Seoul, Korea) were used.

RNA isolation—Total RNA was prepared by using the RNeasy Mini kit (Qiagen). Briefly, after two ice-cold PBS washes, 500 µl of RLT lysis buffer containing β-mercaptoethanol was added to the bead and cell mixture to isolate total RNA. The bead and lysate mixture was centrifuged for three minutes at 1,500 RPM to separate the beads from the RNA, and the RNA was pipetted to the homogenizing column in the RNeasy kit. The RNA was purified with the kit and stored at –80°C until needed.

Affymetrix Gene Microarrays— All RNA samples passed the Affymetrix test for RNA quality and concentration before proceeding to the gene chip study carried out in the Microarray Core Facility at the Baylor College of Medicine (Houston, TX). The samples used for these studies were obtained from three independent biological experiments as follows: We pooled cells from 3 independent RWV experiments carried out at the same time to obtain a single sample (total RNA) that was used for a single microarray. This process minimized inter-experimental variations and provided a sufficient amount of RNA for each microarray. We repeated this process three different times to obtain a final sample size of three microarray chips for the static control samples and three microarray chips for the RWV samples. The array used was Affymetrix GeneChip® Mouse 430 2.0, and the data were background adjusted and normalized to median intensity. The data were transformed so that fold changes were obtained by dividing the averaged normalized intensities of the RWV samples by the averaged normalized intensities of the static samples. Thus, a fold change above 1.0 indicates a gene upregulated by the RWV and below 1.0 indicates a gene downregulated by the RWV. The data were statistically analyzed by DNA chip analyzer (dChip) as described below in the statistical analysis section and filtered for fold change threshold, and the genes that changed in response to the RWV by more than two-fold above or below the static 1g controls with p-values of less than 0.05 were deemed considerable and statistically significant. The number of differentially expressed genes and false discovery rate (FDR) were calculated for each of 500 permutations, and 1,934 genes had p-values less than 0.05 at median FDR. Roughly, half of these genes were false positives. GoMiner software (http://www.miblab.gatech.edu/gominer) was used to sort the genes by biological processes and to assign some of the molecular functions of each known gene (31).

Reverse Transcriptase and Real-Time Polymerase Chain Reaction (RTPCR)—Total RNA was reverse transcribed by using random primers and a Superscript-II kit (Life Technology) (24). The synthesized and purified cDNA was amplified using a LightCycler (Roche Applied Science), and the size of each PCR product was verified by agarose gel electrophoresis as described by us (24). The mRNA copy numbers were determined based on standard curves generated with the genes of interest and *18S* rRNA templates. The *18S* gene (50 nM at 61ºC annealing temperature; Ambion) was used as an internal control for real time RTPCR carried out with capillaries (Roche Applied Science), recombinant Taq polymerase (Invitrogen), and Taq start antibody (Clontech). The primer pairs for the quantitative real time RTPCR are listed in Table 5.1 along with Light Cycler conditions. Real time RTPCR for the listed genes were carried out in RTPCR buffer (20mM Tris-Cl, pH 8.4 at 25°C, 4mM $MgCl_2$, 250 µg/ml bovine serum albumin, and 200 µM deoxynucleotides) containing SYBR green (1:84,000 dilution), 0.05unit/µl Taq DNA polymerase, and Taq Start antibody (1:100 dilution) as described previously (24).

Table 5.1 Primer pairs and Lightcycler conditions for Real Time RTPCR

Accession #	Gene		Primers (5'-3')	bp	LightCycler Conditions
NM_009820	*Runx2*	Fw	GACAGAAGCTTGATGACTCTAAACC	171	7 sec; 62ºC
		Rv	TCTGTAATCTGACTCTGTCCTTGT		9 sec; 72ºC
NM_007554	*BMP4*	Fw	CTGCGGGACTTCGAGGCGACACTTCT	150	7 sec; 65ºC
		Rv	TCTTCCTCCTCCTCCTCCCCAGACTG		7 sec; 72ºC
NM_011199	*PTHR1*	Fw	GCACACAGCAGCCAACATAA	531	7 sec at 63ºC
		Rv	CGCAGCCTAAACGACAGGAA		22 sec at 72ºC
NM_012050	*OMD*	Fw	GACGGGCTGGTGAATGTGACTATGCTTGA	147	7 sec; 63ºC
		Rv	CCAAGGGGCATTGATTCTAATCTGTTATT		10 sec; 72ºC

Statistical analysis—Data are expressed as mean $\pm$ SEM with n numbers representing biological replicates from independently repeated experiments. Statistical analysis was

97

performed using the Student's t-test for ALP enzyme activity experiments. A significance level of p<0.05 was considered statistically significant. The microarray data was analyzed with dChip, a program based on the Model-Based Expression Index (MBEI) method (14, 15). The raw data were normalized using the invariant set normalization, and the average expression values were represented as model-based expression indices. We used the 'PM only model', and the expression values were expressed in log2 scale. Differential gene expression between two groups of samples was analyzed by the t-test built in dChip.

Results

The RWV inhibited ALP activity.

Expression of ALP increases as osteoblasts mature and differentiate, and its enzyme activity is often used as a marker for bone formation. Thus, we examined the effects of the RWV on ALP enzyme activity in 2T3 preosteoblasts. Exposure of 2T3 cells to the RWV for three days significantly decreased ALP activity (Figure 5.2A) and mRNA (Figure 5.2B) in comparison to static 1g controls. This finding, which is consistent to our previously reported data with the RPM (19), suggests that the simulated microgravity or disuse conditions induced by either the RWV or the RPM result in a similar inhibitory effect on osteoblast differentiation.

The RWV altered gene expression profiles of 2T3 cells.

DNA microarray studies were performed on samples obtained from 2T3 cells exposed to static 1g or the RWV for three days. Among approximately 40,000 genes
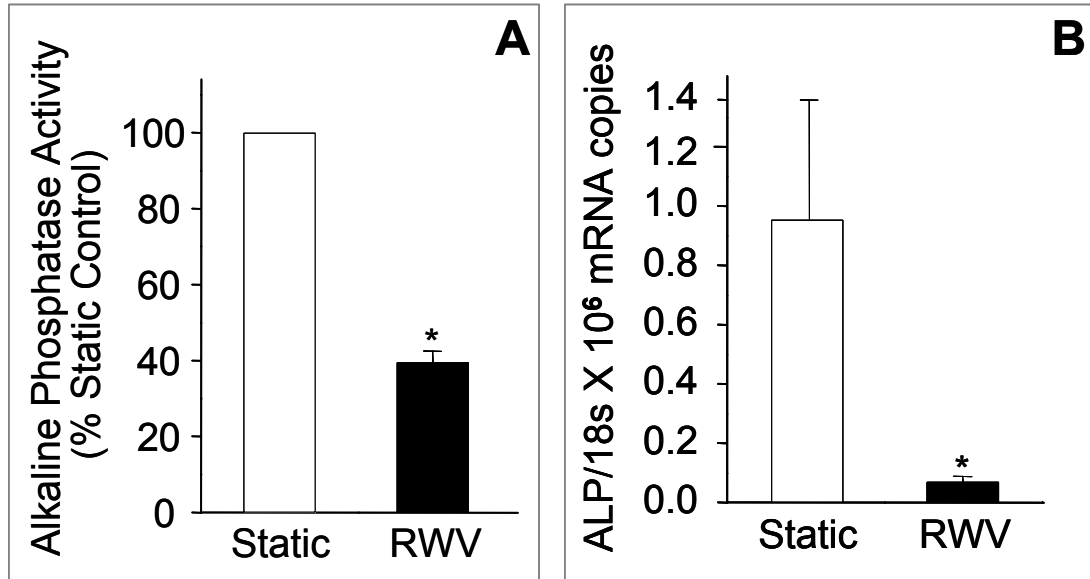
Figure 5.2 RWV exposure inhibited alkaline phosphatase activity and mRNA expression in 2T3 cells. Confluent 2T3 cells grown on microcarriers were placed in the RWV or exposed to static 1g conditions for three days. ALP activity (A) was determined by a colorimetric assay and normalized to total protein, and *ALP* mRNA level (B) was determined by real time RTPCR with *18S* as an internal control. Data are shown as mean ± SEM (n=6 for A, n=3 for B, *p<0.05).
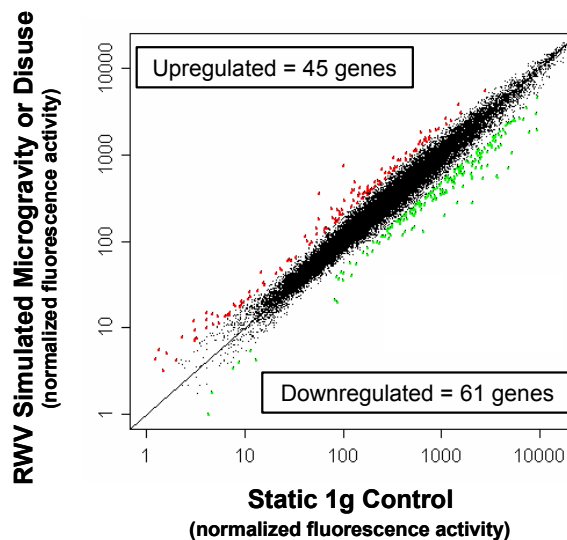
Figure 5.3 The effects of the RWV on gene expression profiles of 2T3 cells. Total RNA was isolated from 2T3 cells exposed to RWV or static 1g control conditions for three days. The samples were reverse transcribed and analyzed by Affymetrix microarrays corresponding to 40,000 mouse genes. The scatter plot shows mean intensities of each gene probe using the data obtained from all microarrays. Statistical analysis identified 61 genes upregulated (red dots) and 45 genes downregulated (green dots) by more than two-fold compared to static 1g control (p<0.05, n=3 each static 1g and RWV). Unchanged genes are shown in black along the diagonal line in the scatter plot.

tested by the Affymetrix array, 61 were downregulated while 45 were upregulated statistically significantly (p<0.05) by more than two-fold above the static 1g control as shown in a scatter plot of the genes (Figure 5.3). In Figure 5.3, dots aligned with the diagonal line represent unchanged genes while genes further from the line were either upregulated (above line) or downregulated (below line) by the RWV. Additionally, Table 5.2 provides a list of significantly changed genes from the microarray that may be implicated in bone formation or mineralization as determined by literature survey, and these genes are organized by fold change with molecular function as defined by GoMiner. Table A.1 shows a larger subset of mechanosensitive genes organized by biological process. Table A.2 lists genes that may be involved in osteoblast function with relaxed p-value stringency. The entire RWV array data can be accessed from Gene Expression Omnibus (GEO) with accession number GSE4658. The RPM microarray data that we previously published can be accessed with numbers GDS928 or GSE1367 (19).

Quantitative real time RTPCR and immunoblotting validated the microarray data for select osteogenic genes.

To confirm our microarray data, we performed real time RTPCR and immunoblot analyses for a select subset of genes that may be implicated in bone formation. The same samples that were used for the microarrays were used for the real time RTPCR, and additional RWV experiments were performed to obtain protein samples for the Western blots. The 2T3 cells exposed to the RWV had decreased expression of *runx2*, *bone morphogenic protein 4 (BMP4), parathyroid hormone receptor 1 (PTHR1)*, and *OMD* genes by a fold change of 0.69, 0.40, 0.54, and 0.10, respectively, as evaluated by the Affymetrix microarray. The gene expression fold changes by real time PCR for *runx2*, *BMP4*, *PTHR1,* and *OMD*, were 0.38, 0.26, 0.59, and 0.10, respectively (Figure

Table 5.2 The effect of the RWV on selected genes that may be involved in osteoblast differentiation and matrix mineralization. Genes are sorted based on fold changes.

Accession #	Gene Name	*Fold Δ	p-value	Molecular Function
NM_012050	osteomodulin	0.10	<0.05	also called osteoadherin, may mediate cell attachment
NM_008760	osteoglycin	0.23	<0.05	binds to TGF-beta, no GAG in bone, keratan sulfate in other tissues
NM_025711	asporin	0.28	<0.05	porin activity; cartilage extracellular protein
BC002065	serine (or cysteine) proteinase inhibitor, clade A, member 3G	0.35	<0.05	may be involved in osteoclast function with MMPs and cathepsins
NM_007729	procollagen, type XI, alpha 1	0.37	<0.05	present in cartilage
NM_011581	thrombospondin 2	0.39	<0.025	involved in cell attachment
NM_016873	WNT1 inducible signaling pathway protein 2	0.39	<0.05	involved in WNT pathway, WNT stimulated by BMPs
BB781435	nidogen 2	0.39	<0.005	calcium binding
NM_007554	bone morphogenetic protein 4	0.40	<0.0025	growth factor and cytokine activity
NM_011693	vascular cell adhesion molecule 1	0.41	<0.025	cell adhesion molecule activity
NM_012043	immunoglobulin superfamily containing leucine rich repeat (ISLR)	0.42	<0.05	involved in cell attachment
NM_009144	secreted frizzled-related sequence protein 2	0.43	<0.05	WNT signaling pathway antagonist
BB431535	matrix metalloproteinase 16	0.47	<0.05	involved in osteoclast function and bone resorption
BC014690	transforming growth factor, beta 3	0.59	<0.05	growth factor and cytokine activity
AF053954 **	cbfa1/runx2 (osf2)	0.69	>0.05	essential transcription factor for osteoblast differentiation and bone formation
NM_008216	hyaluronan synthase 2	0.74	<0.05	with versican-like protein works to captures space destined to become bone
NM_007833	decorin	0.76	<0.025	binds to collagen and may regulate fibril diameter
NM_007431	alkaline phosphatase 2, liver	0.82	<0.05	essential for hydroxyapatite formation and matrix mineralization
BG092290	insulin-like growth factor 2 receptor	1.43	<0.025	signal transduction and hormone activity
NM_020275	tumor necrosis factor receptor superfamily, member 10b	1.43	<0.05	growth factor and cytokine activity
NM_010554	interleukin 1α	1.58	<0.05	potent stimulators of bone resorption
BM935811	integrin α6	2.47	<0.05	cell adhesion molecule
AK003744	cystatin E/M	3.45	<0.05	antagonist to cathepsin family

*Fold=RWV/static 1g
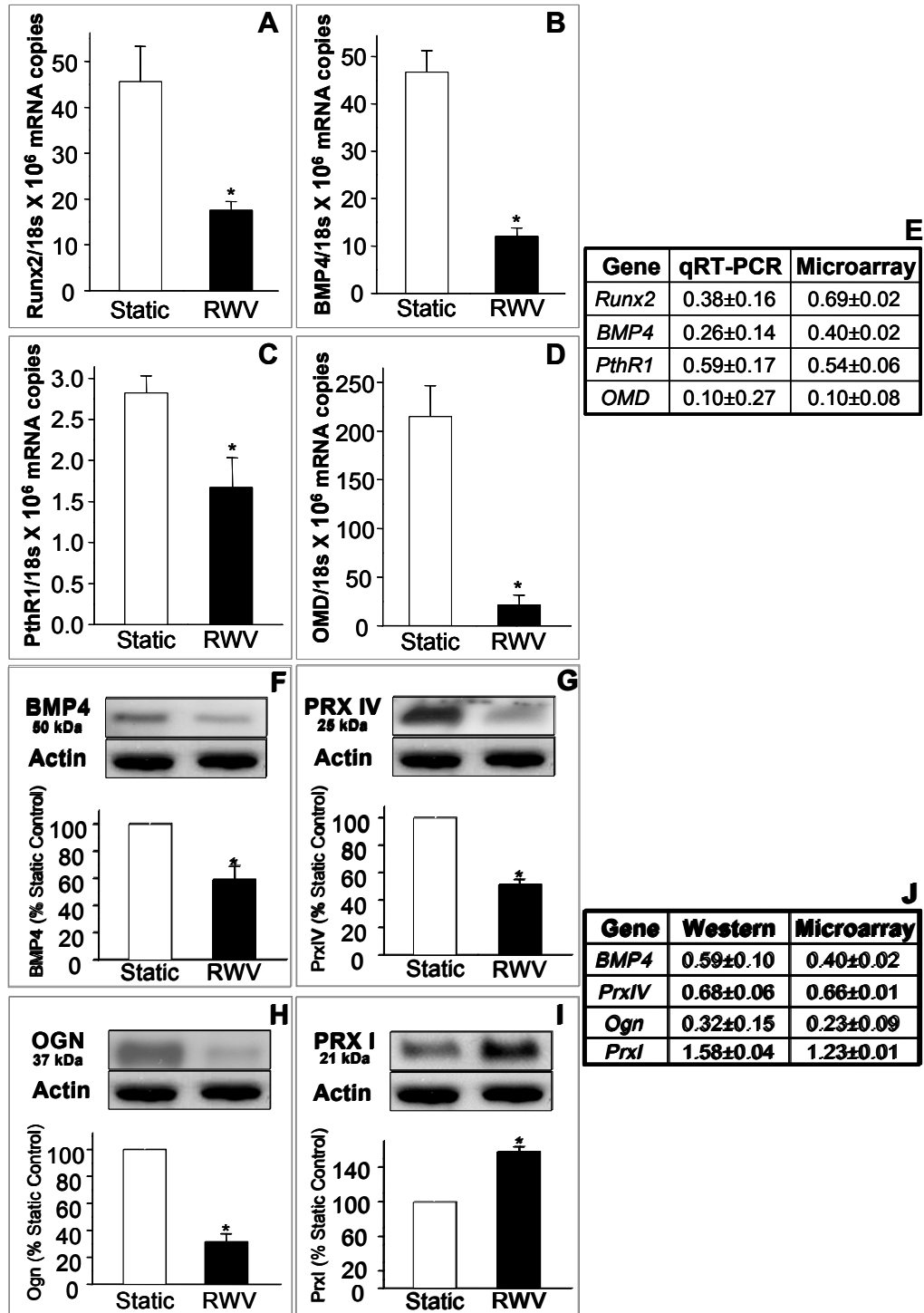
Figure 5.4 Verification of microarray results by real time PCR and immunoblot. Aliquots of total RNA used for the microarray studies (n=3) were used for real time RTPCR for *runx2* (A), *BMP4* (B), *PTHR1* (C), *and OMD (D)* using *18S* rRNA as an internal control. Additional experiments were performed to obtain cell lysate for immunoblots for BMP4 (F), PRXIV (G), OGN (H), and PRXI (I) using actin as an internal control. Also shown is the comparison of the microarray fold changes to the real time RTPCR (E) or immunoblot results (J). Data are shown as mean±SEM (n≥3, * p< 0.05).

5.4 A-E). Additionally, we confirmed the expression of downregulated genes *BMP4, peroxiredoxin IV (PRXIV),* and *osteoglycin (OGN)* and upregulated gene *peroxiredoxin I (PRXI)* by immunoblotting. The Affymetrix fold changes for *BMP4*, *PRXIV, OGN,* and *PRXI* were 0.40, 0.66, 0.23, and 1.23. We showed that the fold changes for the proteins by Western blot were 0.59, 0.68, 0.32, and 1.58, respectively (Figure 5.4 F-J). The different methodologies used, the microarray assay, real time RTPCR, and immunoblotting, produced highly consistent results, providing a level of assurance regarding the validity of the microarray data.

Comparison of the RPM and RWV microarrays revealed 17 genes that changed in the same direction.

There was a subset of genes that demonstrated similar expression changes when exposed to simulated microgravity or disuse using either the RPM or RWV. Table 5.3 displays the genes that changed statistically significantly with $p<0.05$, showing 16 downregulated genes and 1 upregulated gene in this group. Table 5.3 organizes the significant genes by biological process as defined by GoMiner and associates each gene with a molecular function, if known.

Comparison of the RWV and RPM microarrays to a mechanical loading microarray showed that three genes changed in opposite directions between disuse and mechanical loading.

Recently, Xing, et al. published microarray data on mouse tibiae that were mechanically loaded (29). Briefly, they loaded mice in a four point bending mechanical loading device for four days, and total RNA was obtained from the region of the mechanically stimulated tibia. The untreated tibiae of the same mice were used as unloaded controls, and a 22,000 gene Agilent Technologies microarray was utilized for

Table 5.3 A list of statistically significant common genes sensitive to disuse in 2T3 cells using both the RWV and the RPM. Genes are sorted based on typical biological process ($p<0.05$).

Accession #	Gene Name	*Fold Δ RWV	#Fold Δ RPM	Molecular Function
Cell Adhesion				
NM_012050	osteomodulin	0.10	0.18	aka osteoadherin, may mediate cell attachment
NM_007729	procollagen, type XI, alpha 1	0.37	0.29	extracellular matrix structural constituent
NM_012043	immunoglobulin superfamily containing leucine rich repeat	0.18	0.42	involved in cell attachment
AK004179	platelet-derived growth factor receptor-like	0.45	0.52	involved in cell attachment and possibly cell proliferation
Cell Cycle				
NM_011817	growth arrest and DNA damage inducible, gamma	0.40	0.49	structural constituent of ribosome
Development				
NM_009144	secreted frizzled-related sequence protein 2	0.43	0.41	transmembrane receptor and signal transduction activity
Regulation of Cell Growth				
NM_030127	serine protease	0.74	0.22	serine-type endopeptidase activity
NM_008760	osteoglycin	0.23	0.38	growth factor activity
Protein Biosynthesis				
NM_026631	nucleolar protein family A, member 2	1.69	2.04	RNA binding; structural constituent of ribosome
Transport				
AK018504	ras association (RalGDS/AF-6) domain family 2	0.27	0.43	protein binding
Cell Differentiation				
NM_025711	asporin	0.15	0.28	porin activity; cartilage extracellular protein
Metabolism				
NM_007934	glutamyl aminopeptidase	0.40	0.35	aminopeptidase activity
%NM_007431	alkaline phosphatase 2, liver	0.82	0.21	essential for hydroxyapatite formation and matrix mineralization
Skeletal Development				
NM_054077	proline arginine rich end leucine rich repeat	0.43	0.45	extracellular matrix structural constituent
%AF053954	cbfa1/runx2 (osf2)	0.69	0.53	essential transcription factor for osteoblast differentiation and bone formation
%NM_011199	parathyroid hormone receptor 1	0.54	0.20	transmembrane receptor activity
Unknown				
NM_021355	fibromodulin	0.45	0.45	unknown

*Fold= RWV/static 1g
#Fold=RPM/static 1g
%p<0.05 and/or fold change>2.0 as shown by RTPCR

the gene expression studies. We compared the RPM and RWV microarrays to their published data and found that three genes changed in opposite directions with p<0.05. Table 5.4 lists the three genes that were upregulated in mouse tibiae by mechanical loading and were downregulated in cells exposed to disuse. Since the experimental sample sizes (n=3 each) were relatively small, we also evaluated which genes changed commonly in both simulators and opposite to mechanical loading with less stringent p-value cutoffs (p<0.1). Under this non-stringent condition, we found that there were an additional 13 genes that changed in opposite directions as shown in Table A.3.

Table 5.4 Comparison of gene expression changes among RWV, RPM, and mechanical load microarrays. Sorted by biological process.

Accession #	Gene Name	Fold Δ RWV	p-value RWV	#Fold Δ RPM	p-value RPM	*Fold Δ in vivo	p-value in vivo	Molecular Function
Cell Growth & Differentiation								
AK014259	*osteoglycin*	0.22	p<0.05	0.38	p<0.005	2.47	p<0.005	binds to TGF-Beta
Proteolysis								
NM_008788	*procollagen C-proteinase enhancer protein*	0.56	p<0.01	0.52	p<0.05	2.15	p<0.005	nucleic acid binding
Other								
AK004179	*platelet-derived growth factor receptor-like*	0.45	p<0.005	0.52	p<0.05	2.18	p<0.005	receptor activity

#RPM data previously published (19)
*in vivo refers to mechanical loading data previously published (29)

Discussion

We have previously shown that exposure of 2T3 cells grown in Opticell disks to the RPM inhibits ALP activity while gene transcript studies scanning 10,000 mouse genes produced a list of 52 upregulated and 88 downregulated genes altered by more than two-fold compared to the static 1g control (19). Here, we used a distinct approach to expose 2T3 cells to simulated microgravity using the RWV, which maintains the cells in continuous free-fall in culture medium, mimicking a disuse condition. The RWV is a

bioreactor developed by NASA and most commonly used in the United States (17, 21, 22). In contrast, the RPM has been developed by the Japanese and the European Space Agency and is used mostly by scientists outside of the United States, with the exception of our group (4, 6, 19). Unlike the RPM system where the cells were attached to OptiCell membranes and exposed to disuse conditions, the RWV does not have a similar platform and adherent cells have to be grown on microcarriers for exposure to the RWV. Given the need for validated ground-based microgravity simulators, it is imperative that these simulators be compared not only to each other but also to other *in vivo* mechanical loading and unloading systems.

To compare the results of the RWV to those published with the RPM, we aimed to feasibly match the conditions between the two experiments. Most importantly, we found that exposure of 2T3 cells to either the RPM or RWV produced a similar inhibitory effect on ALP enzyme activity. These results suggest that the RPM and RWV inhibit cell differentiation of preosteoblasts, a finding that is consistent with the expected disuse- or microgravity-induced decrease in bone mass.

Previously, it has been controversial whether the RWV decreased or increased ALP activity, but this may be due to a difference of whether the cells were grown as attached or suspended cultures. In one study, Rucci, et al. found that *ALP* activity and mRNA expression increased when exposed to the RWV for two days using a rat osteoblast-like cell line that was grown as aggregate suspension (21). In contrast, Klement, et al. showed that exposure to the RWV for up to 14 days blunted ALP activity and bone matrix mineralization of mouse embryonic pre-metatarsal tissue explants (10). It should be noted that in the Klement et al. study, the cells comprising the bone explants were still attached to the extracellular matrix within the embryonic bone tissues. Similarly, in our current RWV and the previous RPM study, preosteoblasts were grown as adherent cells either on microcarriers or on the OptiCell membranes before and

during exposure to the simulators. These results suggest that the inhibitory effect of the RWV and RPM on the osteoblast function requires bone cells grown in adherent conditions during exposure to simulated microgravity or disuse conditions. Additionally, our finding partially validates and supports the use of ground-based simulators to study disuse- or microgravity-induced changes in bone cell biology and pathology.

We also performed gene microarray analysis to determine changes in gene expression profiles of the preosteoblasts and compared the results to our published findings with the RPM. We found that 17 genes changed in the same manner, and many of these genes are involved in skeletal remodeling. For example, we confirmed expression levels of *runx2,* which was downregulated by approximately 1.5-fold, and is believed to be a "master gene" that plays a critical role in the formation of the skeleton. When *runx2* is genetically knocked out in a mouse model, there is a complete lack of skeleton formation (8, 11). Additionally, we confirmed the downregulation of *PTHR1* levels by the RWV. A decrease in parathyroid hormone related protein, which plays a role in calcium mobilization, has been linked to decreases in bone density and subsequent bone loss in space-flown rats (26). *OMD* belongs to the SLRP family and may be involved in bone matrix formation (2), and simulated microgravity- or disuse-induced decrease in *OMD* is consistent with our hypothesis.

Furthermore, we confirmed the downregulated expression levels of *BMP4*, which is involved in skeleton development, including cartilage formation and various joint developments (27, 28). Moreover, oxidative stress is involved in the etiology of various pathologies, and oxidants are produced under physiological conditions during phagocytosis by macrophages, mitochondrial electron transport, and bone resorption by osteoclasts (13). Bone resorption is known to increase beyond normal physiological levels in spaceflight (23), potentially increasing the levels of oxidative stress in the human body. Peroxiredoxins are a family of antioxidants that are often made by cells in

response to oxidant production. It has been found that *PRXI* is upregulated during bone cell differentiation (9, 13). We found that PRXI protein level was upregulated while PRXIV protein was downregulated by the RWV, corroborating with gene expression data from the microarray. These peroxiredoxins may play a differential role in the cells attempting to compensate for changes in oxidative state.

To further investigate the functional significance of the disuse-associated changes in gene expression, we compared our microarray results to independently published data from mechanically loaded tibiae in a mouse model (29). When we compared their gene expression results to those of the RPM and RWV microarrays, we found three genes that were upregulated by mechanical loading and were contrastingly downregulated by disuse conditions. Also, when less stringent statistical p-values were applied, we found 13 additional genes displaying the same trends. For example, *OGN* was downregulated by the RPM and RWV but upregulated by mechanical loading. *OGN* is a small leucine-rich proteoglycan found in the extracellular matrix of bone, and knockout mice for this gene display collagen fibril diameter abnormalities (25). These comparisons suggest that a subset of the genes in 2T3 cells are mechanosensitive and may be implicated in microgravity- or disuse-induced decreased bone mass. Microgravity occurring during spaceflight is characterized as an environment in which the human body is no longer loaded as on Earth, and disuse due to long term illness or paraplegia dramatically reduces the normal loading on the body. Therefore, it is interesting that many genes that are changed by increased mechanical loading are also changed in the opposite direction by "unloading".

The widely accepted model of animal-based simulated microgravity or disuse is the rodent hindlimb unloading (HLU) experiment. To date, there has not been a large scale gene expression study performed from bones of animals exposed to HLU. However, there have been a few small scale studies investigating specific gene

expression. After four days of HLU using BALB mice, two independent studies found decreases in *type I collagen, osteonectin, osterix, and matrix metalloproteinase 2 (MMP2)* (7, 32). However, in both the RWV and RPM, the expression levels of these genes did not reach statistical significance but did show a trend towards decreased expression.   Additionally, Judex et al. found no change in *cathepsin K (ctsk)* due to HLU exposure while the RPM increased it and the RWV did not alter it. As well, Judex et al. showed no change in *runx2*, which was decreased by both the RWV and RPM (7). Moreover, Zhong, et al. showed that *ALP* expression decreased with HLU exposure, corroborating with the RWV and RPM results (32). Recently, Hughes-Fulford, et al. examined the effects of spaceflight microgravity with or without a centrifugal 1g field intervention on the expression of 24 genes in MC3T3-E1 preosteoblasts (5). In this study, there was a significant reduction in expression of genes such as *cyclooxygenase 2 (cox-2), transforming growth factor beta 1 (TGFβ1), fibroblast growth factor 2 (fgf-2),* and *osteocalcin (OCN)* with exposure to spaceflight microgravity (5). In comparison, *TGFβ1* expression was downregulated by the RWV, comparable to spaceflight, but it was upregulated by the RPM. Additionally, *prostaglandin E1 (EP1)* was not altered in spaceflight, corroborating with the RPM data, but the RWV upregulated its expression. Furthermore, spaceflight did not alter *cyclin A, cyclin E, actin, or fibronectin*, which correlates to both the RWV and RPM microarray data.   Our detailed large scale gene expression studies and comparisons may allow investigators the information needed to select specific genes on which to focus, potentially narrowing the pool of therapeutic targets for bone loss.

In conclusion, we have shown that the two different simulators of microgravity or disuse conditions produce similar results with regard to bone cell differentiation and osteoblast function. We have shown that both simulators reproduce a decreased bone formation response as also seen in spaceflight. Furthermore, we have compiled a short

list of genes that change in response to the two different types of disuse conditions and to mechanical loading, which may serve as specific targets for interventions to prevent decreased bone mass in spaceflight, disuse, or osteoporosis.

References

1. **Boo YC, Sorescu G, Boyd N, Shiojima I, Walsh K, Du J, and Jo H.** Shear stress stimulates phosphorylation of endothelial nitric-oxide synthase at Ser1179 by Akt-independent mechanisms: role of protein kinase A. *J Biol Chem* 277: 3388-3396, 2002.

2. **Buchaille R, Couble ML, Magloire H, and Bleicher F.** Expression of the small leucine-rich proteoglycan osteoadherin/osteomodulin in human dental pulp and developing rat teeth. *Bone* 27: 265-270, 2000.

3. **Carmeliet G and Bouillon R.** The effect of microgravity on morphology and gene expression of osteoblasts in vitro. *FASEB J* 13: 129-134, 1999.

4. **Hoson T.** Evaluation of the three-dimensional clinostat as a simulator of weightlessness. *Planta* 203: S187-197, 1997.

5. **Hughes-Fulford M, Rodenacker K, and Jutting U.** Reduction of anabolic signals and alteration of osteoblast nuclear morphology in microgravity. *J Cell Biochem*, 2006.

6. **Huijser RH.** Desktop RPM: New Small Size Microgravity Simulator for the Bioscience Laboratory. Fokker Space, 1-5, 2000.

7. **Judex S, Zhong N, Squire ME, Ye K, Donahue LR, Hadjiargyrou M, and Rubin CT.** Mechanical modulation of molecular signals which regulate anabolic and catabolic activity in bone tissue. *J Cell Biochem* 94: 982-994, 2005.

8. **Katagiri T and Takahashi N.** Regulatory mechanisms of osteoblast and osteoclast differentiation. *Oral Dis* 8: 147-159, 2002.

9. **Kawai S, Takeshita S, Okazaki M, Kikuno R, Kudo A, and Amann E.** Cloning and characterization of OSF-3, a new member of the MER5 family, expressed in mouse osteoblastic cells. *J Biochem (Tokyo)* 115: 641-643, 1994.

10. **Klement B, Young Q, George B, and Nokkaew M.** Skeletal tissue growth, differentiation and mineralization in the NASA rotating wall vessel. *Bone* 34: 487-498, 2004.

11. **Komori T, Yagi H, Nomura S, Yamaguchi A, Sasaki K, Deguchi K, Shimizu Y, Bronson RT, Gao YH, Inada M, Sato M, Okamoto R, Kitamura Y, Yoshiki S, and**

Kishimoto T. Targeted disruption of Cbfa1 results in a complete lack of bone formation owing to maturational arrest of osteoblasts. *Cell* 89: 755-764, 1997.

12.	**Lang T, LeBlanc A, Evans H, Lu Y, Genant H, and Yu A.** Cortical and trabecular bone mineral loss from the spine and hip in long-duration spaceflight. *J Bone Miner Res* 19: 1006-1012, 2004.

13.	**Li B, Ishii T, Tan CP, Soh JW, and Goff SP.** Pathways of induction of peroxiredoxin I expression in osteoblasts: roles of p38 mitogen-activated protein kinase and protein kinase C. *J Biol Chem* 277: 12418-12422, 2002.

14.	**Li C and Wong WH.** Model-based analysis of oligonucleotide arrays: Expression index computation and outlier detection. *PNAS* 98: 31-36, 2001.

15.	**Li C and Wong WH.** Model-based analysis of oligonucleotide arrays: model validation, design issues and standard error application. *Genome Biology* 2: research0032.0031 - research0032.0011, 2001.

16.	**Nakamura H, Kumei Y, Morita S, Shimokawa H, Ohya K, and Shinomiya K.** Suppression of osteoblastic phenotypes and modulation of pro- and anti-apoptotic features in normal human osteoblastic cells under a vector-averaged gravity condition. *J Med Dent Sci* 50, 2003.

17.	**Ontiveros C, Irwin R, RW, and McCabe L.** Hypoxia Suppresses Runx2 Independent of Modeled Microgravity. *J Cell Physiology* 200: 169-176, 2004.

18.	**Ontiveros C, McCabe, Laura R.** Simulated microgravity suppresses osteoblast phenotype, Runx2 levels and AP-1 transactivation. *Journal of Cellular Biochemistry* 88: 427-437, 2003.

19.	**Pardo SJ, Patel MJ, Sykes MC, Platt MO, Boyd NL, Sorescu GP, Xu M, van Loon JJWA, Wang MD, and Jo H.** Simulated microgravity using the Random Positioning Machine inhibits differentiation and alters gene expression profiles of 2T3 preosteoblasts. *Am J Physiol Cell Physiol* 288: C1211-1221, 2005.

20.	**Pellis NR, Goodwin TJ, Risin D, McIntyre BW, Pizzini RP, Cooper D, Baker TL, and Spaulding GF.** Changes in gravity inhibit lymphocyte locomotion through type I collagen. *In Vitro Cell Dev Biol Anim* 33: 398-405, 1997.

21.	**Rucci N, Migliaccio S, Zani BM, Taranta A, and Teti A.** Characterization of the osteoblast-like cell phenotype under microgravity conditions in the NASA-approved Rotating Wall Vessel bioreactor (RWV). *J Cell Biochem* 85: 167-179, 2002.

22.   **Schwarz RP, Goodwin TJ, and Wolf DA.** Cell culture for three-dimensional modeling in rotating-wall vessels: an application of simulated microgravity. *J Tissue Cult Methods* 14: 51-57, 1992.

23.   **Smith S, Wastney M, O'Brien K, Morukov B, Larina I, Abrams S, Davis-Street J, Oganov V, and Shackelford L.** Bone markers, calcium metabolism, and calcium kinetics during extended-duration space flight on the mir space station. *J Bone Miner Res* 20: 208-218, 2005.

24.   **Sorescu GP, Sykes M, Weiss D, Platt MO, Saha A, Hwang J, Boyd N, Boo YC, Vega JD, Taylor WR, and Jo H.** Bone Morphogenic Protein 4 Produced in Endothelial Cells by Oscillatory Shear Stress Stimulates an Inflammatory Response. *J Biol Chem* 278: 31128-31135, 2003.

25.   **Tasheva E.** Mimecan/osteoglycin-deficient mice have collagen fibril abnormalities. *Molecular Vision* 8: 407-415, 2002.

26.   **Torday JS.** Parathyroid hormone-related protein is a gravisensor in lung and bone cell biology. *Adv Space Res* 32: 1569-1576, 2003.

27.   **Tsumaki N, Nakase T, Miyaji T, Kakiuchi M, Kimura T, Ochi T, and Yoshikawa H.** Bone morphogenetic protein signals are required for cartilage formation and differently regulate joint development during skeletogenesis. *J Bone Miner Res* 17: 898-906, 2002.

28.   **Wijgerde M, Karp S, McMahon J, and McMahon AP.** Noggin antagonism of BMP4 signaling controls development of the axial skeleton in the mouse. *Dev Biol* 286: 149-157, 2005.

29.   **Xing W, Baylink D, Kesavan C, Hu Y, Kapoor S, Chadwick RB, and Mohan S.** Global gene expression analysis in the bones reveals involvement of several novel genes and pathways in mediating an anabolic response of mechanical loading in mice. *Journal of Cellular Biochemistry* 9999: n/a, 2005.

30.   **Zayzafoon M, Gathings WE, and McDonald JM.** Modeled microgravity inhibits osteogenic differentiation of human mesenchymal stem cells and increases adipogenesis. *Endocrinology* 145: 2421-2432, 2004.

31.   **Zeeberg B, Feng W, Wang G, Wang M, Fojo A, Sunshine M, Narasimhan S, Kane D, Reinhold W, Lababidi S, Bussey K, Riss J, Barrett J, and Weinstein J.** GoMiner: a resource for biological interpretation of genomic and proteomic data. *Genome Biology* 4: R28, 2003.

32.   **Zhong N, Garman RA, Squire ME, Donahue LR, Rubin CT, Hadjiargyrou M, and Judex S.** Gene expression patterns in bone after 4 days of hind-limb unloading in two inbred strains of mice. *Aviat Space Environ Med* 76: 530-535, 2005.

Chapter 6

Bone Adaptation to the Mechanical Environment:
High vs. Low Impact Loading

"Every change in the form and function of bone or of their function alone is followed by certain definite changes in their internal architecture and equally definite alteration in their external conformation, in accordance with mathematical laws."
—J. Wolff, 1892 (38)

Summary

From specific aims 1 and 2, we showed that mechanical unloading altered cellular and molecular responses in osteoblasts. We established an *in vitro* model system to study disuse and provided a relatively short list of genes that may be significant in bone loss pathologies. In specific aim 3, it is our goal to both to expound the mechanism driving *in vivo* bone adaptation to extremely low magnitude and high frequency (LMHF) mechanical loading and explore its use as a novel countermeasure device for bone loss in spaceflight. In the next two chapters, we provide background on bone adaptation at the macroscopic and microscopic levels to support specific aim 3, which will be discussed in Chapter 8.

High impact mechanical stimulation such as exercise is often classically regarded as an anabolic signal to instigate bone remodeling. The theory that normal bone adapts to its mechanical environment dates back to Julius Wolff (1892), who was the first to suggest that stress imparted to bone impacted its architecture (38). Harold Frost (1987) elucidated the role of a mechanical stimulus to bone (8, 10) by

defining a minimum effective strain that was required from the stimulus in order to stimulate bone adaptation. Frost defined the mechanostat as the biological machinery that determines bone strength (7). In this chapter, we review bone adaptation to alterations in mechanical loading at the macroscopic level, focusing on the impact of exercise versus externally applied LMHF loading.

General Bone Adaptation

One of the primary functions of bone is providing mechanical integrity for both protection and locomotion. Bone adaptation is the inherent change in bone mass and architecture in response to strain induced by mechanical loads. Three rules govern bone adaptation as follows: 1) adaptation is driven by a dynamic stimulus, 2) adaptation requires only a relatively short duration of loading, and 3) bone cells become accustomed to routine mechanical loading (35). The response of bone to loading or unloading is dependent on both genetic and epigenetic factors. While genetics outlines the general shape, length, and architecture, changes in mechanical environment elicit adaptive responses. According to Wolff's law, bone architecture is defined by mathematical laws, which state that thickness, number, and distribution of trabeculae must correspond to distribution of mechanical stresses, and the trabeculae should be loaded axially in compression and tension (35, 38). It was later elucidated that strain resulting from mechanical stress itself could cause adaptive responses, and Frost defined a minimum effective strain that had be induced to instigate such a response (9). Additionally, it was shown that bone responded to dynamic and not static strain (29). These findings regarding bone adaptation have been formed into mathematical laws, calculating that a strain stimulus is a function of both strain magnitude and frequency. Since strain loading is dynamic, the strain stimulus can be defined using the Fourier method as shown in equation 6.1:

$$E = k_1 \sum_{i=1}^{n} \epsilon_i f_i$$

6.1

where E=strain stimulus, k=proportionality constant, ε=peak to peak strain magnitude, and f=frequency. This equation is critical in bone adaptation because it dictates that a static load would not cause a response since $f = 0$ and that adaptation is proportional to strain magnitude. However, it should be noted that this model predicts a linear relationship between strain magnitude and frequency, and it is well known that biology seldom encompasses precise linearity.

Strain is defined as a change in length relative to the object's original length, and it is widely accepted that strain is a means by which a mechanical force is translated into a signal that can be recognized by the mechanotransduction machinery of the body (22). Both the intensity and duration of the load play critical roles in defining adaptation to mechanical deformation. To avoid failure, the applied load must not induce strain beyond the bone tissue yield, and this level has been measured to be over 0.7% or 7000 microstrain (με) (22). To determine functional strain levels in bone, strain gauges have been inserted *in vivo* in a host of animals, including dog, pig, turkey, sheep, and horse, and strain was measured during physical activity such as galloping or trotting. Remarkably, regardless of size, the maximum peak strain was measured to be within the range of 2000-3000 με for all animals, and this species-independent uniform peak strain is a concept called dynamic strain similarity (DSS) (29). DSS states that peak functional strain is independent of body size and species type, and evolution has defined a safety factor

117

of 2-3 between functional and yield strain such that activity elicits a specific strain level to bone tissue for homeostatic skeletal response (29). It is possible that the peak strain magnitude is similar in animals of disparate size because larger animals have evolved such that weight-related axial stress in the bone is decreased during movement at the expense of decreased agility. For example, a fish can rapidly swim and immediately change course of direction more simply than an elephant (29). For humans, a strain of 3000 $\mu\varepsilon$ for a femur of approximate length of 45 cm (17.7 in) elicits a change in length on the order of magnitude of 1 mm (~0.039 in). If bone cells are responsible for sensing and responding to this strain, which would only be on the order of angstroms relative to the length of a cell, the mechansensory system must be extremely sensitive to generate an adequate adaptive reaction.

In mechanical testing of bone, diverse loading conditions have been used to assess bone properties. Previous studies have shown that in cortical bone tissue, application of 2000 $\mu\varepsilon$ at a frequency of 0.5 Hz maintained bone mass (31, 33). According to equation 1, a similar response should be observed if the frequency was increased to 10 Hz and strain decreased to 100 $\mu\varepsilon$. This trend bound by equation 6.1 was observed experimentally when the frequency was increased to 1 Hz and only a strain of 1000 $\mu\varepsilon$ was needed to maintain bone mass. Further, at a frequency of 30 Hz, only 70 $\mu\varepsilon$ was needed to inhibit bone resorption (32, 33). Thus, bone response to mechanical signals seems to correlate to increased frequency, meaning smaller strains induced by a lower force applied more frequently is ample to stimulate bone formation and maintain bone mass.

Bone adaptation occurs at both the macroscopic and microscopic levels, altering bone mass and architecture to maintain mechanical integrity for posture control and movement. It has been well accepted that high impact activity improves skeletal mass while disuse impedes it. It is also well known that muscle strength

greatly impacts bone health as muscles constantly strain bone, causing adaptive responses within them. In the following sections, we review the accumulating evidence that exercise and muscle contraction both benefit the musculoskeletal system, despite delivering disparate signals to bone.

Exercise: High Magnitude and Low Frequency

Osteopenia is a condition of decreased bone mass, and when bone mass has reduced to the point of fracture risk, the condition is called osteoporosis. It is clear that there is an abundance of data suggesting that exercise promotes skeletal benefits, and the variation among studies is partially due to the type of exercise tested, patient population, and data analysis. However, there remains a common conclusion in the vast majority of studies that exercise provides skeletal benefit, albeit sometimes site-specific.

Exercise or physical activity beyond normal, daily routine exists in copious forms and induces distinct loads on the body. For instance, walking imposes a load of 1g (1 times body weight) while running increases the load to 3-4g, and jumping hurdles further augments the loading to 5g (21). Exercise can be regarded as a high magnitude (greater than 1g) and low frequency (1-2 Hz) impact. The benefits of exercise have been inexorably tested, documented, and relayed to the general public, and it has been shown to increase bone and muscle mass (11, 34, 36). The last two decades have provided insight into exercise intervention trials in the normal population, beyond that of comparing elite athletes to sedentary controls. The exercise regimes in these experiments ranged from aerobic versus stretching control to high weight and low repetition resistance weight training versus low weight and high repetition weight training. Subjects varied within a gamut of ages from a young 10 years to post-menopausal women over 50 years old. Studies continued for at

least eight months and used bone mineral density (BMD) as a marker of skeletal improvement.

In one study involving young women ages 20-35, researchers investigated the use of exercise and calcium supplementation on peak bone mass. These women were divided into an exercise group consisting of weight training combined with aerobic activity or a stretching control group. After two years of exercise or control, there was a significant increase in BMD in the spine, femoral neck and trochanter, and calcaneus due to exercise, but calcium supplementation did not improve BMD in any tested location (5). In another study with post-menopausal women, researchers explored the effects of resistance training (high load, low repetitions) versus endurance training (low load, high repetitions) on bone mass in the forearm and hip. After one year of exercise intercession, there were significant increases in BMD at the femoral trochanter in the hip and the distal radius of the arm with resistance training while endurance training only improved mid-radius BMD. Using the one repeat maximum (1-RM) method, the researchers also found that muscle strength increased in both groups. The study concluded that the peak load was more important than the number of repetition cycles to increase bone mass in early post-menopausal women (18). In another study of pre-menopausal women (age range of 28-39 years), subjects were assigned to exercise or non-exercise control groups and monitored for 1.5 years. The exercise group showed an increase in femur trochanter BMD by one year but no change in total, arm, or leg BMD compared to control. In addition, they used the 1-RM method to evaluate muscle strength and found a 58% increase in the exercise group when compared to baseline and no increase in the control group (20).

However, not all studies have reported increases in BMD at the femur, a site at which many fractures occur in osteoporotic patients. One study explored whether

aerobic or weight training benefited the skeletal system in young college-aged women (mean age 19.9 years) over an eight month period. They found increases in spine lumbar BMD in both running and weight training groups compared to a non-exercise control group but no significant changes at the hip (34). In another study evaluating the effects of jumping in pre- and post-menopausal women, the subjects were assigned to perform 50 vertical jumps for six times per week. Mechanical loads induced to the joints were measured by ground reaction forces, amounting to 3g/jump for pre-menopausal women and 4g/jump for post-menopausal subjects. After five months, there was a 2.8% increase in BMD at the femur in the pre-menopausal group but no change in the post-menopausal women after one year or 1.5 years (2). Thus, there was a clear benefit for younger women but not older, post-menopausal subjects.

It is clear that there is an abundance of data suggesting that exercise promotes skeletal benefits, and the variation among the studies is probably partially due to the type of exercise tested. These discrepancies allow for appreciation of the complex nature of mechanical loading and subsequent bone adaptation. For example, during jumping, there is loading due to absorption of the impact as well as muscle-generated forces applied to the bone. In gymnasts, dismounting from the parallel bars stimulates an immense load amounting to approximately 11g, which partially expounds why gymnasts encompass a hip BMD greater than other athletes (21, 23). However, in the Bassey study, jumping applied no more than 4g reaction forces to the joints of the subjects, equivalent to forces from running (2). Running has been generally shown to not improve femur BMD, and thus, in this study, the pre-menopausal women probably achieved increased femoral BMD because of strain induced by muscle-derived tension to the bone rather than impact (21). However, with the complexity of mechanical loading and bone adaptation, there is

most likely a host of other reasons as to why lower impact did not improve BMD in older women but did in younger women. We can only surmise conclusions from the clinical data available and continue to investigate other treatment options for bone loss.

It is generally well accepted that the growing skeleton is most likely to benefit from exercise as bone modeling and remodeling ensure optimal mechanical properties of bone, removing old, aged bone and replacing it with new, stronger bone. Exercise during childhood assists in the acquisition of bone as well as remodeling its architecture. It has been shown that tennis players who began training during childhood had increased BMD, bone mineral content, and cortical wall thickness compared to players who began playing during adulthood (15). Furthermore, a study investigating the effects of exercise on pre-pubertal young boys (mean age 10.4 years) found that not only did the BMD of all boys increase over the course of the study as expected but also physical education intervention for eight months increased BMD twice that of controls in the exercise group. The researchers concluded based on all parameters measured that exercise before puberty may increase femur volumetric BMD by increasing cortical thickness (3).

Mounting data as summarized in Table 6.1 makes it quite lucid that exercise provides benefit to the musculoskeletal system, despite the variation among clinical trials. There is currently no defined exercise regime that seems to be best suited for improving bone mass, and if the field of research can adequately compare premium exercise routines for various age groups, this would be beneficial to the general public.

Table 6.1 Summary of exercise studies

Subjects	Stimulation	Length	Result	Ref
Boys, 10 yr, pre-puberty	Regular P.E. class with various exercises	8 mos.	Increase in BMD in all subjects; 2-fold further increase in exercise group	Bradney
Women, 20-35 yr, pre-menopausal	Exercise+Calcium, Aerobic exercise, stretching control	2 yrs.	Increase in BMD in spine, femoral neck and trochanter, calcaneus; No effect of calcium	Friendlander
Women, 20 yr, pre-menopausal	Aerobic vs resistance training	8 mos.	Increase in spine lumbar BMD in both groups; no changes in femur at hip	Snow-Harter
Women, 28-39 yr, pre-menopausal	Resistance exercise vs. non-exercise	1.5 yrs.	Increase in femur trochanter BMD in 1 yr but no change in total, arm, or leg BMD; Increased muscle strength by 1-RM method	Lohman
Women, post-menopausal	Resistance (high load, low reps) and endurance (low load, high reps)	1 yr.	Increase in BMD at femoral trochanter and distal radius with resistance; Increase in radius BMD in endurance; Peak load more important than frequency	Kerr
Women, pre- and post-menopausal	50 vertical jumps 6X/week 3g in pre-menopausal and 4g in post-menopausal	5-18 mos.	2% increase in BMD at femur in pre-menopausal but not post-menopausal group; Gymnasts 11g and have high hip BMD; Perhaps muscle-derived tension played larger role than impact	Bassey

Muscle Contraction: Low Magnitude and High Frequency

As humans age, the harsh effects of high impact exercise becomes a burden that the ailing mature skeleton can no longer efficiently tolerate. While several factors dictate osteoporosis, the pathology is exacerbated by increased age, coinciding with decreased muscle strength and posture stability. As ageing continues, there is a drastic degeneration in muscle strength (sarcopenia), leading to decreases in muscle-bone movement. Thus, the elderly population is prone to accidental falls and subsequent injury, leading to bone fractures. At each joint in the body, muscles apply forces to attached bones such that these signals are fired rapidly at low level movements that are imperceptible at the macroscopic level. Muscle contractions are constantly applied to the bone in everyday tasks such as maintaining posture while standing or sitting (25). As muscle atrophies with age,

these signals to the skeleton also diminish. The notion of stimulating bone formation or inhibiting bone resorption in patients with musculoskeletal diseases such as cerebral palsy (14, 37), osteopenia (33), and post-menopausal osteoporosis (24) with a low magnitude (0.1-0.4g) and high frequency (30-90Hz) mechanical load is a new, non-invasive treatment ideal for elderly patients or those with a disability that would inhibit them from high impact exercise. It has been shown through animal and clinical trials that a LMHF mechanical stimulation is anabolic to bone (17, 24, 26-28, 37). Although not yet experimented in space, this potential osteoporosis countermeasure may provide benefit to the musculoskeletal system in a microgravity environment.

While impact from exercise induces strain levels of 2000-3000 με, muscle contractions inflict strains much lower in magnitude on the order of 10 με. With conventional thought, these strains would not be hypothesized to play a role in regulating bone adaptation, growth, or remodeling. However, as discussed earlier, equation 6.1 demonstrates that a lower peak-to-peak strain fired more frequently could provide a strain stimulus capable of inducing an adaptive response. Previous studies have been performed to log the strain history of bone in various animals, defining specific features such as peak magnitudes and frequencies over a specified time range (6). It is classically thought that the peak strain magnitudes during high impact activities have the largest effect on bone response, leading to many strain gage analyses of bone centered on maximum strains (4, 19, 30). These peak strains have been shown to be non-uniformly located over the cortex of the bone (30), meaning not all bone cells sense the same strain. Moreover, these peak strains are only experienced for short periods of the day, leaving the majority of the strain history to be defined by other strain magnitudes. In fact, in a turkey model, the maximum peak strain movements lasted for a total of 2 minutes/day, consisting of wing flaps or

body shakes. However, turkey bones are still well adapted and strong enough to support flight, suggesting that other portions of the strain history must be involved in bone adaptation (1).

The vast majority of the strain history of various animals encompasses low level strains from long periods of standing or sitting. In fact, standing intervention for 3 hours/day during bed rest prevented bone loss, suggesting that the effect of muscle contractions needed for postural stability aided in preventing bone loss (16). Studies performed in sheep showed that low magnitude strains were experienced frequently (Figure 6.1, left) in the range of 40 Hz (Figure 6.1, middle). In another study examining the strain history in three distinct species, *in vivo* bone strains were recorded from the weight-bearing tibia of an adult dog, turkey, and sheep and non-weight bearing ulna of turkey. They found that over the course of 12-24 hours, the turkey ulnae had strains of 1000 με once per day, 100 με about 100 times/day, and 5 με thousands of times per day as seen in Figure 6.1 (right). In the tibia, all three animals had one event of 1000 με, more events at 100με than the ulnae, and thousands of events at <10με as depicted in Figure 6.1 (right). Animals were videotaped to correlate the type of movement to points in the strain history, and walking induced the maximum strain from -1500 to 1000 με in the turkey tibia at a frequency of 0.6 Hz but a continued strain history through 40 Hz. Standing caused strains of ±10 με at a frequency of 40 Hz (6).

These studies show that a dominant contributor to the strain history recordings is non-vigorous activity, where muscle contraction is required during activities such as standing. As such, the question is whether these low magnitude strains impact bone remodeling and adaptation. Subsequent investigations have shown the utility of these low level signals in bone adaptation in a host of subjects, preventing or normalizing bone loss. In growing BALB mice, 0.3g mechanical
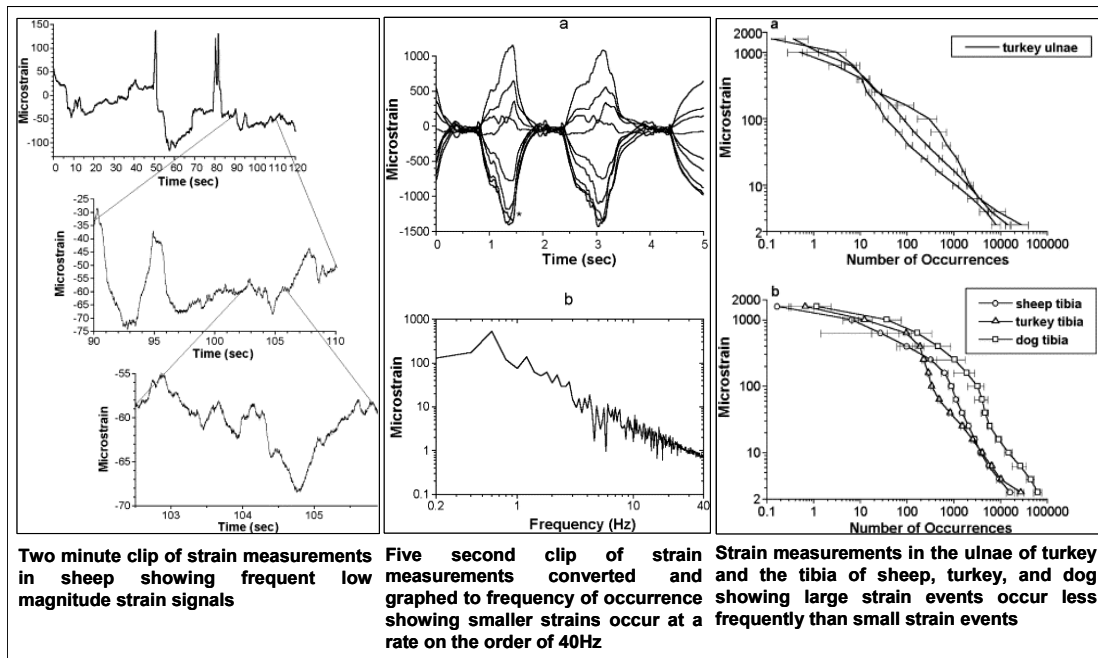
Figure 6.1 Strain history recordings of various animals during normal daily activities. These data show that low strain movements occur (left) in the frequency range of 40Hz (middle) more frequently than peak strain movements (right) (6). (Figure printed with permission from *Journal of Biomechanics*)

loading at 45Hz induced strain oscillations of 10 µε on the periosteal surface of the tibia as measured by *in vivo* strain gages. After treatment for three weeks for 15 minutes/day, there was a decrease in osteoclast activity compared to age-matched controls while bone formation rates (BFR) in the trabecular bone and mid-diaphyseal cortical bone were unchanged (39). However, BFR in the endocortical surface of the metaphysis was increased in this study (39) while cortical bone has also been shown to not respond to these signals in other studies (26) . Total body mass, bone length, and matrix composition were not negatively altered by the LMHF load (39). In another study, the left tibias of wildtype C57BL/6J mice were exposed to 0.3g or 0.6g loading at 45 Hz for 10 minutes/day while the right tibia acted as an internal control. Strain levels were as low as 3 µε, and after three weeks of 0.3g or 0.6g loading,

126

there was an increase in trabecular BFR in the metaphysis. Bone morphology in the epiphysis was altered by increased cortical area and thickness (12). Furthermore, the effects of LMHF loading on bone adaptation caused by disuse were investigated using the hindlimb unloading (HLU) model. Adult BALB mice were exposed to 0.3g load at 45 Hz for 10 minutes/day for a total of four or 21 days. There was a decrease in BFR due to HLU and an increase due to LMHF loading after 21 days treatment in both trabecular and cortical surfaces. After four days, there were decreases in gene expression for several genes, including *type 1 collagen, osterix, matrix metalloproteinase protein 2 (MMP2)*, and *osteonectin* due to HLU. There was no change in expression at four days due to LMHF loading; however, after 21 days, there were increases in *inducible nitric oxide synthase (iNOS), MMP2, receptor activator of the nuclear factor κB (RANKL),* and *type I collagen*. There were no changes due to HLU or LMHF loading in *cathepsin K (ctsk)*, *runt homology domain transcription factor 2 (cbfa1/runx2),* or *MMP9* gene expression after four or 21 days (17).

Studies involving LMHF loading then advanced to rat models, and in one study, adult rats were subjected to control, LMHF mechanical stimulation, disuse by HLU, HLU intervened by LMHF loading for 10 minutes/day, or HLU intervened with normal weight bearing for 10 minutes/day. After 28 days, there was an increase in BFR in the proximal tibia with exposure to LMHF loading. HLU inhibited BFR while intervention with normal weight bearing slightly increased BFR. However, LMHF loading normalized BFR in the HLU group compared to age-matched controls (28). There have also been investigations in larger animal models such as turkey and sheep. In one study, the hindlimbs of adult sheep were exposed to approximately 5 με induced by 0.3g loading for 20 minutes/day. After one year of treatment, trabecular bone were evaluated with micro-computed tomography (μ-CT) and

mechanically tested. Mechanical loading increased mineral content and trabecular number while trabecular spacing decreased, displaying increased trabecular quantity and thickening. There was an increase in stiffness and mechanical strength in the longitudinal direction of weight bearing. This study was critical because it showed that not only does LMHF loading increase bone mass but also the quality of the trabecular bone, and these effects were observed in a larger animal at a considerably longer time point than previous findings (27).

While animal studies were imperative in moving toward testing this device in humans, the most critical information supporting the hypothesis that such low magnitude mechanical signals can induce bone mass and adaptation were obtained as studies advanced to humans. LMHF mechanical loading has been shown to benefit various groups, including children with disabilities, young women with low bone mineral density (BMD), and post-menopausal women with osteoporosis. In a pilot clinical trial, children with disabilities affecting muscular strength such as cerebral palsy and muscular dystrophy were treated with mechanical loading at 0.3g at 90 Hz for 10 minutes/day for 5 days/week for a total of six months. There was a 6.3% increase in tibia volumetric trabecular bone mineral density (vTBMD) with treatment compared to placebo control after brief exposure to LMHF loading, which was remarkable since compliance in this study was fairly low at 44% or about 4.4 minutes/day of treatment. However, there was no effect on vTBMD in the spine (37). The disabilities endured by these children results in poor muscular strength and limited mobility. Therefore, it is possible that these physiological signals of muscle contraction to the bone are also diminished in these patients. Since LMHF loading mimics the signals outputted by the musculature to the bone, it is possible that the children had increased BMD, at least in specific sites, because the diminished muscular signals were replaced by the LMHF loading device.

There have also been clinical trials investigating the effects of LMHF loading on young women, and in one study, 48 women (age range of 15-20 years) with low BMD and a history of at least one skeletal fracture were exposed to either control or treatment conditions for 10 minutes/day at 0.3g and 30 Hz for one year. There was an increase in trabecular bone in the lumbar vertebrae and cortical bone of the femur midshaft compared to controls. Moreover, there was an increase in muscle cross section area, and these beneficial results were dependent on compliance level (13). Furthermore, clinical trials in post-menopausal women have been performed, and in one study, treatment at 0.2g at 30 Hz for two 10 minutes/day treatments for one year increased BMD in the femur compared to placebo control. The women in the placebo control group lost 2% BMD over the experimental time frame. There was less bone loss in the spine in the treated group compared to controls, and these effects were dependent on compliance. As such, those who complied with the treatment protocol most stringently had the greatest beneficial effects (24).

Thus, LMHF mechanical loading as summarized in Table 6.2 has been shown to benefit the musculoskeletal system despite some variation among studies. The device has recently been approved for treatment of osteoporosis, but long term studies will provide the most beneficial information as to its safety and efficacy in preventing or normalizing bone loss.

Conclusion

There is overwhelming evidence that exercise creates large magnitude strain sensed by bone tissue and bone cells, leading to increased bone mass and bone adaptation. These large strains are on the order of 1000 $\mu\varepsilon$ and only represent a small part of the strain history of normal daily activities, such as when humans exercise or horses trot. The larger portion of strain history is encompassed by

Table 6.2 Summary of LMHF studies

Subjects	Stimulation	Length	Result	Ref
BALB mice	0.3g, 45Hz, 15 min/day, 10 microstrain	3 weeks	Decrease in osteoclast activity; No change in BFR in trabecular bone and mid-diaphysis; Increase in BFR at endocortical surface	Xie
BALB mice	0.3g, 45Hz, 10min/day Disuse +/- intervention	3 weeks	Increase in trabecular and cortical bone surface area; after 4 days, decrease in genes due to disuse; after 21 days of loading, increase in gene expression	Judex
C57 WT mice	0.3g or 0.6g, 45Hz, 10min/day	3 weeks	Both loads increased trabecular BFR in metaphysis; increase in cortical area and thickness of epiphysis	Garman
Adult sheep	0.3g, 20min/day	1 year	Increase in mineral content and trabecular number, decrease in spacing, and increase in stiffness and strength	Rubin
Children with disabilities	0.3g, 90Hz, 10min/day	6 mos.	6.3% increase in tibia volumetric BMD; no change in spine BMD	Ward
Women, 15-20 yr, pre-menopausal	0.3g, 30Hz, 10min/day	1 year	Increase in trabecular bone BMD at lumbar spine, cortical bone of femur midshaft, and in muscle area	Gilsanz
Women, post-Menopausal	0.2g, 10Hz, two 10min/day	1 year	Increase in BMD in femur; less bone loss in spine	Rubin

extremely low signals on the order of 10 $\mu\varepsilon$, and it has been shown that these signals when applied at a high frequency induce an adaptive response. However, while systemic loading of an entire animal has shown beneficial effects of low magnitude mechanical loading, it is unknown whether bone cells can actually sense and respond in an anabolic manner. Previous evidence suggests that bone cells would not be able to sense such low level strains. In fact, stretch-activated channels, one potential mechanosensory molecule, have been shown to detect strains only as low as 30 $\mu\varepsilon$ (6). Another potential path of mechanotransduction from the tissue to the cellular level is through fluid flow produced when bone is mechanically loaded *in vivo* during movement. In some studies, it has been shown that shear stresses similar to *in vivo* levels can be produced when 1000-2000 $\mu\varepsilon$ is applied at 1-2 Hz or if 100-200 $\mu\varepsilon$ is applied at 20-30Hz. Thus, a 10 $\mu\varepsilon$ signal applied at 30 Hz would only amount

to stresses on the order of 0.1 dyn/cm^2, still below the range of 6-30 dyn/cm^2 known to induce intracellular calcium *in vitro*. However, the modeled shear stress depends on many factors, such as the assumed canalicular annular space, which if reduced would increase the shear stress prediction (6). Mechanical loading induces many changes and deformation to the tissue and cells that it is possible to construe the hypothesis that low level signals can be sensed by the skeletal system through the cellular network. If this is true, it would be of further interest to determine how these signals, as low as they may be, are sensed and used to elicit a bone formation promoting or bone resorption inhibiting response. Thus, it was our goal to expound this question by applying LMHF loading to an isolated osteoblast system as discussed in Chapter 8.

References

1.   **Adams DJ, Spirt AA, Brown TD, Fritton SP, Rubin CT, and Brand RA.** Testing the daily stress stimulus theory of bone adaptation with natural and experimentally controlled strain histories. *J Biomech* 30: 671-678, 1997.

2.   **Bassey EJ, Rothwell MC, Littlewood JJ, and Pye DW.** Pre- and postmenopausal women have different bone mineral density responses to the same high-impact exercise. *J Bone Miner Res* 13: 1805-1813, 1998.

3.   **Bradney M, Pearce G, Naughton G, Sullivan C, Bass S, Beck T, Carlson J, and Seeman E.** Moderate exercise during growth in prepubertal boys: changes in bone mass, size, volumetric density, and bone strength: a controlled prospective study. *J Bone Miner Res* 13: 1814-1821, 1998.

4.   **Carter DR, Smith DJ, Spengler DM, Daly CH, and Frankel VH.** Measurement and analysis of in vivo bone strains on the canine radius and ulna. *J Biomech* 13: 27-38, 1980.

5.   **Friedlander AL, Genant HK, Sadowsky S, Byl NN, and Gluer CC.** A two-year program of aerobics and weight training enhances bone mineral density of young women. *J Bone Miner Res* 10: 574-585, 1995.

6.   **Fritton SP, McLeod KJ, and Rubin CT.** Quantifying the strain history of bone: spatial uniformity and self-similarity of low-magnitude strains. *J Biomech* 33: 317-325, 2000.

7.   **Frost HM.** A 2003 update of bone physiology and Wolff's Law for clinicians. *Angle Orthod* 74: 3-15, 2004.

8.   **Frost HM.** Bone "mass" and the "mechanostat": a proposal. *Anat Rec* 219: 1-9, 1987.

9.   **Frost HM.** *The Laws of Bone Structure*. Springfield, IL: Thomas, 1964.

10.   **Frost HM.** The mechanostat: a proposed pathogenic mechanism of osteoporoses and the bone mass effects of mechanical and nonmechanical agents. *Bone Miner* 2: 73-85, 1987.

11.   **Galloway MT and Jokl P.** Aging successfully: the importance of physical activity in maintaining health and function. *J Am Acad Orthop Surg* 8: 37-44, 2000.

12.   **Garman R, Gaudette G, Donahue LR, Rubin C, and Judex S.** Low-level accelerations applied in the absence of weight bearing can enhance trabecular bone formation. *J Orthop Res* 25: 732-740, 2007.

13.   **Gilsanz V, Wren TA, Sanchez M, Dorey F, Judex S, and Rubin C.** Low-level, high-frequency mechanical signals enhance musculoskeletal development of young women with low BMD. *J Bone Miner Res* 21: 1464-1474, 2006.

14.   **Gray B, Hsu JD, and Furumasu J.** Fractures caused by falling from a wheelchair in patients with neuromuscular disease. *Dev Med Child Neurol* 34: 589-592, 1992.

15.   **Haapasalo H, Sievanen H, Kannus P, Heinonen A, Oja P, and Vuori I.** Dimensions and estimated mechanical characteristics of the humerus after long-term tennis loading. *J Bone Miner Res* 11: 864-872, 1996.

16.   **Issekutz B, Jr., Blizzard JJ, Birkhead NC, and Rodahl K.** Effect of prolonged bed rest on urinary calcium output. *J Appl Physiol* 21: 1013-1020, 1966.

17.   **Judex S, Zhong N, Squire ME, Ye K, Donahue LR, Hadjiargyrou M, and Rubin CT.** Mechanical modulation of molecular signals which regulate anabolic and catabolic activity in bone tissue. *J Cell Biochem* 94: 982-994, 2005.

18.   **Kerr D, Morton A, Dick I, and Prince R.** Exercise effects on bone mass in postmenopausal women are site-specific and load-dependent. *J Bone Miner Res* 11: 218-225, 1996.

19.   **Lanyon LE and Smith RN.** Bone strain in the tibia during normal quadrupedal locomotion. *Acta Orthop Scand* 41: 238-248, 1970.

20.   **Lohman T, Going S, Pamenter R, Hall M, Boyden T, Houtkooper L, Ritenbaugh C, Bare L, Hill A, and Aickin M.** Effects of resistance training on regional and total bone mineral density in premenopausal women: a randomized prospective study. *J Bone Miner Res* 10: 1015-1024, 1995.

21.   **Marcus R.** Exercise: moving in the right direction. *J Bone Miner Res* 13: 1793-1796, 1998.

22.   **Marcus R, Feldman D, and Kelsey JL.** *Osteoporosis*. San Diego, CA: Academic Press, 2001.

23.   **Robinson TL, Snow-Harter C, Taaffe DR, Gillis D, Shaw J, and Marcus R.** Gymnasts exhibit higher bone mass than runners despite similar prevalence of amenorrhea and oligomenorrhea. *J Bone Miner Res* 10: 26-35, 1995.

24.   **Rubin C, Recker R, Cullen D, Ryaby J, McCabe J, and McLeod K.** Prevention of postmenopausal bone loss by a low-magnitude, high-frequency mechanical stimuli: a clinical trial assessing compliance, efficacy, and safety. *J Bone Miner Res* 19: 343-351, 2004.

25.   **Rubin C, Turner AS, Bain S, Mallinckrodt C, and McLeod K.** Anabolism. Low mechanical signals strengthen long bones. *Nature* 412: 603-604, 2001.

26.   **Rubin C, Turner AS, Mallinckrodt C, Jerome C, McLeod K, and Bain S.** Mechanical strain, induced noninvasively in the high-frequency domain, is anabolic to cancellous bone, but not cortical bone. *Bone* 30: 445-452, 2002.

27.   **Rubin C, Turner AS, Muller R, Mittra E, McLeod K, Lin W, and Qin YX.** Quantity and quality of trabecular bone in the femur are enhanced by a strongly anabolic, noninvasive mechanical intervention. *J Bone Miner Res* 17: 349-357, 2002.

28.   **Rubin C, Xu G, and Judex S.** The anabolic activity of bone tissue, suppressed by disuse, is normalized by brief exposure to extremely low-magnitude mechanical stimuli. *Faseb J* 15: 2225-2229, 2001.

29.   **Rubin CT and Lanyon LE.** Dynamic strain similarity in vertebrates; an alternative to allometric limb bone scaling. *J Theor Biol* 107: 321-327, 1984.

30.   **Rubin CT and Lanyon LE.** Limb mechanics as a function of speed and gait: a study of functional strains in the radius and tibia of horse and dog. *J Exp Biol* 101: 187-211, 1982.

31.   **Rubin CT and Lanyon LE.** Regulation of bone formation by applied dynamic loads. *J Bone Joint Surg Am* 66: 397-402, 1984.

32.   **Rubin CT and Lanyon LE.** Regulation of bone mass by mechanical strain magnitude. *Calcif Tissue Int* 37: 411-417, 1985.

33.   **Rubin CT, Sommerfeldt DW, Judex S, and Qin Y.** Inhibition of osteopenia by low magnitude, high-frequency mechanical stimuli. *Drug Discov Today* 6: 848-858, 2001.

34.   **Snow-Harter C, Bouxsein ML, Lewis BT, Carter DR, and Marcus R.** Effects of resistance and endurance exercise on bone mineral status of young women: a randomized exercise intervention trial. *J Bone Miner Res* 7: 761-769, 1992.

35.   **Turner CH.** Three rules for bone adaptation to mechanical stimuli. *Bone* 23: 399-407, 1998.

36.   **Vuori I.** Exercise and physical health: musculoskeletal health and functional capabilities. *Res Q Exerc Sport* 66: 276-285, 1995.

37.   **Ward K, Alsop C, Caulton J, Rubin C, Adams J, and Mughal Z.** Low magnitude mechanical loading is osteogenic in children with disabling conditions. *J Bone Miner Res* 19: 360-369, 2004.

38.   **Wolff J.** *Das Gesetz der Transformation der Knochen*. Berlin, Hirschwald: Stuttgart : Schattauer, 1892.

39.   **Xie L, Jacobson JM, Choi ES, Busa B, Donahue LR, Miller LM, Rubin CT, and Judex S.** Low-level mechanical vibrations can influence bone resorption and bone formation in the growing skeleton. *Bone* 39: 1059-1066, 2006.

Chapter 7

Bone Adaptation to the Mechanical Environment:
Cell Signaling in Osteoblasts

Summary

The various bones of the skeleton are surrounded by a microenvironment controlled by local signals and systemic hormones, and the cells present in bone regulate homeostasis by maintaining the tightly regulated process of bone remodeling. In the previous chapter, we reviewed the macroscopic level of bone adaptation to changes in the mechanical environment, focusing on high and low impact loading. Here, we delve into the microscopic level of cellular adaptation to alterations in mechanical loading conditions. The human body is exposed to a multitude of forces and their resulting effects on the tissue and cellular structure, including mechanical strain magnitude and rate, pressure, fluid shear stress, compression, tension, and electric streaming currents. The process by which the body senses these signals at various levels, either the whole body, organ, tissue, or cell, is still largely not understood.

Bone adaptation occurs at the cellular level, where cells secrete a multitude of growth factors and cytokines, instigating cell signaling cascades leading to cell differentiation, osteoid formation, and mineralization in response to alterations in the mechanical environment. In this chapter, we partially review bone cell adaptation by covering mechanotransduction and gravity, fluid flow-induced shear stress, and the bone morphogenic protein (BMP) signaling pathway. It is known that the human body has adapted to the gravitational field of Earth, as observed in the vast number of changes instigated in the body by spaceflight. Among these changes, bone loss remains one of the most critical pathologies hindering the expansion of human-based, long term missions. In developing countermeasures for bone loss in astronauts, few studies have

elucidated the cellular and molecular changes impressed upon the skeletal microenvironment. These changes could be essential in understanding general principles such as how cells sense mechanical signals, including gravity, and perhaps can lead to the development of more efficient methods to mitigate bone loss both in spaceflight and other bone pathologies. Additionally, the cellular environment consists of various mechanical loads, including the resultant shear stress from interstitial fluid flow. Mature osteoblasts that are responsible for maintaining the mineralized matrix are called osteocytes, which occupy spaces within the bone and are exposed to interstitial fluid flow and subsequent shear stress. It is widely hypothesized that this shear stress acts as a signal to osteocytes, which stimulates inactive bone lining cells and preosteoblasts to begin the bone formation cascade (15, 20, 37). With these various micro-signals, bone remodeling sustains a healthy balance between bone formation and bone resorption through a gamut of cellular control, including local feedback mechanisms, intracellular signaling cascades, and growth factor binding. Perturbations to the bone remodeling cycle lead to an imbalance between bone formation and bone resorption, ultimately triggering skeletal pathologies. Thus, bone loss occurs when bone resorption outweighs bone formation, as observed in osteoporosis, disuse, and spaceflight (6, 63, 67, 85). Lastly, the bone morphogenic proteins (BMPs) comprise a portion of the factors cultivated by osteoblasts, directly influencing cell differentiation and proliferation as well as regulating osteoclastogenesis (9). In this chapter, we partially review osteoblast cell signaling as relevant to the broad picture of this research. We include mechanotransduction and gravity, fluid shear-induced responses in osteoblasts, and the BMP signaling cascade as it relates to bone formation, including the downstream canonical smad pathway and the mitogen-activated protein kinase (MAPK) pathway.

General Mechanotransduction

Mechanotransduction is the intricate way in which individual cells comprising whole tissues and organs sense mechanical loads and convert the signals into useful biochemical information. This biochemical information is required for seemingly simple commands such as wiggling a toe or daunting tasks such as preventing cancer. Mechanotransduction is still not completely understood, although many critical components have been implicated for their roles in sensing a signal and instigating subsequent pathways to induce a physiological response. Among these identified mechansensory components are stretch-activated ion channels, integrins, cadherins, caveolae, growth factor receptors, cytoskeletal filaments, and the extracellular matrix (Figure 7.1) (31). Figure 7.2 shows mechanisms by which some of these mechanosensors work such as stretch activated ion channels (A) altering their conformation and changing their opening and closing rate when the membrane is distorted or a channel that experiences tension from the cytoskeleton (B). Also, Figure 7.2 shows mechanotransduction through tension applied to enzymes (C) or other proteins (D) and the chemical potential of these proteins when under either compression or tension (E). These mechanically sensitive cellular components can be activated by a host of signals, including external forces such as gravity, fluid flow-induced shear stress, and impact from exercise. Many organs and tissues in the human body are mechanosensitive, including bone, cartilage, muscle, heart, and the gastrointestinal tract (32). Mechanical signals play an essential role in maintaining homeostasis as observed in tissue degradation and atrophy due to disuse or microgravity. For example, immobilization during bed rest or paralysis results in a large absence of mechanical stimulation such as walking, leading to acute and rapid bone and muscle loss (5, 68, 85).

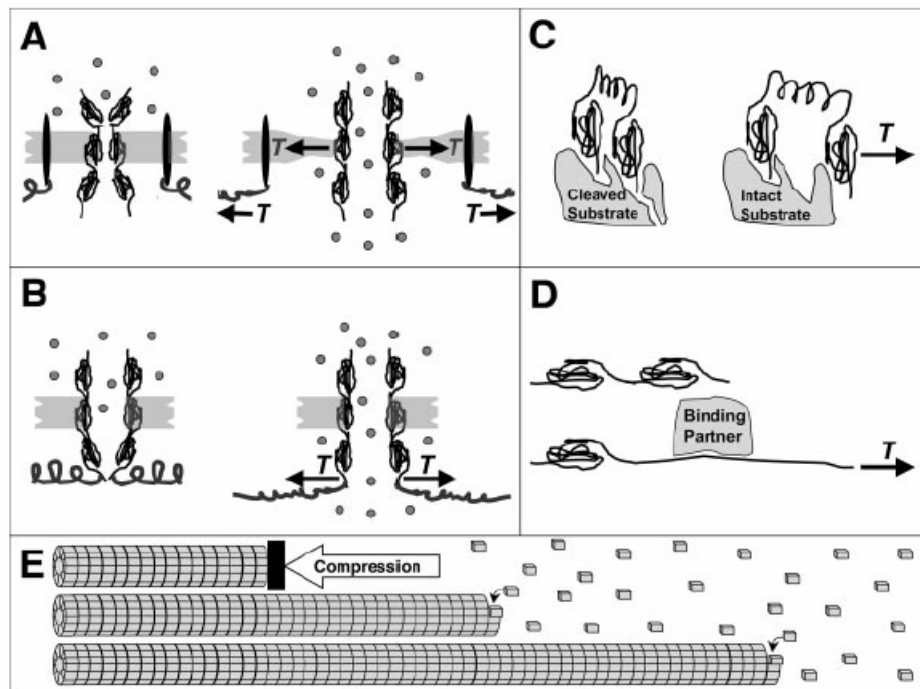There have been common signaling molecules established to play roles in mechanotransduction by various cell types. In general, integrins are one class of

138
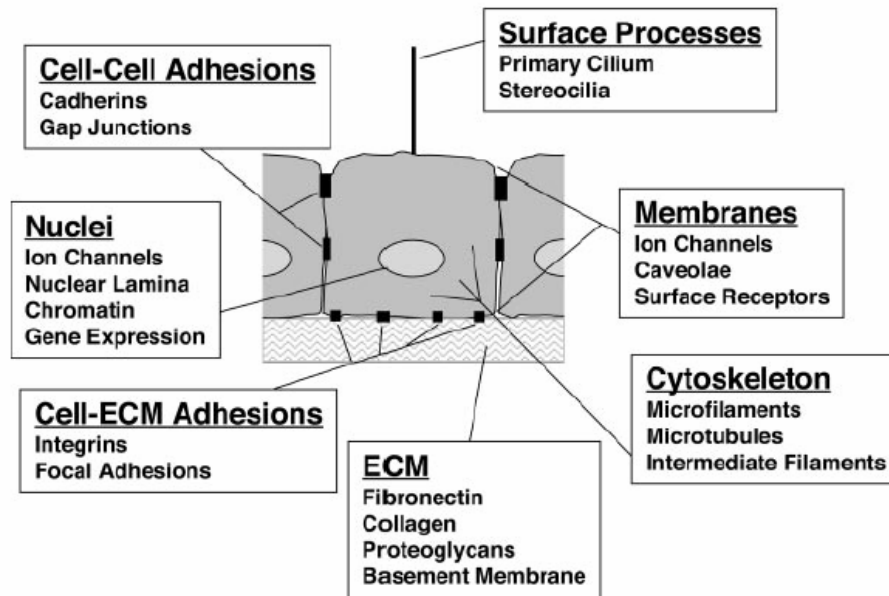
Figure 7.1 Mediators of cellular mechanotransduction (31)
(Figure printed with permission from *FASEB Journal*)

Figure 7.2 Molecular mechanism of conversion from mechanical signal to chemical information (31)
(Figure printed with permission from *FASEB Journal*)

universal mechanoreceptors, and the interaction of integrins with the extracellular matrix mediates an increase in intracellular calcium (Ca^{2+}) and subsequent activation of the MAPK pathway. The MAPK cascade involves the activation of extracellular signaling-regulated kinases 1/2 (ERK1/2) by phosphorylation and an ensuing activation of the activator protein 1 (AP-1) family of transcription factors. This signaling cascade leads to pro-growth responses in a variety of cells (32). In particular, the osteocyte, which is the mature bone cell responsible for bone maintenance and hypothesized bone mechanosensor, responds to mechanical signals by extracellular Ca^{2+} influx through stretch-activated ion channels, leading to increases in intracellular Ca^{2+} (32). Additionally, osteocytes are unique cells because they create long processes, which are believed to be their means of communication to other bone cells such as bone lining cells and osteoblasts. As such, osteocytes use these cell-cell connections to transmit signals through gap junctions leading to biological responses.

There have been detailed investigations performed to elucidate the pathways ensuing after a mechanical signal is detected, revealing individual molecules responsible for mediating specific responses. Because of the breadth of detailed knowledge available, it is not the goal of this chapter to provide a comprehensive review of signaling pathways involved in skeletal maintenance. However, we provide insight into key cell signaling pathways, including mechanotransduction and gravity, fluid flow-induced shear stress on bone formation, and the role of the BMP family in bone formation.

Mechanotransduction and Gravity

The structure-function relationship of bone has evolved over the course of human life, and it is well known since the time of Julius Wolff (1892) that bone adapts to its mechanical environment. As such, it is no surprise that the skeleton has adapted to the gravitational field on Earth, and the launch of the space program in the 1960s confirmed

that the human body, when exposed to long term, near-zero gravitational impact, endures harsh biomedical alterations such as cardiovascular deconditioning and musculoskeletal atrophy (67, 76). The unique environment of spaceflight most likely alters the skeleton at the whole organ, tissue, and cellular levels. However, the details of such changes are only partially understood. In particular, the mechanosensory machinery cells use to sense mechanical loading, such as gravity, is still largely unidentified. Bone adaptation to changes in the mechanical environment depends at least partially on the transduction of mechanical signals to chemical information.

It is fairly well understood how the human body perceives gravity to maintain orientation, and in most invertebrates and vertebrates, there is some type of specialized organ that allows maintenance of equilibrium with respect to gravity and movement. In humans, the otolith organs called the utricle and saccule, which are located in the inner ear, are responsible for the perception of gravity and maintenance of balance. Hair cells in the inner ear are activated by movement and transmit signals through nerve fibers to the brain, signifying changes in position, acceleration, and gravity. As observed in spaceflight, there is an abrupt loss of constant linear acceleration due to gravity, and the otolith stimulus responsible for maintaining vertical orientation is removed, leading to abnormal spatial orientation and movement control. These effects are diminished over time as the neurovestibular system adapts to microgravity, which results in the need for readaptation when astronauts return to Earth (8, 55).

However, the question at hand is whether individual cells of various organs and tissues in the human body themselves sense gravity, leading to the pathologies induced by spaceflight such as site-specific rather than systemic loss of bone. For instance, it is reasonable to conjecture that without gravity, the body no longer walks as on Earth. As such, there is no cyclic motion, which regulates the fluid movement in the skeletal system. Without this ensuing oscillatory flow, there could be a lack of a bone formation

141

signal to the mechanosensing cell, leading to decreased bone formation and inevitable bone loss. Likewise, it is reasonable to surmise that without a mechanical load as essential as gravity, there is a change in mechanotransduction, impeding the expression of signals imperative for genes regulating bone formation. However, to test these hypotheses, we must have ways to study isolated cell systems in a microgravity system, and as spaceflight has become more sporadic, scientists have turned to simulators of microgravity.

Much of what is known regarding how cells sense gravity has been studied in the plant cell. Weight causes differential mass displacement, due to differences in masses among different organelles. The cytoskeleton has traditionally been regarded as a mediator in the perception of gravity both in animals and plants (11, 29, 30, 62, 77). In plants, the mechanism used to sense gravity is most likely through the movement of statoliths. A statolith is a specialized form of an amyloplast, which are plant organelles responsible for storing and converting sugar into energy, found in the root tip cells called statocytes of higher order plants. Statoliths are more dense than the cell cytoplasm and sediment with exposure to gravity, and they are entangled with the cytoskeleton actin filaments. It is widely hypothesized that sedimentation of statoliths emanates a mechanosensory pathway leading to reorientation of the cytoskeleton and a cellular response such as turning of the root in response to a change in motion (27). Additionally, there has been research performed to understand whether there are temporal effects of plant responses to gravity. The concept of perception time is the minimum duration of the stimulation interval necessary to induce gravitropic bending of the root. Hejnowicz, et al. stated that the shortest stimulation time was one second, and, therefore, they assumed that the perception time is shorter than one second (27). The notion of perception time is important because it implies that the sensitivity to gravity involves not only exposure to the magnitude of the gravity vector but also constant

alignment of the vector to the subject for some minimal time. In spaceflight, cell signaling by gravitropic organelles is altered because there is no force displacing them to a specific gravity-dependent target for gravity-sensing signaling. Thus, a method of continually changing the direction of the gravity vector more rapidly than the cell's perception time may inhibit gravitropic responses. Consequently, simulating microgravity under normal ground conditions by using devices such as the Random Positioning Machine (RPM) or the Rotating Wall Vessel (RWV) bioreactor, which continuously rotate and move the gravity vector relative to the subject, are based on the hypothesis that sensing no weight would have similar effects as being weightless. These gravity vector-averaging systems have enabled scientists to advance knowledge in both microgravity-based science and general mechanotransduction.

There has been some research performed on the effects of spaceflight and simulated microgravity on mammalian cells, namely changes in gene expression as covered previously in Chapters 3, 4, and 5. However, how cells sense gravity is a continually evolving field because statoliths do not account for how all mechanosensitive cells in the body perceive gravity as there is no evidence of statoliths in bone cells, muscle cells, or other tissue cells of the human body. It is well accepted that individual cells must be able to detect changes in mechanical load as evidenced by bone remodeling by osteoblasts and osteoclasts. It is hypothesized that mammalian cells sense gravity through the cytoskeleton, whereby movement distorts the cell surface and its connections to the cytoskeleton (30). Cells are attached to their extracellular matrix (ECM) through special proteins called integrins, whose receptors form clusters called focal adhesions. The focal adhesions are physically connected to the actin cytoskeleton by interactions between the cytoplasmic tail of integrin receptors and actin-associated molecules in the cytoplasm like vinculin (30). Thus, it has been shown that activation of many of the signaling molecules with exposure to a mechanical load is mediated through

143

integrins and subsequent mitogenic receptors, and moreover, these molecules are not floating about in the cell but rather are connected to the cytoskeleton in the focal adhesion complex. As such, it seems that cells are "hardwired" such that the cytoskeletal filaments form the physical connections between the cell surface, which is exposed to mechanical loads, and the nucleus, where gene programming takes place. This theory is called the tensegrity model, a bridged word describing tensional integrity, depicting that the cell is pre-stressed to gives cells mechanical stiffness. Thus, with its physical connections, perturbations to the cell environment alters the cell surface, modifies its connection to the ECM, and causes resultant changes to the nucleus (30).

Although it is well understood how the whole body senses gravity and how plant cells respond to changes in gravity, it is only partially understood how mammalian cells react to microgravity. Future studies may elucidate this mechanosensory pathway, which would not only lead to advanced spaceflight but also general improved understanding of mechanotransduction.

Fluid Shear Signaling*

Bone cells are among the most mechanically sensitive cells in the body, and their response to mechanical loading is an important factor in bone formation. Mechanical loading, as shown through *in vitro* studies using fluid flow (44), results in highly adaptive responses of bone-forming and bone-resorbing cells that together maintain homeostasis in bone tissue (64). Mechanical unloading of bone causes disruptions to these mechanisms, resulting in pathological changes that lead to increased bone resorption and subsequent bone loss (5). For example, studies have previously suggested that

*Adapted from Vadoothker, SV and Patel, MJ, et al., *Fluid Shear Stress Induces Differential Responses of Bone Formation Proteins in Preosteoblast Cells*, 2007, In preparation

144

astronauts and bed-ridden patients experience unloading due to a decrease in osteoblast function (33, 56). It is widely hypothesized that fluid flow in bone may signal osteoblast differentiation (15, 20, 37) and induce osteoblasts to secrete key bone formation markers and matrix proteins (66). Mechanical loading as a result of fluid flow is known to result in a dynamic and oscillatory flow profile in bone tissue, and, thus, oscillatory fluid flow is hypothesized to be the most likely flow profile present in bone during physical activity (61, 64, 79). When bone is loaded (foot strike to ground), a hydrostatic pressure gradient is created, and interstitial fluid is forced into the canalicular network of bone. Unloading (time in between foot strikes) induces an adverse pressure gradient causing reversal of fluid flow. Together, loading and unloading create the bidirectional and oscillatory fluid flow inside bone tissue (41, 48, 79). Because microgravity or bed rest results in the lack of a loading and unloading cycle, it is possible that the detrimental effects to the musculoskeletal system are due to an absence of signals normally induced by cyclic fluid flow.

Shear Sensitive Proteins in Osteoblasts

Several studies have linked changes in osteoblast morphology and protein expression to fluid flow exposure. Oscillatory fluid flow upregulates various proteins involved in bone formation, including prostaglandin E_2 (PGE_2), cyclooxegenase-2 (cox-2), osteopontin (OPN), alkaline phosphatase (ALP), and osteocalcin (OCN) (44, 48, 61). Ponik, et al. and Malone, et al. determined that both osteoblasts and osteocytes elongated and actin stress fibers increased in response to a unidirectional fluid flow stimulus, similar to how endothelial cells lining the blood vessel wall react to constant blood flow (69). ALP is found in bone cells prior to cell differentiation and matrix mineralization (17), and fluid flow and the resulting shear stress have been found to increase levels of ALP (19, 28, 57, 60). Fluid shear has also been shown to temporally

activate signal transduction pathways involving cox-2 and OPN, both proteins necessary for bone mechanotransduction (61, 83). Specifically, primary bone cells with no mechanical stimulation experienced great decreases in OPN production, suggesting that inactivity may decrease the emergence of an osteoblastic phenotype (40). Other proteins of interest studied through fluid flow exposure include nitric oxide (NO), PGE_2, receptor activator of nuclear factor kappa B ligand (RANKL), and osteoprotegerin (OPG). Signaling molecules NO and PGE_2 were upregulated by fluid flow in osteoblasts and were found to be active in actin cytoskeleton disruption (50). Furthermore, bone cells have been shown to release prostaglandins in response to fluid flow and have contributed to either bone growth or bone resorption depending on G-protein coupled receptors (GPCR) activated by fluid flow (13). An increase in NO production has also been shown to decrease osteoclastogenesis and bone resorption (45), allowing for the continued maintenance of bone tissue. Similarly, RANKL, a marker for bone resorption and osteoclastogenesis, is competitively blocked by OPG in response to oscillatory fluid flow (39), and a decrease in RANKL production as a result of a mechanical stimulus has been shown to increase levels of NO in bone tissue, reducing bone resorption (45). Correspondingly, when bone cells were subjected to tensile mechanical stress, the cells increased OPN expression, suggesting that OPN may also play a role in mediating bone cell mechanotransduction (51). Studies of these and other proteins involved in bone formation as a result of fluid flow allow a greater understanding of how bone cells respond to mechanical stimuli to maintain skeletal homeostasis.

*Two Novel Shear Sensitive Proteins in Osteoblasts*

While the previously mentioned markers have been studied greatly in depth, many more markers exist that have never been studied in response to shear stress. These proteins could enhance the knowledge regarding bone mechanotransduction in

response to fluid flow and ultimately how bone formation occurs. New insight into the cellular and molecular events leading to bone formation provides the necessary information for expanding the development of pharmaceutical treatments targeting formation since most drugs target bone resorption (www.nof.org). An increase in the expression of bone morphogenic protein 4 (BMP4), an osteogenic marker of bone formation present since skeletogenesis (74), has been found *in vitro* in endothelial cells as a result of shear stress from oscillating fluid flow (69). BMP4, when studied in bone, has also been shown to be an osteoinductive growth factor that regulates signaling in osteoblasts (54). Studies have also determined that if BMP4 is delivered through gene therapy, ectopic endochondral bone formation occurred in skeletal muscle (43). Similarly, an increase in exposure to BMP4 improved bone healing *in vivo* when BMP4 was delivered to the appropriate osteoprogenitor cells (46, 58). Thus, various reports have established BMP4 as an important bone formation marker with a key role in osteoblast differentiation and proliferation; however, to date, no studies have examined the effects of fluid flow on BMP4 in bone cells. Additionally, osteoglycin (OGN), another osteogenic marker, is understudied in bone formation but has been shown to regulate collagen fibrillogenesis (24). Patel et al. and Xing et al. have both also found through microarray studies that mechanical unloading or loading regulates OGN. However, its response to fluid shear stress has never been reported.

Most bone cell mechanotransduction studies have exposed cells from approximately 5 dyn/cm^2 to 20 dyn/cm^2 (39, 42, 48, 50, 73), although models have predicted that osteocytes experience anywhere from 8 to 30 dyn/cm^2 of shear stress *in vivo* depending on the activity performed (79). While both unidirectional (laminar) and bidirectional (oscillatory) fluid flow profiles have been employed through *in vitro* studies to gain a better understanding of mechanotransduction in bone cells, few studies have *directly* compared the response of osteoblasts to both fluid flow profiles (28, 35, 61).

Thus, we have shown that oscillatory shear stress induces the expression of alkaline phosphatase (ALP) activity, BMP4, and OGN while laminar shear stress inhibits these same markers. In our studies, 2T3 cells were exposed to laminar shear stress at 15 dyn/cm^2 and oscillatory shear stress at ±5 dyn/cm^2. The cells responded to mechanical stress by aligning in the direction of unidirectional, laminar fluid flow but not in response to oscillatory fluid flow (Figure 7.3). Additionally, laminar shear stress blunted ALP activity in comparison to static and oscillatory shear stress conditions (Figure 7.4). This phenomenon has been shown by others, but more importantly, we report that this effect is independent of the shear magnitude and rather depends on the direction of the flow. As shown in Figure 7.5, ALP activity was decreased by laminar shear at varying magnitudes of shear stress between 5-15 dyn/cm^2 compared to both static and oscillatory shear stress conditions.

Both BMP4 and OGN have not been studied under shear stress, but our studies show they may be highly shear-sensitive bone formation proteins. Laminar shear stress at 15 dyn/cm^2 decreased BMP4 and OGN expression compared to oscillatory shear stress at ±5dyn/cm^2 (Figure 7.6). Since both the magnitude and direction of the shear stress differed in this experiment, we sought to evaluate whether this effect remained when the magnitude of the shear stress was held constant. As a result, we found that the direction of the flow was indeed the key player in regulating both BMP4 and OGN since the decreased expression of both proteins was exhibited at all magnitudes of shear stress (Figure 7.7). Furthermore, we show the effects of shear stress on BMP4 and OGN expression are dose-dependent (Figure 7.8) where at least 10 dyn/cm^2 of laminar shear stress is required to decrease BMP4 expression. For OGN, laminar shear stress at 5 or 10 dyn/cm^2 is sufficient to induce decreased expression. In this figure, the laminar sample at 15 dyn/cm^2 was mistakenly left out of the gel for the Western blot; however, previous data (Figure 7.7) shows that laminar shear stress at 15 dyn/cm^2 also
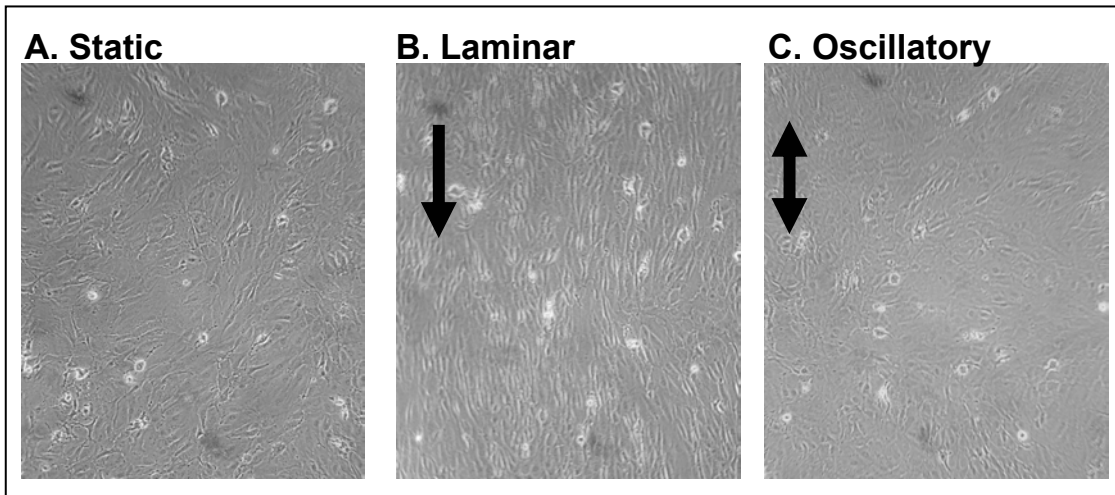
Figure 7.3 2T3 cells aligned in the direction of unidirectional laminar fluid flow. Confluent 2T3 cells were exposed to static (A), laminar (15 dyn/cm^2) shear stress (B), or oscillatory (± 5 dyn/cm^2) shear stress (C) for 24 hours. Cells were photomicrographed with a phase contrast microscope at the end of the experiement. Arrows indicate fluid flow direction. (n ≥ 13)
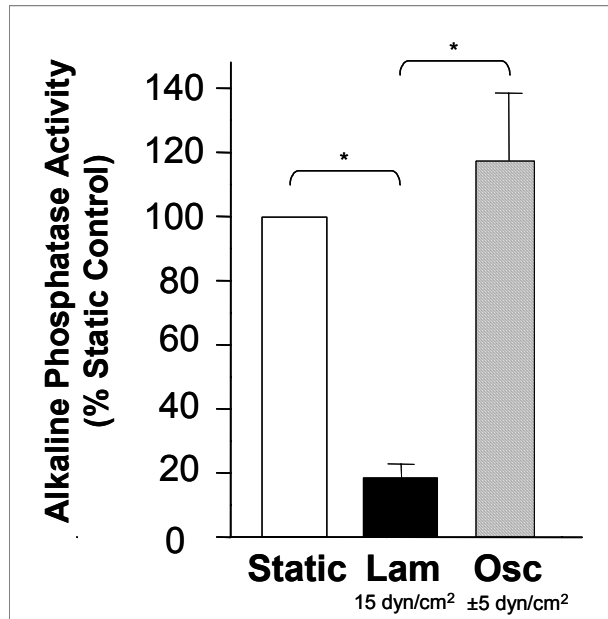
Figure 7.4 Oscillatory shear stress increased ALP activity in 2T3 cells. Cells were exposed to static, laminar (Lam), or oscillatory (Osc) shear stress conditions as in Figure 7.1. Cell lysate was obtained after 24 hours, and ALP activity was measured using a colormetric assay and normalized to total protein. Data are represented as mean ± SEM and graphed as a % of control (* $p < 0.05$, n ≥ 13).
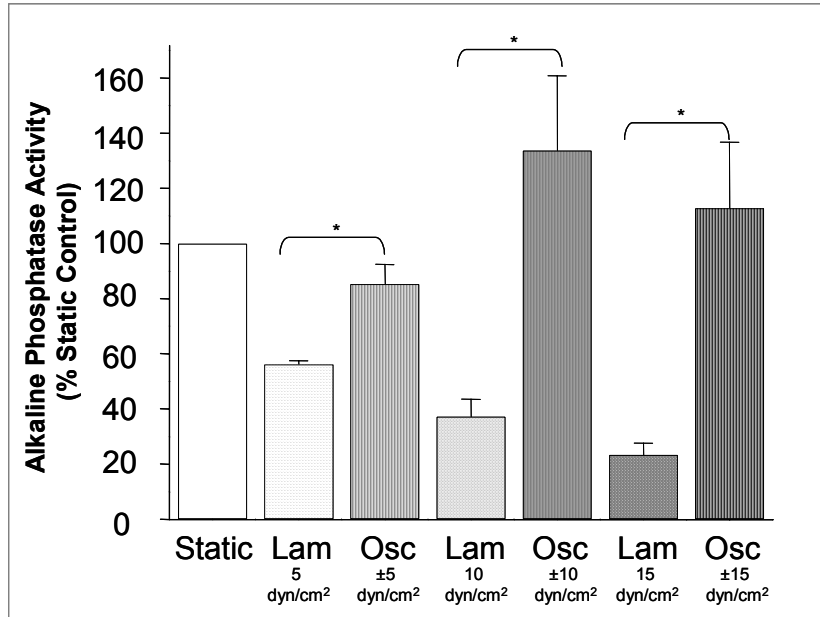
Figure 7.5 Oscillatory shear stress increased ALP in a dose-dependent manner compared to laminar shear stress. Cells were exposed to static, laminar (Lam), or oscillatory (Osc) shear stress conditions at varying magnitudes. Cell lysate was obtained after 24 hours, and ALP activity was measured using a colormetric assay and normalized to total protein. Data are represented as mean ± SEM and graphed as a % of control (* $p < 0.05$, n=3-9).
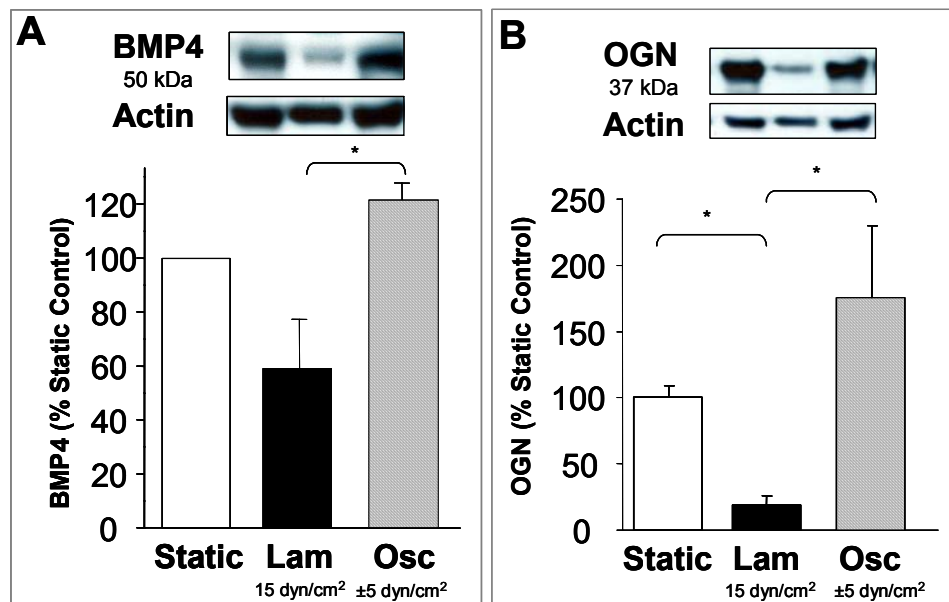
Figure 7.6 Oscillatory shear stress increased expression of BMP4 and OGN compared to laminar shear stress. Cells were exposed to static, laminar (Lam), or oscillatory (Osc) shear stress conditions as in Figure 7.1. Cell lysate was obtained after 24 hours, and specific antibodies against BMP4 (A) and OGN (B) were used to detect protein expression by Western blot. Data are represented as mean ± SEM and graphed as a % of control (* $p < 0.05$, n=3-9)

150
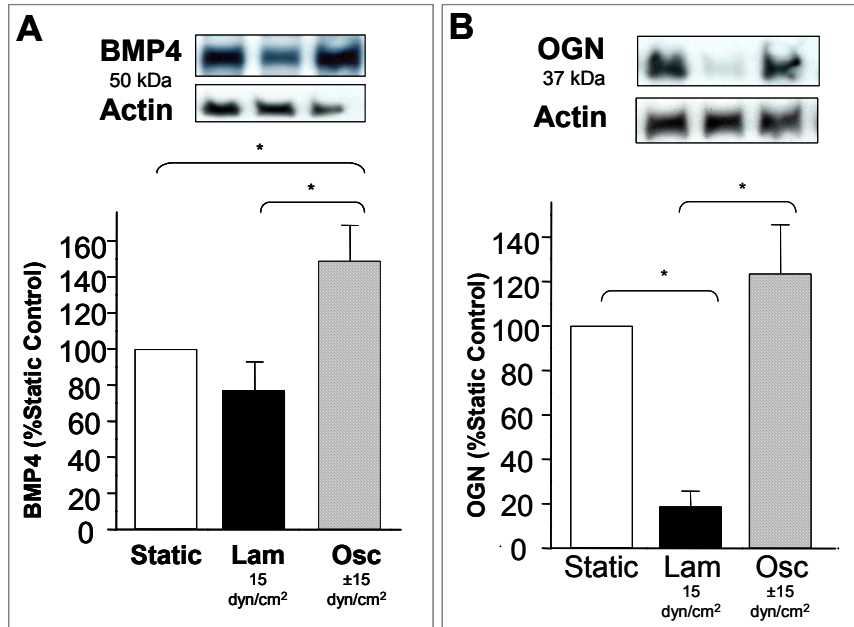
Figure 7.7 Oscillatory shear stress increased BMP4 and OGN compared to laminar shear stress at identical magnitudes. Cells were exposed to static, laminar (Lam), or oscillatory (Osc) shear stress conditions at a constant magnitude of 15 dyn/cm^2. Cell lysate was obtained after 24 hours, and specific antibodies against BMP4 (A) and OGN (B) were used to detect protein expression by Western blot. Data are represented as mean ± SEM and graphed as a % of control (*p<0.05, n = 6)
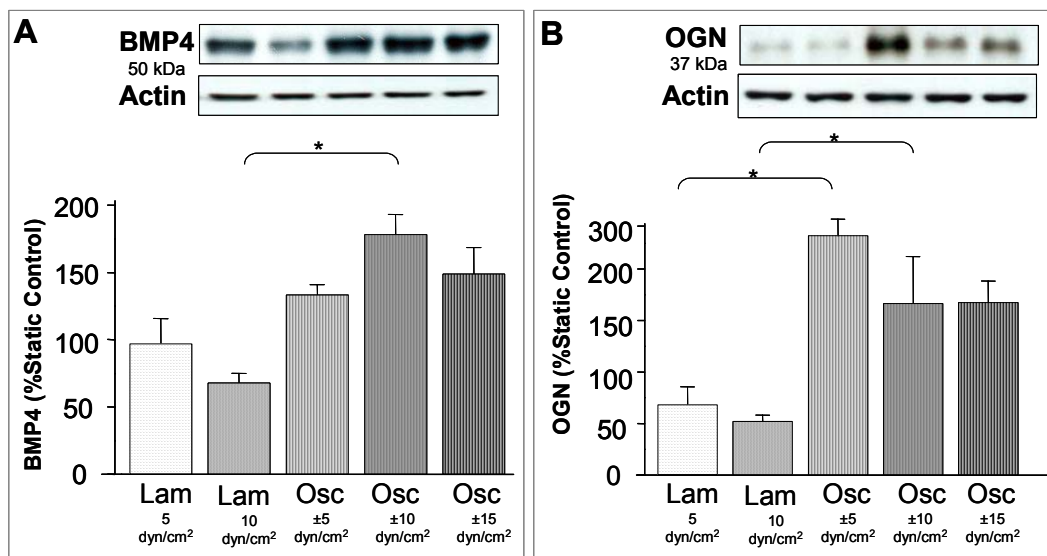
Figure 7.8 Oscillatory shear stress increased BMP4 and OGN in a dose-dependent manner compared to laminar shear stress. Cells were exposed to static, laminar (Lam), or oscillatory (Osc) shear stress conditions at varying magnitudes. Cell lysate was obtained after 24 hours, and specific antibodies against BMP4 (A) and OGN (B) were used to detect protein expression by Western blot. Data are represented as mean ± SEM and graphed as a % of control (*p<0.05, n=3-9).

decreased OGN expression compared to the appropriate oscillatory shear conditions. OGN has been shown to play a role in collagen fibril regulation and is a member of the small leucine-rich proteoglycan (SLRP) family, whose members are hypothesized to play roles in bone matrix mineralization (72). In our studies, both BMP4 and OGN expression were regulated by shear stress exposure, suggesting that the expression of both proteins is controlled by a mechanically sensitive pathway. Changes in shear magnitude did not affect the increased expression of BMP4. When laminar and oscillatory shear stress magnitude were held constant, oscillatory flow still increased expression of both proteins compared to laminar flow, suggesting that the flow direction plays a role in regulating BMP4 and OGN expression. These findings are consistent with previous work showing that oscillatory fluid flow is the physiological flow naturally present in bone (79), and it suggests that oscillatory shear stress may cause an osteogenic response while distinctly differing flow profiles such as laminar flow inhibit bone formation.

Fluid flow inevitably induces signaling cascades, regulating diverse sets of proteins, cytokines, and growth factors responsible for maintaining appropriate cellular function and ultimately bone remodeling. Fluid-induced shear stress is one of the many mechanical signals to which bone cells must respond, and the reviewed molecules are only a small fraction of the numerous factors involved in maintaining the highly complex process of skeletal homeostasis.

Bone Morphogenic Protein (BMP) Signal Transduction

There are a number of cell signaling pathways altered by mechanical loading, leading to a multitude of anabolic responses. Here, we aim to review the signaling cascades induced by the BMPs, which are members of the Transforming Growth Factor Beta (TGF-β) superfamily and have been shown in numerous studies to instigate potent osteogenic effects such as stimulating the differentiation of mesenchymal stem cells to

osteoblast lineage (7, 38, 59, 82). While BMPs were first identified in the context of bone and cartilage formation (75), they have since been implicated in various processes including neural development (47, 65) and cardiovascular pathogenesis (12, 14). They are multi-functional growth factors whose cellular and molecular mechanisms of action have recently been ascertained and utilized in the development of clinical applications for bone and cartilage regeneration (16, 21, 53).

BMP Structure and Function

To date, there have been approximately 15-20 BMPs identified (7, 26, 81), and each BMP has a precursor and a cleaved, secreted mature form (81). There is a conserved seven cysteine-rich region, where six of these cysteines form a knot while the seventh is involved in dimerization. The large precursor protein, at an approximate weight of 50 kDa, contains a signal peptide, a pro-domain, and a mature domain. Once the signal peptide is cleaved, the precursor protein undergoes glycosylation and dimerization. To secrete the active BMP, the cell proteolytically cleaves the pro-domain at a dibasic site, rendering the C-terminal active domain available for release (81). BMPs can form active homodimers and heterodimers, both composed of polypeptide chains connected by disulfide bonds (26).

As the name suggests, BMPs are morphogenes, those regulating the shape of the organism, whereas the TGFβ proteins are classified as cytokines, which are small biological factors that have specific effects on cell-cell interactions and communication. While BMPs are members of the TGFβ superfamily and share 40-50% structural similarity with TGFβ, they can have drastically disparate effects on osteoblast differentiation markers (26). BMP-2 has been shown to enhance ALP activity and OCN expression, but TGFβ has also been shown to inhibit these same markers (70).   One of the most critical functions of the BMPs for clinical applications is their ability to induce

153

ectopic bone and cartilage, rendering them useful for joint defects and injuries. Among the many BMPs, the ones with the immense osteogenic capabilities are BMP2, BMP4, and BMP7 (9, 81). Currently, only BMP2 and BMP7 have been shown clinically to provide an *in vivo* induction of bone for fracture healing, spinal fusion, and other skeletal deformations (16, 36).

SMAD Pathway

The canonical BMP pathway begins with a BMP binding to its cell surface receptor (Figure 7.9) (9). It has been shown that when BMP2 binds to a pre-formed heteromeric receptor complex, it activates the smad pathway. If, however, BMP2 binds to a receptor complex induced by BMP2 itself, the MAPK pathway is instigated, as discussed later (52). The BMP receptors are serine/threonine kinase receptors, and there are two groups of BMP receptors distinguished as type I and type II. There are two subclasses of type I receptors called type IA or activin receptor-like kinase (ALK)-3 and type IB or ALK-6. The first receptor to which a BMP binds is BMP receptor II (BMPRII), and this ligand-receptor complex initiates a cascade of events starting with the recruitment of and dimerization to BMP receptor I (BMPRI). Once BMPRII binds to BMPRI, the constitutive kinase activity of type II activates type I and commences the smad cascade. It begins with the phosphorylation of smads 1, 5, 8 by the BMPRII/BMPRI heterodimer. Once phosphorylated, smads 1, 5, 8 can induce many different responses, including signaling to smad 4 and its translocation to the nucleus to act as a transcription factor for downstream BMP signaling targets (9). Osteoblast differentiation depends on interactions of smads with *runt homology domain transcription factor 2 (runx2),* as shown in the differentiation of mesenchymal cells. If *runx2* is mutated yielding a truncated runx2 protein, there is no interaction with smads 1, 2, 3, and 5, halting osteoblast differentiation even in the presence of smads or BMPs
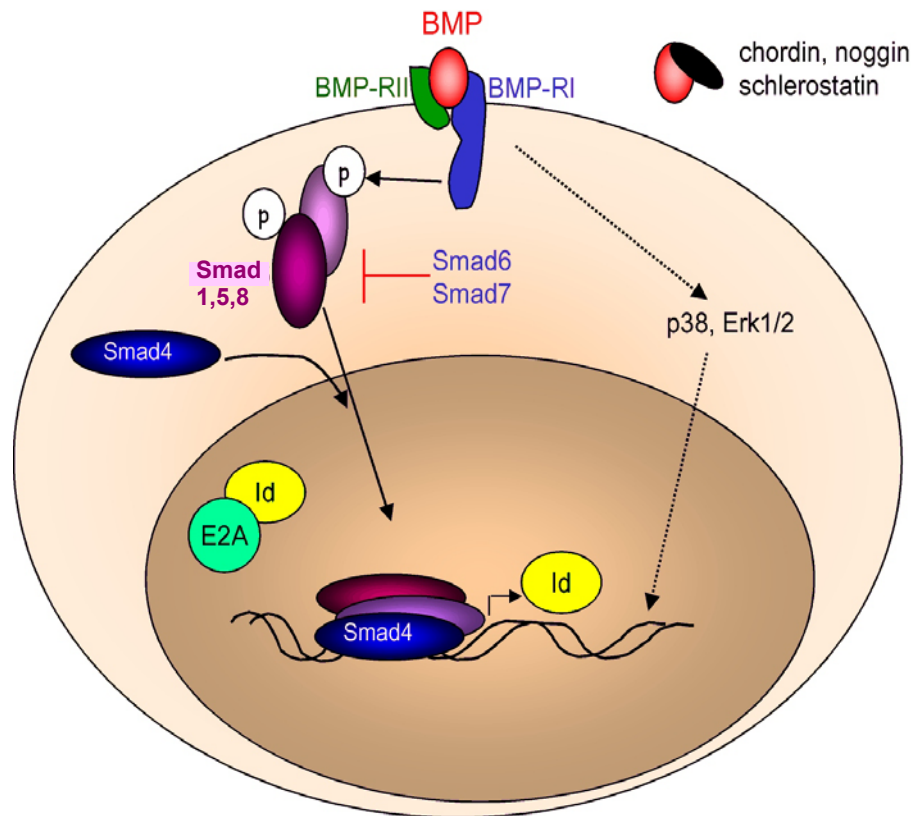
Figure 7.9 BMP signaling pathway showing smad phosphorylation and translocation of smad 4 to nucleus for transcriptional regulation and alternative MAPK pathway
(Ref: Norwegian Radium Hospital)

(84). Thus, smad proteins play an essential role in relaying signals from the cell surface to the nucleus for gene transcription, some of which are critical to bone formation.

Mitogen Activated Protein Kinase (MAPK) Pathway

Both BMP and TGFβ activate smad-independent pathways, namely the Ras/MAPK pathway (Figure 7.10). There have been three major subclasses of MAPKs identified in mammalian cells including the extracellular signaling-regulated kinases (ERK), the c-Jun N-terminal kinases (JNK), and the p38 family (71). In osteoblast cell culture, there have been reports of ERK activation in response to growth factors that act through receptor tyrosine kinases (RTKs). These RTKs include platelet-derived growth factor (PDGF), insulin-like growth factor-1 (IGF-1), basic fibroblast growth factor (bFGF), and GPCRs such as prostaglandin $F_{2\alpha}$ (71). ERK activation has been linked to collagen cross-linking with integrins and interleukin-6 as well as increased cell proliferation and bone cell differentiation (71). It has been shown that BMP2 stimulates Ras activity and downstream ERK and p38 (3, 80). This signaling cascade results in downstream effects, including increased expression of Fos/Jun family members and activating transcription factors 2 (ATF2). Activation of p38 MAPK is essential for BMP2-induced increases in *type I collagen*, *ALP*, and *OCN* while induction of *fibronectin* and *OPN* requires both p38 and ERK (9). It has additionally been shown that p38 incites ALP activity, marking the role of MAPKs in cell differentiation and bone formation (71). Many signaling cascades regulate various bone cell responses, and MAPKs are only one group that controls bone remodeling. However, it is established that MAPKs play an essential role in maintaining cellular adaptation.

156
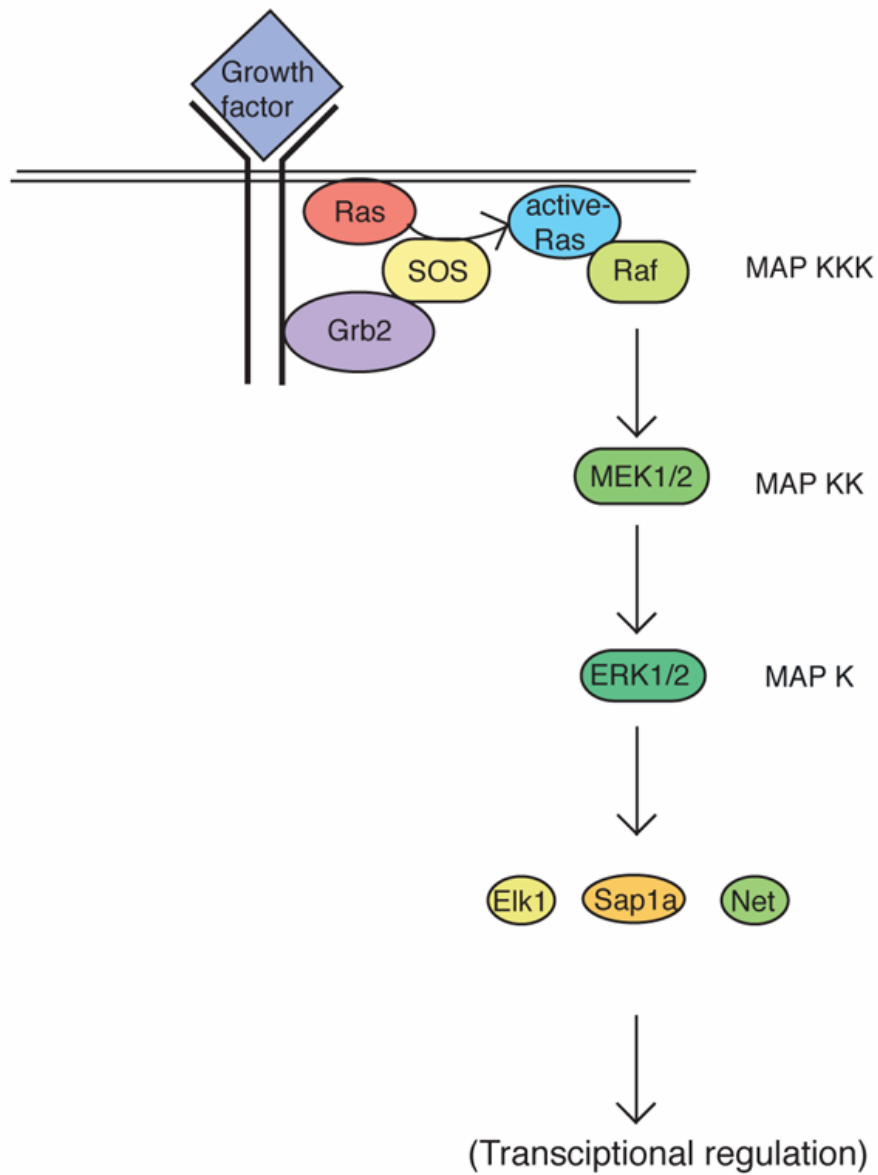
Figure 7.10 Summary of general MAPK pathway showing activation by growth factor such as a BMP and subsequent activation of a MAPKKK (first MAP activated) to MAPK (last MAPK activated) and eventual transcriptional regulation

BMP Antagonists

Cellular control of the BMP pathway is performed by both intracellular and extracellular antagonists. These control systems that inhibit BMP activity include blocking the smad pathway by inhibitory smads 6/7, smad degradation or intracellular blocking, and blocking of BMPs by extracellular binding proteins such as noggin, chordin, and DAN. Smad 6 and 7 interfere with smad 1 and 5 phosphorylation and subsequent dimerization with smad 4. They are activated by phosphorylation by type I BMP or TGFβ receptors, and smad 6 is a more specific BMP inhibitor than smad 7 (9). It has been shown that BMP2, TGFβ, and activin can induce the expression of smad 6 in stromal and muscle cells (34). Since smads are modulated by BMPs, it is possible that osteoblast cells exposed to rBMPs may increase smad 1, 5, 8 complex in the short term but also increase smad 6 and 7 over longer periods of exposure for endogenous BMP signaling control by negative feedback (9). Smads themselves are regulated by various factors, including intracellular binding proteins such as ski, an oncogene that blocks BMP, activin, and TFGβ signaling by corepressor activity. Ski mutations result in failure to bind to signaling smads and to inhibit the BMP pathway (78). Additionally, there are smad ubiquitination regulatory factors (smurf) 1 and 2 that are specific to activated smads and consequently regulate their degradation (9). There are many extracellular antagonists that are secreted polypeptides tempering BMP signaling by prohibiting binding to cell surface receptors. Table 7.1 shows the various antagonists and whether they are expressed and/or induced by BMPs.

*Table 7.1 Selected extracellular BMP antagonists

Antagonist	Expressed	Induced by BMPs
Noggin	Yes	Yes
Chordin	Yes	No
Dan	Yes	No
Twisted Gastrulation (Tsg)	Yes	No
Follistatin	Yes	No
Gremlin	Yes	Yes

(*Modified from Canalis, et al., 2003) (9)

In our studies, noggin was used to inhibit BMP activity, and we focus on it in this section. Noggin was originally identified for its actions in the development of the Spemann Organizer, a region of the central nervous system which blocks BMP4 to allow neural folding and eventual formation of the spinal cord and brain. Noggin, like the other extracellular antagonists, binds BMPs and prevents them from binding to their cell surface receptors. It binds to BMP2, 4, 5, 6, and 7 and does not seem to have any effects independent of BMP signaling (9). In cell culture, osteoblasts express noggin, and expression of it is enhanced by treatment with rBMP 2, 4, and 6. Noggin blocks BMPs in differentiated and undifferentiated osteoblast cells, preventing BMP effects such as collagenous and non-collagenous protein expression, ALP activity, and mineralization (23, 59). It has been shown that stromal cells from noggin overexpresser mice do not undergo osteoblastic differentiation (18, 22), which in turn also prevents osteoclastogenesis since osteoblasts express necessary signals such as RANKL, the ligand for receptor activator of NF-κB (RANK) essential for osteoclast differentiation (1). *In vivo*, noggin prevents chondrogenesis, membranous ossification, and development of limbs (2, 10). Noggin overexpresser mice develop osteopenia and suffer fractures (18), and human heterozygous mutations in the noggin gene results in joint lesions (25).

Chordin is also secreted by the Spemann Organizer and blocks BMP activity similarly to noggin. It is specific to BMPs, and double noggin/chordin mutations lead to diverse abnormalities, including disrupted mesoderm development and patterning (4). Follistatin was identified as a binding protein to activin but also binds to BMP4, repressing BMP signaling (9). Follistatin knockouts endure neonatal death, a result of varying deficiencies including those to the skeleton (49). The Dan family of secreted glycoproteins has the capability to bind BMPs, in particular BMP2 and 4 with varying affinity. However, dan knockout mice display modest phenotypic changes compared to other BMP antagonist knockout models (9).

BMPs play a critical role in a sundry of processes, including development and skeletal maintenance. There are inherent feedback mechanisms in play to balance BMP signaling by intracellular and extracellular antagonists. Skeletal homeostasis depends on this control to maintain osteoblast function and bone remodeling.

Conclusion

Bone adaptation occurs at the cellular level where cells such as osteoblasts and osteocytes sense deformation due to mechanical loading or unloading, instigating a cell signaling cascade leading to changes in cell proliferation, death, or differentiation. Bone cells are among the most mechanically sensitive in the body, and there are many different ways in which mechanical loads, including gravity, are sensed. The means by which gravity is sensed by cells still evades science, but there is continuing research in this field. There have been many studies using simulated microgravity to study changes in cellular architecture and gene expression, illuminating some insight into downstream effects due to alterations in the gravitational field. Additionally, other bone pathologies such as osteoporosis, depend on our knowledge on how the skeletal system adapts to changes in hormones, decreased exercise and subsequent fluid flow, and muscle

160

atrophy. Fluid flow-induced cell signaling plays a critical role in instigating bone remodeling, which is regulated by a multitude of factors. Among the many proteins that play roles in cell signaling leading to bone formation, osteoblasts secrete BMPs, which cause signaling cascades mediated by either smad proteins or MAPKs. Through numerous means, bone adaptation to changes in mechanical environment occurs not only at the macroscopic level but also at the cellular level.

References

1.   **Abe E, Yamamoto M, Taguchi Y, Lecka-Czernik B, O'Brien CA, Economides AN, Stahl N, Jilka RL, and Manolagas SC.** Essential requirement of BMPs-2/4 for both osteoblast and osteoclast formation in murine bone marrow cultures from adult mice: antagonism by noggin. *J Bone Miner Res* 15: 663-673, 2000.

2.   **Aspenberg P, Jeppsson C, and Economides AN.** The bone morphogenetic proteins antagonist Noggin inhibits membranous ossification. *J Bone Miner Res* 16: 497-500, 2001.

3.   **Attisano L and Wrana JL.** Signal transduction by the TGF-beta superfamily. *Science* 296: 1646-1647, 2002.

4.   **Bachiller D, Klingensmith J, Kemp C, Belo JA, Anderson RM, May SR, McMahon JA, McMahon AP, Harland RM, Rossant J, and De Robertis EM.** The organizer factors Chordin and Noggin are required for mouse forebrain development. *Nature* 403: 658-661, 2000.

5.   **Bikle DD and Halloran BP.** The response of bone to unloading. *J Bone Miner Metab* 17: 233-244, 1999.

6.   **Bikle DD, Harris J, Halloran BP, and Morey-Holton E.** Altered skeletal pattern of gene expression in response to spaceflight and hindlimb elevation. *Am J Physiol* 267: E822-827, 1994.

7.   **Bilezikian JP, Raisz LG, and Rodan GA.** *Principles of bone biology.* San Diego: Academic Press, 1996.

8.   **Black FO, Paloski WH, Doxey-Gasway DD, and Reschke MF.** Vestibular plasticity following orbital spaceflight: recovery from postflight postural instability. *Acta Otolaryngol Suppl* 520 Pt 2: 450-454, 1995.

9.   **Canalis E, Economides AN, and Gazzerro E.** Bone morphogenetic proteins, their antagonists, and the skeleton. *Endocr Rev* 24: 218-235, 2003.

10.   **Capdevila J and Johnson RL.** Endogenous and ectopic expression of noggin suggests a conserved mechanism for regulation of BMP function during limb and somite patterning. *Dev Biol* 197: 205-217, 1998.

11.   **Carmeliet G and Bouillon R.** The effect of microgravity on morphology and gene expression of osteoblasts in vitro. *FASEB J* 13: 129-134, 1999.

12.   **Chang K, Weiss D, Suo J, Vega JD, Giddens D, Taylor WR, and Jo H.** Bone morphogenic protein antagonists are coexpressed with bone morphogenic protein 4 in endothelial cells exposed to unstable flow in vitro in mouse aortas and in human coronary arteries: role of bone morphogenic protein antagonists in inflammation and atherosclerosis. *Circulation* 116: 1258-1266, 2007.

13.   **Cherian PP, Cheng B, Gu S, Sprague E, Bonewald LF, and Jiang JX.** Effects of mechanical strain on the function of Gap junctions in osteocytes are mediated through the prostaglandin EP2 receptor. *J Biol Chem* 278: 43146-43156, 2003.

14.   **Csiszar A, Smith KE, Koller A, Kaley G, Edwards JG, and Ungvari Z.** Regulation of bone morphogenetic protein-2 expression in endothelial cells: role of nuclear factor-kappaB activation by tumor necrosis factor-alpha, H2O2, and high intravascular pressure. *Circulation* 111: 2364-2372, 2005.

15.   **Datta N, Pham QP, Sharma U, Sikavitsas VI, Jansen JA, and Mikos AG.** In vitro generated extracellular matrix and fluid shear stress synergistically enhance 3D osteoblastic differentiation. *Proc Natl Acad Sci U S A* 103: 2488-2493, 2006.

16.   **De Biase P and Capanna R.** Clinical applications of BMPs. *Injury* 36 Suppl 3: S43-46, 2005.

17.   **Deligianni DD, Katsala ND, Koutsoukos PG, and Missirlis YF.** Effect of surface roughness of hydroxyapatite on human bone marrow cell adhesion, proliferation, differentiation and detachment strength. *Biomaterials* 22: 87-96, 2001.

18.   **Devlin RD, Du Z, Pereira RC, Kimble RB, Economides AN, Jorgetti V, and Canalis E.** Skeletal overexpression of noggin results in osteopenia and reduced bone formation. *Endocrinology* 144: 1972-1978, 2003.

19.   **Donahue HJ, Li Z, Zhou Z, and Yellowley CE.** Differentiation of human fetal osteoblastic cells and gap junctional intercellular communication. *Am J Physiol Cell Physiol* 278: C315-322, 2000.

20.   **Fan X, Rahnert JA, Murphy TC, Nanes MS, Greenfield EM, and Rubin J.** Response to mechanical strain in an immortalized pre-osteoblast cell is dependent on ERK1/2. *J Cell Physiol* 207: 454-460, 2006.

21.   **Gautschi OP, Frey SP, and Zellweger R.** Bone morphogenetic proteins in clinical applications. *ANZ J Surg* 77: 626-631, 2007.

22.   **Gazzerro E, Du Z, Devlin RD, Rydziel S, Priest L, Economides AN, and Canalis E.** Noggin arrests stromal cell differentiation in vitro. *Bone* 32: 111-119, 2003.

23.   **Gazzerro E, Gangji V, and Canalis E.** Bone morphogenetic proteins induce the expression of noggin, which limits their activity in cultured rat osteoblasts. *J Clin Invest* 102: 2106-2114, 1998.

24.   **Ge G, Seo NS, Liang X, Hopkins DR, Hook M, and Greenspan DS.** Bone morphogenetic protein-1/tolloid-related metalloproteinases process osteoglycin and enhance its ability to regulate collagen fibrillogenesis. *J Biol Chem* 279: 41626-41633, 2004.

25.   **Gong Y, Krakow D, Marcelino J, Wilkin D, Chitayat D, Babul-Hirji R, Hudgins L, Cremers CW, Cremers FP, Brunner HG, Reinker K, Rimoin DL, Cohn DH, Goodman FR, Reardon W, Patton M, Francomano CA, and Warman ML.** Heterozygous mutations in the gene encoding noggin affect human joint morphogenesis. *Nat Genet* 21: 302-304, 1999.

26.   **Granjeiro JM, Oliveira RC, Bustos-Valenzuela JC, Sogayar MC, and Taga R.** Bone morphogenetic proteins: from structure to clinical use. *Braz J Med Biol Res* 38: 1463-1473, 2005.

27.   **Hejnowicz Z, Sondag C, Alt W, and Sievers A.** Temporal course of graviperception in intermittently stimulated cress roots. *Plant Cell Environ* 21: 1293-1300, 1998.

28.   **Hillsley MV and Frangos JA.** Alkaline phosphatase in osteoblasts is down-regulated by pulsatile fluid flow. *Calcif Tissue Int* 60: 48-53, 1997.

29.   **Hou G, Mohamalawari DR, and Blancaflor EB.** Enhanced gravitropism of roots with a disrupted cap actin cytoskeleton. *Plant Physiol* 131: 1360-1373, 2003.

30.   **Ingber D.** How cells (might) sense microgravity. *Faseb J* 13 Suppl: S3-15, 1999.

31.   **Ingber DE.** Cellular mechanotransduction: putting all the pieces together again. *Faseb J* 20: 811-827, 2006.

32.   **Iqbal J and Zaidi M.** Molecular regulation of mechanotransduction. *Biochem Biophys Res Commun* 328: 751-755, 2005.

33.   **Ishijima M, Rittling SR, Yamashita T, Tsuji K, Kurosawa H, Nifuji A, Denhardt DT, and Noda M.** Enhancement of osteoclastic bone resorption and suppression of osteoblastic bone formation in response to reduced mechanical stress do not occur in the absence of osteopontin. *J Exp Med* 193: 399-404, 2001.

34.   **Ishisaki A, Yamato K, Hashimoto S, Nakao A, Tamaki K, Nonaka K, ten Dijke P, Sugino H, and Nishihara T.** Differential inhibition of Smad6 and Smad7 on bone morphogenetic protein- and activin-mediated growth arrest and apoptosis in B cells. *J Biol Chem* 274: 13637-13642, 1999.

35.   **Jacobs CR, Yellowley CE, Davis BR, Zhou Z, Cimbala JM, and Donahue HJ.** Differential effect of steady versus oscillating flow on bone cells. *J Biomech* 31: 969-976, 1998.

36.   **Kain MS and Einhorn TA.** Recombinant human bone morphogenetic proteins in the treatment of fractures. *Foot Ankle Clin* 10: 639-650, viii, 2005.

37.   **Kapur S, Baylink DJ, and Lau KH.** Fluid flow shear stress stimulates human osteoblast proliferation and differentiation through multiple interacting and competing signal transduction pathways. *Bone* 32: 241-251, 2003.

38.   **Katagiri T, Yamaguchi A, Komaki M, Abe E, Takahashi N, Ikeda T, Rosen V, Wozney JM, Fujisawa-Sehara A, and Suda T.** Bone morphogenetic protein-2 converts the differentiation pathway of C2C12 myoblasts into the osteoblast lineage. *J Cell Biol* 127: 1755-1766, 1994.

39.   **Kim CH, You L, Yellowley CE, and Jacobs CR.** Oscillatory fluid flow-induced shear stress decreases osteoclastogenesis through RANKL and OPG signaling. *Bone* 39: 1043-1047, 2006.

40.   **Klein-Nulend J, Roelofsen J, Semeins CM, Bronckers AL, and Burger EH.** Mechanical stimulation of osteopontin mRNA expression and synthesis in bone cell cultures. *J Cell Physiol* 170: 174-181, 1997.

41.   **Knothe Tate ML, Steck R, Forwood MR, and Niederer P.** In vivo demonstration of load-induced fluid flow in the rat tibia and its potential implications for processes associated with functional adaptation. *J Exp Biol* 203: 2737-2745, 2000.

42.   **Kreke MR and Goldstein AS.** Hydrodynamic shear stimulates osteocalcin expression but not proliferation of bone marrow stromal cells. *Tissue Eng* 10: 780-788, 2004.

43.   **Li G, Peng H, Corsi K, Usas A, Olshanski A, and Huard J.** Differential effect of BMP4 on NIH/3T3 and C2C12 cells: implications for endochondral bone formation. *J Bone Miner Res* 20: 1611-1623, 2005.

44.   **Li YJ, Batra NN, You L, Meier SC, Coe IA, Yellowley CE, and Jacobs CR.** Oscillatory fluid flow affects human marrow stromal cell proliferation and differentiation. *J Orthop Res* 22: 1283-1289, 2004.

45.   **Liedert A, Kaspar D, Blakytny R, Claes L, and Ignatius A.** Signal transduction pathways involved in mechanotransduction in bone cells. *Biochem Biophys Res Commun* 349: 1-5, 2006.

46.   **Luk KD, Chen Y, Cheung KM, Kung HF, Lu WW, and Leong JC.** Adeno-associated virus-mediated bone morphogenetic protein-4 gene therapy for in vivo bone formation. *Biochem Biophys Res Commun* 308: 636-645, 2003.

47.   **Machold RP, Kittell DJ, and Fishell GJ.** Antagonism between Notch and bone morphogenetic protein receptor signaling regulates neurogenesis in the cerebellar rhombic lip. *Neural Develop* 2: 5, 2007.

48.   **Malone AM, Batra NN, Shivaram G, Kwon RY, You L, Kim CH, Rodriguez J, Jair K, and Jacobs CR.** The role of actin cytoskeleton in oscillatory fluid flow-induced signaling in MC3T3-E1 osteoblasts. *Am J Physiol Cell Physiol* 292: C1830-1836, 2007.

49.   **Matzuk MM, Lu N, Vogel H, Sellheyer K, Roop DR, and Bradley A.** Multiple defects and perinatal death in mice deficient in follistatin. *Nature* 374: 360-363, 1995.

50.   **McGarry JG, Klein-Nulend J, and Prendergast PJ.** The effect of cytoskeletal disruption on pulsatile fluid flow-induced nitric oxide and prostaglandin E2 release in osteocytes and osteoblasts. *Biochem Biophys Res Commun* 330: 341-348, 2005.

51.   **Morinobu M, Ishijima M, Rittling SR, Tsuji K, Yamamoto H, Nifuji A, Denhardt DT, and Noda M.** Osteopontin expression in osteoblasts and osteocytes during bone formation under mechanical stress in the calvarial suture in vivo. *J Bone Miner Res* 18: 1706-1715, 2003.

52.   **Nohe A, Hassel S, Ehrlich M, Neubauer F, Sebald W, Henis YI, and Knaus P.** The mode of bone morphogenetic protein (BMP) receptor oligomerization determines different BMP-2 signaling pathways. *J Biol Chem* 277: 5330-5338, 2002.

53.   **Oshin AO and Stewart MC.** The role of bone morphogenetic proteins in articular cartilage development, homeostasis and repair. *Vet Comp Orthop Traumatol* 20: 151-158, 2007.

54.   **Osyczka AM and Leboy PS.** Bone morphogenetic protein regulation of early osteoblast genes in human marrow stromal cells is mediated by extracellular signal-regulated kinase and phosphatidylinositol 3-kinase signaling. *Endocrinology* 146: 3428-3437, 2005.

55.   **Paloski WH, Black FO, Reschke MF, Calkins DS, and Shupert C.** Vestibular ataxia following shuttle flights: effects of microgravity on otolith-mediated sensorimotor control of posture. *Am J Otol* 14: 9-17, 1993.

56.   **Pardo SJ, Patel MJ, Sykes MC, Platt MO, Boyd NL, Sorescu GP, Xu M, van Loon JJWA, Wang MD, and Jo H.** Simulated microgravity using the Random Positioning Machine inhibits differentiation and alters gene expression profiles of 2T3 preosteoblasts. *Am J Physiol Cell Physiol* 288: C1211-1221, 2005.

57.   **Pavlin D, Dove SB, Zadro R, and Gluhak-Heinrich J.** Mechanical loading stimulates differentiation of periodontal osteoblasts in a mouse osteoinduction model: effect on type I collagen and alkaline phosphatase genes. *Calcif Tissue Int* 67: 163-172, 2000.

58.   **Peng H, Usas A, Gearhart B, Olshanski A, Shen HC, and Huard J.** Converse relationship between in vitro osteogenic differentiation and in vivo bone healing elicited by different populations of muscle-derived cells genetically engineered to express BMP4. *J Bone Miner Res* 19: 630-641, 2004.

59.   **Phimphilai M, Zhao Z, Boules H, Roca H, and Franceschi RT.** BMP signaling is required for RUNX2-dependent induction of the osteoblast phenotype. *J Bone Miner Res* 21: 637-646, 2006.

60.   **Pittenger MF, Mackay AM, Beck SC, Jaiswal RK, Douglas R, Mosca JD, Moorman MA, Simonetti DW, Craig S, and Marshak DR.** Multilineage potential of adult human mesenchymal stem cells. *Science* 284: 143-147, 1999.

61.   **Ponik SM, Triplett JW, and Pavalko FM.** Osteoblasts and osteocytes respond differently to oscillatory and unidirectional fluid flow profiles. *J Cell Biochem* 100: 794-807, 2007.

62.   **Ross MD.** The influence of gravity on structure and function of animals. *Adv Space Res* 4: 305-314, 1984.

63.   **Rubin CT, Sommerfeldt DW, Judex S, and Qin Y.** Inhibition of osteopenia by low magnitude, high-frequency mechanical stimuli. *Drug Discov Today* 6: 848-858, 2001.

64.   **Rubin J, Rubin C, and Jacobs CR.** Molecular pathways mediating mechanical signaling in bone. *Gene* 367: 1-16, 2006.

65.   **See J, Mamontov P, Ahn K, Wine-Lee L, Crenshaw EB, 3rd, and Grinspan JB.** BMP signaling mutant mice exhibit glial cell maturation defects. *Mol Cell Neurosci* 35: 171-182, 2007.

66.   **Sikavitsas VI, Bancroft GN, Holtorf HL, Jansen JA, and Mikos AG.** Mineralized matrix deposition by marrow stromal osteoblasts in 3D perfusion culture increases with increasing fluid shear forces. *Proc Natl Acad Sci U S A* 100: 14683-14688, 2003.

67.   **Smith S, Wastney M, O'Brien K, Morukov B, Larina I, Abrams S, Davis-Street J, Oganov V, and Shackelford L.** Bone markers, calcium metabolism, and calcium kinetics during extended-duration space flight on the mir space station. *J Bone Miner Res* 20: 208-218, 2005.

68.   **Smith SM, Davis-Street JE, Fesperman JV, Calkins DS, Bawa M, Macias BR, Meyer RS, and Hargens AR.** Evaluation of treadmill exercise in a lower body negative pressure chamber as a countermeasure for weightlessness-induced bone loss: a bed rest study with identical twins. *J Bone Miner Res* 18: 2223-2230, 2003.

69.   **Sorescu GP, Sykes M, Weiss D, Platt MO, Saha A, Hwang J, Boyd N, Boo YC, Vega JD, Taylor WR, and Jo H.** Bone Morphogenic Protein 4 Produced in Endothelial Cells by Oscillatory Shear Stress Stimulates an Inflammatory Response. *J Biol Chem* 278: 31128-31135, 2003.

70.   **Spinella-Jaegle S, Roman-Roman S, Faucheu C, Dunn FW, Kawai S, Gallea S, Stiot V, Blanchet AM, Courtois B, Baron R, and Rawadi G.** Opposite effects of bone morphogenetic protein-2 and transforming growth factor-beta1 on osteoblast differentiation. *Bone* 29: 323-330, 2001.

71.   **Suzuki A, Guicheux J, Palmer G, Miura Y, Oiso Y, Bonjour JP, and Caverzasio J.** Evidence for a role of p38 MAP kinase in expression of alkaline phosphatase during osteoblastic cell differentiation. *Bone* 30: 91-98, 2002.

72.   **Tasheva E.** Mimecan/osteoglycin-deficient mice have collagen fibril abnormalities. *Molecular Vision* 8: 407-415, 2002.

73.   **Thi MM, Kojima T, Cowin SC, Weinbaum S, and Spray DC.** Fluid shear stress remodels expression and function of junctional proteins in cultured bone cells. *Am J Physiol Cell Physiol* 284: C389-403, 2003.

74.   **Tsumaki N, Nakase T, Miyaji T, Kakiuchi M, Kimura T, Ochi T, and Yoshikawa H.** Bone morphogenetic protein signals are required for cartilage formation and differently regulate joint development during skeletogenesis. *J Bone Miner Res* 17: 898-906, 2002.

75.   **Urist MR.** Bone: formation by autoinduction. *Science* 150: 893-899, 1965.

76.   **Vaziri ND, Ding Y, Sangha DS, and Purdy RE.** Upregulation of NOS by simulated microgravity, potential cause of orthostatic intolerance. *J Appl Physiol* 89: 338-344, 2000.

77.   **Wang N, Naruse K, Stamenovic D, Fredberg JJ, Mijailovich SM, Tolic-Norrelykke IM, Polte T, Mannix R, and Ingber DE.** Mechanical behavior in living cells consistent with the tensegrity model. *Proc Natl Acad Sci U S A* 98: 7765-7770, 2001.

78.   **Wang W, Mariani FV, Harland RM, and Luo K.** Ski represses bone morphogenic protein signaling in Xenopus and mammalian cells. *Proc Natl Acad Sci U S A* 97: 14394-14399, 2000.

79.   **Weinbaum S, Cowin SC, and Zeng Y.** A model for the excitation of osteocytes by mechanical loading-induced bone fluid shear stresses. *J Biomech* 27: 339-360, 1994.

80.   **Weston CR, Lambright DG, and Davis RJ.** Signal transduction. MAP kinase signaling specificity. *Science* 296: 2345-2347, 2002.

81.   **Xiao YT, Xiang LX, and Shao JZ.** Bone morphogenetic protein. *Biochem Biophys Res Commun* 362: 550-553, 2007.

82.   **Yamaguchi A, Katagiri T, Ikeda T, Wozney JM, Rosen V, Wang EA, Kahn AJ, Suda T, and Yoshiki S.** Recombinant human bone morphogenetic protein-2 stimulates osteoblastic maturation and inhibits myogenic differentiation in vitro. *J Cell Biol* 113: 681-687, 1991.

83.   **You J, Reilly GC, Zhen X, Yellowley CE, Chen Q, Donahue HJ, and Jacobs CR.** Osteopontin gene regulation by oscillatory fluid flow via intracellular calcium mobilization and activation of mitogen-activated protein kinase in MC3T3-E1 osteoblasts. *J Biol Chem* 276: 13365-13371, 2001.

84.	**Zhang YW, Yasui N, Ito K, Huang G, Fujii M, Hanai J, Nogami H, Ochi T, Miyazono K, and Ito Y.** A RUNX2/PEBP2alpha A/CBFA1 mutation displaying impaired transactivation and Smad interaction in cleidocranial dysplasia. *Proc Natl Acad Sci U S A* 97: 10549-10554, 2000.

85.	**Zwart SR, Hargens AR, Lee SM, Macias BR, Watenpaugh DE, Tse K, and Smith SM.** Lower body negative pressure treadmill exercise as a countermeasure for bed rest-induced bone loss in female identical twins. *Bone* 40: 529-537, 2007.

Chapter 8

The Effects of Disuse and Low Magnitude Mechanical Loading on Osteoblast Function*

Summary

From specific aims 1 and 2, we developed an *in vitro* disuse system to study cellular alterations in osteoblasts caused by disuse. We evaluated system gene expression, providing insight into how osteoblasts respond through molecular transformations to unloading. In specific aim 3, it is our goal to explore a countermeasure device and its cellular and molecular effects in osteoblasts.

Bone loss due to osteoporosis or disuse such as in paraplegia or microgravity is a significant health problem. As a treatment for osteoporosis, brief exposure of intact animals or humans to low magnitude and high frequency (LMHF) mechanical loading has been shown to normalize and prevent bone loss. However, the underlying mechanisms and the target cells by which LMHF mechanical loading alleviate bone loss are not known. Here, we hypothesized that direct application of LMHF mechanical loading to osteoblasts alters their cell responses, preventing decreased bone formation induced by disuse or microgravity conditions. To test our hypothesis, preosteoblast 2T3 cells were exposed to a disuse condition using the Random Positioning Machine (RPM) and intervened with a LMHF mechanical load (0.1-0.4g at 30Hz for 10-60 min/day). Exposure of 2T3 cells to the RPM decreased bone formation responses as determined by alkaline phosphatase (ALP) activity and mineralization even in the presence of a

submaximal dose of bone morphogenic protein 4 (BMP4, 20ng/ml). However, LMHF mechanical loading prevented the RPM-induced decrease in ALP activity and mineralization. Mineralization induced by LMHF mechanical loading was enhanced by treatment with BMP4 and blocked by the BMP antagonist noggin, suggesting a role for BMPs in this response. In addition, LMHF mechanical loading rescued the RPM-induced decrease in gene expression of *ALP*, *runt homology domain transcription factor 2 (runx2)*, *osteomodulin (OMD)*, *parathyroid hormone receptor 1 (PTHR1)*, and *osteoglycin (OGN)*. These findings show that osteoblasts directly respond to LMHF mechanical loading to induce bone formation responses, potentially leading to normalization or prevention of bone loss caused by disuse or microgravity conditions. The mechanosensitive genes identified here provide potential targets for pharmaceutical treatments that may be used in combination with LMHF mechanical loading to better treat osteoporosis, disuse-induced bone loss, or microgravity-induced bone loss.

Introduction

Musculoskeletal pathologies associated with decreased bone mass, including osteopenia, osteoporosis, disuse-induced bone loss, and microgravity-induced bone loss, affect millions of Americans annually. Bone loss is particularly dangerous since it is at first asymptomatic and leads to severe fractures of bones, typically those in the hip, spine, and wrist (3).   While osteoporosis usually affects the elderly, it can afflict both men and women of any age. Additionally, bone loss occurs in spaceflight, rendering astronauts at-risk for fractures during long term space travel. On average, astronauts lose 1-2% of bone mass per month during space missions (14), and there are no known countermeasures that can effectively mitigate this bone loss.

It has long been regarded that mechanical stimuli are anabolic to bone. High magnitude, low frequency impact such as running has been recognized to increase bone and muscle mass (2, 31, 34). However, the opposite stimulus, a low magnitude and high frequency (LMHF) mechanical load experienced in activities as low impact as standing, has also been shown to be anabolic to bone (24). This type of signal is transmitted by the musculature to the skeleton during the majority of each day, assisting in maintenance of posture and other non-strenuous activities. If it is true that muscle atrophy (sarcopenia) parallels ageing (15, 16, 22), then these intrinsic, LMHF mechanical signals would diminish with it, leaving the musculoskeletal system without potentially key signals critical to the regulation and retention of skeletal mass and morphology.

Recently, a LMHF mechanical loading device has been developed to treat bone loss by applying a low magnitude mechanical signal at a high frequency to the whole animal or human. The LMHF mechanical load has been shown to be effective in treating musculoskeletal pathologies in a number of subjects during research and clinical trials, including animals (26), children with musculoskeletal diseases such as cerebral palsy or muscular dystrophy (7, 35), young women with low bone mass (6), and post-menopausal osteoporotic women (23). While several pre-clinical and clinical trials have demonstrated that the LMHF mechanical loading affects bone formation *in vivo*, the target tissues of the mechanical load and underlying mechanisms mediating the responses are not known. Here, we hypothesized that a LMHF mechanical loading applied directly to osteoblasts would prevent decreased bone formation responses in osteoblasts by altering gene expression and cell function.

To test our hypothesis, pre-osteoblast 2T3 cells were exposed to the RPM to model a decreased bone formation response (20) and intervened with the LMHF mechanical signals (0.1-0.4g acceleration at 30Hz frequency) for 10-60 min per day. We

developed an *in vitro* method to apply LMHF mechanical loading to osteoblast cells, examined various bone formation markers, and performed BMP inhibitor studies. We found that vibration stimulated an osteogenic response in a BMP-dependent manner, inducing alkaline phosphatase (ALP) activity, enhancing subsequent mineralization, and increasing osteogenic gene expression.

Materials and Methods

Cell culture – 2T3 murine osteoblast precursor cells were kindly provided to us by Dr. Steve Harris, University of Texas Health Science Center at San Antonio. The cells were cultured in a growth medium (α-minimal essential medium) containing 10% fetal bovine serum (Atlanta Biologicals) with 100 units/ml of penicillin and 100µg/ml of streptomycin and grown in a standard humidified incubator (37°C, 5% CO_2) as previously described by us (20, 21).   For mineralization experiments, the growth medium was supplemented with ascorbic acid (50 µg/ml) and β-glycerolphosphate (5 mM) with or without BMP2 or BMP4 (0-50 ng/ml) and/or noggin (100 ng/ml).

Random Positioning Machine (RPM) – A desktop RPM manufactured by the Dutch Space Agency was used to simulate disuse or microgravity conditions as previously described by us (20). Briefly, OptiCell disks seeded with cells were mounted on the center of the platform located on the inner frame, and the RPM was operated in random modes of speed and direction via a computer user interface with dedicated control software inside a humidified incubator (5% CO_2 at 37^oC).

Low Magnitude and High Frequency (LMHF) Mechanical Loading Platform—LMHF mechanical loading was delivered to the cells using a vertically oscillating platform custom manufactured by Juvent, Inc (Figure 8.1A). The magnitude of mechanical

174

loading is defined as a peak-to-peak load (Figure 8.1B), and cells were exposed to 0.1-0.4g acceleration (where 1g is Earth's gravitational field) at 30 Hz frequency for 10-60 minutes per day for 3-21 days (Figure 8.1C). The loading platform dimensions are 17"X17", and the loading conditions were controlled through a program installed on a laptop.
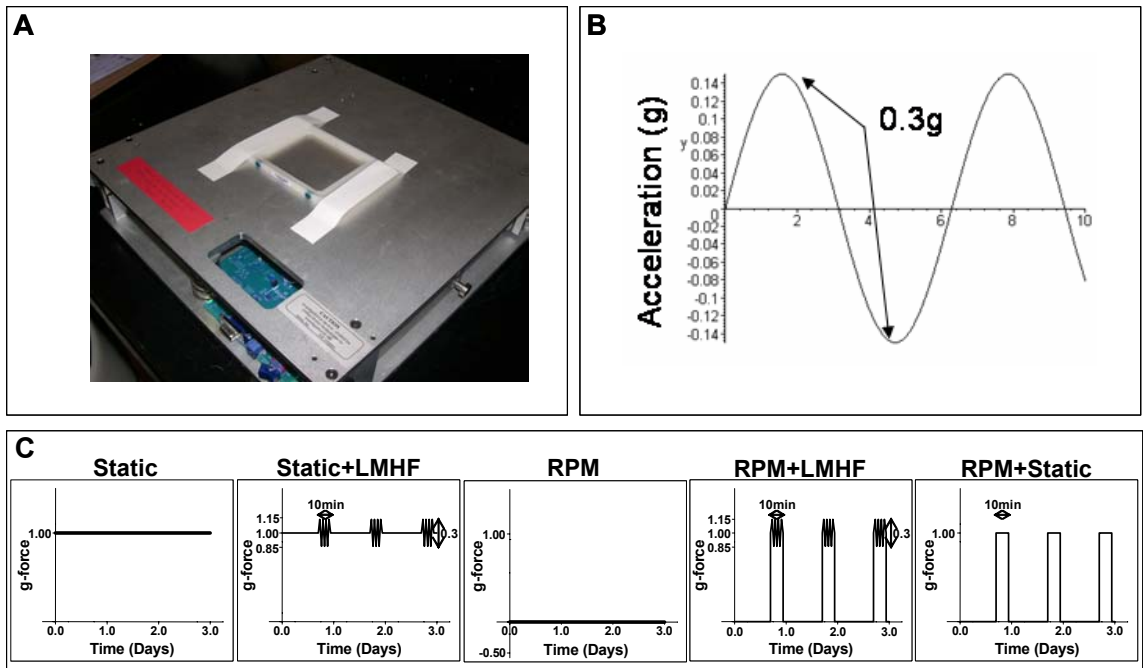
Figure 8.1 LMHF mechanical loading using a custom built platform. Confluent 2T3 cells grown in OptiCell chambers were exposed to LMHF loading using a platform (A) designed to produce dynamic, vertical oscillations, where the peak to peak acceleration is the magnitude of the load (B). Cells were exposed to five different experimental conditions (C) with varying g-loads as shown on the y-axis using the LMHF platform and/or the RPM.

Experimental Design— Confluent 2T3 cells grown in OptiCells were exposed to static (1g) or RPM conditions with or without a brief, daily LMHF mechanical load inside a humidified incubator (5% CO_2 at 37°C). As shown in Figure 1C, 2T3 cells were exposed to five different conditions: 1) *Static*: cells were exposed to control 1g conditions continuously throughout the experimental duration, 2) *Static+LMHF*: cells were exposed

to static 1g conditions and treated once with LMHF mechanical loading for 10-60 minutes/day, 3) *RPM*: cells were continuously rotated on the RPM, simulating a disuse or microgravity environment,   4) *RPM+LMHF*: cells were exposed to the RPM and removed once from the RPM and mechanically loaded daily as in the Static+LMHF group, and 5) *RPM+Static*: Since the RPM+LMHF group not only was treated with the LMHF mechanical loading but also was returned to static 1g conditions briefly, we employed the RPM+Static group as a control. This group of cells was exposed to the RPM and intervened with the static 1g conditions daily (10-60 min/day).

Whole cell lysate and alkaline phosphatase (ALP) enzyme activity—Following the experiment, cells were washed with ice-cold phosphate buffered saline (PBS) two times and lysed in 500 µl of a lysis buffer containing 0.5% Triton X-100, 1 mM $MgCl_2$, and 10 mM Tris-HCl. Samples were stored at -80ºC until needed. Alkaline phosphatase (ALP) activity was determined using a Diagnostics ALP assay kit (Sigma) as previously described by us (20, 21).

Alizarin Red Stain—Following the experiment, cells were washed with ice-cold PBS two times and fixed in 70% ethanol for 15 minutes. Cultures were stained for two minutes with a 1% Alizarin red solution for calcium detection. Following the stain, cultures were rinsed with a 0.01%HCl-ethanol solution and dH_20. The plates were dried overnight before being scored for percent mineralization using ImageJ analysis software. Quantification graphs express mineralization as a percent of the experimental control.

Fourier Transform Infrared (FTIR) Spectroscopy— After 15-21 days of exposure to stimulus, cells were scraped in 100% ethanol and dried at 50°C overnight. Samples were mixed with potassium bromide (Sigma), pressed into pellets, and analyzed with a

Nexus 470 FTIR spectrometer (ThermoNicolet, Madison, WI), which was equipped with a deuterated triglycine sulfate (DTGS) detector. A nitrogen purge was performed, and sixty four scans were acquired (4).

Reverse Transcriptase and Real Time Polymerase Chain Reaction (RTPCR)–Total RNA was prepared and amplified as previously described by us (20, 21). Briefly, total RNA was prepared using the RNeasy Mini Kit (Qiagen) and reverse transcribed by using random primers and a Superscript-II kit (Life Technology). The synthesized and purified cDNA was amplified using a LightCycler (Roche Applied Science), and mRNA copy numbers were determined based on standard curves generated with the genes of interest and normalized against *18S* ribosomal RNA. The primer pairs for quantitative real time RTPCR for *ALP*, *runx2*, *BMP4*, *OMD*, and *PTHR1* were previously published by us (20, 21) and for *OGN* by others (37). Real time RTPCR for the listed genes were carried out in RTPCR buffer as described previously by us (20, 21).

Statistical analysis—Data are expressed as mean ± SEM with n numbers representing biological replicates pooled from independent experiments. Statistical analysis was performed using the Student's t-test. A significance level of $p < 0.05$ was considered statistically significant.

Results

LMHF mechanical loading did not alter cell morphology or cell number of 2T3 preosteoblasts.

2T3 cells exposed to Static, Static+LMHF, RPM, or RPM+LMHF conditions for three days showed no apparent change in cell morphology after stimulus exposure as

shown in Figure 8.2A. Additionally, cell number did not change between static and experimental groups with exposure to LMHF mechanical loading or RPM (Figure 8.2B). These results suggest that the RPM or LMHF mechanical loading did not significantly affect cell shape and growth.
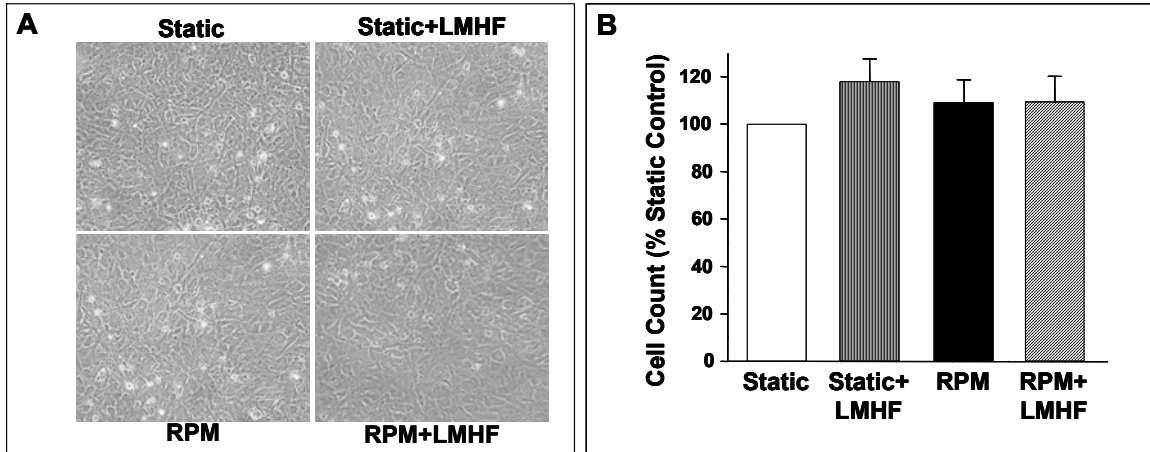
Figure 8.2 LMHF mechanical loading did not alter morphology or cell number of 2T3 cells. Confluent 2T3 cells were exposed to Static, Static+LMHF, RPM, or RPM+LMHF conditions for 3 days. LMHF loading was applied to the appropriate groups at 0.3g for 10 min/day. Cultured cells were photomicrographed with a phase microscope at the end of the experiment (A), and cell proliferation was assessed by counting cells using a Coulter counter and graphed as % of static control. Data are expressed as mean ± SEM (n=5-11, p>0.15).

LMHF mechanical loading increased ALP activity in a magnitude- and time-dependent manner.

Here, we examined whether LMHF mechanical loading regulated ALP activity, an early bone formation marker, in a magnitude-dependent manner. LMHF mechanical loading applied to 2T3 cells for 10 min/day for three days induced an increase in ALP activity in a magnitude-dependent manner, where 0.3g and 0.4g induced significant changes compared to static control (Figure 8.3A). Next, we investigated the time-dependent effects of LMHF mechanical loading. Exposure to 0.3g LMHF mechanical
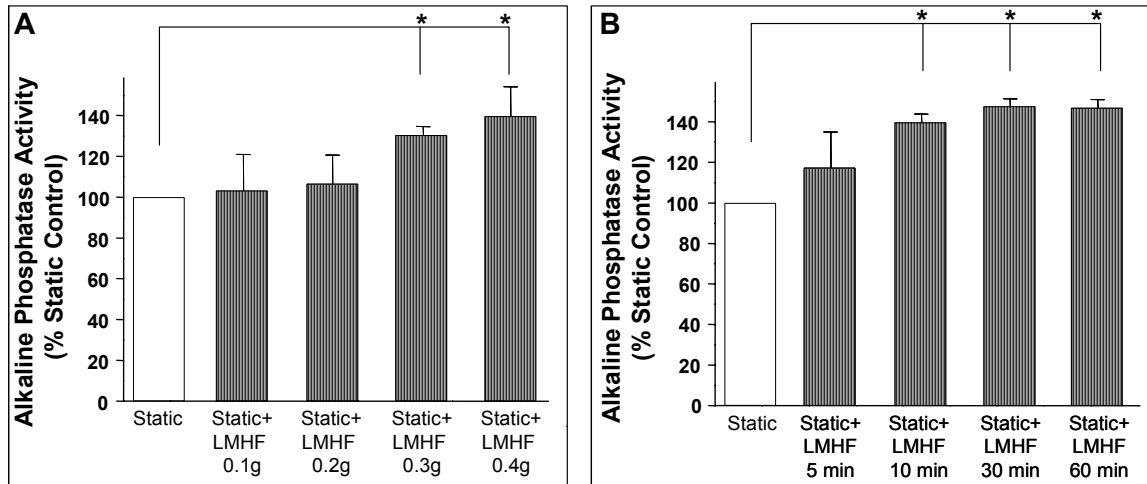
Figure 8.3 LMHF loading increased alkaline phosphatase (ALP) activity in a magnitude- and time-dependent manner. 2T3 cells were exposed to Static or Static+LMHF conditions at varying loading magnitudes (A) or varying treatment-time/day (B), and cell lysates were obtained. After 3 days exposure, ALP activity was determined using a colorimetric assay, normalized to total protein, and graphed as a % of static control. Data are expressed as mean ± SEM (n=6, *p<0.05).

loading for as few as 10 minutes/day for three days was sufficient to increase ALP activity in 2T3 cells. Exposure for 30 minutes or one hour per day did not further increase ALP activity compared to 10 minutes/day (Figure 8.3B). These results suggest that LMHF mechanical loading increases ALP activity in a magnitude- and time-dependent manner.

LMHF mechanical loading prevented inhibition of ALP activity induced by RPM.

Previously, we have shown that exposure of 2T3 cells to either the RPM or RWV induces bone loss responses as determined by ALP activity (20, 21). Here, we examined whether LMHF mechanical loading prevents ALP activity inhibition induced by exposing 2T3 cells to RPM. As expected, RPM exposure (three days) decreased ALP activity by 30% of static control (Figure 8.4). This RPM-induced decrease was completely normalized to the static level by exposing cells to LMHF mechanical loading

(RPM+LMHF) at either 0.3g (Figure 8.4A) or 0.4g (Figure 8.4B) for 10 min/day. In contrast, exposure to static conditions for 10 min/day (RPM+Static) was not able to prevent RPM-inhibition of ALP activity (Figure 8.4B), suggesting a specific effect of the mechanical loading and not the static 1g conditions. In addition, LMHF mechanical loading (Static+LMHF) for 10 min/day at both 0.3g and 0.4g increased ALP activity by 30% above static control as shown in Figure 8.4. These results are consistent with the following mineralization studies.
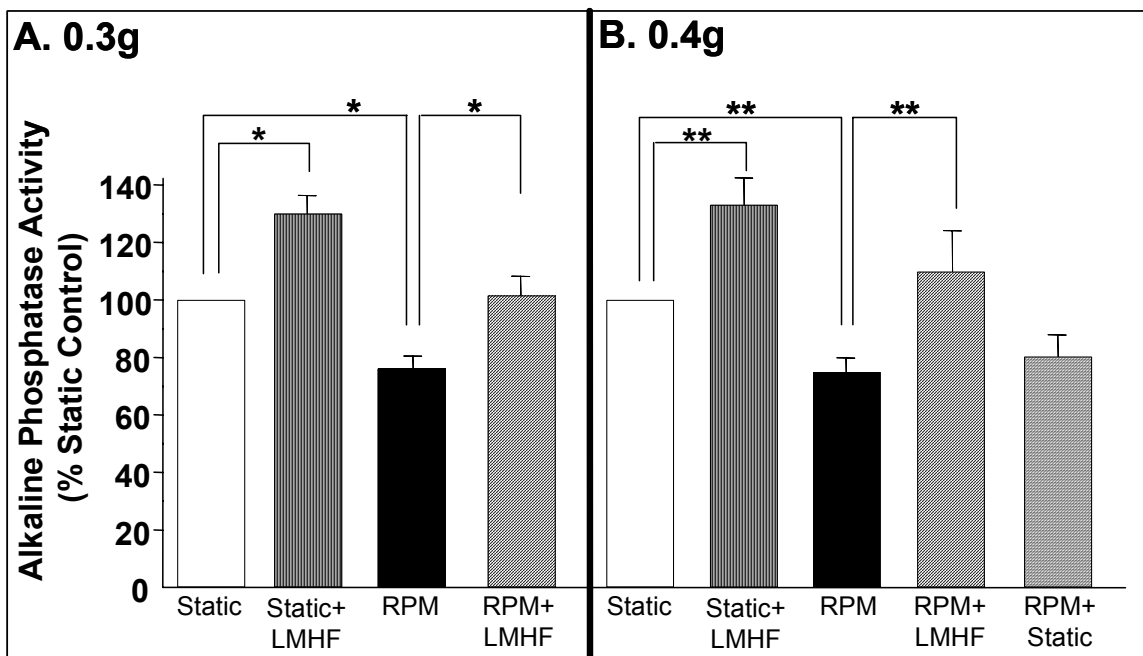
Figure 8.4 LMHF mechanical loading prevented inhibition of alkaline phosphatase activity caused by RPM. 2T3 cells were exposed to Static, Static+LMHF, RPM, RPM+LMHF, and RPM+Static conditions for 3 days. LMHF was applied to the appropriate groups at 0.3g (A) or 0.4g (B) for 10 min/day. ALP activity was measured using a colormetric assay, normalized to total protein, and graphed as a % of static control. Data are expressed as mean ± SEM (n=6-9 *p<0.01, **p<0.05).

LMHF mechanical loading stimulated mineralization in a magnitude-dependent manner.

2T3 cells show no apparent mineralization in an experimental time frame of 15-21 days unless osteogenic factors such as BMP2 or BMP4 are added to the culture medium (5). Here, we examined whether LMHF mechanical loading stimulates mineralization of 2T3 cells without supplementing the culture medium with exogenous BMPs. As expected, the static cells cultured for 21 days in the absence of added BMPs (Static) did not show any significant calcium deposits as identified by Alizarin Red staining (Figure 8.5A and B). Also as expected, supplementing the media with 20 ng/ml of BMP4 (Static+BMP4) induced a dramatic increase in calcium deposits (Figure 8.5A and B). Exposure of 2T3 cells to LMHF mechanical loading alone (without exogenously added BMP4) significantly increased calcium deposits by 10 to 40-fold over the static conditions (Static+LMHF). Additionally, the effect of LMHF signals was magnitude-dependent, as calcium deposition significantly increased when cells were loaded at levels as low as 0.1g up to 0.4g. To further demonstrate whether LMHF loading induced physiologically relevant mineralization in 2T3 cells, FTIR analysis was performed. Figure 8.5C is a representative FTIR analysis showing adsorption bands at 1650 cm^{-1} (Amide I, C=O) and 1530 cm^{-1} (Amide II, N-H and C-N), which represent bonds in the extracellular matrix and lipid content (4). Additionally, mineral samples had peaks at 1030 cm^{-1} (P-O), at 870 cm^{-1} (C-O), and a split peak at 600 cm^{-1} (P-O). These bands are characteristic of carbonate-containing, poorly crystalline hydroxyapatite (4). These results suggest that LMHF loading alone can stimulate mineralization of 2T3 cells without requiring exogenously added BMPs.
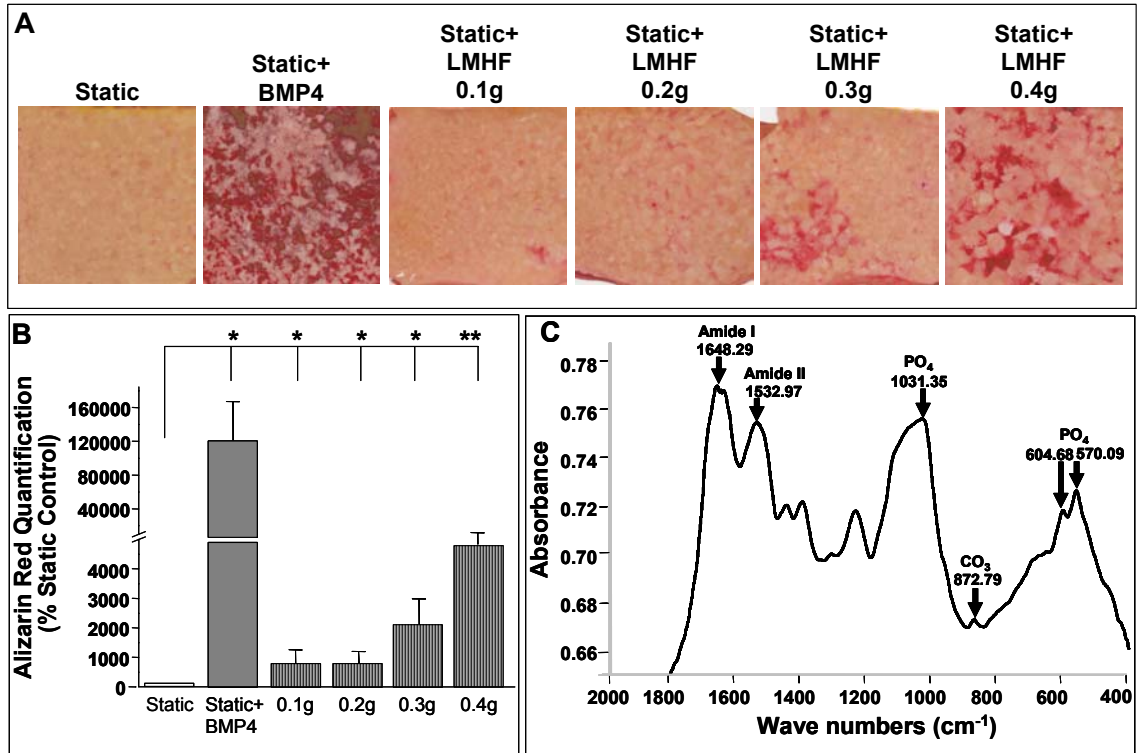
Figure 8.5 LMHF mechanical loading induced mineralization in a magnitude-dependent manner. Confluent 2T3 cells were exposed to Static, Static+BMP4, or Static+LMHF conditions at varying loading magnitudes (0.1-0.4g for 10 min/day) for 21 days and stained for calcium deposition using Alizarin Red and analyzed with FTIR for chemical composition (C). The Opticell membrane was scanned (A), and quantification (B) was determined using imaging software and graphed as a % of static control. Data are expressed as mean ± SEM (n=6-10, *p<0.01, **p<0.05).

LMHF mechanical loading stimulated and RPM inhibited mineralization in 2T3 cells in a BMP4 concentration-dependent manner.

We next investigated the effects of LMHF loading and the RPM on 2T3 cell mineralization in a BMP4 concentration-dependent manner. We carried out experiments for a shorter duration of 15 days (rather than the 21 day experiments in Figure 8.5) to detect differences among BMP4-treated groups. 2T3 cells were exposed to Static, Static+LMHF, or RPM conditions and treated with or without recombinant BMP4 in concentrations varying from 0-50 ng/ml (Figure 8.6). BMP4 alone induced mineralization in static cultures at 20 or 50 ng/ml treatment, while 10 ng/ml showed a moderate but not statistically significant increase. The LMHF loading significantly augmented the BMP4 effect (Static+LMHF) at 20 ng/ml of BMP4 by more than two-fold above the corresponding static group. We also found that the LMHF loading tended to enhance the effect of 10 ng/ml BMP4 above that of the corresponding static group, although it did not reach statistical significance. The RPM prevented mineralization at submaximal concentrations of BMP4 (1 to 20ng/ml) compared to those of both the Static and Static+LMHF groups. This anti-osteogenic effect of RPM in the presence of submaximal BMP4 concentrations was also observed when cells were treated with 20 ng/ml BMP2 (data not shown). However, when treated with a higher concentration of BMP4 (50 ng/ml), 2T3 cells showed maximal mineralization in all three groups (Static, Static+LMHF, and RPM), and no differences were observed among them. These results suggest that BMP4 and LMHF provide pro-mineralization effects in an additive manner, and the RPM completely prevents the pro-mineralization effect of submaximal concentration of BMPs (up to 20 ng/ml). However, treating cells with a supermaximal BMP4 concentration (50 ng/ml) saturates the RPM and LMHF effects, suggesting a key role for BMPs as a mediator of mineralization in response to either mechanical condition.
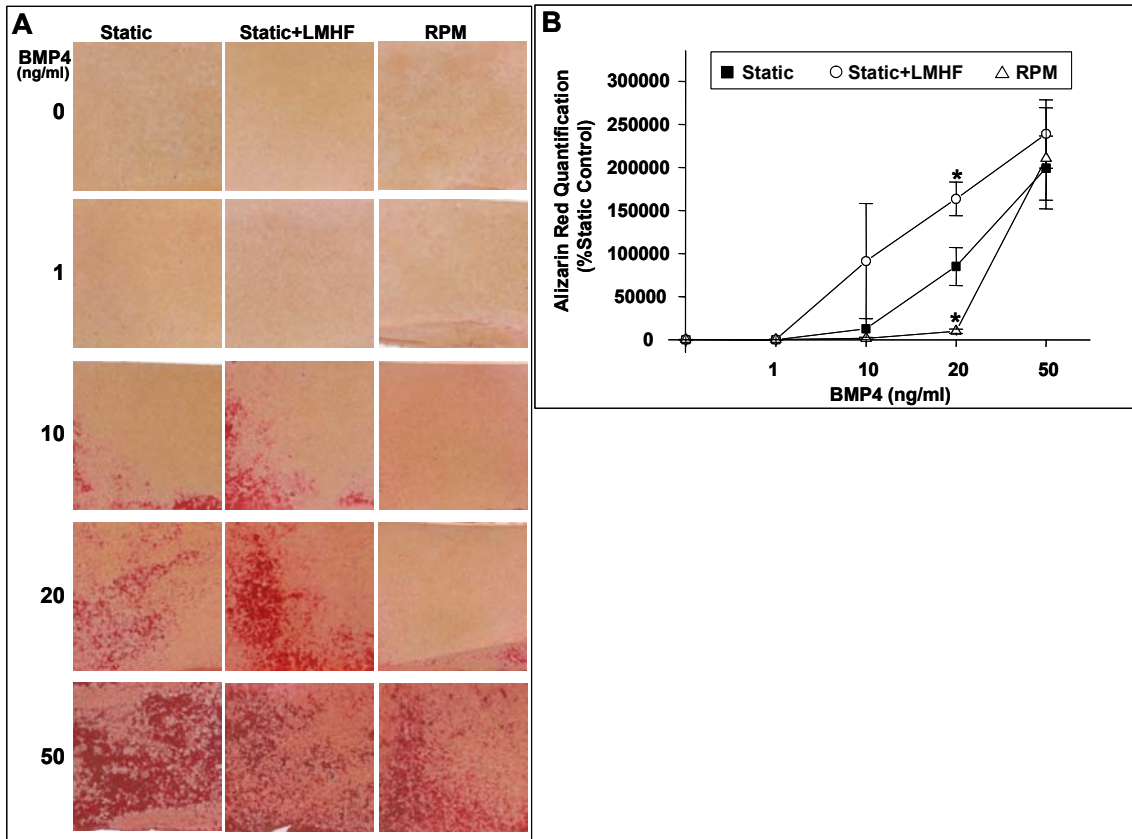
Figure 8.6 LMHF loading induced and RPM inhibited mineralization in 2T3 cells in a BMP4 concentration-dependent manner. Confluent 2T3 cells were exposed to Static, Static+LMHF, or RPM conditions in the presence of varying concentrations of BMP4 for 15 days. LMHF was applied to the appropriate groups at a magnitude of 0.4g for 10 min/day.   Cell cultures were stained with Alizarin Red (A), and the intensity was quantified (B) as in Figure 3. Data are expressed as mean ± SEM (n=4, *p<0.05).

LMHF mechanical loading prevented RPM-induced inhibition of 2T3 cell mineralization.

Previously, we have shown that exposure of 2T3 cells to either the RPM or RWV induces bone loss responses as determined by ALP activity, mineralization, and osteogenic gene expression (20, 21). Here, we examined whether daily LMHF loading of 2T3 cells could prevent the inhibition of mineralization induced by the RPM. For this study, 2T3 cells were exposed to Static, Static+LMHF, RPM, RPM+LMHF, and RPM+Static conditions in the presence of BMP4 (20 ng/ml) for 15 days and stained with Alizarin Red. As shown in Figure 8.7, LMHF loading of static cells (Static+LMHF) increased mineralization by 50% above the Static group, while the RPM dramatically inhibited mineralization by ~90% of the Static group. This RPM-induced inhibition was completely normalized to the level of the Static+LMHF group by exposing the cells to LMHF loading for 10 min/day (RPM+LMHF). However, exposure of the RPM group to static conditions for 10 min/day (RPM+Static) could not rescue the inhibition of mineralization by the RPM (Figure 8.7), suggesting a specific effect of LMHF loading and not the static 1g conditions. However, osteocalcin (OCN), a downstream target protein of *runx2*, was not changed with LMHF loading or RPM exposure (Figure 8.7C). These results suggest that RPM inhibits mineralization of 2T3 cells, which can be completely rescued by exposure to brief, daily LMHF loading.

LMHF mechanical loading induced mineralization in a BMP-dependent manner.

The result in Figure 8.6 suggested that the osteogenic effect of LMHF may be mediated by a BMP-dependent mechanism. To further test this hypothesis, we examined whether the specific BMP antagonist noggin (8) could block the osteogenic response induced by LMHF loading. As shown in Figure 8.8, LMHF loading, BMP4 (20 ng/ml), and BMP4+LMHF loading significantly increased mineralization compared to the

185
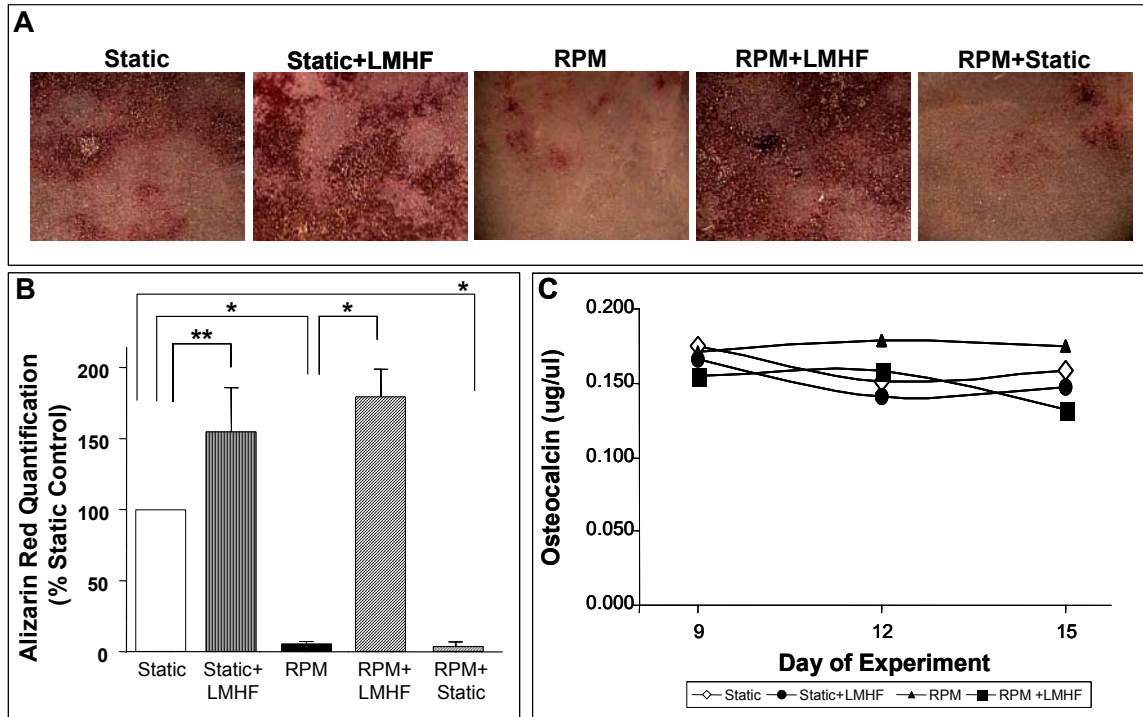
Figure 8.7 LMHF loading prevented inhibition of mineralization caused by RPM. 2T3 cells were exposed to Static, Static+LMHF, RPM, RPM+LMHF, and RPM+Static conditions in the presence of BMP4 for 15 days. LMHF was applied to the appropriate groups at 0.3g for 10 min/day. Alizarin Red staining was quantified and data are expressed as mean ± SEM (n=6, *p<0.005, **p<0.05).

Static group. However, treatment with noggin (100 ng/ml) completely blocked mineralization in all groups (Static, Static+LMHF, Static+BMP4, and Static+BMP4+LMHF). This result suggests an essential role of BMPs in the mineralization response induced by LMHF.

LMHF mechanical loading rescued RPM-induced decrease in osteogenic gene expression.

We have previously identified genes in 2T3 cells that change in response to the RPM and the RWV (20, 21). Here, we investigated alterations in a subset of osteogenic genes induced by LMHF loading. Consistent with our previous findings (20, 21), real
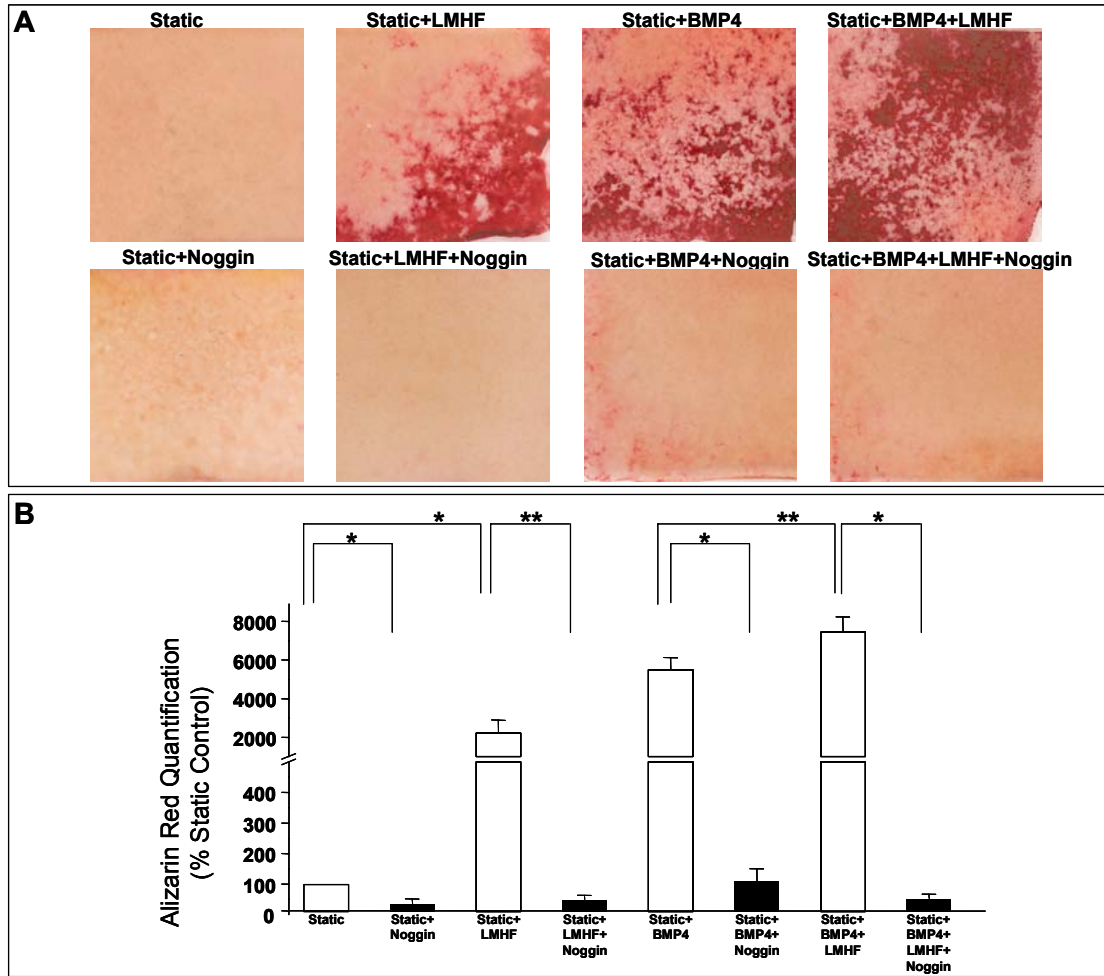
Figure 8.8 LMHF loading induced mineralization in a BMP-dependent manner.
2T3 cells were exposed to Static, Static+LMHF, Static+BMP4, and
Static+LMHF+BMP4 with or without noggin for 18-21 days. LMHF loading was
applied to the appropriate groups at 0.4g for 10 min/day. Alizarin Red staining was
quantified and data are expressed as mean ± SEM (n=6-10, *p<0.005, **p<0.05).

time RTPCR data (Figure 8.9) showed that RPM exposure for three days significantly inhibited the expression of *ALP*, *runx2*, *OMD, PTHR1*, and *OGN*. LMHF loading significantly increased the expression of all the tested genes except for osteoglycin in the Static+LMHF group (Figure 8.9). Moreover, LMHF prevented the RPM-induced decrease in expression of *ALP*, *runx2*, *OMD, PTHR1*, and *OGN* (RPM+LMHF). Unlike other genes studied here, regulation of *BMP4* mRNA level was unique. RPM exposure did not decrease *BMP4* mRNA level compared to static control, which is consistent with our previous findings (20). However, LMHF loading of static cells (Static+LMHF) increased *BMP4* level by ~two-fold above Static control and increased *BMP4* level by ~2.5-fold in RPM-exposed cells (RPM+LMHF) compared to the RPM (Figure 8.9). These data demonstrate that LMHF regulates expression of osteogenic genes, providing a potential molecular mechanism by which LMHF stimulates bone formation responses in 2T3 cells.

Discussion

One of the most significant findings of the current study is that cultured osteoblasts can directly sense and respond to an extremely low magnitude mechanical stimulus when applied at a high frequency, leading to osteogenic changes. The data presented here suggest that osteoblasts are partially responsible for the anabolic effects of LMHF loading observed *in vivo* in both animals and humans (7, 26, 35). These results are significant because they suggest that low impact loading in intact animals and humans may directly stimulate osteoblasts and stimulate bone formation responses. It is widely accepted that bone is responsive to signals that create peak strain magnitudes of 2,000-3,500 microstrains (με), such as those created from physical activities like running (19, 27, 30). However, muscle contractions during standing impose strains in the spectral range of 10-50 Hz of at least two orders of magnitude lower than high impact or
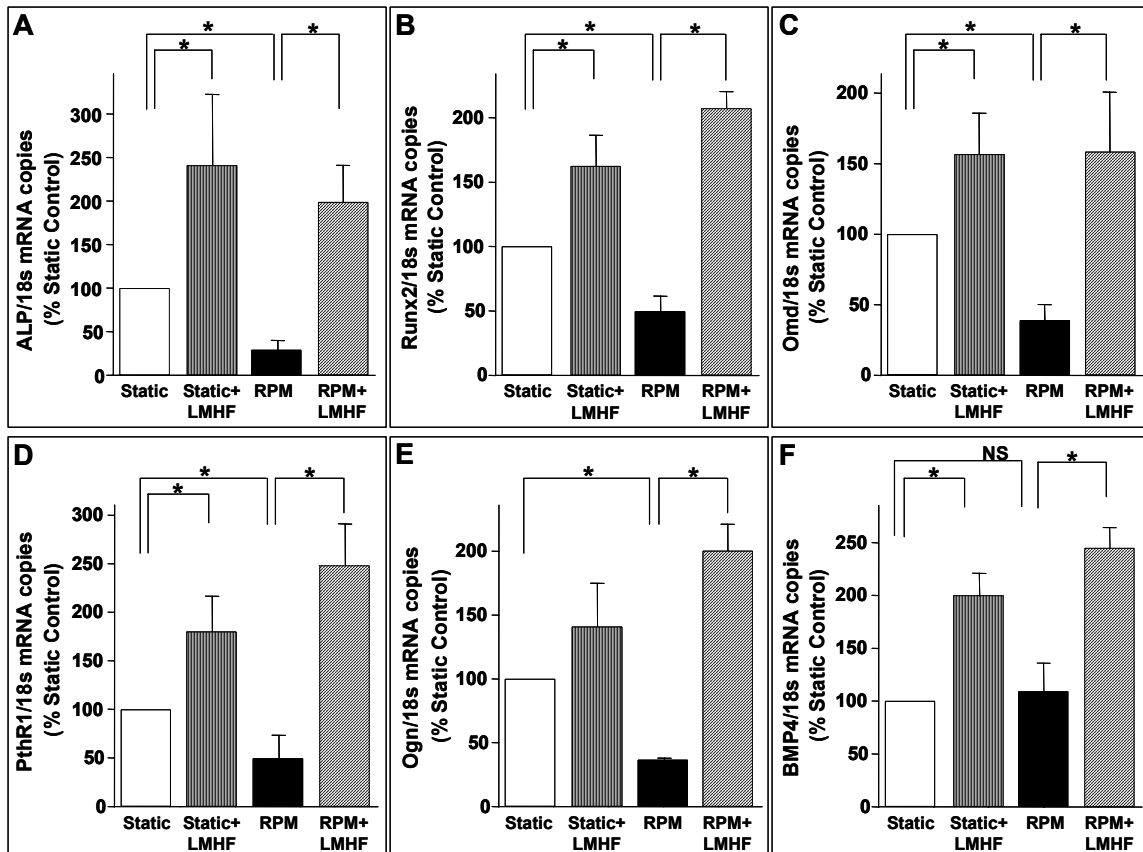
Figure 8.9 LMHF loading rescued RPM-induced decrease in osteogenic gene expression. Confluent 2T3 cells were exposed to Static, Static+LMHF, RPM, and RPM+LMHF conditions for 3 days. LMHF loading was applied to the appropriate groups at 0.3g for 10 min/day. Total RNA was obtained from the cell lysates, purified, and reverse transcribed to obtain cDNA. Quantitative real time PCR was performed for ALP (A), runx2 (B), osteomodulin (C), parathyroid hormone receptor 1 (D), and osteoglycin (E) using 18s rRNA as an internal control. Data are expressed as mean ± SEM (n=3-10, *p<0.05).

strenuous activities (30) and have recently been shown to normalize bone loss (23, 25, 26). Previous studies have shown that in cortical bone tissue, application of 2,000 $\mu\varepsilon$ at a frequency of 0.5 Hz (high magnitude and low frequency) maintained bone mass (28, 30). When the frequency was increased to 1 Hz, only a strain of 1,000 $\mu\varepsilon$ was needed to maintain bone mass, and at 30 Hz, only 70 $\mu\varepsilon$ (low magnitude, high frequency) was needed to inhibit bone resorption (29, 30).   Thus, bone response to mechanical loading appears to correlate with the product of frequency and load magnitude, meaning small strains induced by a low force could stimulate bone formation and maintain bone mass if applied at a high frequency. However, the underlying molecular mechanisms regulating how such a low level signal can be anabolic to bone tissue and which cells or tissues sense and mediate the response are unknown.

The current study provides insight into the potential mechanisms regarding how such low level mechanical loads can prevent or normalize bone loss. To examine the underlying mechanisms of the observed *in vivo* anabolic effects in response to LMHF loading, we used the RPM to induce a bone loss response *in vitro* using 2T3 cells. As expected, the RPM decreased ALP activity (Figure 8.4) and mineralization (Figure 8.7), and LMHF treatment increased both markers in static cells (Static+LMHF) in a magnitude-dependent manner (Figures 8.3 and 8.5). Moreover, LMHF prevented the RPM inhibition of ALP activity (Figure 8.4) and mineralization (Figure 8.7), preventing bone loss responses induced by the disuse or simulated microgravity conditions. The effects of both the RPM and LMHF loading were much more dramatic on mineralization than ALP activity of 2T3 cells. This may be because ALP activity is an early indicator of bone formation and is transient (17), making it a less sensitive marker of osteogenesis, especially in response to mechanical stimuli. These findings show that osteoblasts can directly respond to the LMHF signal at least *in vitro* by induction of osteogenic markers, suggesting that bone may respond to LMHF signals *in vivo* through osteoblast cells.

190

Importantly, we found that LMHF loading *alone* can induce mineralization of 2T3 cells (Figure 8.5) in a magnitude-dependent manner, and up to 20 ng/ml of BMP4 or BMP2 supplementation further increased this response in an additive manner (Figure 8.6). However, a supermaximal concentration (50 ng/ml) of BMP4 added to the cells was able to overcome both the RPM inhibition and LMHF increase (Figure 8.6). More importantly, treatment with the BMP antagonist noggin completely blocked mineralization induced by the LMHF stimuli. One of the limitations of this study was the range of low magnitude force due to physical limitations of the LMHF loading platform. Nevertheless, we tested LMHF loading magnitudes of 0.1-0.4g, and observed a 10 to 40-fold increase in mineralization in a magnitude-dependent manner with exposure to LMHF loading. Together, these results clearly demonstrate a key role of BMPs in the osteogenic responses of osteoblasts in response to LMHF mechanical loading. Moreover, these data suggest that while either BMP2/4 treatment or LMHF alone may be used, a combination of the mechanical and humoral stimuli may be a better therapeutic modality to prevent or normalize bone loss. However, it is important to point out that chronic systemic supplementation of BMP4 has been shown to induce hypertension at least in a mouse model (18), suggesting a caution must be raised in its use.

The current study reveals some of the osteogenic genes that are regulated by LMHF and/or RPM. We have previously shown by DNA microarray analysis that the RPM and RWV inhibit expression of a subset of osteogenic genes (20, 21). Here, we investigated *ALP, runx2, PTHR1, OMD, OGN, and BMP4*. *Runx2* is considered a "master gene" that plays a critical role in the formation of the skeleton, and without *runx2*, there is a complete lack of skeleton formation in a mouse model (12, 13). Parathyroid hormone related protein plays a role in calcium mobilization and has been linked to loss of bone density in space-flown rats (32) while *OMD* and *OGN* belong to the small leucine rich proteoglycan (SLRP) family, members of which have been

hypothesized to play roles in bone matrix formation and mineralization (1). LMHF loading induced the expression of each of these genes (Static+LMHF) and prevented the RPM-inhibition of their expression (RPM+LMHF) (Figure 8.9).

We found that regulation of *BMP4* by the RPM and LMHF was unique compared to the other genes. *BMP4* is involved in the development of the skeleton, including cartilage formation and various joint developments (33, 36). The RPM did not alter *BMP4* mRNA levels, which is consistent to our previous report (20). However, LMHF loading induced an increase in *BMP4* mRNA in both static (Static+LMHF) and RPM-exposed cells (RPM+LMHF). This result suggests that the mechanism of action of the RPM and LMHF loading are distinct. While the bone loss response of osteoblasts in response to RPM is not dependent on changes in *BMP4* mRNA level, LMHF loading is BMP-dependent. Together, these data suggest that LMHF regulates expression of osteogenic genes, providing a potential molecular mechanism by which LMHF stimulates bone formation responses in 2T3 cells. The mechanosensitive genes identified here provide potential targets for pharmaceutical treatments that may be used in combination with LMHF mechanical loading to more effectively treat bone pathologies.

In this study, we show that osteoblasts respond directly to a LMHF mechanical load. It has not been reported how the LMHF may be sensed and transmitted in to the cells to induce the osteogenic responses. Potential mechanotransduction pathways may involve integrins (11), stretch-activated channels and the ensuing influx of extracellular calcium (11), or cell deformations and cytoskeleton (9, 10). Elucidating the mechanosensors and mechanotransduction pathways would be interesting future work.

We have revealed that LMHF mechanical loading, which has been shown to prevent bone loss in animals and humans, elicits cellular and molecular changes in osteoblasts, which may mediate bone formation responses to extremely low magnitude loading. As summarized in Figure 8.10, the RPM inhibits markers of bone formation

such as ALP activity and mineralization as well as critical gene expression such as *runx2*. However, LMHF mechanical loading prevents these effects in a BMP-dependent manner. This research provides critical insight into how such low level mechanical loading prevents or normalizes bone loss in animals and humans, and this mechanical loading platform may be also used as a novel countermeasure in spaceflight.
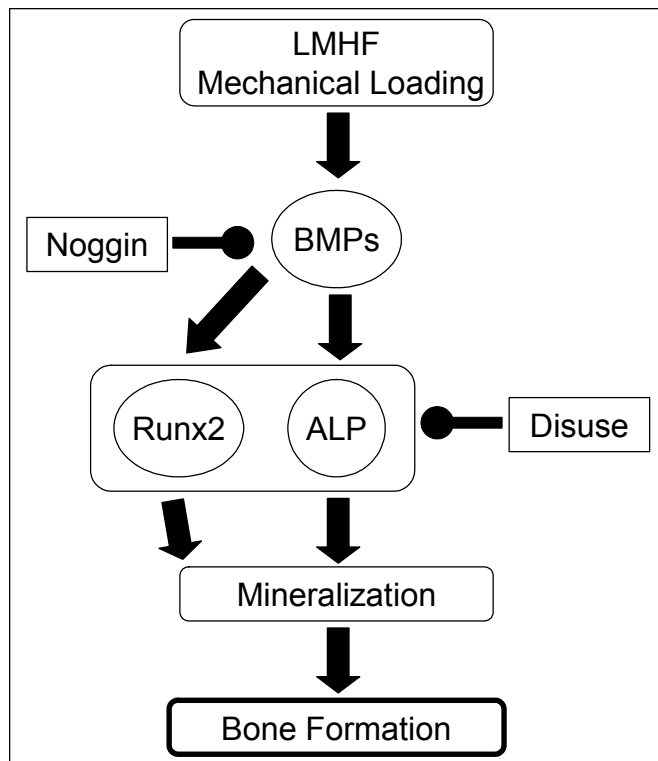
Figure 8.10 Summary pathway showing mechanistic insight into RPM inhibition and mechanical loading induction of bone formation

References

1. **Buchaille R, Couble ML, Magloire H, and Bleicher F.** Expression of the small leucine-rich proteoglycan osteoadherin/osteomodulin in human dental pulp and developing rat teeth. *Bone* 27: 265-270, 2000.

2. **Galloway MT and Jokl P.** Aging successfully: the importance of physical activity in maintaining health and function. *J Am Acad Orthop Surg* 8: 37-44, 2000.

3. **Gass M and Dawson-Hughes B.** Preventing osteoporosis-related fractures: an overview. *Am J Med* 119: S3-S11, 2006.

4. **Gersbach CA, Byers BA, Pavlath GK, and Garcia AJ.** Runx2/Cbfa1 stimulates transdifferentiation of primary skeletal myoblasts into a mineralizing osteoblastic phenotype. *Exp Cell Res* 300: 406-417, 2004.

5. **Ghosh-Choudhury N, Windle JJ, Koop BA, Harris MA, Guerrero DL, Wozney JM, Mundy GR, and Harris SE.** Immortalized murine osteoblasts derived from BMP 2-T-antigen expressing transgenic mice. *Endocrinology* 137: 331-339, 1996.

6. **Gilsanz V, Wren TA, Sanchez M, Dorey F, Judex S, and Rubin C.** Low-level, high-frequency mechanical signals enhance musculoskeletal development of young women with low BMD. *J Bone Miner Res* 21: 1464-1474, 2006.

7. **Gray B, Hsu JD, and Furumasu J.** Fractures caused by falling from a wheelchair in patients with neuromuscular disease. *Dev Med Child Neurol* 34: 589-592, 1992.

8. **Groppe J, Greenwald J, Wiater E, Rodriguez-Leon J, Economides AN, Kwiatkowski W, Affolter M, Vale WW, Belmonte JC, and Choe S.** Structural basis of BMP signalling inhibition by the cystine knot protein Noggin. *Nature* 420: 636-642, 2002.

9. **Ingber D.** How cells (might) sense microgravity. *Faseb J* 13 Suppl: S3-15, 1999.

10. **Ingber DE.** Cellular mechanotransduction: putting all the pieces together again. *Faseb J* 20: 811-827, 2006.

11. **Iqbal J and Zaidi M.** Molecular regulation of mechanotransduction. *Biochem Biophys Res Commun* 328: 751-755, 2005.

12.   **Katagiri T and Takahashi N.** Regulatory mechanisms of osteoblast and osteoclast differentiation. *Oral Dis* 8: 147-159, 2002.

13.   **Komori T, Yagi H, Nomura S, Yamaguchi A, Sasaki K, Deguchi K, Shimizu Y, Bronson RT, Gao YH, Inada M, Sato M, Okamoto R, Kitamura Y, Yoshiki S, and Kishimoto T.** Targeted disruption of Cbfa1 results in a complete lack of bone formation owing to maturational arrest of osteoblasts. *Cell* 89: 755-764, 1997.

14.   **Lang T, LeBlanc A, Evans H, Lu Y, Genant H, and Yu A.** Cortical and trabecular bone mineral loss from the spine and hip in long-duration spaceflight. *J Bone Miner Res* 19: 1006-1012, 2004.

15.   **Lee WS, Cheung WH, Qin L, Tang N, and Leung KS.** Age-associated decrease of type IIA/B human skeletal muscle fibers. *Clin Orthop Relat Res* 450: 231-237, 2006.

16.   **Lees SJ, Rathbone CR, and Booth FW.** Age-associated decrease in muscle precursor cell differentiation. *Am J Physiol Cell Physiol* 290: C609-615, 2006.

17.   **Lian JB and Stein GS.** Development of the osteoblast phenotype: molecular mechanisms mediating osteoblast growth and differentiation. *Iowa Orthop J* 15: 118-140, 1995.

18.   **Miriyala S, Gongora Nieto MC, Mingone C, Smith D, Dikalov S, Harrison DG, and Jo H.** Bone morphogenic protein-4 induces hypertension in mice: role of noggin, vascular NADPH oxidases, and impaired vasorelaxation. *Circulation* 113: 2818-2825, 2006.

19.   **Murfee WL, Hammett LA, Evans C, Xie L, Squire M, Rubin C, Judex S, and Skalak TC.** High-frequency, low-magnitude vibrations suppress the number of blood vessels per muscle fiber in mouse soleus muscle. *J Appl Physiol* 98: 2376-2380, 2005.

20.   **Pardo SJ, Patel MJ, Sykes MC, Platt MO, Boyd NL, Sorescu GP, Xu M, van Loon JJWA, Wang MD, and Jo H.** Simulated microgravity using the Random Positioning Machine inhibits differentiation and alters gene expression profiles of 2T3 preosteoblasts. *Am J Physiol Cell Physiol* 288: C1211-1221, 2005.

21.   **Patel MJ.** Identification of Mechanosensitive Genes in Osteoblasts by Comparative Microarray Studies Using the Rotating Wall Vessel and the Random Positioning Machine. *Journal of Cellular Biochemistry* 101: 587-599, 2007.

22.   **Rosenberg IH.** Sarcopenia: origins and clinical relevance. *J Nutr* 127: 990S-991S, 1997.

23.   **Rubin C, Recker R, Cullen D, Ryaby J, McCabe J, and McLeod K.** Prevention of postmenopausal bone loss by a low-magnitude, high-frequency mechanical stimuli: a clinical trial assessing compliance, efficacy, and safety. *J Bone Miner Res* 19: 343-351, 2004.

24.   **Rubin C, Turner AS, Bain S, Mallinckrodt C, and McLeod K.** Anabolism. Low mechanical signals strengthen long bones. *Nature* 412: 603-604, 2001.

25.   **Rubin C, Turner AS, Muller R, Mittra E, McLeod K, Lin W, and Qin YX.** Quantity and quality of trabecular bone in the femur are enhanced by a strongly anabolic, noninvasive mechanical intervention. *J Bone Miner Res* 17: 349-357, 2002.

26.   **Rubin C, Xu G, and Judex S.** The anabolic activity of bone tissue, suppressed by disuse, is normalized by brief exposure to extremely low-magnitude mechanical stimuli. *Faseb J* 15: 2225-2229, 2001.

27.   **Rubin CT and Lanyon LE.** Dynamic strain similarity in vertebrates; an alternative to allometric limb bone scaling. *J Theor Biol* 107: 321-327, 1984.

28.   **Rubin CT and Lanyon LE.** Regulation of bone formation by applied dynamic loads. *J Bone Joint Surg Am* 66: 397-402, 1984.

29.   **Rubin CT and Lanyon LE.** Regulation of bone mass by mechanical strain magnitude. *Calcif Tissue Int* 37: 411-417, 1985.

30.   **Rubin CT, Sommerfeldt DW, Judex S, and Qin Y.** Inhibition of osteopenia by low magnitude, high-frequency mechanical stimuli. *Drug Discov Today* 6: 848-858, 2001.

31.   **Snow-Harter C, Bouxsein ML, Lewis BT, Carter DR, and Marcus R.** Effects of resistance and endurance exercise on bone mineral status of young women: a randomized exercise intervention trial. *J Bone Miner Res* 7: 761-769, 1992.

32.   **Torday JS.** Parathyroid hormone-related protein is a gravisensor in lung and bone cell biology. *Adv Space Res* 32: 1569-1576, 2003.

33.   **Tsumaki N, Nakase T, Miyaji T, Kakiuchi M, Kimura T, Ochi T, and Yoshikawa H.** Bone morphogenetic protein signals are required for cartilage formation

and differently regulate joint development during skeletogenesis. *J Bone Miner Res* 17: 898-906, 2002.

34.	**Vuori I.** Exercise and physical health: musculoskeletal health and functional capabilities. *Res Q Exerc Sport* 66: 276-285, 1995.

35.	**Ward K, Alsop C, Caulton J, Rubin C, Adams J, and Mughal Z.** Low magnitude mechanical loading is osteogenic in children with disabling conditions. *J Bone Miner Res* 19: 360-369, 2004.

36.	**Wijgerde M, Karp S, McMahon J, and McMahon AP.** Noggin antagonism of BMP4 signaling controls development of the axial skeleton in the mouse. *Dev Biol* 286: 149-157, 2005.

37.	**Xing W, Baylink D, Kesavan C, Hu Y, Kapoor S, Chadwick RB, and Mohan S.** Global gene expression analysis in the bones reveals involvement of several novel genes and pathways in mediating an anabolic response of mechanical loading in mice. *Journal of Cellular Biochemistry* 9999: n/a, 2005.

Chapter 9

Discussion

Summary and Conclusions

Musculoskeletal pathologies associated with decreased bone mass, including osteoporosis, disuse-induced bone loss, and microgravity-induced bone loss, affect millions of Americans annually. Many pharmaceutical treatments have slowed osteoporosis, but there is still no countermeasure for bone loss observed in astronauts. Additionally, high magnitude and low frequency impact such as running has been recognized to increase bone and muscle mass under normal but not microgravity conditions. However, a low magnitude and high frequency (LMHF) mechanical load experienced in activities such as postural control, has also been shown to be anabolic to bone. While several clinical trials have demonstrated that LMHF mechanical loading normalizes bone loss *in vivo*, the target tissues and cells of the mechanical load and underlying mechanisms mediating the responses are unknown.

As such, the *objectives* of this project were to analyze any cellular and molecular changes induced in osteoblasts by LMHF loading and to investigate the utility of a LMHF mechanical load in mitigating microgravity-induced bone loss. The *central hypothesis* of the project was that simulated microgravity or disuse conditions induce bone loss by inhibiting expression of genes critical in regulating bone formation, osteoblast differentiation, and subsequent mineralization while a LMHF mechanical load prevents these effects. Thus, the central hypothesis of this project was tested with three specific aims, as follows:

199

- Specific Aim 1: To determine the effect of simulated microgravity disuse on cell differentiation and mineralization of mouse calvarial 2T3 pre-osteoblasts

- Specific Aim 2: To compile a confined list of selected genes that change upon exposure to simulated microgravity or disuse

- Specific Aim 3: To determine whether LMHF mechanical loading prevents microgravity- or disuse-induced decrease in bone formation

To achieve these aims, we developed an *in vitro* disuse system using the Random Positioning Machine (RPM). For the first time, we reported systemic gene expression studies in 2T3 preosteoblasts using the RPM disuse system showing that 140 genes were altered by RPM exposure with over two-fold statistically significant changes. Moreover, we also utilized an independent simulator called the Rotating Wall Vessel (RWV) to partially validate the *in vitro* disuse systems and to confine the list of genes to those most critical in regulating bone formation. After comparative studies, we constricted the list to 17 commonly changed genes, three of which were not only decreased with disuse but also increased with mechanical loading *in vivo*. Furthermore, we employed the RPM disuse system to evaluate the mechanism by which a LMHF load mitigates bone loss. Exposure of osteoblasts to the RPM decreased bone formation markers such as alkaline phosphatase (ALP) activity and mineralization even in the presence of bone morphogenic protein 4 (BMP4), and the LMHF mechanical loading prevented the RPM-induced decrease in both markers.

In conventional thought, high impact exercises instigate large strains, which initiate bone adaptation and remodeling. However, these large strains are only a small portion of the strain history recorded over a 24 hour period of various animals. As such, the dominant portion of the strain history is composed of smaller, more frequent strains.

The LMHF mechanical loading platform mimics these strains that are characteristic of physiological musculature loading on bones during activities such as postural control.

In this dissertation, we examined the hypothesis that direct application of LMHF mechanical loading to osteoblasts alters their cell responses, preventing decreased bone formation induced by disuse as marked by ALP activity and gene expression. Exposure of 2T3 cells to the RPM decreased bone formation responses as determined by ALP activity and mineralization even in the presence of a submaximal dose of BMP4 (20ng/ml). However, LMHF mechanical loading prevented the RPM-induced decrease in ALP activity and mineralization. Mineralization induced by mechanical loading was enhanced by treatment with BMP4 and blocked by the BMP antagonist noggin, suggesting a role for BMPs in this response. In addition, mechanical loading rescued the RPM-induced decrease in gene expression of *ALP*, *runx2*, *osteomodulin (OMD)*, *parathyroid hormone receptor 1 (PTHR1)*, and *osteoglycin (OGN)*. These genes are part of a larger set of mechanosensitive genes identified in this dissertation. Additionally, for the first time, these findings show that osteoblasts respond directly to extremely low magnitude mechanical loading to induce bone formation responses, potentially leading to normalization or prevention of bone loss caused by disuse or microgravity conditions.

Therefore, by achieving the three specific aims set forth, this dissertation has shown that LMHF mechanical loading promotes anabolic responses at the cellular and molecular level, partially providing mechanistic understanding by which such a low magnitude load prevents or prolongs bone loss *in vivo* in animals and humans. In addition, we have shown that LMHF loading prevents simulated microgravity-induced decrease in bone formation response at the *in vitro* level, supporting use of the platform in spaceflight to countermeasure bone loss. Furthermore, we provided systemic gene expression analyses and confined the list of genes to those that may play critical roles in regulating bone formation in normal and disuse conditions. In conclusion, this research

is *significant* because it sought to evaluate whether the extremely low level mechanical loading induced changes in an isolated osteoblast system, and if so, what the underlying molecular mechanisms were regulating those changes.   This information not only provides further understanding of how osteoblasts sense and respond to various mechanical loads but also imparts potential targets for pharmaceutical treatments that could be combined with LMHF loading to better treat bone loss due to osteoporosis, disuse, or spaceflight.

Limitations

There are limitations to the studies performed in this dissertation including, but not limited to, the following points:

1. Simulated environments

2. Experiments compared in Aim 2 but not performed at same time

3. Defining "mechanosensitive" when observing gene changes

4. Molecular effects of LMHF loading beyond BMPs

5. Experiments performed in cell line

6. Detailed mechanistic studies in future work

7. LMHF loading dependent on more factors than strain magnitude and frequency

The environments used for these studies with the RPM and RWV are designed to simulate disuse or microgravity conditions and have been shown to recapitulate some responses observed *in vivo* in isolated cells, animals, and humans. However, it should be noted that the both environments are only simulations, and therefore, the results must be tested in actual spaceflight or disuse conditions.

Additionally, in aim 2, we compare the results from the RPM to the RWV; however, these experiments were not performed side-by-side. This caveat must be noted as a limitation to the comparative studies performed. Furthermore, the effects observed from the microarray gene expression analyses after exposure to both simulators are dependent on the definition of "mechanosensitive". For instance, if a gene was upregulated by the RPM but its downstream targets were unaffected, the gene could be labeled as not mechanosensitive even though its expression level changed with exposure to the stimulus. An example from both microarrays is the *runx2* gene, whose expression level was downregulated by both the RPM and RWV and upregulated by LMHF. However, *osteocalcin*, which is a downstream target of *runx2*, was unchanged

by exposure to each stimulus. Thus, although the gene expression level was changed, the activity of *runx2* may not be changed. Future work would need to perform detailed studies using a truncated form of the *runx2* gene inserted into cells and exposed to the stimulus to determine if the gene is truly mechanosensitive. However, in this dissertation, a gene whose expression level was changed by the stimulus was labeled mechanosensitive.

Moreover, the goal of this dissertation was to develop a method to study the effects of disuse at the cellular and molecular level and to investigate whether LMHF loading normalized bone loss *in vivo* by acting on osteoblasts directly. As such, the project is now developed so that future work can focus on the changes noted in this dissertation. Thus far, we have only partially implicated BMPs in potentially playing a role in the LMHF loading effects on osteoblasts, and future work should center about investigating the entire pathway. Additionally, there are many other pathways independent of BMPs that may play roles in mediating the effects of both the RPM and LMHF loading, including adhesion molecules such as focal adhesion kinases (FAK) and integrins. This conclusions of this dissertation were limited to the data presented here, which show that the effects of LMHF requires BMPs and that simulated disuse alters many genes, the specific roles of which should be the focus of future studies. Additionally, the work performed here was in an immortalized cell line that no longer mimics in tact *in vivo* osteoblasts. The results would need to be confirmed in a primary cell type, which could then be used for future mechanistic work.

Lastly, LMHF loading depends not only on magnitude and frequency of the applied load, but also it depends on the effects caused at the tissue and cellular level. For instance, perhaps there is a role for bone microdamage, which occurs physiologically as part of the adaptation and remodeling cycle of bone. Additionally, we showed in this dissertation that the effects of LMHF were magnitude-dependent.

However, we did not perform frequency dose curves. Frequency is most likely the larger contributor to the osteogenic effects of LMHF loading as the strain magnitude is much lower than the levels needed to induce bone adaptation but is also applied much more frequently than the larger strain events. Additionally, as previously discussed, there are most likely many changes induced by LMHF loading, including the activation of various mechanical signaling pathways. This project did not evaluate the effects on specific mechanosensitive elements such as ion-gated channels, stretch-activated channels, adhesion complexes, or g-protein coupled receptors. These studies were limited to gene expression and the role of BMP4/BMPs in the effects of the RPM and LMHF loading. However, it should be noted that there is most likely a host of other downstream factors that may play roles in mediating the effects of disuse and LMHF loading on bone loss.

Future Directions

This dissertation has set up a method by which disuse and LMHF mechanical loading can be tested *in vitro* to explore changes at the cellular and molecular level of osteoblasts. To advance these experiments, the ensuing steps could revolve around targeting a specific gene or molecular pathway altered by both disuse and LMHF loading as identified in this dissertation. To develop sophisticated cell signaling pathways, the next steps should revolve around functional tests by knocking down gene expression using pharmacological agents or siRNA and overexpressing gene expression by plasmid or adenovirus. This type of functional knowledge could directly implicate a specific mechanosensitive gene in mediating osteoblast responses to disuse or LMHF mechanical loading and be specifically used for pharmaceutical treatments.

We have begun studies involving *OGN*, which is a gene that is decreased by the RPM and RWV and increased by LMHF mechanical loading as shown in Figure 9.1. *OGN* is a small leucine-rich proteoglycan found in the extracellular matrix of bone, and knockout mice for this gene display collagen fibril diameter abnormalities. Most investigations of *OGN* are in the eye extracellular matrix, and there is also an *OGN* knockout mouse available from the Tasheva lab. An overall x-ray of the skeleton of the *OGN-/-* mouse does not show macroscopic alterations to the bones due to *OGN* deletion. However, there have not been sophisticated studies examining the mechanical properties of the bones of these mice. Future work could image the bones using micro-computed tomography (μ-CT) to assess morphological changes to the trabecular and cortical bone due to the gene deletion by comparing to an appropriate background control. Additionally, the bones could be mechanically tested, evaluating parameters such as modulus of elasticity and load to failure. Lastly, the bones could be sectioned and stained by immunohistochemistry for various proteins involved in bone resorption

and bone formation. This type of information is unavailable and would greatly enhance the role of *OGN* in bone remodeling.

We currently have molecular reagents targeting *OGN*, including a working antibody for Western blots (Figure 9.1A and C),   primers for real time RTPCR (Figure 9.1B and D), and DNA plasmid for overexpression (Figure 9.2).   The plasmid transfection conditions are partially optimized, but cell death during transfection may still be too high. Moreover, preliminary data shown in Figure 9.2 suggest that *OGN* may be linked to the BMP pathway through BMP4.   However, these results shown in two independent experiments (Figure 9.2 B and C) were inconsistent. It may be of interest to pursue the link between *OGN* and *BMP4* because we have previously observed that treatment of 2T3 cells with recombinant OGN (rOGN) protein combined with rBMP4 increases mineralization compared to treatment with either rOGN or rBMP4 alone (data not shown).

Additionally, we have tested various siRNA sequences from Dharmacon, including their smart pool siRNA available for *OGN*. It, however, does not provide substantial knockdown of *OGN* in 2T3 cells at concentrations less than 100uM. However, at 100uM, there was knockdown, but this result was inconsistent (Figure 9.3). As such, we are currently testing additional siRNA sequences targeting osteoglycin. Therefore, there are ample molecular reagents available to pursue the role of *OGN* not only in osteoblast function but also in LMHF mechanical loading-induced prevention of decreased bone formation.

Moreover, we have collaborations available to perform hindlimb unloading (HLU) studies using a mouse model. To elevate the *in vitro* studies in this dissertation, *OGN-/-* mice could be used in an HLU *in vivo* experiment intervened with LMHF loading. We have the capability to evaluate the bone morphology of these mice using μ-CT analysis

A

B

C

D
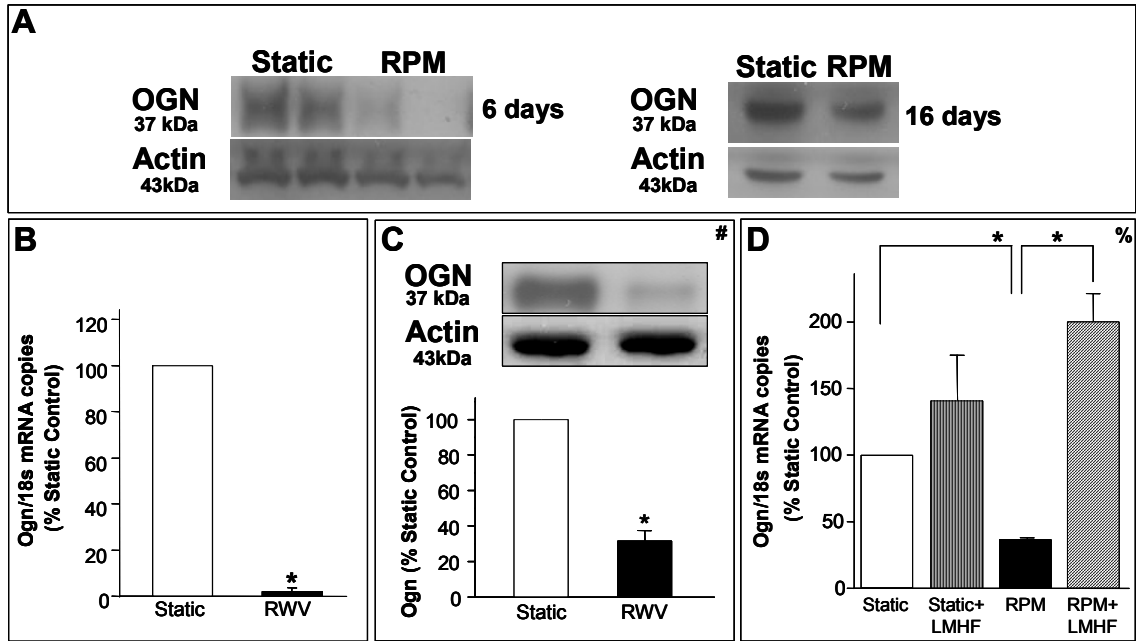
*p<0.05
#Patel, et al., JCell Biochem, 2007
%Patel, et al., JBC, 2007 (In Review)

Figure 9.1 RPM decreased while LMHF loading increased expression of *OGN* protein and transcript levels.
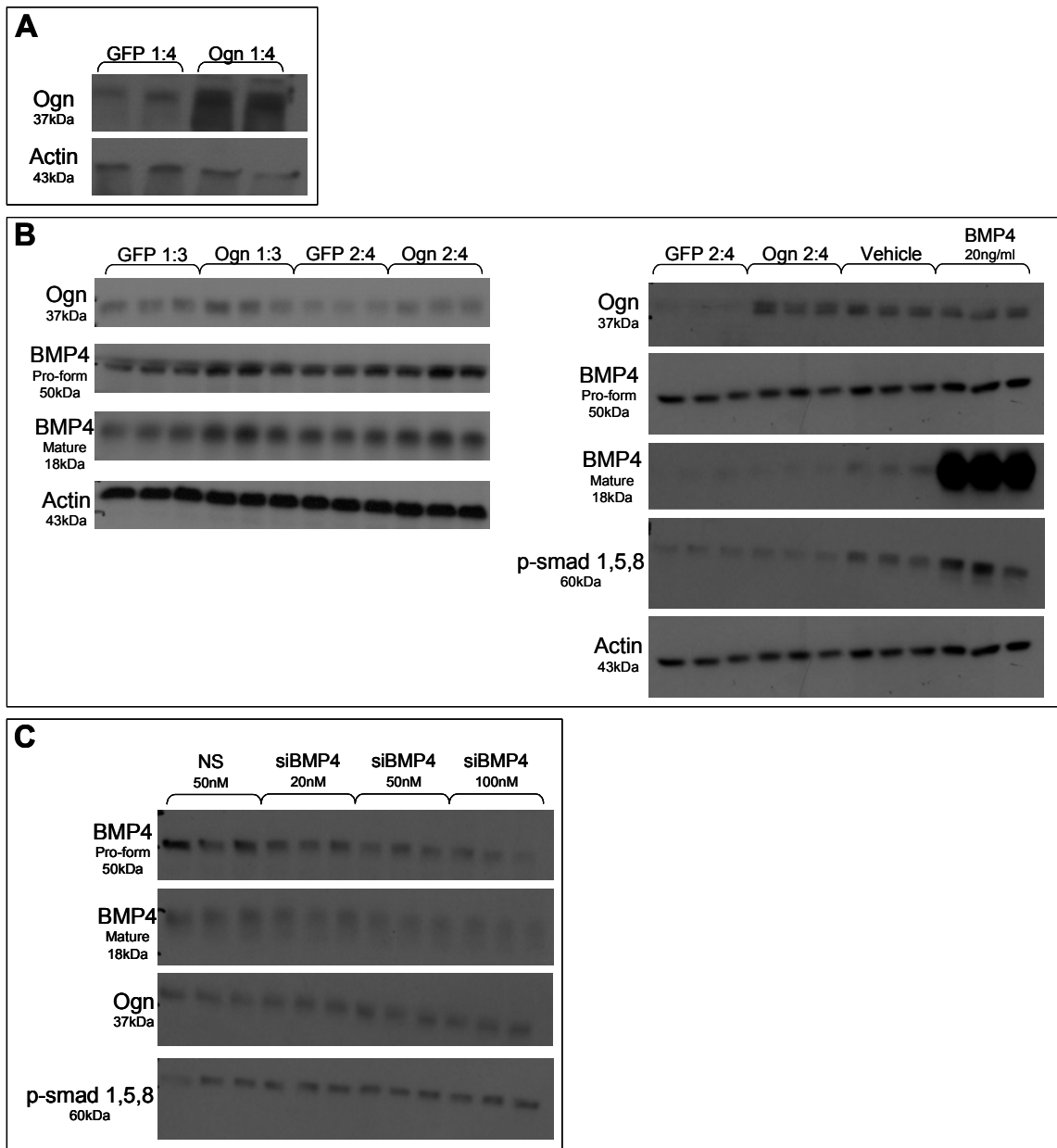
Figure 9.2 *OGN* plasmid induced overexpression of OGN protein compared to a GFP control plasmid and may be involved in regulation of BMP4. OGN plasmid transfection conditions are shown in A and B. Inconsistent preliminary results in B and C suggest OGN may be related to the BMP pathway through BMP4.
(Experiments shown here were for three days for OGN plasmid and two days for siBMP4 treatment.)
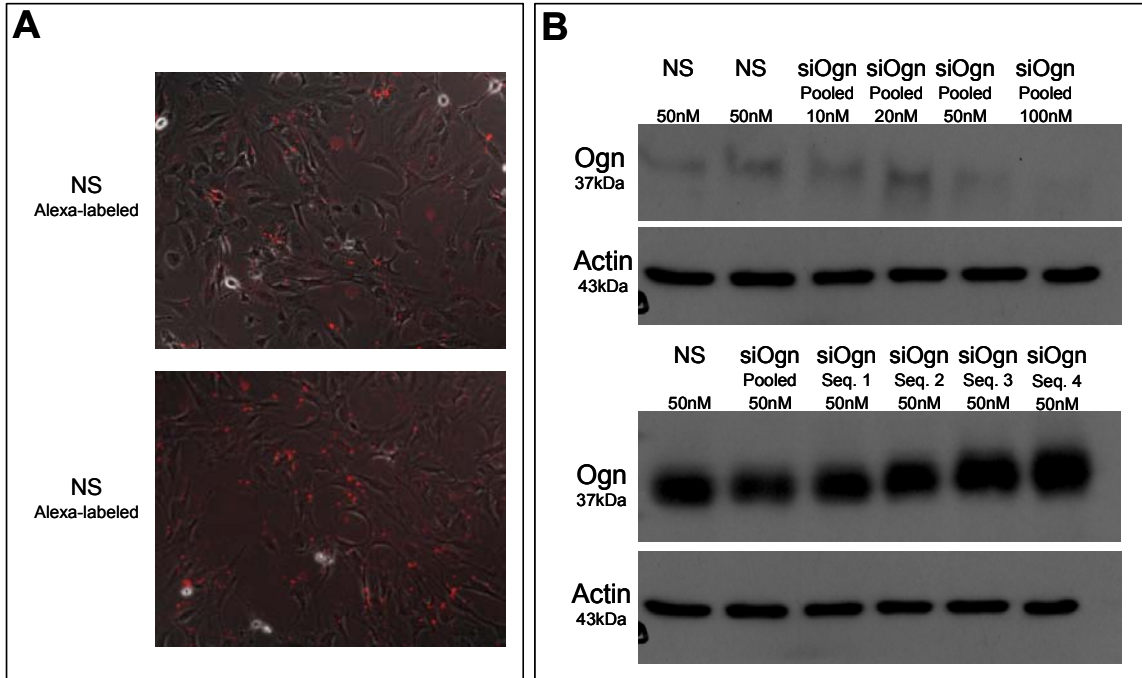
Figure 9.3 *OGN* **siRNA did not knockdown OGN protein.** Cells were treated with siOGN or non-silencing control (NS) siRNA. Transfection of siRNA occurred as noted by NS-labeled siRNA while multiple sequences of siOGN were not effective.
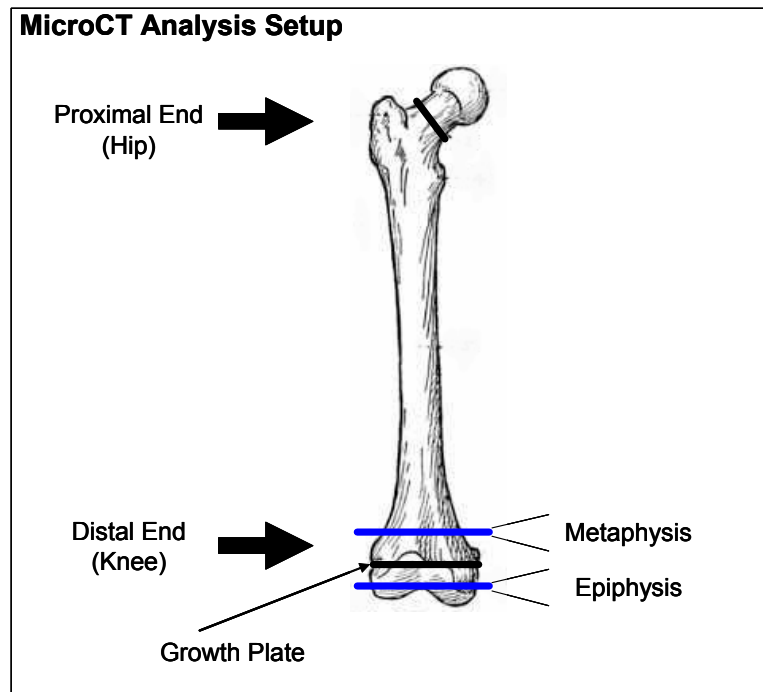
Figure 9.4 MicroCT setup of analysis for HLU studies

as shown in Figure 9.4. Additionally, µ-CT can evaluate the morphology and properties of bone architecture as shown in Figures 9.5, 9.6, and 9.7.

Additionally, although the BMP pathway as shown in Figure 9.8 is well established for its role in bone formation, this dissertation is the first to provide insight into the direct effects of LMHF loading on osteoblast function. Thus, it is feasible and would be interesting to further establish the effect of LMHF loading on the BMP molecular signaling pathway. We have shown by antagonist studies that the effects of LMHF mechanical loading require BMPs. However, future work may surround studying downstream signaling molecules such as smad 1,5,8 phosphorylation and mitogen activating protein kinases (MAPK). We have preliminary data suggesting differential regulation of some members of the BMP pathway with MAPKs in Figure 9.9 and smad-dependent factors in Figure 9.10. However, most of the preliminary data is inconclusive. The preliminary data included here was obtained from samples exposed to three days of RPM or LMHF loading. Since many of the signaling proteins are phosphorylated and typically are activated acutely, it may be necessary to perform short time courses to accurately determine the molecular mechanisms regulating both responses. If any of these molecules change with LMHF loading or RPM exposure, their functional roles may be analyzed easily because of available blocking agents. Furthermore, there are a number of other genes such as *OMD*, *PTHR1*, and *runx2* that may be further investigated for their role in how the LMHF loading prevents bone loss.

Lastly, the effects of LMHF loading and RPM on osteoblast mineralization may be dependent on lots or shelf life of the recombinant BMP4 used. As shown in Figure 9.11, a new lot of BMP4 was shown by smad 1,5,8 phosphorylation to be much stronger than the lot used in these experiments presented in this dissertation. However, we cannot decipher whether it was the lot or the shelf life of the BMP4 that yielded a stronger BMP activity response. As such, current tests are being performed to

Figure 9.5 HLU for 13 days decreased bone volume in the femur metaphysis of BALB mice.

Property	p-value	% Change
Bone Volume	0.004	64.4
BV/TV	0.002	60.3
Connectivity	0.002	79.5
Tb Number	0.02	23.4
Tb Thickness	0.008	22.7
Tb Spacing	0.03	26.9
Mineral Density	0.006	23.2

Figure 9.6 HLU for 13 days did not alter bone volume in the femur epiphysis of BALB mice.

Property	p-value	% Change
Bone Volume	0.14	28.8
BV/TV	0.08	19.2
Connectivity	0.09	14.3
Tb Number	0.18	7.8
Tb Thickness	0.03	12.1
Tb Spacing	0.21	6.9
Mineral Density	0.53	1.5

A. Tibia Metaphysis

Control — Hindlimb Unloading (HLU)

B. Trabecular Bone Architecture Analysis

Property	p-value	% Change
Bone Volume	0.28	20.9
BV/TV	0.24	22.5
Connectivity	0.77	8.3
Tb Number	0.41	8.5
Tb Thickness	0.25	8.5
Tb Spacing	0.27	12.5
Mineral Density	0.09	6.1

Figure 9.7 HLU for 13 days did not alter bone volume in the tibia metaphysis of BALB mice.

BMP/Wnt Signaling Pathway: Alkaline Phosphatase and Mineralization

Figure created by M. Patel from manuscript:
Rawadi, et al., *BMP-2 Controls Alkaline Phosphatase Expression and Osteoblast Mineralization by a Wnt Autocrine Loop*. JBMR 2003

Figure 9.8 BMP pathway leading to runx2 and ALP expression as well as mineralization in osteoblasts.
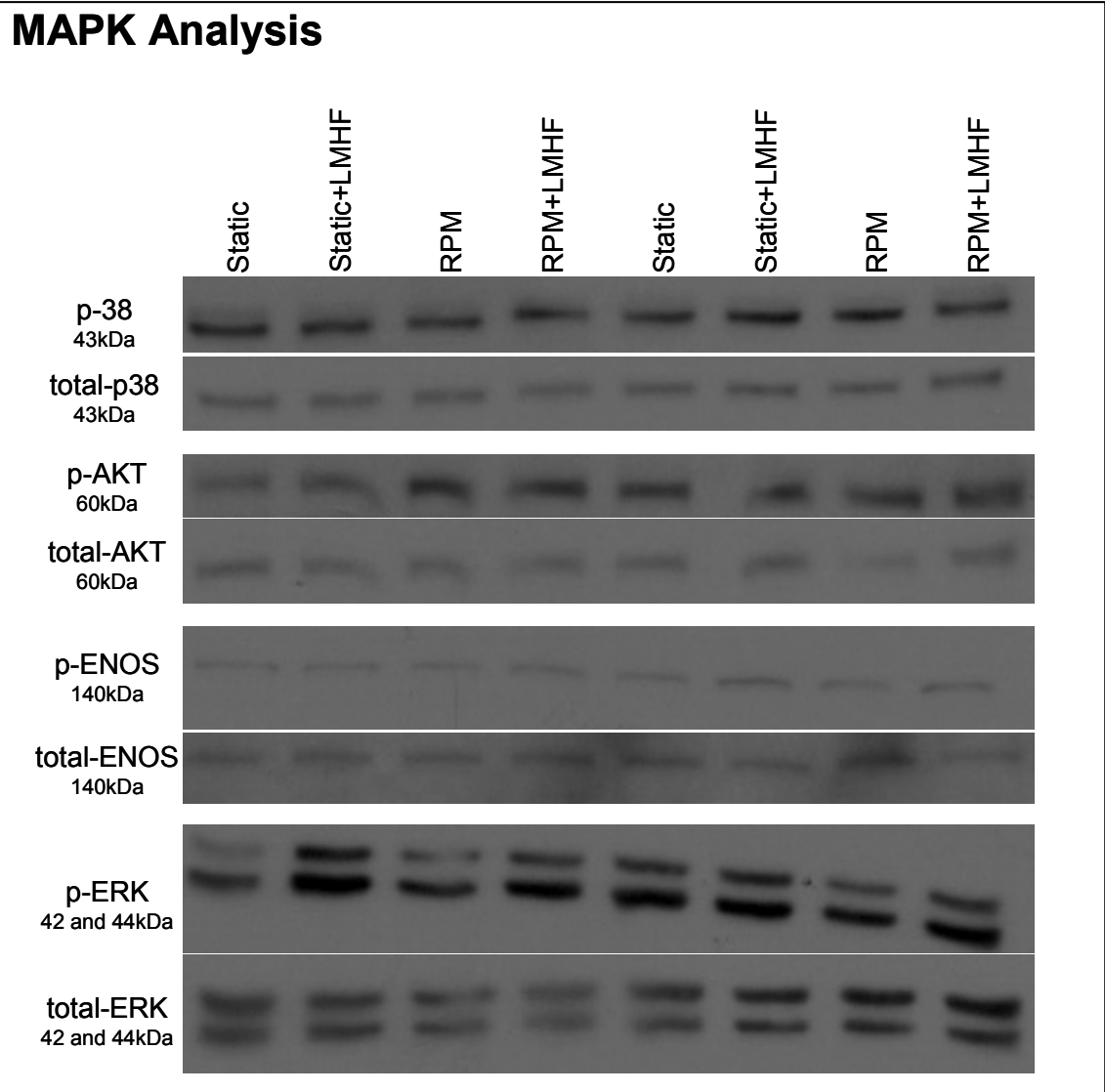
Figure 9.9 Preliminary data showing effects of RPM and LMHF loading on MAPKs.
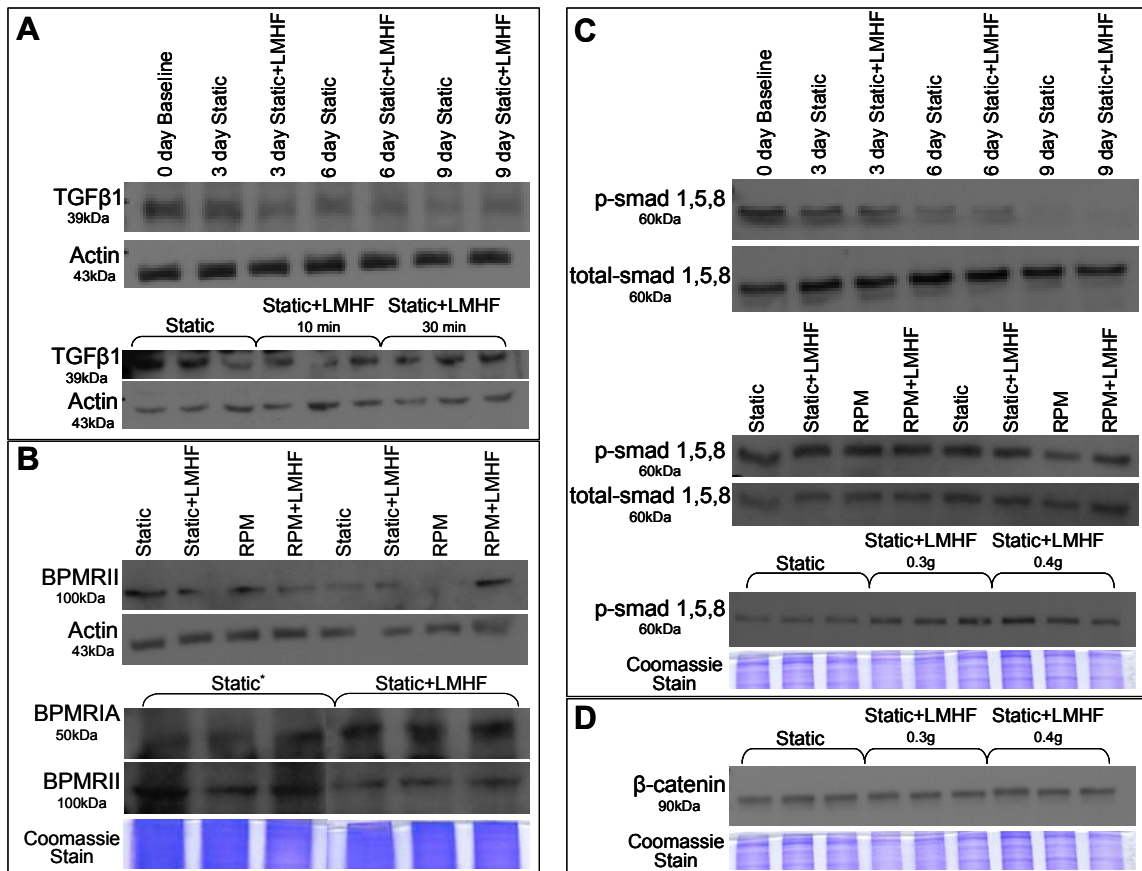
Figure 9.10 Preliminary data showing effects of RPM and LMHF loading on Smad-dependent factors.
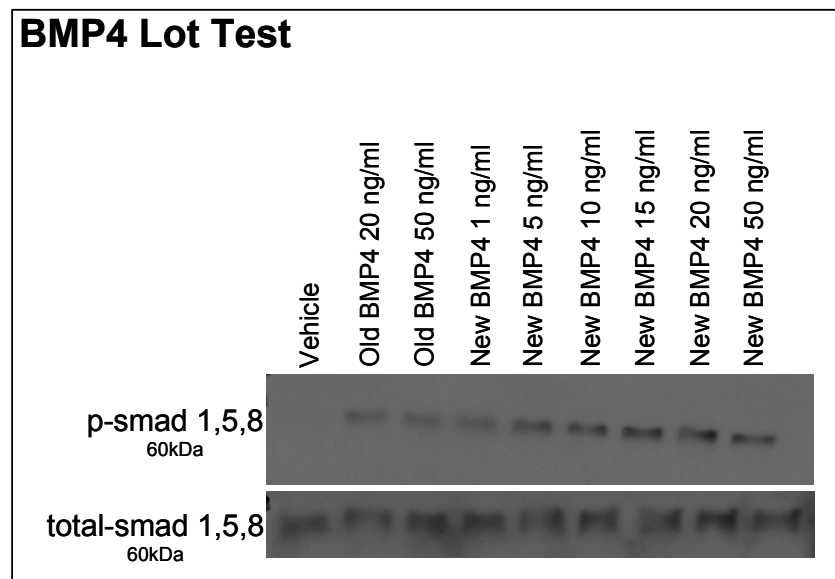
Figure 9.11 BMP4 lot test at varying concentrations

determine if the effects of LMHF loading and RPM are BMP-lot dependent. If so, then future studies will need to repeat the BMP4 concentration-dependent experiments to determine the ideal concentration where the effects of the RPM and LMHF loading can be observed.

If it is truly the goal of this project to understand how such low level mechanical loads can mediate bone adaptation, then future directions such as those discussed here must be considered. This biological information will further elucidate our knowledge of how the skeletal system maintains its integrity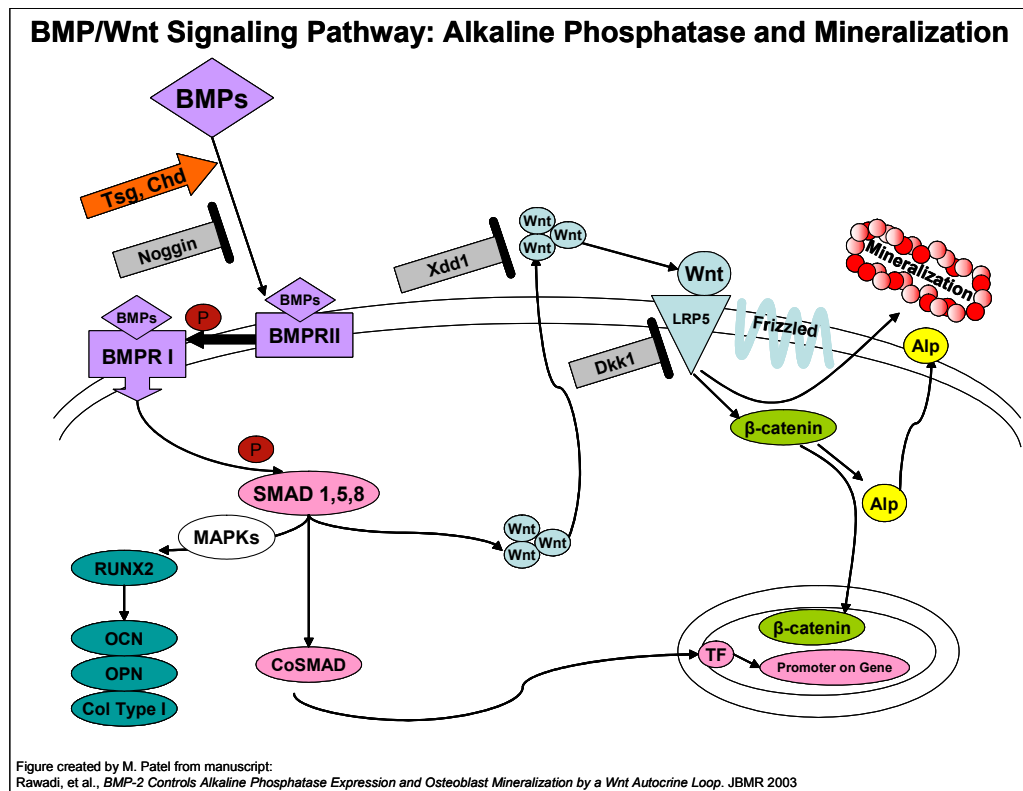 to fully provide its protective and supportive functions to the body, and as such, it will render opportunities to develop new techniques to better treat bone pathologies. Additionally, the success of clinical trials exploring the utility of the LMHF mechanical loading platform in mitigating osteoporotic bone loss combined with the research performed in this dissertation strongly support the use of LMHF loading as a novel countermeasure in spaceflight.

Appendix A

Chapter 5 Supplemental Tables

Table A.1 A list of selected statistically significant RWV-mechanosensitive genes in 2T3 cells. Sorted based on typical biological process.

Accession #	Gene Name	*Fold Δ	p-value	Molecular Function
Cell Adhesion				
NM_012050	*Osteomodulin*	0.10	0.04	aka osteoadherin, may mediate cell attachment
NM_011581	*thrombospondin 2*	0.39	0.03	structural molecule activity; calcium ion binding
BB781435	*nidogen 2*	0.39	0.004	calcium ion binding
NM_007729	*procollagen, type XI, alpha 1*	0.40	0.04	extracellular matrix structural constituent
NM_012043	*immunoglobulin superfamily containing leucine rich repeat (ISLR)*	0.42	0.02	involved in cell attachment
BB250384 L08431	*vascular cell adhesion molecule 1*	0.45	0.02	protein binding
BF225985	*discoidin domain receptor family, member 1*	0.49	0.04	protein kinase activity; protein serine/threonine kinase activity
BC013560	*procollagen, type IV, alpha 2*	2.02	0.03	structural molecule activity; extracellular matrix structural constituent
BG073728	*RGM domain family, member B*	2.24	0.05	protein self binding
BM935811	*integrin alpha 6*	2.47	0.01	receptor activity; protein binding
BF158638	*procollagen, type IV, alpha 1*	2.59	0.002	structural molecule activity; extracellular matrix structural constituent
Cell Cycle				
NM_011817 AK007410	*growth arrest and DNA damage inducible, gamma*	0.40	0.009	structural constituent of ribosome
AK004608	*heat shock protein 8*	2.27	0.04	protein binding; ATP binding
Cell Differentiation				
NM_025711	*Asporin*	0.15	0.05	porin activity; cartilage extracellular protein
Development				
NM_031258	*chordin-like 1*	0.16	0.03	unknown
NM_009144	*secreted frizzled-related sequence protein 2*	0.43	0.03	transmembrane receptor and signal transduction activity
BB549310	*olfactomedin 1*	2.66	0.02	unknown
Skeletal Development				
NM_007554	*bone morphogenetic protein 4*	0.40	0.002	cytokine activity
NM_054077	*proline arginine-rich end leucine-rich repeat*	0.43	0.05	extracellular matrix structural constituent
NM_011641	*transformation related protein 63*	0.47	0.04	DNA binding; transcription factor activity
Cell Growth				
NM_010516	*cysteine rich protein 61*	0.24	0.02	protein binding; insulin-like growth factor binding

*Fold=RWV/static 1g

Table A.1-Continued

Accession #	Gene Name	*Fold Δ	p-value	Molecular Function
NM_016873	WNT1 inducible signaling pathway protein 2	0.39	0.01	phospholipase A2 activity; calcium ion binding
BC020038	endothelial cell-specific molecule 1	0.46	0.01	insulin-like growth factor binding
Cytoskeletal Regulation				
NM_008857	protein kinase C, iota	0.45	0.04	actin filament organization
AV297945	myosin X	0.46	0.046	motor activity; actin binding
AW491660	tubulin, alpha 4	2.42	0.007	microtubule based movement; GTPase activity; structural molecule activity
Metabolism				
NM_007934	glutamyl aminopeptidase	0.40	0.03	DNA binding; protein binding
AY057913	brain derived neurotrophic factor	0.46	0.02	mechanoreceptor differentiation; protein binding; growth factor activity
NM_007436	aldehyde dehydrogenase family 3, subfamily A1	2.56	0.04	aldehyde dehydrogenase activity
Proteolysis				
NM_011269	Rhesus blood group-associated A glycoprotein	0.36	0.01	cysteine-type endopeptidase activity
AF282844	matrix metalloproteinase 16	0.47	0.04	metalloendopeptidase activity
BB658835	a disintegrin-like and metalloprotease (reprolysin type) with thrombospondin type 1 motif, 5 (aggrecanase-2)	0.48	0.03	metalloendopeptidase activity; peptidase activity
AK011596	transferrin receptor	2.40	0.05	receptor activity; transferrin receptor activity
Signal Transduction				
NM_008046	follistatin	0.39	0.02	BMP signaling pathway
Protein Folding				
NM_013560	heat shock protein 1	2.03	0.04	unknown
NM_011020	heat shock 70kDa protein 4 like	2.06	0.02	ATP binding; unfolded protein binding
Transport				
AK018504	ras association (RalGDS/AF-6) domain family 2	0.43	0.27	protein binding
AV344473	sorting nexin associated golgi protein 1	0.48	0.008	unknown
BB280137	RAB guanine nucleotide exchange factor (GEF) 1	0.48	0.02	DNA binding; zinc ion binding
BB144704	ATP-binding cassette, sub-family A (ABC1), member 1	0.48	0.02	ATP binding; ATPase activity
Chromosome Organization				
BB533903	histone 1, H1c	0.29	0.03	DNA binding; protein binding
M25487 NM_023422	histone 1, H2bc	0.44	0.03	DNA binding

*Fold=RWV/static 1g

Table A.1-Continued

Accession #	Gene Name	*Fold Δ	p-value	Molecular Function
Nitric Oxide Synthesis				
BF166000	high mobility group box 1	0.41	0.04	nitric-oxide synthase regulator activity
Multidrug Transport				
BB291885	ATP-binding cassette, sub-family C (CFTR/MRP), member 4	2.35	0.003	multidrug efflux pump activity
Endocytosis				
AI848122	low density lipoprotein receptor-related protein 8, apolipoprotein e receptor	2.30	0.04	receptor activity; calcium ion binding
Stress or Immune Response				
NM_007705	cold inducible RNA binding protein	0.21	0.003	
D67017	heat shock protein 105	2.54	0.02	protein binding; ATP binding
AW763765	heat shock protein 1A	3.18	0.04	ATP binding
Regulation of Cell Growth				
NM_008760	osteoglycin	0.23	0.03	growth factor activity
Negative Regulation of Cell Growth				
NM_009517	wild-type p53-induced gene 1	2.18	0.03	unknown
Unknown				
BC002065	serine (or cysteine) proteinase inhibitor, clade A, member 3G	0.35	0.02	endopeptidase inhibitor activity
NM_133859	olfactomedin-like 3	0.40	0.02	unknown
NM_016753	latexin	0.44	0.01	enzyme inhibitor activity; metalloendopeptidase inhibitor activity
NM_007984	fascin homolog 1, actin bundling protein	0.47	0.04	actin binding; actin filament binding
NM_029632	protein phosphatase 1, regulatory (inhibitor) subunit 11	2.17	0.03	unknown
AI266910	ceroid-lipofuscinosis, neuronal 2	2.07	0.04	serine-type endopeptidase activity
NM_009266	selenophosphate synthetase 2	2.02	0.004	catalytic activity

*Fold=RWV/static 1g

Table A.2 The effect of the RWV on selected genes that may be involved in osteoblast differentiation and matrix mineralization. Genes are sorted based on fold changes with relaxed p-value stringency.

Accession #	Gene Name	*Fold Δ	p-value	Molecular Function
NM_012050	osteomodulin	0.10	<0.05	aka osteoadherin, may mediate cell attachment
NM_008760	osteoglycin	0.23	<0.05	binds to TGF-beta, no GAG in bone, keratan sulfate in other tissues
NM_025711	asporin	0.28	<0.05	porin activity; cartilage extracellular protein
BC002065	serine (or cysteine) proteinase inhibitor, clade A, member 3G	0.35	<0.05	may be involved in osteoclast function with MMPs and cathepsins
NM_007729	procollagen, type XI, alpha 1	0.37	<0.05	present in cartilage
NM_011581	thrombospondin 2	0.39	<0.025	involved in cell attachment
NM_016873	WNT1 inducible signaling pathway protein 2	0.39	<0.05	involved in WNT pathway, WNT stimulated by BMPs
BB781435	nidogen 2	0.39	<0.005	calcium binding
NM_007554	bone morphogenetic protein 4	0.40	<0.0025	growth factor and cytokine activity
BM218630	protocadherin 18	0.40	0.075	calcium ion binding
NM_011693	vascular cell adhesion molecule 1	0.41	<0.025	cell adhesion molecule activity
NM_012043	immunoglobulin superfamily containing leucine rich repeat (ISLR)	0.42	<0.05	involved in cell attachment
NM_009144	secreted frizzled-related sequence protein 2	0.43	<0.05	WNT signaling pathway antagonist
NM_021355	fibromodulin	0.45	0.051	binds to collagen, may regulate fibril formation, binds to TGF-beta
BB431535	matrix metalloproteinase 16	0.47	<0.05	involved in osteoclast function and bone resorption
AW412729	procollagen, type XII, alpha 1	0.48	0.072	present in collagen; extracellular matrix structural constituent
NM_010511	interferon gamma receptor 1	0.52	0.087	inhibit bone resorption
AF153440	BMP and activin membrane-bound inhibitor, homolog (Xenopus laevis)	0.53	0.065	antagonist to BMPs; involved in TGF-beta signaling pathway
BC014690	transforming growth factor, beta 3	0.59	<0.05	growth factor and cytokine activity
AF053954	cbfa1/runx2 (osf2)	0.69	0.086	essential transcription factor for osteoblast differentiation and bone formation
NM_020273	glucocorticoid modulatory element binding protein 1	0.70	0.059	transcription factor activity
NM_008216	hyaluronan synthase 2	0.74	<0.05	with versican-like protein works to captures space destined to become bone
NM_007833	decorin	0.76	<0.025	binds to collagen and may regulate fibril diameter
NM_007431	alkaline phosphatase 2, liver	0.82	<0.05	essential for hydroxyapatite formation and matrix mineralization
BB082407	hyaluronan and proteoglycan link protein 4	1.22	0.082	present in articular cartilage
BM251152	chondroitin sulfate proteoglycan 2	1.23	0.070	present in cartilage
BG092290	insulin-like growth factor 2 receptor	1.43	<0.025	signal transduction and hormone activity
NM_020275	tumor necrosis factor receptor superfamily, member 10b	1.43	<0.05	growth factor and cytokine activity
BG069059	leucine rich repeat (in FLII) interacting protein 1	1.52	0.082	leucine rich repeats involved in bone mineralization
NM_010554	interleukin 1α	1.58	<0.05	potent stimulators of bone resorption
NM_011361	serum/glucocorticoid regulated kinase	1.65	0.072	transferase activity, transferring phosphorus-containing groups
M94967	prostaglandin-endoperoxide synthase 2	2.05	0.062	prostaglandins important in fluid shear over bone cells
BM935811	integrin α6	2.47	<0.05	cell adhesion molecule
AK003744	cystatin E/M	3.45	<0.05	antagonist to cathepsin family
NM_011111	serine (or cysteine) proteinase inhibitor, clade B, member 2	7.14	0.078	may be involved in osteoclast function with MMPs and cathepsins
X75557	proliferin	14.4	0.059	involved in cell adhesion; may regulate cathepsin L; involved in cell proliferation

* Fold= RWV/static 1g

Table A.3 Comparison of gene expression changes among RWV, RPM, and mechanical load microarrays. Genes are sorted by biological process.

Accession #	Gene Name	Fold Δ RWV	p-value RWV	Fold Δ RPM	p-value RPM	Fold Δ in vivo	p-value in vivo	Molecular Function
Cell Growth & Differentiation								
AK014259	osteoglycin	0.22	<0.05	0.38	<0.005	2.47	<0.005	binds to TGF-Beta
NM_008409	integral membrane protein 2A	0.31	0.17	0.53	<0.05	2.85	<0.005	marker gene of osteoblastic cells in bone formation
NM_007792	cysteine and glycine-rich protein 2	0.65	<0.05	0.68	0.15	4.12	<0.0025	zinc ion binding
AK011346	pleiotrophin	0.43	0.17	0.36	<0.05	4.29	<0.0025	involved in bone mineralization; growth factor binding
Cell Adhesion								
NM_015734	procollagen, type V, alpha 1	0.56	0.06	0.65	0.11	1.97	<0.0025	present in cartilage ECM
NM_007739	procollagen, type VIII, alpha 1	0.57	p>0.05	0.68	p>0.1	2.56	p<0.0025	present in cartilage ECM
Cell Death								
NM_008086	growth arrest specific 1	0.59	0.16	0.53	<0.01	2.26	<0.0025	protein binding
Proteolysis								
NM_008788	procollagen C-proteinase enhancer protein	0.56	<0.01	0.52	<0.05	2.15	<0.005	nucleic acid binding
NM_011175	legumain	0.64	0.25	0.66	0.08	3.25	<0.005	cysteine-type endopeptidase activity
Signal Transduction								
NM_008809	platelet derived growth factor receptor, beta polypeptide	0.74	0.25	0.61	0.07	1.97	<0.01	protein serine/threonine kinase activity
NM_009037	reticulocalbin	0.69	<0.05	0.85	0.36	2.31	<0.005	calcium ion binding
Transcription regulation								
NM_010351	goosecoid	0.58	0.20	0.68	0.13	2.3	<0.005	DNA binding
NM_019791	melanoma antigen, family D, 1	0.54	0.14	0.55	<0.005	2.33	<0.0025	transcription coactivator activity
Cytoskeletal Movement								
NM_007392	actin, alpha 2, smooth muscle, aorta	0.64	p>0.1	0.85	p>0.1	1.97	p<0.0025	structural constituent of cytoskeleton
Other								
NM_009128	stearoyl-coenzyme A desaturase 2	0.4	0.28	0.35	<0.0025	2.56	<0.0025	iron ion binding
AK004179	platelet-derived growth factor receptor-like	0.45	<0.005	0.52	<0.05	2.18	<0.005	receptor activity

Vita

Mamta Jashvantlal Patel

Mamta Jashvantlal Patel was born in Anaheim, California on November 13, 1979 to the immensely proud parents Jashvantlal (JK) and Laxmiben (LJ) Patel. She is preceded in the family by two older sisters Hima and Daxa and followed by a younger sister Pritty and a brother RajuorBhikhu (no kidding, that is on the birth certificate). Mamta also had the joy of living with her maternal grandparents Vallabhbhai and Jamnaben Patel. JK and LJ immigrated to the United States of America on October 1, 1978 in pursuit of the American Dream…to the Home of the Brave…in the Land of the Free, leaving behind two daughters, Hima and Daxa, in the care of LJ's parents in a small village outside of Surat, India. JK and LJ managed to amass an appropriate amount of money to reunite with Hima and Daxa, and two weeks after Mamta's birth, the family moved to the ever popular town of San Angelo, Texas, the place she still calls home. Mamta attended preschool at Bradford Headstart, advanced to Holy Angels and Day Elementary for the succeeding years, progressed to Edison Junior High (Go Tide Go!), and finished her secondary education at Central High School (Go Bobcats!).

One of the most humorous memories of Mamta's early years was Catholic school, where all things in uniform plaid graced the hallways. However, there was Color Day. That's right: Color Day. On this day, any student whose parent attended the school PTA meeting was allowed to wear anything she wanted. ANYTHING. Mamta would love to say that her parents graciously attended this meeting, but she distinctly remembers planning with her siblings to connive her dad into attending a meeting that was clearly pointless, all the way across the city, and absolutely way too long. For merely placing his name on the sign-in sheet, the days of plaid shoes, plaid dresses, and all things plaid were forced to capitulate to the wonderful world of color, of the reds, the yellows, the greens, and of all things *not* plaid. Truth be told, it was the finest day in Mamta's Catholic do-good school days.

Although difficult for any of Mamta's friends and family to now believe, Mamta was painfully shy in her early years. In school, she was labeled the "nice, quiet" one. However, the winds of fate brought her to Mrs. Sickenius' seventh grade speech classroom where she was punched in the diaphragm to demonstrate what she sounded like at audible levels. No kidding, her teacher punched her daily in the stomach. Soon, Mamta felt so comfortable in her own skin that she discovered her calling as an actress. No really, Mamta still thinks she can act (she is a bit miffed at Aishwarya Rai and Parminda Nagra for taking *her* spot as the first successful Indian actress in Hollywood). She was chosen for the lead in the school play called "Of Winners, Losers, and Game", a part for which she was actually awarded Best Actress (it is even in the school trophy case!).

Mamta's siblings claim that she was a "true teenager", but aside from always being on the phone and loving shopping, Mamta was an odd mix of tomboy and girl. Her incredibly girly best friend, Tamara, had the bright idea that since Mamta loved sports and was all about school spirit, she should be a cheerleader. Yes, that is right. Mamta became a cheerleader. Although, in theory, Tamara's idea was beautiful, she was sorely proven wrong when Mamta would come in late or altogether miss the cheer because she was so involved in whether number 9 was going to go for the layup or pull back and shoot the jumper. Gone were the days Mamta listened to Tamara!

Perhaps the most impacting memory from her teenage years was Mrs. Adkins ninth grade English and Literature class, where Mamta first heard someone tell her she should be both a writer and an engineer (oxymoron, anyone, anyone...). She distinctly remembers that with every essay turned in, it was her goal to receive the highest grade, which from Mrs. Adkins was a note that said "I'm impressed". As her sophomore English teacher suggested (on a post-it Mamta still has to this day), Mamta would love to write children's literature someday.

Mamta has always been an avid activist and a true busy body, leading her high school class as sophomore, junior, and senior class president, holding student body office, singing in the choir, planning prom, and is not ashamed to say participating in JETS (Junior Engineering and Technical Society). Mamta graduated number 9 of her high school class of 767 and was voted Most Likely to Succeed by both the student body and faculty.

In the fall of 1998, Mamta pursued her higher education at Texas A&M University (Whoop!) and received a Bachelor of Science in Aerospace Engineering with honors in 2003. In college, she joined the women's lacrosse team and learned that she was by far the weakest link but claims joining the team was one of the best decisions of her collegiate career. Mamta became a Fish Camp (Freshmen Orientation Program) counselor each year of college, and she enjoyed helping freshmen transition into the years of Aggieland full of college football, school pride, and lifelong friends. Additionally, Mamta had learned from an old friend (Nicholas) that to fulfill her childhood dream of working for NASA meant that she would have to co-op there. This news shattered Mamta's sincere aspiration to finish college in under four years (yes, Mamta has always been an overachiever). At that time, NASA only hired full time employees from their past co-op students, and as such, Mamta made it her freshmen year goal to get that co-op! She still remembers "the phone call" she received from Bob Musgrove in HR and running up and down the hallways of her dorm in sheer joy and excitement. She now blushes that she carried the phone with her while Bob was on the line. Luckily, he still offered her the position! It was during these co-op years that Mamta unclenched and learned that life was about more than good grades and perfect records.

In 2003, Mamta made the arduous decision to decline an offer from NASA to pursue her Ph.D. in Bioengineering at the Georgia Institute of Technology and Emory University (Note: Mamta never left the southern part of the country. She just kept moving laterally west to east! *Y'all* never can take the *South* out of a *Southern gal*.) During her tenure at Georgia Tech and Emory University, Mamta was awarded the NASA Harriet Jenkins Pre-doctoral Fellowship, Gandy/Diaz Teaching Fellowship, and numerous travel awards. In 2005, Mamta was granted her Master of Science in Mechanical Engineering, and finally, at the summit of her four and half graduate years of diligence and bits of fun sprinkled about, Mamta defended her dissertation in Bioengineering in 2007.

In these years, Mamta achieved her lifelong dream of developing her own photography, fiddled with learning the guitar, ran a couple of marathons, traveled to Europe and across the United States, continued to play lacrosse, and managed to share these memories with a great set of friends. Mamta now resides in Houston, TX working in the Astronaut Training and Mission Control division of NASA and enjoys cooking, succulent dining, reading, playing Jeopardy, traveling, hanging out with friends, cheering on her alma mater in college football, spending time with her Wolverine, sharing in the new and independent lives of her siblings, and hearing her parents' stories about India.